Supplementary Information

Divergent Photochemical Remodeling of Furans

Da Hye Lee[1,†], Sumitava Mallik[1,†], Seok Yeol Yoo[2], Kyungbae Kim[1], and Yoonsu Park[1,3,]*

[1]Department of Chemistry, Korea Advanced Institute of Science and Technology (KAIST), Daejeon 34141, Republic of Korea

[2]Center for Catalytic Hydrocarbon Functionalizations, Institute for Basic Science (IBS), Daejeon 34141, Republic of Korea

[3]InnoCORE AI Co-Research & Education for Innovative Drug (AI-CRED) Institute, KAIST, Daejeon 34141, Republic of Korea

[†]These authors contributed equally.

**yoonsu.park@kaist.ac.kr*

Table of Contents

I. General Consideration

All air- and moisture-sensitive manipulations were carried out using vacuum line, Schlenk, and cannula techniques or in an inert atmosphere (nitrogen) glovebox unless otherwise noted. All glassware was stored in a pre-heated oven prior to use. The solvents used for air- and moisture-sensitive manipulations were dried and deoxygenated using literature procedures[1].

2,5-dimethylfuran, 2-pentylfuran, and furan were purchased from Sigma-Aldrich or TCI chemical company and distilled over a high vacuum line before use. 3,6-di-*tert*-butyl-9-mesityl-10-methylacridin-10-ium tetrafluoroborate, hydrazine monohydrochloride, sodium benzoate, scandium (III) triflate, 2,5-diphenyl furan, benzohydrazide, diosbulbin B, and isonicotinic acid hydrazide were purchased from Sigma-Aldrich or TCI chemical company or BLD pharm and dried under high vacuum prior to use. Sodium thiosulfate pentahydrate and sodium sulfate were purchased from Samchun chemical company and dried under high vacuum prior to use. All purified starting materials were stored in an N_2-filled glovebox. Hydrazine solution (1.0 M in MeCN), ethyl 3-(furan-2-yl)propanoate, and (+)-menthofuran were purchased from TCI chemical company or Sigma-Aldrich and used without further purification. Unless otherwise stated, all commercial reagents and solvents were used without additional purification.

^{1}H NMR spectra were recorded on Bruker AVANCE III HD (400 MHz), AVANCE NEO Nanobay (400 MHz), AVANCE NEO (500 MHz) or Agilent Technologies DD2 (600 MHz) at room temperature, unless otherwise noted. Chemical shifts were quoted in parts per million (ppm) referenced to the residual solvent peak. The following abbreviations were used to describe peak splitting patterns when appropriate s = singlet, d = doublet, dd = doublet of doublet, ddd = doublet of doublet of doublet, ddt = doublet of doublet of triplet, dt = doublet of triplet, t = triplet, td = triplet of doublet, tt = triplet of triplet, ttt = triplet of triplet of triplet, appt = apparent triplet, q = quartet, p = pentet, m = multiplet, br = broad. Coupling constants, *J*, were reported in hertz (Hz). ^{13}C NMR spectra were obtained on Bruker AVANCE III HD (400 MHz), AVANCE NEO Nanobay (400 MHz), AVANCE NEO (500 MHz), or Agilent Technologies DD2 (600 MHz), fully decoupled by broadband

proton decoupling. Chemical shifts were reported in ppm referenced to the residual solvent peak. ^{19}F NMR spectra were recorded on Bruker AVANCE III HD (400 MHz), AVANCE NEO Nanobay (400 MHz), or AVANCE NEO (500 MHz), and chemical shifts were reported in ppm referenced to external α,α,α-trifluorotoluene as -63.72 ppm.

Analytical thin-layer chromatography (TLC) was performed on Merck precoated silica gel 60 F254 plates. Visualization on TLC was achieved by UV light (254 nm). Silica-gel chromatography was performed using a CombiFlash® R_f^+ system with RediSep® R_f Silica columns using a proper eluent. Basic alumina (Al_2O_3) column chromatography was performed with standard grade, Brockmann I, activated, basic, using a proper eluent. High-resolution mass spectrometry (HRMS) data were obtained using ESI method via a reversed-phase liquid chromatography system (UPLC) connected to a Waters Xevo G2-XS Q-TOF mass spectrometer, operated with MassLynx software. UV-Vis absorption spectra were recorded on a Cary 60 UV-Vis S5 spectrometer (Agilent Technologies, Santa Clara, California) by using a custom-made 10 mm cuvette fitted with a J-Young valve. The data collection for X-ray single crystal structure analysis was performed at the given temperature on a Bruker D8 QUEST diffractometer and Bruker D8 VENTURE diffractometer equipped with Iμs 3.0 Mo X-ray tube (λ = 0.71073 Å) and Photon II detector. The parabar-coated crystals were mounted on a goniometer for a diffraction experiment. The diffraction data were integrated, scaled, and reduced by using the Bruker APEX5 software. The crystal structures were solved by SHELX structure solution program and refined by full-matrix least-squares calculations with the SHELXL[2,3].

II. Preparation of Starting Materials

Preparation of furan derivatives

3-phenylfuran[4], 3-(*p*-tolyl)furan[4], 3-(4-methoxyphenyl)furan[4], 3-(4-fluorophenyl)furan[4], 3-(4-(trifluoromethyl)phenyl)furan[4], 3-(furan-3-yl)benzonitrile[5], 2-(furan-3-yl)pyridine[4], 2-(furan-3-yl)pyrazine[4], 3-(naphthalen-2-yl)furan[4], 3-benzylfuran[6], 2-phenylfuran[4], 2-(furan-2-yl)pyridine[7], 2-(furan-2-ylmethyl)isoindoline-1,3-dione[8], 3,4-diphenylfuran[4], 3,4-di-*p*-tolylfuran[9], 2-methyl-4-phenylfuran[4], and 1,3,5-tri(furan-3-yl)benzene[10] were synthesized according to the previously reported methods.

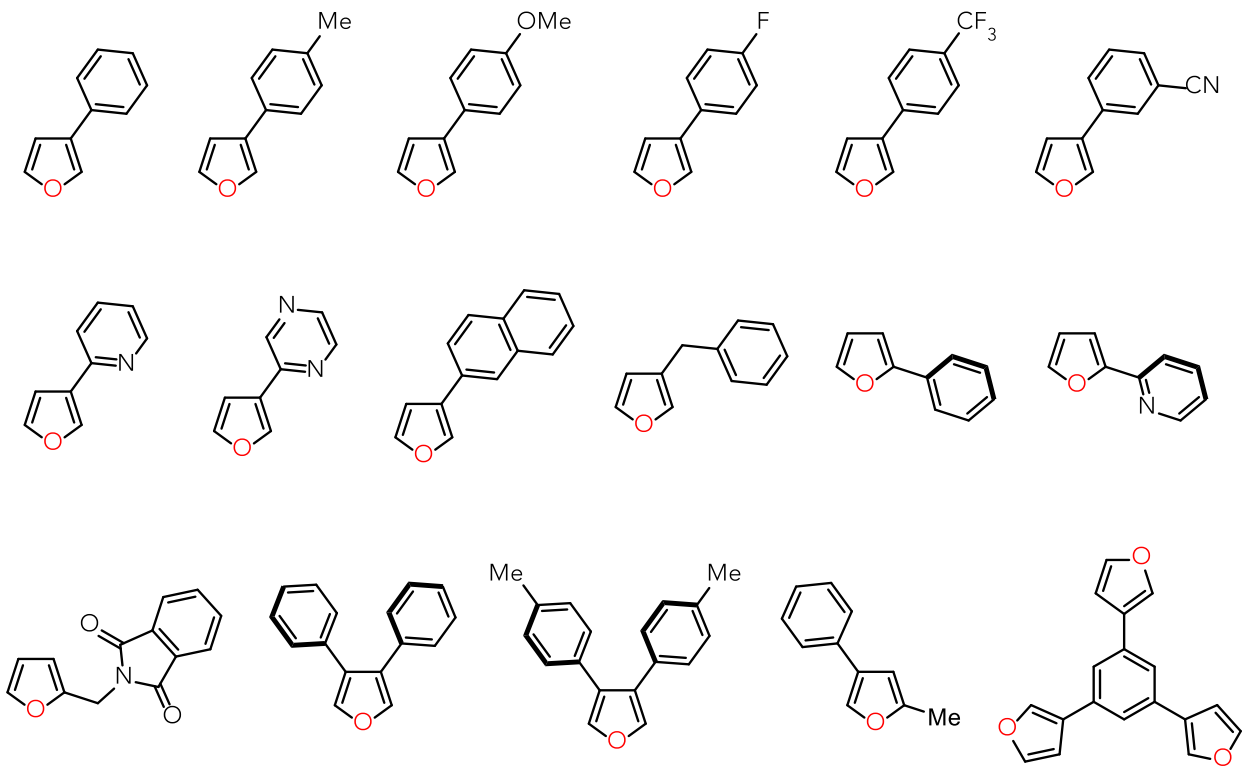

Figure S1. Molecular structures of the synthesized furans according to the literature methods

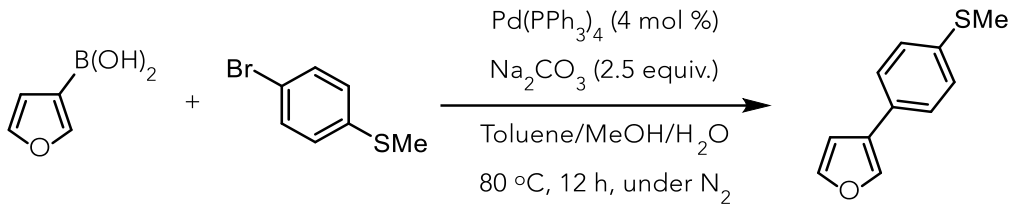

Preparation of 3-(4-(methylthio)phenyl)furan. A modified procedure was used based on the literature[4]. A 100 mL Schlenk flask was charged with a magnetic stir bar and $Pd(PPh_3)_4$ (4 mol %) under N_2 atmosphere. A toluene (12 mL) solution of aryl bromide (5.66 mmol) was added, followed by the addition of a 2 M aqueous solution of Na_2CO_3 (10 mL) and a solution of furan-3-boronic acid (6.5 mmol) in MeOH (3 mL). The reaction mixture was stirred at 80 °C for 12 h. Upon completion, the reaction mixture was cooled and extracted with CH_2Cl_2 three times. The combined organic layer was washed with brine and dried over Na_2SO_4. The resultant was filtered and concentrated under reduced pressure. The crude mixture was purified by silica gel flash column chromatography (Eluent: *n*-hexane/EtOAc = 9:1).

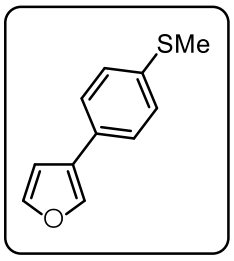

White solid (742.0 mg, 60%); **^{1}H NMR (400 MHz, Chloroform-*d*)** δ 7.72 (dd, *J* = 1.6, 0.9 Hz, 1H), 7.48 (appt, *J* = 1.7 Hz, 1H), 7.44 – 7.38 (m, 2H), 7.32 – 7.23 (m, 2H), 6.68 (dd, *J* = 1.9, 0.9 Hz, 1H), 2.50 (s, 3H); **^{13}C{^{1}H} NMR (151 MHz, Chloroform-*d*)** δ 143.84, 138.44, 137.10, 129.53, 127.30, 126.41, 126.08, 108.85, 16.20; **HRMS** (ESI) m/z calcd. for $C_{11}H_{10}OS$ $[M+H]^+$: 191.0525, found: 191.0520.

Preparation of photocatalyst

9-Mesityl-3,6-di-*tert*-butyl-10-mesitylacridinium tetrafluoroborate (**PC 1**) was synthesized according to the previously reported methods[11].

Neutralization of hydrazinium salts to free hydrazines

According to a procedure reported by Yoshiya Fukumoto and coworkers[12], *tert*-butyl hydrazinecarboxylate hydrochloride, and *tert*-butylhydrazine hydrochloride were free-based prior to use. In brief, to the suspension of hydrazinium salt in CH_2Cl_2 was added 2.0 equivalents of aqueous 1 M KOH solution at room temperature. After stirring for 30 min at room temperature, the resulting suspension was extracted to CH_2Cl_2, and the organic phase was further washed with brine, dried over sodium sulfate, and concentrated under reduced pressure to afford the desired free hydrazines.

Preparation of hydrazine derivatives

(1*R*,2*S*,5*R*)-2-isopropyl-5-methylcyclohexyl hydrazinecarboxylate[13] and phenethylhydrazine[14] were synthesized according to previously reported methods.

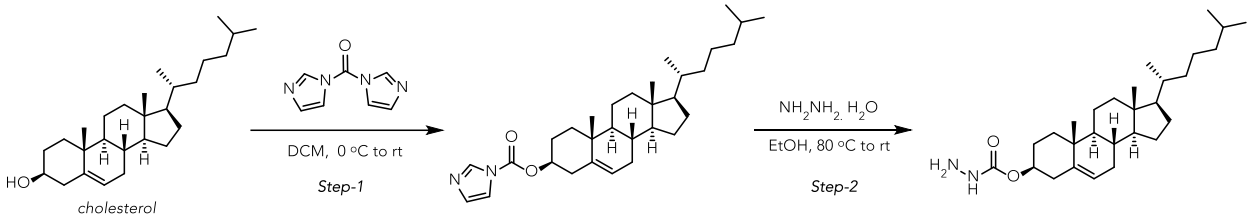

Preparation of (3*S*,8*S*,9*S*,10*R*,13*R*,14*S*,17*R*)-10,13-dimethyl-17-((*R*)-6-methylheptan-2-yl)-2,3,4,7,8,9,10,11,12,13,14,15,16,17-tetradecahydro-1*H*-cyclopenta[*a*]phenanthren-3-yl hydrazinecarboxylate. A modified procedure was used based on the literature[13,15]. A 50 mL Schlenk flask equipped with a magnetic stir bar was charged with cholesterol (2.5 mmol). Dichloromethane (10 mL) was added, and the reaction mixture was cooled to 0 °C. CDI (1.05 equiv.) was then added portion-wise, and the resulting solution was stirred at room temperature for 3 h. Upon completion of the reaction, the mixture was diluted with dichloromethane and washed three times with Na_2CO_3. The combined organic layers were washed with brine, dried

over Na_2SO_4, filtered, and concentrated under reduced pressure. The crude carbonate product was used for the next step without further purification.

Step-2: A modified procedure was used based on the literature.[16] A round-bottom flask was charged with the crude carbonate (2.0 mmol) was dissolved in EtOH (5 mL), treated with hydrazine hydrate (2.0 equiv.), and heated at 80 °C for 3 h. After completion, the reaction was quenched with 1 M NaOH and extracted with EtOAc (50 mL × 3). The combined organic layers were dried over Na_2SO_4, filtered, and concentrated under reduced pressure. Purification by silica gel column chromatography (Hexane/EtOAc = 1:1) afforded the corresponding carbazate.

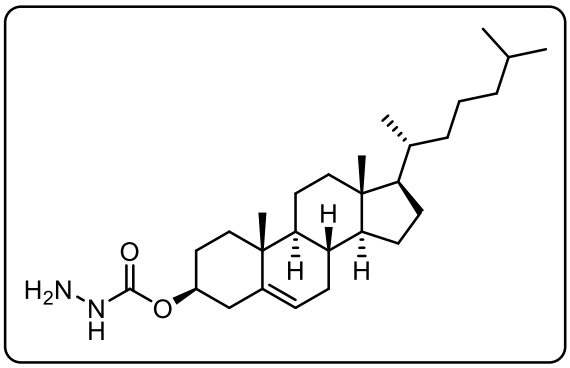

White solid (355.0 mg, 40%); **^{1}H NMR (600 MHz, Chloroform-*d*)** δ 5.94 (s, 1H), 5.38 (dd, *J* = 5.1, 2.3 Hz, 1H), 4.54 (t, *J* = 5.2 Hz, 1H), 3.57 (br, 2H), 2.44 – 2.24 (m, 2H), 2.03 – 1.92 (m, 2H), 1.91 – 1.78 (m, 3H), 1.65 – 1.40 (m, 7H), 1.39 – 1.30 (m, 3H), 1.29 – 1.21 (m, 1H), 1.20 – 1.04 (m, 7H), 1.03 – 0.93 (m, 6H), 0.93 – 0.80 (m, 9H), 0.67 (s, 3H).; **^{13}C{^{1}H} NMR (151 MHz, Chloroform-*d*)** δ 158.52, 139.70, 122.89, 75.43, 56.81, 56.25, 50.13, 42.44, 39.85, 39.65, 38.61, 37.07, 36.68, 36.31, 35.93, 32.03, 31.98, 28.37, 28.23, 28.15, 24.42, 23.96, 22.97, 22.70, 21.17, 19.45, 18.85, 11.99.

III. General Catalytic Procedures

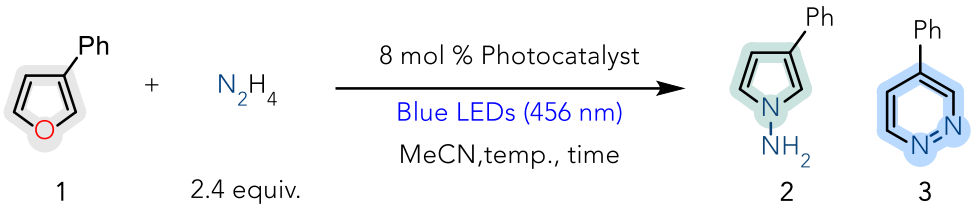

General procedure for reaction optimization studies. In a typical experiment, an oven-dried 4 mL vial was charged with 3-phenylfuran **1** (0.1 mmol, 1.0 equiv.), N_2H_4 (0.24 mmol, 2.4 equiv.), 8 mol % of photocatalyst (0.008 mmol, 0.08 equiv.), followed by the additive in an N_2-filled glovebox. After the addition of the proper reagent, solvent was added to the vial. A magnetic stir bar was charged, sealed with a screw cap and electrical tape, then removed from the glovebox. For the light reaction, the reaction vessel was stirred under irradiation with Kessil™ PR160L-456 nm blue lamps (40 W, 100% intensity) using a household fan. After completion, about 10 mg of 1,3,5-trimethoxybenzene was added to the reaction mixture under an ambient atmosphere. Then, an aliquot of 0.05 mL of the resulting crude mixture was taken and directly transferred to an NMR tube. An additional 0.6 mL of $CDCl_3$ was added to the NMR cell, and the crude yield was analyzed by either 400 MHz or 500 MHz ^{1}H NMR spectroscopy using 1,3,5-trimethoxybenzene as an internal standard. The relaxation delay (d1), scan numbers (ns), and dummy scans (ds) were set to 20 seconds, 3 scans, and 1 scan, respectively, to accurately quantify the yield using ^{1}H NMR spectra.

Figure S2. Typical reaction setup for irradiation experiments: 23 °C (left), 80 °C (right).

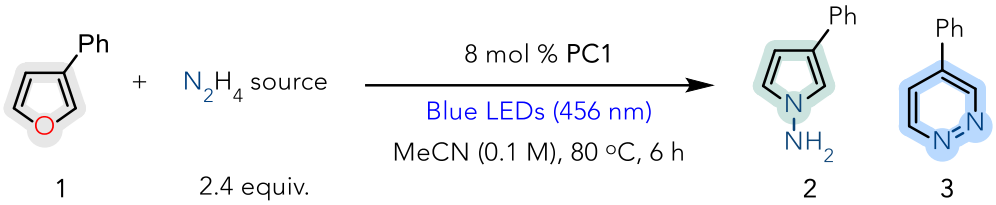

Table S1. Reaction optimization studies for *N*-aminopyrrole conversion: effect of N_2H_4 source

Entry	N_2H_4 source	^{1}H NMR Yield of **2** (%)	^{1}H NMR Yield of **3** (%)	Unreacted furan **1** (%)
1	1.0 M in MeCN	51	13	25
2	1.0 M in Tetrahydrofuran	26	10	42
3	N_2H_4 H_2O	23	5	48

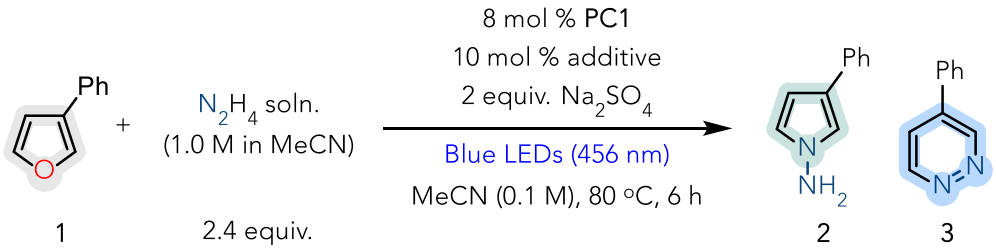

Table S2. Reaction optimization studies for *N*-aminopyrrole conversion: effect of additive

Entry	Additive	^{1}H NMR Yield of **2** (%)	^{1}H NMR Yield of **3** (%)	Unreacted furan **1** (%)
1	$Sc(OTf)_3$	69	12	11
2	$Zn(OTf)_2$	14	11	32
3	$Cu(acac)_2$	47	9	23
4	Acetic acid	49	10	20

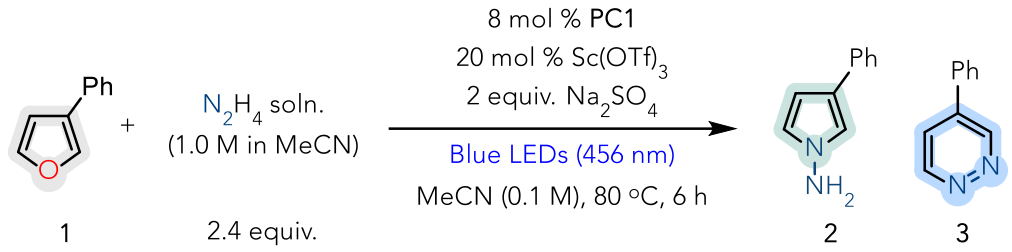

Table S3. Reaction optimization studies for *N*-aminopyrrole conversion: other variation

Entry	Deviation from optimal conditions	^{1}H NMR Yield of **2** (%)	^{1}H NMR Yield of **3** (%)	Unreacted furan **1** (%)
1	none	86	13	0
2	Without $Sc(OTf)_3$	61	11	26
3	Without Na_2SO_4	68	16	0
4	$N_2H_4 \cdot HCl$	0	0	43
5	**PC2** instead of **PC1**	67	13	0
6	**PC3** instead of **PC1**	29	9	52
7	**PC4** instead of **PC1**	63	14	16

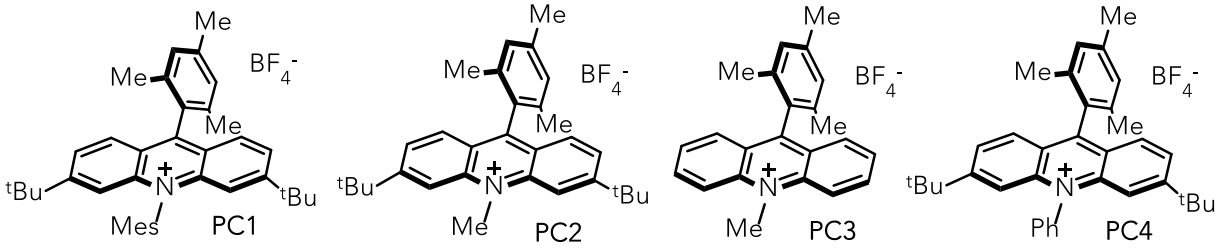

Table S4. Control studies for the *N*-aminopyrrole reaction system.

Entry	Deviation from optimal conditions	^{1}H NMR Yield of **2** (%)	^{1}H NMR Yield of **3** (%)	Unreacted furan **1** (%)
1	none	86	13	0
2	w/o Blue LED irradiation	0	0	99
3	w/o **PC1**	0	0	96
4	w/o irradiation, **PC1**	0	0	99

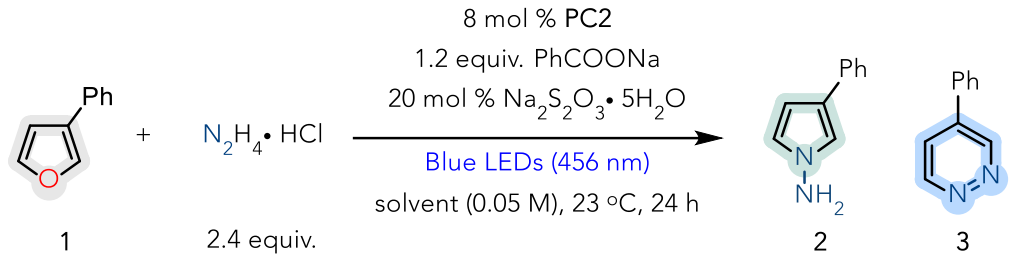

Table S5. Reaction optimization studies for pyridazine conversion: effect of solvent

Entry	Solvent	^{1}H NMR Yield of **2** (%)	^{1}H NMR Yield of **3** (%)	Unreacted furan **1** (%)
1	MeCN:H_2O (4:1)	0	90	0
2	MeCN	18	25	28

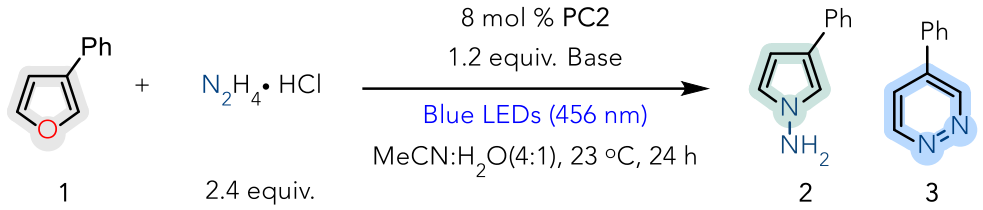

Table S6. Reaction optimization studies for pyridazine conversion: effect of base

Entry	Base	^{1}H NMR Yield of **2** (%)	^{1}H NMR Yield of **3** (%)	Unreacted furan **1** (%)
1	1.2 equiv. Sodium benzoate 20 mol % $Na_2S_2O_3 \cdot 5H_2O$	0	90	0
2	1.2 equiv. Sodium benzoate 1.2 equiv. $Na_2S_2O_3 \cdot 5H_2O$	0	79	0
3	Sodium benzoate	0	71	0
4	$Na_2S_2O_3 \cdot 5H_2O$	0	57	0
5	Disodium succinate	0	43	0

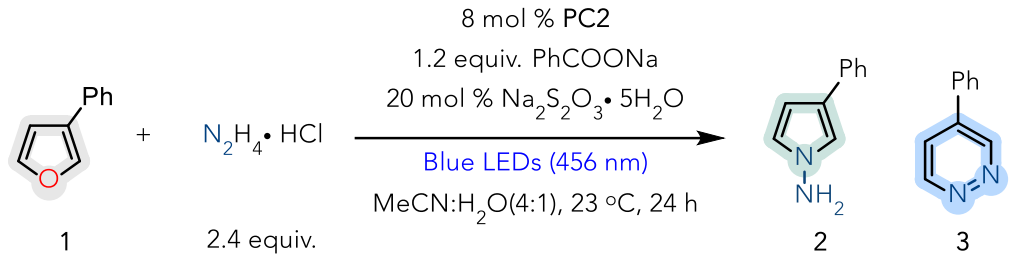

Table S7. Reaction optimization studies for pyridazine conversion: other variation

Entry	Deviation from optimal conditions	^{1}H NMR Yield of **2** (%)	^{1}H NMR Yield of **3** (%)	Unreacted furan **1** (%)
1	none	0	90	0
2	Without PhCOONa	0	39	0
3	**PC1** instead of **PC2**	0	67	0
4	**PC3** instead of **PC2**	0	10	0
5	**PC4** instead of **PC2**	0	65	0
6	4-CN pyridine instead of PhCOONa	0	46	0

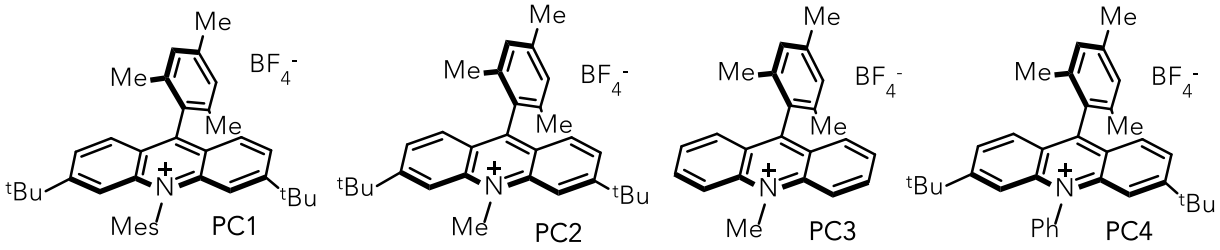

Table S8. Control studies for the pyridazine reaction system.

Entry	Deviation from optimal conditions	^{1}H NMR Yield of **2** (%)	^{1}H NMR Yield of **3** (%)	Unreacted furan **1** (%)
1	none	0	90	0
2	w/o Blue LED irradiation	0	0	98
3	w/o **PC2**	0	0	96
4	w/o irradiation, **PC2**	0	0	99

General photocatalytic procedure for skeletal diversification

1) Furan-to-*N*-aminopyrrole conversion

In a typical experiment, an oven-dried 4 mL vial was charged with furan (0.2 mmol, 1.0 equiv.), scandium (III) triflate (0.04 mmol, 0.2 equiv.), and sodium sulfate (0.4 mmol, 2.0 equiv.), followed by 8 mol % of **PC1** (0.016 mmol, 0.08 equiv.) in an N_2-filled glovebox. After the addition of the proper reagent, acetonitrile (1.52 mL) was added to the vial. A magnetic stir bar was charged, sealed with a screw cap and electrical tape, then removed from the glovebox. Under an N_2 atmosphere, hydrazine solution (1.0 M in MeCN) (0.48 mL, 2.4 equiv.) was added to the vial, and the mixture was stirred for 6 h under irradiation at 80 °C with Kessil™ PR160L 456 nm blue lamps (40 W, 100% intensity) using a household fan. After completion, the crude mixture was concentrated under reduced pressure, then purified with silica gel flash column chromatography to afford the desired product.

2) Furan-to-Pyridazine conversion

In a typical experiment, an oven-dried 4 mL vial was charged with furan (0.2 mmol, 1.0 equiv.), hydrazine monohydrochloride (0.48 mmol, 2.4 equiv.), sodium benzoate (0.24 mmol, 1.2 equiv.), and sodium thiosulfate pentahydrate (0.04 mmol, 0.2 equiv.), followed by 8 mol % of **PC2** (0.016 mmol, 0.08 equiv.) in an N_2-filled glovebox. After the addition of the proper reagent, acetonitrile (1.6 mL) was added to the vial. A magnetic stir bar was charged, sealed with a screw cap and electrical tape, then removed from the glovebox. Under an N_2 atmosphere, degassed water (0.4 mL) was added to the vial, and the mixture was stirred for 24 h under irradiation at 23 °C with Kessil™ PR160L 456 nm blue lamps (40 W, 100% intensity) using a household fan. After completion, quenched with saturated $NaHCO_3$, extracted with ethyl acetate three times, and dried over Na_2SO_4. The resultant was filtered and concentrated under reduced pressure, then purified with silica gel flash column chromatography to afford the desired product.

*Note: Substrate **41, 42** purified by basic alumina column chromatography.*

3-phenyl-1*H*-pyrrol-1-amine (2)

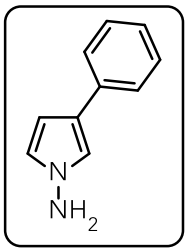

Yellow solid (24.0 mg, 76%); Purified by silica chromatography with EtOAc/*n*-hexane (1:5) eluent; **^{1}H NMR (600 MHz, Chloroform-*d*)** δ 7.51 (dd, *J* = 8.2, 1.5 Hz, 2H), 7.36 (appt, *J* = 7.7 Hz, 2H), 7.20 (tq, *J* = 7.6, 1.1 Hz, 1H), 6.99 (appt, *J* = 2.2 Hz, 1H), 6.73 (appt, *J* = 2.6 Hz, 1H), 6.38 (appt, *J* = 2.4 Hz, 1H), 4.86 (s, 2H); **^{13}C{^{1}H} NMR (151 MHz, Chloroform-*d*)** δ 135.70, 128.74, 125.57, 125.00, 123.16, 122.97, 119.01, 104.36; **HRMS** (ESI) m/z calcd. for $C_{10}H_{10}N_2$ $[M+H]^+$: 159.0917, found: 159.0914; Solid-state structure and its absolute configuration was characterized by X-ray diffraction analysis (CCDC 2554884).

3-(*p*-tolyl)-1*H*-pyrrol-1-amine (5)

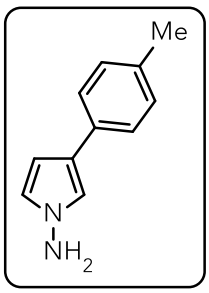

Yellow solid (26.1 mg, 76%); Purified by silica chromatography with EtOAc/*n*-hexane (1:4) eluent; **^{1}H NMR (500 MHz, Chloroform-*d*)** δ 7.41 (d, J = 7.8 Hz, 2H), 7.18 (d, J = 7.8 Hz, 2H), 6.95 (appt, J = 2.2 Hz, 1H), 6.71 (appt, J = 2.6 Hz, 1H), 6.35 (appt, J = 2.5 Hz, 1H), 4.84 (s, 2H), 2.38 (s, 3H); **^{13}C{^{1}H} NMR (126 MHz, Chloroform-*d*)** δ 135.10, 132.86, 129.42, 124.94, 123.02, 122.99, 118.69, 104.23, 21.16; **HRMS** (ESI) m/z calcd. for $C_{11}H_{12}N_2$ $[M+H]^+$: 173.1073, found: 173.1069.

3-(4-methoxyphenyl)-1*H*-pyrrol-1-amine (6)

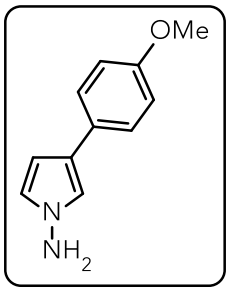

Yellow solid (19.5 mg, 52%); Purified by silica chromatography with EtOAc/*n*-hexane (1:4) eluent; **^{1}H NMR (500 MHz, Chloroform-*d*)** δ 7.46 – 7.35 (m, 2H), 6.94 – 6.84 (m, 3H), 6.70 (appt, *J* = 2.6 Hz, 1H), 6.29 (dt, *J* = 4.4, 2.2 Hz, 1H), 4.86 (s, 2H), 3.82 (d, *J* = 2.5 Hz, 3H); **^{13}C{^{1}H} NMR (126 MHz, Chloroform-*d*)** δ 157.83, 128.60, 126.15, 123.00, 122.81, 118.31, 114.20, 104.13, 55.41; **HRMS** (ESI) m/z calcd. for $C_{11}H_{12}N_2O$ $[M+H]^+$: 189.1022, found: 189.1018.

3-(4-(methylthio)phenyl)-1*H*-pyrrol-1-amine (7)

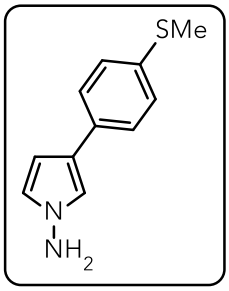

Yellow solid (13.4 mg, 33%); Purified by silica chromatography with EtOAc/*n*-hexane (1:4) eluent; **^{1}H NMR (500 MHz, Chloroform-*d*)** δ 7.41 (d, *J* = 7.8 Hz, 2H), 7.30 – 7.18 (m, 2H), 6.98 (s, 1H), 6.72 (s, 1H), 6.32 (s, 1H), 4.90 (s, 2H), 2.49 (s, 3H); **^{13}C{^{1}H} NMR (126 MHz, Chloroform-*d*)** δ 134.85, 133.09, 127.73, 125.51, 123.24, 122.53, 118.94, 104.34, 16.64; **HRMS** (ESI) m/z calcd. for $C_{11}H_{12}N_2S$ $[M+H]^+$: 205.0794, found: 205.0790.

3-(4-fluorophenyl)-1*H*-pyrrol-1-amine (8)

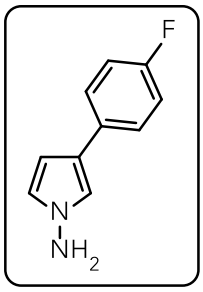

Pale white solid (23.3 mg, 66%); Purified by silica chromatography with EtOAc/*n*-hexane (1:4) eluent; **^{1}H NMR (400 MHz, Chloroform-*d*)** δ 7.52 – 7.36 (m, 2H), 7.03 (appt, *J* = 8.7 Hz, 2H), 6.93 (appt, *J* = 2.2 Hz, 1H), 6.72 (appt, *J* = 2.6 Hz, 1H), 6.30 (appt, *J* = 2.4 Hz, 1H), 4.88 (s, 2H); **^{13}C{^{1}H} NMR (101 MHz, Chloroform-*d*)** δ 161.26 (d, *J* = 243.5 Hz), 131.89 (d, *J* = 3.2 Hz), 126.39 (d, *J* = 7.7 Hz), 123.24, 122.14, 118.80, 115.49 (d, *J* = 21.4 Hz), 104.34; **^{19}F NMR (377 MHz, Chloroform-*d*)** δ -117.91; **HRMS** (ESI) m/z calcd. for $C_{10}H_9FN_2$ $[M+H]^+$: 177.0823, found: 177.0818.

3-(4-(trifluoromethyl)phenyl)-1*H*-pyrrol-1-amine (9)

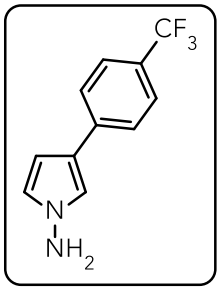

Yellow solid (24.9 mg, 55%); Purified by silica chromatography with EtOAc/*n*-hexane (1:4) eluent; **^{1}H NMR (600 MHz, DMSO-d$_6$)** δ 7.69 (d, *J* = 8.1 Hz, 2H), 7.59 (d, *J* = 8.1 Hz, 2H), 7.40 – 7.12 (m, 1H), 6.75 – 6.71 (m, 1H), 6.39 (appt, *J* = 2.4 Hz, 1H), 6.08 (s, 2H); **^{13}C{^{1}H} NMR (151 MHz, DMSO-d$_6$)** δ 140.08, 125.46 (q, *J* = 4.2 Hz), 124.80 (q, *J* = 31.2 Hz), 124.68 (q, *J* = 271.8 Hz), 124.26, 123.44, 120.19, 119.25, 103.40; **^{19}F NMR (377 MHz, DMSO-d$_6$)** δ -60.51; **HRMS** (ESI) m/z calcd. for $C_{11}H_9F_3N_2$ $[M+H]^+$: 227.0791, found: 227.0787.

3-(1-amino-1*H*-pyrrol-3-yl)benzonitrile (10)

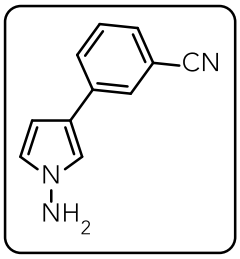

Yellow solid (14.6 mg, 40%); Purified by silica chromatography with EtOAc/*n*-hexane (1:1.5) eluent; **^{1}H NMR (600 MHz, Chloroform-*d*)** δ 7.71 (d, *J* = 1.8 Hz, 1H), 7.66 (dt, *J* = 7.1, 1.9 Hz, 1H), 7.45 – 7.37 (m, 2H), 7.04 (appt, *J* = 2.2 Hz, 1H), 6.75 (appt, *J* = 2.6 Hz, 1H), 6.33 (dd, *J* = 2.9, 2.1 Hz, 1H), 4.95 (s, 2H); **^{13}C{^{1}H} NMR (151 MHz, Chloroform-*d*)** δ 137.05, 129.50, 129.12, 128.83, 128.34, 123.83, 120.85, 119.73, 119.39, 112.75, 104.49; **HRMS** (ESI) m/z calcd. for $C_{11}H_9N_3$ $[M+H]^+$: 184.0869, found: 184.0863.

3-(naphthalen-2-yl)-1*H*-pyrrol-1-amine (11)

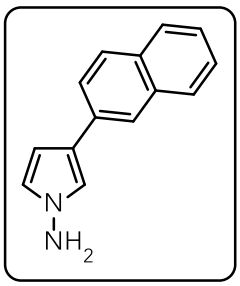

Yellow solid (14.6 mg, 67%); Purified by silica chromatography with EtOAc/*n*-hexane (1:5) eluent; **^{1}H NMR (600 MHz, Chloroform-*d*)** δ 7.92 (d, *J* = 1.8 Hz, 1H), 7.88 – 7.75 (m, 3H), 7.65 (dd, *J* = 8.6, 1.8 Hz, 1H), 7.46 (ddd, *J* = 8.1, 6.8, 1.4 Hz, 1H), 7.41 (ddd, *J* = 8.1, 6.8, 1.3 Hz, 1H), 7.11 (appt, *J* = 2.1 Hz, 1H), 6.77 (appt, *J* = 2.5 Hz, 1H), 6.50 (dd, *J* = 2.9, 2.0 Hz, 1H), 4.89 (s, 2H); **^{13}C{^{1}H} NMR (151 MHz, Chloroform-*d*)** δ 134.09, 133.14, 132.01, 128.26, 127.76, 127.74, 126.17, 124.99, 124.49, 123.42, 122.96, 122.39, 119.51, 104.59; **HRMS** (ESI) m/z calcd. for $C_{14}H_{12}N_2$ $[M+H]^+$: 209.1073, found: 209.1070.

3-benzyl-1*H*-pyrrol-1-amine (12)

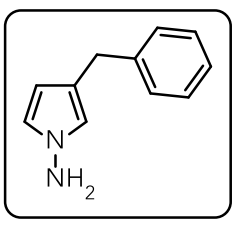

Orange oil (14.8 mg, 43%); Purified by silica chromatography with EtOAc/*n*-hexane (1:4) eluent; **^{1}H NMR (600 MHz, Chloroform-*d*)** δ 7.30 (appt, *J* = 7.5 Hz, 2H), 7.25 (d, *J* = 7.3 Hz, 2H), 7.20 (appt, *J* = 7.4 Hz, 1H), 6.62 (appt, *J* = 2.5 Hz, 1H), 6.44 (s, 1H), 5.89 (s, 1H), 4.76 (s, 2H), 3.79 (s, 2H); **^{13}C{^{1}H}**

NMR (151 MHz, Chloroform-*d*) δ 142.27, 128.68, 128.41, 125.83, 122.22, 121.61, 120.24, 106.71, 33.66; **HRMS** (ESI) m/z calcd. for $C_{11}H_{12}N_2$ $[M+H]^+$: 173.1073, found: 173.1068.

2-methyl-4-phenyl-1*H*-pyrrol-1-amine (13)

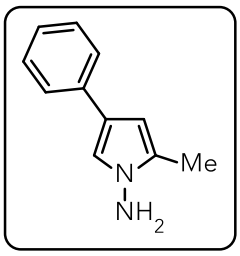

Yellow solid (21.7 mg, 63%); Purified by silica chromatography with EtOAc/*n*-hexane (1:4) eluent; **^{1}H NMR (600 MHz, Chloroform-*d*)** δ 7.49 – 7.44 (m, 2H), 7.32 (appt, *J* = 7.8 Hz, 2H), 7.18 – 7.12 (m, 1H), 6.97 (d, *J* = 2.2 Hz, 1H), 6.13 (dd, *J* = 2.2, 1.1 Hz, 1H), 4.56 (s, 2H), 2.27 (s, 3H); **^{13}C{^{1}H} NMR (151 MHz, Chloroform-*d*)** δ 135.91, 130.33, 128.69, 125.37, 124.91, 121.27, 118.01, 102.54, 11.28; **HRMS** (ESI) m/z calcd. for $C_{11}H_{12}N_2$ $[M+H]^+$: 173.1073, found: 173.1067.

ethyl 3-(1-amino-1*H*-pyrrol-2-yl)propanoate (14)

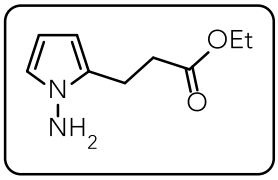

Orange liquid (7.5 mg, 21%); Purified by silica chromatography with EtOAc/*n*-hexane (1:19) eluent; **^{1}H NMR (600 MHz, Chloroform-*d*)** δ 6.66 (appt, *J* = 2.5 Hz, 1H), 5.96 (d, *J* = 3.4 Hz, 1H), 5.80 (d, *J* = 3.0 Hz, 1H), 4.72 (s, 2H), 4.13 (q, *J* = 7.2 Hz, 2H), 2.93 (t, *J* = 7.4 Hz, 2H), 2.65 (t, *J* = 7.4 Hz, 2H), 1.24 (t, *J* = 6.0 Hz, 3H); **^{13}C{^{1}H} NMR (151 MHz, Chloroform-*d*)** δ 173.42, 131.97, 121.59, 104.99, 103.79, 60.70, 34.35, 20.72, 14.34; **HRMS** (ESI) m/z calcd. for $C_9H_{14}N_2O_2$ $[M+H]^+$: 183.1128, found: 183.1120.

2-pentyl-1*H*-pyrrol-1-amine (15)

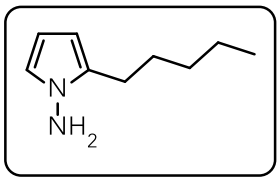

Yellow liquid (7.6 mg, 25%); Purified by silica chromatography with EtOAc/*n*-hexane (1:19) eluent; **^{1}H NMR (600 MHz, Chloroform-*d*)** δ 6.65 (dd, *J* = 2.9, 2.0 Hz, 1H), 5.97 (dd, *J* = 3.8, 2.8 Hz, 1H), 5.83 – 5.68 (m, 1H), 4.51 (s, 2H), 2.73 – 2.46 (m, 2H), 1.78 – 1.57 (m, 2H), 1.48 – 1.31 (m, 4H), 1.00 – 0.85 (m,

3H); **^{13}C{^{1}H} NMR (151 MHz, Chloroform-*d*)** δ 133.99, 121.05, 104.78, 103.37, 31.82, 28.89, 25.59, 22.67, 14.19; **HRMS** (ESI) m/z calcd. for $C_9H_{16}N_2$ [M+H]$^+$: 153.1386, found: 153.1381.

3-(3,5-di(furan-3-yl)phenyl)-1*H*-pyrrol-1-amine (16)

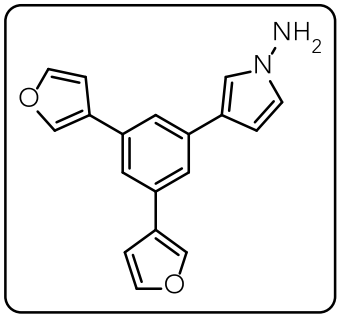

Use 7.2 equiv. of N_2H_4 solution (1.0 M in MeCN); Yellow solid (53.4 mg, 92%); Purified by silica chromatography with EtOAc/*n*-hexane (1:2.5) eluent; **^{1}H NMR (600 MHz, Chloroform-*d*)** δ 7.79 (appt, *J* = 1.2 Hz, 2H), 7.61 – 7.46 (m, 4H), 7.40 (appt, *J* = 1.6 Hz, 1H), 7.07 (appt, *J* = 2.1 Hz, 1H), 6.76 (dd, *J* = 1.8, 0.9 Hz, 3H), 6.41 (dd, *J* = 2.9, 2.0 Hz, 1H), 4.93 (s, 2H); **^{13}C{^{1}H} NMR (151 MHz, Chloroform-*d*)** δ 143.76, 138.81, 138.80, 136.84, 133.36, 126.65, 123.31, 122.68, 121.64, 121.03, 119.39, 109.19, 104.66; **HRMS** (ESI) m/z calcd. for $C_{18}H_{14}N_2O_2$ [M+H]$^+$: 291.1128, found: 291.1125.

***N*-(2-phenyl-1*H*-pyrrol-1-yl)benzamide (17)**

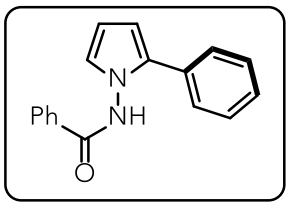

Run with benzoyl hydrazine instead of hydrazine solution; Green solid (47.2 mg, 90%); Purified by silica chromatography with EtOAc/*n*-hexane (1:5) eluent; **^{1}H NMR (600 MHz, Chloroform-*d*)** δ 8.69 (s, 1H), 7.56 (d, *J* = 7.6 Hz, 2H), 7.40 (appt, *J* = 7.5 Hz, 1H), 7.28 (d, *J* = 7.6 Hz, 4H), 7.18 (appt, *J* = 7.5 Hz, 2H), 7.14 – 7.07 (m, 1H), 6.61 (dt, *J* = 3.3, 1.3 Hz, 1H), 6.20 (d, *J* = 3.9 Hz, 1H), 6.13 (d, *J* = 3.5 Hz, 1H); **^{13}C{^{1}H} NMR (151 MHz, Chloroform-*d*)** δ 167.25, 134.21, 132.68, 131.70, 131.54, 128.99, 128.58, 128.04, 127.52, 127.30, 123.71, 107.97, 107.73; **HRMS** (ESI) m/z calcd. for $C_{17}H_{14}N_2O$ [M+H]$^+$: 263.1179, found: 263.1176.

***N*-(3-phenyl-1*H*-pyrrol-1-yl)benzamide (18)**

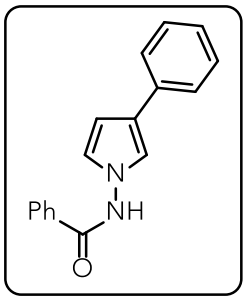

Run with benzoyl hydrazine instead of hydrazine solution; Yellow solid (30.0 mg, 57%); Purified by silica chromatography with EtOAc/*n*-hexane (1:1.5) eluent; **^{1}H NMR (400 MHz, DMSO-d$_6$)** δ 11.83 (s, 1H), 7.96 (d, *J* = 7.2 Hz, 2H), 7.70 – 7.61 (m, 1H), 7.60 – 7.51 (m, 4H), 7.39 – 7.28 (m, 3H), 7.19 – 7.10 (m, 1H), 6.91 (dd, *J* = 3.0, 2.2 Hz, 1H), 6.53 (dd, *J* = 3.0, 1.9 Hz, 1H); **^{13}C{^{1}H} NMR (101 MHz, DMSO-d$_6$)** δ 165.81, 135.16, 132.37, 131.78, 128.67, 128.62, 127.60, 125.32, 124.39, 123.24, 122.14, 119.09, 104.44; **HRMS** (ESI) m/z calcd. for $C_{18}H_{14}N_2O_2$ $[M+H]^+$: 291.1128, found: 291.1125.

***tert*-butyl (3-phenyl-1*H*-pyrrol-1-yl)carbamate (19)**

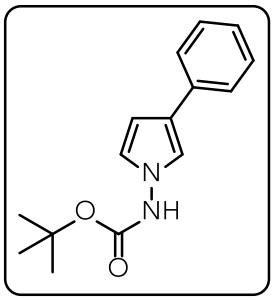

Run with *N*-Boc protected hydrazine instead of hydrazine solution; Yellow solid (25.8 mg, 50%); Purified by silica chromatography with EtOAc/*n*-hexane (1:5) eluent; **^{1}H NMR (600 MHz, Chloroform-*d*)** δ 7.49 (dd, *J* = 8.3, 1.3 Hz, 2H), 7.33 (appt, *J* = 7.8 Hz, 2H), 7.30 (s, 1H), 7.21 – 7.14 (m, 1H), 6.97 (appt, *J* = 2.1 Hz, 1H), 6.71 (appt, *J* = 2.6 Hz, 1H), 6.44 (dd, *J* = 3.1, 1.9 Hz, 1H), 1.51 (s, 9H); **^{13}C{^{1}H} NMR (151 MHz, Chloroform-*d*)** δ 154.56, 135.29, 128.69, 125.88, 125.30, 123.24, 118.94, 105.74, 82.56, 28.29; **HRMS** (ESI) m/z calcd. for $C_{15}H_{18}N_2O_2$ $[M+H]^+$: 259.1441, found: 259.1438.

***N*-(*tert*-butyl)-3-phenyl-1*H*-pyrrol-1-amine (20)**

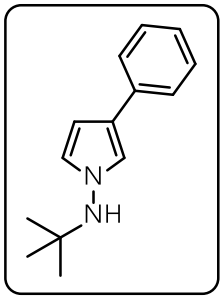

Run with *N*-tertbutyl-protected hydrazine instead of hydrazine solution; Yellow liquid (13.5 mg, 31%); Purified by silica chromatography with EtOAc/*n*-hexane (1:4) eluent; **^{1}H NMR (500 MHz, Chloroform-*d*)** δ 7.51 (dd, *J* = 8.3, 1.4 Hz, 2H), 7.36 – 7.29 (m, 2H), 7.19 – 7.13 (m, 1H), 6.96 (appt, *J* = 2.1 Hz, 1H), 6.67 (appt, *J* = 2.6 Hz, 1H), 6.37 (dd, *J* = 3.0, 1.9 Hz, 1H), 4.45 (s, 1H),

1.20 (s, 9H); **$^{13}C\{^{1}H\}$ NMR (126 MHz, Chloroform-*d*)** δ 135.92, 128.72, 125.42, 124.97, 123.89, 122.05, 119.65, 103.56, 55.67, 28.39; **HRMS** (ESI) m/z calcd. for $C_{14}H_{18}N_2$ $[M+H]^+$: 215.1543, found: 215.1541.

4-phenylpyridazine (3)

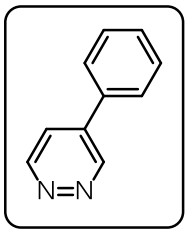

0.1 mmol scale of **1**; Pale white solid (13.2 mg, 85%); Purified by silica chromatography with EtOAc/*n*-hexane (3:2) eluent; **^{1}H NMR (600 MHz, Chloroform-*d*)** δ 9.46 (d, *J* = 2.4 Hz, 1H), 9.22 (d, *J* = 5.3 Hz, 1H), 7.70 – 7.62 (m, 3H), 7.52 (dd, *J* = 11.0, 7.1 Hz, 3H); **$^{13}C\{^{1}H\}$ NMR (151 MHz, Chloroform-*d*)** δ 151.55, 150.11, 138.65, 134.62, 130.26, 129.67, 127.20, 123.40; NMR spectroscopic signatures are matched with that of the previously reported ones[17].

4-(*p*-tolyl)pyridazine (21)

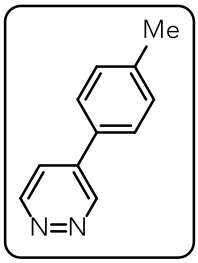

Yellow solid (27.0 mg, 80%); Purified by silica chromatography with EtOAc/n-hexane (4:1) eluent; **^{1}H NMR (600 MHz, Chloroform-*d*)** δ 9.45 (dd, J = 2.5, 1.2 Hz, 1H), 9.19 (dd, J = 5.5, 1.2 Hz, 1H), 7.62 (dd, J = 5.4, 2.5 Hz, 1H), 7.58 (d, J = 8.2 Hz, 2H), 7.34 (d, J = 7.9 Hz, 2H), 2.43 (s, 3H); **$^{13}C\{^{1}H\}$ NMR (151 MHz, Chloroform-*d*)** δ 151.47, 149.96, 140.69, 138.56, 131.65, 130.41, 127.03, 123.02, 21.44; **HRMS** (ESI) m/z calcd. for $C_{11}H_{11}N_2$ $[M+H]^+$: 171.0917, found: 171.0914.

4-(4-methoxyphenyl)pyridazine (22)

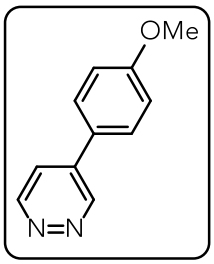

Yellow solid (30.0 mg, 80%); Purified by silica chromatography with EtOAc/*n*-hexane (4:1) eluent; **^{1}H NMR (600 MHz, Chloroform-*d*)** δ 9.45 – 9.41 (m, 1H), 9.15 (d, *J* = 5.4 Hz, 1H), 7.63 (d, *J* = 9.1 Hz, 2H), 7.59 (dd, *J* = 5.5, 2.5 Hz, 1H), 7.05 (d, *J* = 8.7 Hz, 2H), 3.87 (s, 3H); **$^{13}C\{^{1}H\}$ NMR (151 MHz, Chloroform-*d*)**

δ 161.52, 151.42, 149.74, 138.15, 128.48, 126.66, 122.50, 115.18, 55.60; **HRMS** (ESI) m/z calcd. for $C_{11}H_{11}N_2O$ $[M+H]^+$: 187.0866, found: 187.0864.

4-(4-(methylthio)phenyl)pyridazine (23)

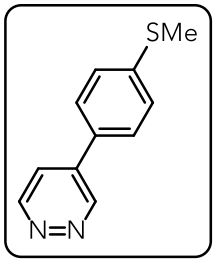

Yellow solid (25.0 mg, 62%); Purified by silica chromatography with EtOAc/*n*-hexane (4:1) eluent; **^{1}H NMR (600 MHz, Chloroform-*d*)** δ 9.44 (s, 1H), 9.19 (d, *J* = 5.4 Hz, 1H), 7.60 (dd, *J* = 8.5, 2.1 Hz, 3H), 7.38 (d, *J* = 8.0 Hz, 2H), 2.54 (s, 3H); **^{13}C{^{1}H} NMR (151 MHz, Chloroform-*d*)** δ 151.51, 149.70, 142.31, 137.98, 130.73, 127.38, 126.85, 122.73, 15.33; **HRMS** (ESI) m/z calcd. for $C_{11}H_{11}N_2S$ $[M+H]^+$: 203.0637, found: 203.0636.

4-(4-fluorophenyl)pyridazine (24)

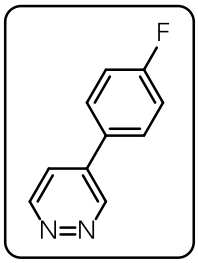

Yellow solid (12.3 mg, 35%); Purified by silica chromatography with EtOAc/*n*-hexane (4:1) eluent; **^{1}H NMR (600 MHz, Chloroform-*d*)** δ 9.42 (dd, *J* = 2.6, 1.2 Hz, 1H), 9.21 (dd, *J* = 5.4, 1.2 Hz, 1H), 7.69 – 7.63 (m, 2H), 7.61 (dd, *J* = 5.4, 2.5 Hz, 1H), 7.23 (appt, *J* = 8.5 Hz, 2H); **^{13}C{^{1}H} NMR (151 MHz, Chloroform-*d*)** δ 164.18 (d, *J* = 251.4 Hz), 151.50, 149.86, 137.66, 130.78 (d, *J* = 3.4 Hz), 129.17 (d, *J* = 8.7 Hz), 123.17, 116.90 (d, *J* = 22.0 Hz); **^{19}F NMR (377 MHz, Chloroform-*d*)** δ -110.28; **HRMS** (ESI) m/z calcd. for $C_{10}H_8FN_2$ $[M+H]^+$: 175.0666, found: 175.0662.

4-(4-(trifluoromethyl)phenyl)pyridazine (25)

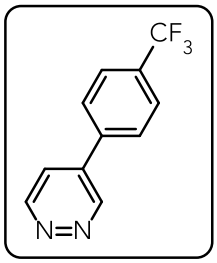

Orange solid (25.1 mg, 56%); Purified by silica chromatography with EtOAc/*n*-hexane (4:1) eluent; **^{1}H NMR (600 MHz, Chloroform-*d*)** δ 9.47 (dd, *J* = 2.5, 1.2 Hz, 1H), 9.29 (dd, *J* = 5.3, 1.2 Hz, 1H), 7.84 – 7.77 (m, 4H), 7.68 (dd, *J* = 5.3, 2.5 Hz, 4H); **^{13}C{^{1}H} NMR (151 MHz, Chloroform-*d*)** δ 151.64, 149.85, 138.30, 137.37, 132.25 (q, *J* = 32.9 Hz), 127.76, 126.68 (q, *J* = 3.7 Hz), 123.83 (q, *J* = 272.2 Hz),

123.73; **^{19}F NMR (471 MHz, Chloroform-*d*)** δ -62.88; **HRMS** (ESI) m/z calcd. for $C_{11}H_8F_3N_2$ $[M+H]^+$: 225.0634, found: 225.0633.

3-(pyridazin-4-yl)benzonitrile (26)

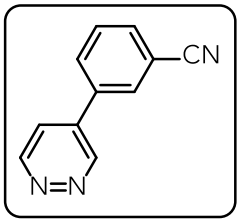

Orange solid (12.6 mg, 35%); Purified by silica chromatography with EtOAc/*n*-hexane (4:1) eluent; **^{1}H NMR (400 MHz, Chloroform-*d*)** δ 9.46 (s, 1H), 9.32 (d, *J* = 5.3 Hz, 1H), 7.96 (s, 1H), 7.91 (d, *J* = 7.9 Hz, 1H), 7.82 (d, *J* = 7.8 Hz, 1H), 7.70 (appt, *J* = 7.8 Hz, 1H), 7.66 (dd, *J* = 5.4, 2.5 Hz, 1H); **^{13}C{^{1}H} NMR (151 MHz, Chloroform-*d*)** δ 151.65, 149.58, 136.72, 136.17, 133.58, 131.51, 130.87, 130.72, 123.67, 117.97, 114.28; **HRMS** (ESI) m/z calcd. for $C_{11}H_8N_3$ $[M+H]^+$: 182.0713, found: 182.0709.

4-(pyridin-2-yl)pyridazine (27)

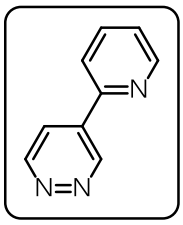

Yellow solid (28.0 mg, 89%); Purified by silica chromatography with EtOAc/*n*-hexane (8:1) eluent; **^{1}H NMR (600 MHz, Chloroform-*d*)** δ 9.80 (dt, *J* = 2.2, 1.0 Hz, 1H), 9.29 (dt, *J* = 5.4, 0.9 Hz, 1H), 8.80 – 8.75 (m, 1H), 8.07 (dd, *J* = 5.4, 2.4 Hz, 1H), 7.87 (dt, *J* = 5.2, 1.4 Hz, 2H), 7.44 – 7.37 (m, 1H); **^{13}C{^{1}H} NMR (151 MHz, Chloroform-*d*)** δ 151.85, 150.75, 149.29, 137.46, 136.59, 124.80, 123.09, 121.25; **HRMS** (ESI) m/z calcd. for $C_9H_8N_3$ $[M+H]^+$: 158.0713, found: 158.0710.

4-(pyrazin-2-yl)pyridazine (28)

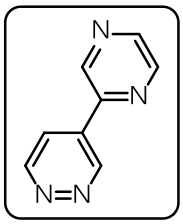

Brown solid (22.5 mg, 71%); Purified by silica chromatography with EtOAc/*n*-hexane (8:1) eluent; **^{1}H NMR (600 MHz, Chloroform-*d*)** δ 9.85 (s, 1H), 9.36 (d, *J* = 4.2 Hz, 1H), 9.17 (d, *J* = 3.2 Hz, 1H), 8.75 (d, *J* = 4.1 Hz, 1H), 8.70 (d, *J* = 3.5 Hz, 1H), 8.09 (dq, *J* = 5.3, 2.5 Hz, 1H); **^{13}C{^{1}H} NMR (151 MHz, Chloroform-*d*)**

δ 151.90, 148.77, 147.68, 145.80, 145.15, 142.55, 134.01, 123.03; **HRMS** (ESI) m/z calcd. for $C_8H_7N_4$ $[M+H]^+$: 159.0665, found: 159.0661.

4-(naphthalen-2-yl)pyridazine (29)

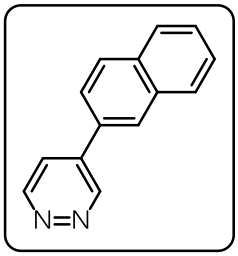

Yellow solid (31.0 mg, 75%); Purified by silica chromatography with EtOAc/*n*-hexane (4:1) eluent; **^{1}H NMR (600 MHz, Chloroform-*d*)** δ 9.60 (dd, *J* = 2.6, 1.2 Hz, 1H), 9.26 (dd, *J* = 5.4, 1.2 Hz, 1H), 8.17 (d, *J* = 1.9 Hz, 1H), 8.01 (d, *J* = 8.5 Hz, 1H), 7.98 – 7.93 (m, 1H), 7.93 – 7.87 (m, 1H), 7.76 (ddd, *J* = 10.4, 7.0, 2.2 Hz, 2H), 7.61 – 7.55 (m, 2H); **^{13}C{^{1}H} NMR (151 MHz, Chloroform-*d*)** δ 151.55, 150.23, 138.64, 133.94, 133.52, 131.84, 129.71, 128.69, 127.96, 127.68, 127.27, 127.20, 123.98, 123.54; **HRMS** (ESI) m/z calcd. for $C_{14}H_{11}N_2$ $[M+H]^+$: 207.0917, found: 207.0916.

3-phenylpyridazine (30)

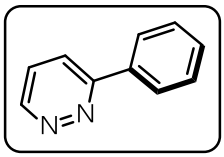

The yield is determined by ^{1}H NMR because of the instability of the product (35%, ^{1}H NMR yield); **^{1}H NMR (600 MHz, Chloroform-*d*)** δ 9.21 – 9.17 (m, 1H), 8.12 – 8.06 (m, 2H), 7.92 (dd, *J* = 8.5, 1.6 Hz, 1H), 7.60 (dd, *J* = 8.6, 4.9 Hz, 1H), 7.57 – 7.50 (m, 3H); NMR spectroscopic signatures are matched with that of the previously reported ones[18].

3-(pyridin-2-yl)pyridazine (31)

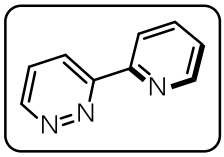

Brown solid (12.6 mg, 40%); Purified by silica chromatography with EtOAc/*n*-hexane (8:1) eluent; **^{1}H NMR (600 MHz, Chloroform-*d*)** δ 9.21 (dd, *J* = 5.0, 1.7 Hz, 1H), 8.86 – 8.66 (m, 2H), 8.57 (dd, *J* = 8.5, 1.7 Hz, 1H), 7.89 (td, *J* = 7.8, 1.8 Hz, 1H), 7.61 (dd, *J* = 8.5, 4.9 Hz, 1H), 7.41 (ddd, *J* = 7.5, 4.8, 1.2 Hz, 1H); **^{13}C{^{1}H} NMR (151 MHz, Chloroform-*d*)** δ 158.80, 153.62, 151.34, 149.54, 137.39, 127.16, 124.95, 124.62, 121.80; NMR spectroscopic signatures are matched with that of the previously reported ones[18].

3-pentylpyridazine (32)

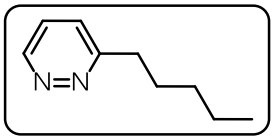

Yellow solid (13.2 mg, 44%); Purified by silica chromatography with EtOAc/*n*-hexane (3:1) eluent; **^{1}H NMR (600 MHz, Chloroform-*d*)** δ 9.04 (dd, *J* = 4.8, 1.7 Hz, 1H), 7.38 (dd, *J* = 8.4, 4.8 Hz, 1H), 7.32 (dd, *J* = 8.5, 1.7 Hz, 1H), 3.00 – 2.94 (m, 2H), 1.78 (dq, *J* = 9.4, 7.3 Hz, 2H), 1.36 (dq, *J* = 6.7, 3.4 Hz, 4H), 0.94 – 0.87 (m, 3H); **^{13}C{^{1}H} NMR (101 MHz, Chloroform-*d*)** δ 164.26, 149.67, 126.45, 126.30, 36.51, 31.56, 29.49, 22.57, 14.10; NMR spectroscopic signatures are matched with that of the previously reported ones[19].

ethyl 3-(pyridazin-3-yl)propanoate (33)

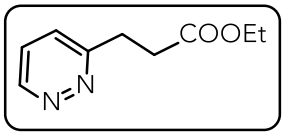

Yellow solid (11.5 mg, 32%); Purified by silica chromatography with EtOAc/*n*-hexane (2.5:1) eluent; **^{1}H NMR (600 MHz, Chloroform-*d*)** δ 9.07 (dd, *J* = 4.5, 2.1 Hz, 1H), 7.41 (appt, *J* = 3.3 Hz, 2H), 4.12 (q, *J* = 7.2 Hz, 2H), 3.28 (t, *J* = 7.2 Hz, 2H), 2.94 (t, *J* = 7.2 Hz, 2H), 1.23 (t, *J* = 7.2 Hz, 3H); **^{13}C{^{1}H} NMR (101 MHz, Chloroform-*d*)** δ 172.81, 162.26, 149.91, 127.13, 126.57, 60.78, 33.04, 31.26, 14.32; **HRMS** (ESI) m/z calcd. for $C_9H_{12}N_2O_2$ [M+H]$^+$: 181.0972, found: 181.0966.

2-(pyridazin-3-ylmethyl)isoindoline-1,3-dione (34)

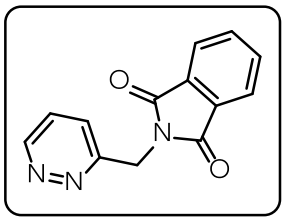

Yellow solid (16.2 mg, 34%); Purified by silica chromatography with EtOAc/*n*-hexane (4:1) eluent; **^{1}H NMR (600 MHz, Chloroform-*d*)** δ 9.11 (dd, *J* = 4.9, 1.7 Hz, 1H), 7.88 (dd, *J* = 5.4, 3.1 Hz, 2H), 7.75 (dd, *J* = 5.4, 3.0 Hz, 2H), 7.51 – 7.42 (m, 2H), 5.21 (s, 2H); **^{13}C{^{1}H} NMR (151 MHz, Chloroform-*d*)** δ 168.01, 157.81, 150.84, 134.38, 132.19, 126.89, 125.44, 123.76, 41.53; **HRMS** (ESI) m/z calcd. for $C_{13}H_9N_3O_2$ [M+H]$^+$: 240.0768, found: 240.0765.

3,6-diphenylpyridazine (35)

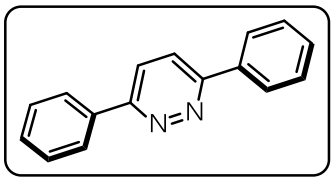

Yellow solid (12.0 mg, 26%); Purified by silica chromatography with EtOAc/*n*-hexane (3:1) eluent; **^{1}H NMR (600 MHz, Chloroform-*d*)** δ 8.19 – 8.14 (m, 4H), 7.94 (s, 2H), 7.62 – 7.47 (m, 6H); **^{13}C{^{1}H} NMR (151 MHz, Chloroform-*d*)** δ 157.78, 136.27, 130.19, 129.20, 127.09, 124.35; NMR spectroscopic signatures are matched with that of the previously reported ones[20].

4,5-diphenylpyridazine (4)

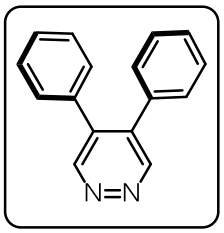

Yellow solid (38.5 mg, 83%); Purified by silica chromatography with EtOAc/*n*-hexane (1:1) eluent; **^{1}H NMR (600 MHz, Chloroform-*d*)** δ 9.18 (s, 2H), 7.32 (dt, J = 14.3, 7.0 Hz, 6H), 7.19 (d, J = 6.8 Hz, 4H); **^{13}C{^{1}H} NMR (151 MHz, Chloroform-*d*)** δ 152.02, 137.24, 134.70, 129.36, 128.94, 128.87; **HRMS** (ESI) m/z calcd. for $C_{16}H_{12}N_2$ $[M+H]^+$: 233.1073, found: 233.1072; Solid-state structure and its absolute configuration was characterized by X-ray diffraction analysis (CCDC 2554882).

4,5-di-*p*-tolylpyridazine (36)

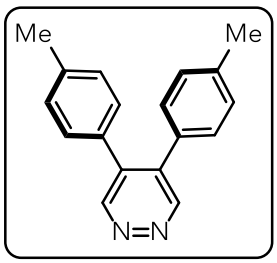

Yellow solid (44.0 mg, 85%); Purified by silica chromatography with EtOAc/*n*-hexane (3:1) eluent; **^{1}H NMR (600 MHz, Chloroform-*d*)** δ 9.15 (s, 2H), 7.16 – 7.10 (m, 8H), 2.36 (s, 6H); **^{13}C NMR (151 MHz, Chloroform-*d*)** δ 152.19, 139.06, 137.27, 132.03, 129.70, 129.33, 21.40; **HRMS** (ESI) m/z calcd. for $C_{18}H_{17}N_2$ $[M+H]^+$: 261.1386, found: 261.1391.

3-methyl-5-phenylpyridazine (37)

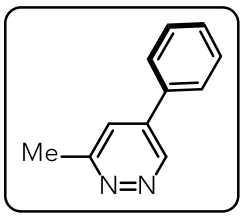

Yellow solid (14.7 mg, 43%); Purified by silica chromatography with EtOAc/*n*-hexane (4:1) eluent; **^{1}H NMR (600 MHz, Chloroform-*d*)** δ 9.30 (d, *J* = 2.2 Hz, 1H), 7.66 (dd, *J* = 8.2, 1.5 Hz, 2H), 7.56 – 7.47 (m, 4H), 2.79 (s, 3H); **^{13}C{^{1}H} NMR (151 MHz, Chloroform-*d*)** δ 160.17, 148.00, 138.67, 134.97, 130.09, 129.62, 127.25, 123.85, 22.56; **HRMS** (ESI) m/z calcd. for $C_{11}H_{11}N_2$ $[M+H]^+$: 171.0917, found: 171.0913.

Pyridazine (38)

0.2 mmol scale of $N_2H_4 \cdot HCl$ with 1.0 mmol of furan; The yield is determined by ^{1}H NMR because of volatility (46%, ^{1}H NMR yield); **^{1}H NMR (600 MHz, Chloroform-*d*)** δ 9.10 (d, *J* = 4.0 Hz, 2H), 7.50 – 7.45 (m, 2H); NMR spectroscopic signatures are matched with that of the previously reported ones[21].

2,5-dimethyl-1*H*-pyrrol-1-amine (39)

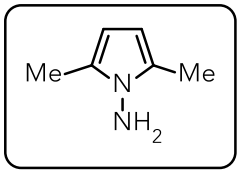

The yield is determined by ^{1}H NMR because of volatility (Yellow liquid, 64%, ^{1}H NMR yield); Purified by silica chromatography with EtOAc/*n*-hexane (1:9) eluent; **^{1}H NMR (600 MHz, Chloroform-*d*)** δ 5.71 (s, 2H), 4.20 (s, 2H), 2.24 (s, 6H); **^{13}C{^{1}H} NMR (151 MHz, Chloroform-*d*)** δ 128.12, 102.51, 11.73; NMR spectroscopic signatures are matched with that of the previously reported ones[22].

3,6-dimethylpyridazine (40)

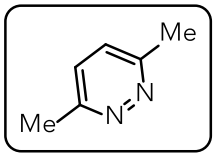

The yield is determined by ^{1}H NMR because of volatility (48%, ^{1}H NMR yield); **^{1}H NMR (600 MHz, Chloroform-*d*)** δ 7.16 (s, 2H), 2.51 (s, 6H); NMR spectroscopic signatures are matched with that of the previously reported ones[23].

(*R*)-4,7-dimethyl-5,6,7,8-tetrahydrocinnoline (41)

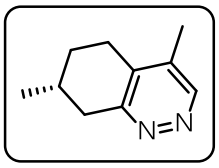

0.1 mmol scale of (+)-menthofuran with 16 mol % of **PC2** in 0.05 M of MeCN:H_2O (4:1); Yellow liquid (13.2 mg, 81%); Purified by basic alumina chromatography with EtOAc/*n*-hexane (1:4) eluent; **^{1}H NMR (500 MHz, Chloroform-*d*)** δ 8.73 (s, 1H), 3.24 (ddd, *J* = 17.2, 4.6, 2.1 Hz, 1H), 2.78 (ddd, *J* = 18.1, 5.8, 2.9 Hz, 1H), 2.68 – 2.54 (m, 2H), 2.19 (s, 3H), 2.05 – 1.87 (m, 2H), 1.42 (dtd, *J* = 13.2, 5.6, 2.2 Hz, 1H), 1.12 (d, *J* = 6.4 Hz, 3H); **^{13}C{^{1}H} NMR (126 MHz, Chloroform-*d*)** δ 159.27, 150.92, 135.36, 135.26, 38.63, 30.13, 28.65, 24.77, 21.60, 15.69; **HRMS** (ESI) m/z calcd. for $C_{10}H_{14}N_2$ $[M+H]^+$: 163.1230, found: 163.1232.

(2*S*,3a*R*,6*R*,6a*R*,7*S*,10*S*,11a*S*,11b*R*)-11b-methyl-2-(pyridazin-4-yl)octahydro-4*H*-3a,6:7,10-dimethanofuro[2,3-*c*]oxepino[4,5-*e*]oxepine-4,8(6*H*)-dione (42)

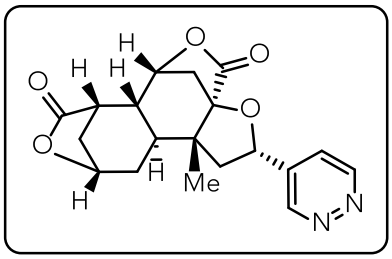

0.05 mmol scale of diosbulbin B with 16 mol % of **PC2**, and 1.0 equiv. of $Na_2S_2O_3 \cdot 5H_2O$ in 0.05 M of MeCN:H_2O (4:1); Yellow solid (10.0 mg, 56%); Purified by basic alumina chromatography with MeOH/CH_2Cl_2 (1:9) eluent; **^{1}H NMR (600 MHz, DMSO-*d*$_6$)** δ 9.10 (d, *J* = 1.9 Hz, 1H), 9.06 (d, *J* = 5.3 Hz, 1H), 7.51 (dd, *J* = 5.3, 2.3 Hz, 1H), 5.93 (s, 1H), 4.82 (t, *J* = 5.3 Hz, 1H), 4.65 (d, *J* = 5.6 Hz, 1H), 2.97 (ddd, *J* = 13.8, 11.8, 5.1 Hz, 1H), 2.69 – 2.60 (m, 2H), 2.35 (dt, *J* = 11.1, 5.5 Hz, 1H), 2.26 – 2.20 (m, 1H), 2.11 – 2.03 (m, 2H), 1.86 (d, *J* = 11.4 Hz, 1H), 1.65 (qt, *J* = 13.7, 6.7 Hz, 2H), 1.46 (d, *J* = 9.7 Hz, 1H), 1.07 (s, 3H); **^{13}C{^{1}H} NMR (151 MHz, DMSO-*d*$_6$)** δ 177.73, 176.28, 152.73, 151.11, 142.71, 125.91, 79.74, 77.08, 76.85, 42.22, 41.72, 40.95, 40.21, 38.31, 38.23, 34.50, 27.71, 27.68, 13.58; **HRMS** (ESI) m/z calcd. for $C_{19}H_{20}N_2O_5$ $[M+H]^+$: 357.1445, found: 357.1450.

(3*S*,8*S*,9*S*,10*R*,13*R*,14*S*,17*R*)-17-((*R*)-heptan-2-yl)-10,13-dimethyl-2,3,4,7,8,9,10,11,12,13,14,15,16,17-tetradecahydro-1*H*-cyclopenta[*a*]phenanthren-3-yl (3-phenyl-1*H*-pyrrol-1-yl) carbamate (43)

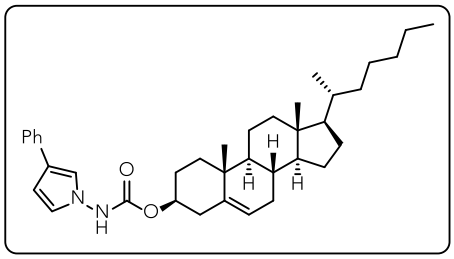

0.05 mmol scale of **1**; Yellow solid (14.8 mg, 52%); Purified by silica chromatography with EtOAc/*n*-hexane (1:19) eluent; **^{1}H NMR (600 MHz, Chloroform-*d*)** δ 7.52 – 7.45 (m, 2H), 7.33 (appt, *J* = 7.8 Hz, 3H), 7.22 – 7.14 (m, 1H), 6.98 (appt, *J* = 2.1 Hz, 1H), 6.72 (appt, *J* = 2.6 Hz, 1H), 6.45 (dd, *J* = 3.1, 1.9 Hz, 1H), 5.39 (dd, *J* = 5.1, 2.5 Hz, 1H), 4.69 – 4.58 (m, 1H), 2.37 (d, *J* = 42.1 Hz, 2H), 2.06 – 1.77 (m, 5H), 1.68 – 1.42 (m, 7H), 1.39 – 1.21 (m, 5H), 1.19 – 0.99 (m, 12H), 0.92 (d, *J* = 6.5 Hz, 3H), 0.87 (dd, *J* = 6.6, 2.8 Hz, 6H), 0.68 (s, 3H); **^{13}C{^{1}H} NMR (101 MHz, Chloroform-*d*)** δ 155.05, 139.41, 135.21, 128.74, 125.99, 125.32, 124.11, 123.22, 123.19, 118.88, 105.92, 56.81, 56.27, 50.10, 42.46, 39.85, 39.66, 38.36, 37.01, 36.67, 36.32, 35.94, 32.04, 31.99, 28.37, 28.16, 28.05, 24.43, 23.98, 22.97, 22.71, 21.19, 19.46, 18.86, 12.00; **HRMS** (ESI) m/z calcd. for $C_{37}H_{52}N_2O_2$ $[M+H]^+$: 571.4258, found: 571.4252.

(1*R*,2*S*,5*R*)-2-isopropyl-5-methylcyclohexyl (3-phenyl-1*H*-pyrrol-1-yl)carbamate (44)

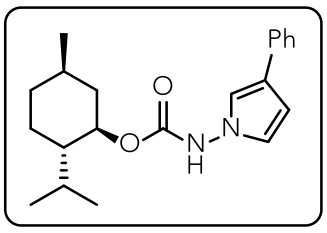

0.1 mmol scale of **1**; Yellow solid (31.3 mg, 92%); Purified by silica chromatography with EtOAc/*n*-hexane (1:9) eluent; **^{1}H NMR (600 MHz, Chloroform-*d*)** δ 7.48 (td, *J* = 4.6, 2.2 Hz, 2H), 7.41 (d, *J* = 4.0 Hz, 1H), 7.33 (td, *J* = 7.7, 4.2 Hz, 2H), 7.19 (dt, *J* = 11.0, 5.3 Hz, 1H), 6.97 (s, 1H), 6.70 (s, 1H), 6.44 (s, 1H), 4.67 (t, *J* = 11.2 Hz, 1H), 2.10 (d, *J* = 11.6 Hz, 1H), 1.91 (s, 1H), 1.67 (d, *J* = 12.7 Hz, 2H), 1.49 (s, 1H), 1.35 (s, 1H), 1.11 – 0.98 (m, 2H), 0.96 – 0.88 (m, 6H), 0.85 – 0.76 (m, 4H); **^{13}C{^{1}H} NMR (101 MHz, Chloroform-*d*)** δ 155.45, 135.23, 128.72, 125.95, 125.29, 124.02, 123.23, 118.90, 105.81, 47.23, 41.10, 34.21, 31.49, 26.47, 23.60, 22.11, 20.87, 16.60; **HRMS** (ESI) m/z calcd. for $C_{21}H_{28}N_2O_2$ $[M+H]^+$: 341.2224, found: 341.2221.

***N*-(3-phenyl-1*H*-pyrrol-1-yl)isonicotinamide (45)**

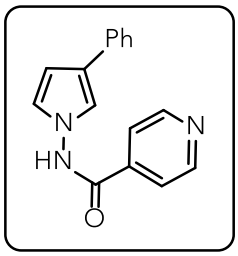

Yellow solid (43.7 mg, 83%); Purified by silica chromatography with EtOAc/*n*-hexane (9:1) eluent; **^{1}H NMR (600 MHz, Chloroform-*d*)** δ 10.69 (s, 1H), 8.90 – 8.37 (m, 2H), 7.64 – 7.49 (m, 2H), 7.45 – 7.32 (m, 2H), 7.28 (appt, *J* = 7.7 Hz, 2H), 7.20 – 7.11 (m, 1H), 6.87 (appt, *J* = 2.0 Hz, 1H), 6.60 (appt, *J* = 2.6 Hz, 1H), 6.51 – 6.37 (m, 1H); **^{13}C{^{1}H} NMR (151 MHz, Chloroform-*d*)** δ 165.40, 150.39, 138.82, 134.64, 129.75, 128.87, 127.17, 126.26, 125.07, 124.37, 122.54, 121.51, 118.04, 106.14; **HRMS** (ESI) m/z calcd. for $C_{16}H_{13}N_3O$ $[M+H]^+$: 263.1131, found: 263.1130; Solid-state structure and its absolute configuration was characterized by X-ray diffraction analysis (CCDC 2554885).

***N*-phenethyl-3-phenyl-1*H*-pyrrol-1-amine (46)**

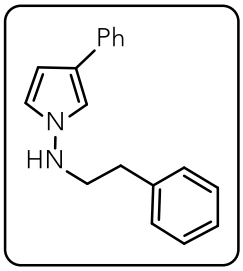

Yellow liquid (12.9 mg, 25%); Purified by silica chromatography with EtOAc/*n*-hexane (1:4) eluent; **^{1}H NMR (600 MHz, Chloroform-*d*)** δ 7.54 – 7.48 (m, 2H), 7.38 – 7.31 (m, 5H), 7.28 – 7.23 (m, 2H), 7.20 – 7.15 (m, 1H), 7.10 – 7.03 (m, 1H), 6.79 (q, *J* = 2.6 Hz, 1H), 6.40 (dd, *J* = 3.9, 2.2 Hz, 1H), 4.76 (s, 1H), 3.44 (t, *J* = 7.2 Hz, 2H), 2.84 (t, *J* = 7.1 Hz, 2H); **^{13}C{^{1}H} NMR (151 MHz, Chloroform-*d*)** δ 138.97, 135.78, 128.84, 128.77, 128.74, 126.64, 125.56, 125.01, 122.88, 121.43, 117.21, 104.36, 54.61, 34.30; **HRMS** (ESI) m/z calcd. for $C_{18}H_{18}N_2$ $[M+H]^+$: 263.1543, found: 263.1544.

IV. Computational Analysis

Computational method.

All calculations were carried out using density functional theory (DFT)[24] as implemented in the ORCA 6.0.0 quantum chemistry program package[25,26]. Transition state and ground state geometry optimizations were performed at the M06-2X/def2-SVP level of theory with TightSCF and TightOpt convergence criteria[27,28]. The RIJCOSX approximation was employed in conjunction with the def2/J auxiliary basis set to accelerate the Coulomb and exchange integral evaluations[29]. Solvation effects were incorporated at all stages of the calculation using the Conductor-like Polarizable Continuum Model (CPCM)[30] with acetonitrile as the solvent. All transition-state searches, geometry optimizations, frequency calculations, and single-point energy refinements were performed with CPCM(MeCN). Vibrational frequencies were computed at the same level of theory (M06-2X/def2-SVP/CPCM(MeCN)) to confirm the nature of the stationary points: all intermediates were verified by the absence of imaginary frequencies, while transition states exhibited a single imaginary frequency corresponding to the relevant bond-making or bond-breaking process. The electronic energies of optimized structures were refined by single-point calculations using the triple-ζ quality def2-TZVP basis set with TightSCF convergence[28].

$$G(sol) = H(sol) - TS(\text{sol})$$

$$H(\text{sol}) = E(\text{SCF}, \text{sol}) + H_{corr}$$

$$\Delta E(\text{SCF}, \text{sol}) = \sum E(\text{SCF}, \text{sol}) \text{ for products} - \sum E(\text{SCF}, \text{sol}) \text{ for reactants}$$

$$\Delta G(\text{sol}) = \sum G(\text{sol}) \text{for products} - \sum G(\text{sol}) \text{for reactants}$$

The energy components were computed using the protocol described above. Here, $E(\mathrm{SCF}, \mathrm{sol})$ denotes the solution-phase electronic energy obtained from CPCM calculations. H_{corr} denotes the thermal enthalpy correction obtained from the frequency calculation, including zero-point and thermal contributions. To properly model the reaction in solution, the standard-state conversion to the 1 M solution-phase state was also accounted for by including a concentration term of 0.082 eV in the individual species energies, consistent with the ORCA 6 manual.

Table S9. Computed energies of the optimized geometries.

Structure	***E*(sol) (SCF/TZ) [eV]** CPCM(MeCN) M06-2X/def2-TZVP	H_{corr} **(CPCM) [kcal/mol]** CPCM(MeCN) M06-2X/def2-SVP	**S(sol) [cal/mol •K]** CPCM(MeCN) M06-2X/def2-SVP	**G(sol) [eV]**
I	-15590.576	138.18	108.77	-15585.990
I_5-TS	-18634.686	175.240	121.72	-18628.661
II_5	-18634.745	176.140	120.71	-18628.668
II_5-TS	-18634.513	172.93	117.09	-18628.528
III_5	-15591.003	138.71	102.7	-15586.316
III_5-TS	-18646.992	182.47	123.09	-18640.671
IV_5	-13511.362	120.49	96.66	-13507.387
I_6-TS	-18634.744	175.66	119.34	-18628.670
II_6	-18634.857	176.39	117.83	-18628.731
II_6-TS	-18634.683	173.57	114.81	-18628.641
III_6	-15591.06	139.23	101.42	-15586.334
III_6-TS	-18647.131	183.29	118.19	-18640.711
IV_6	-13511.035	120.34	94.35	-13507.036
S1	-12540.134	100.85	90.520	-12536.931
S2	-15585.529	139.96	103.170	-15580.794
S3	-15573.482	130.78	103.000	-15569.143
II_5'	-15589.833	-	-	-15589.833
II_6'	-15590.22	-	-	-15590.220
II_5'' (∆E)	-15602.93	-	-	-15602.930
II_6'' (∆E)	-15603.155	-	-	-15603.155
II_5'' (∆G)	-15602.93	148.02	101.66	-15597.826
II_6'' (∆G)	-15603.155	148.55	100.22	-15598.009
SIII_5-TS	-18633.312	173.5	120.61	-18627.348
N_2H_4	-3044.101	35.78	56.41	-3043.279
$N_2H_5^+$	-3056.417	45.18	57.29	-3055.199
H_2O	-2079.873	15.18	45.11	-2079.798

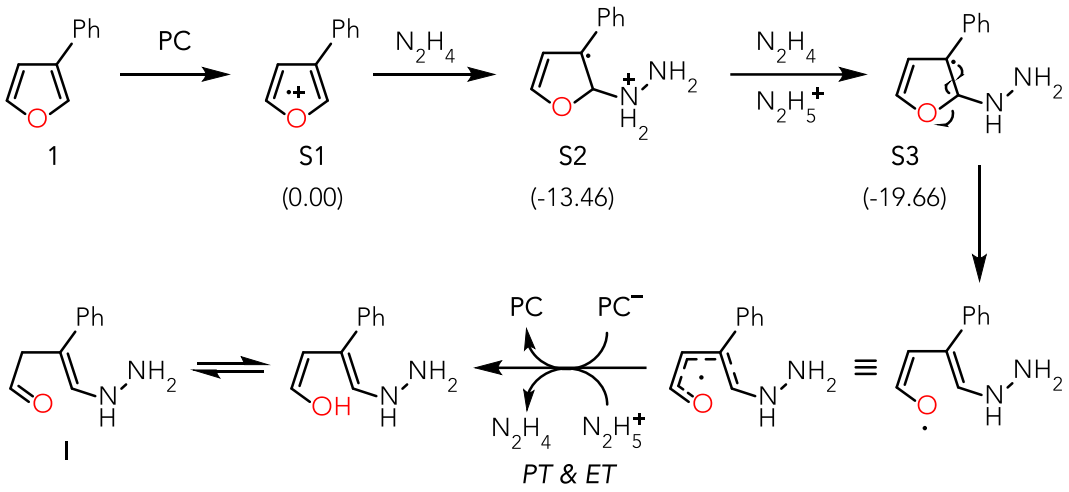

Figure S3. Possible pathway for hydrazinium salt formation from hydrazine.

The mechanism in **Figure S3** is proposed based on our previous work[4]. The possible formation of hydrazinium salts was considered as these species can promote the protonation of the hydroxy group, thereby facilitating water elimination in the dehydration step. The overall process is thermodynamically favorable by 19.7 kcal/mol; therefore, hydrazinium salts were incorporated into the main dehydration profile without an additional energetic penalty.

Hydrazinium salts are not required for the initial ring-closure and subsequent proton-transfer steps, as these transformations already proceed readily in their absence, consistent with the low barriers shown in the main profile.

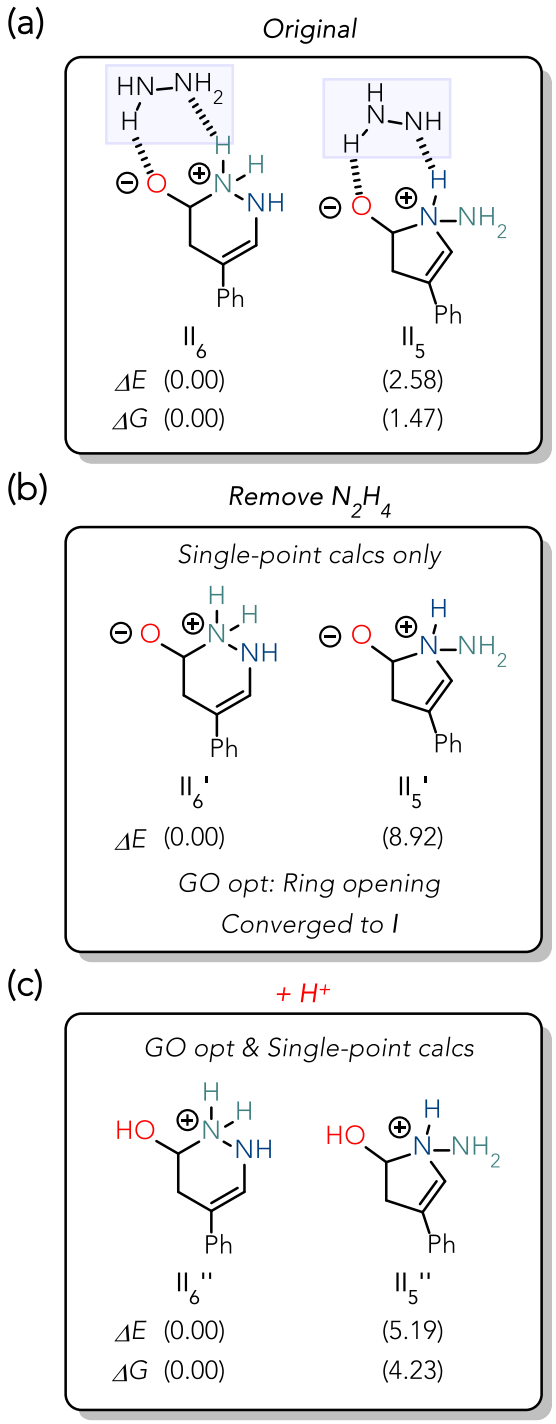

Figure S4. Evaluation of cyclized hydrazine-free zwitterionic intermediates (a) with N_2H_4, (b) without N_2H_4, and (c) with H^+. GO opt, geometry optimization.

To evaluate the origin of the energy difference between **II$_5$** and **II$_6$**, we recalculated the single-point energies after removing hydrazine from the original optimized structures (**Figure S4a,b**). The results show that **II$_5$′** is 8.9 kcal/mol less stable than the corresponding six-membered-ring intermediate **II$_6$′**. Upon geometry optimization, however, **II$_5$′** collapsed to intermediate **I**, indicating that the five-membered zwitterionic structure is intrinsically unstable and requires hydrazine assistance for stabilization. Even when this zwitterionic instability was avoided by artificially protonating the oxygen atom prior to geometry optimization, the six-membered structure (**II$_6$″**) remained more stable than the five-membered structure (**II$_5$″**) by approximately 5.2 kcal/mol (**Figure S4c**).

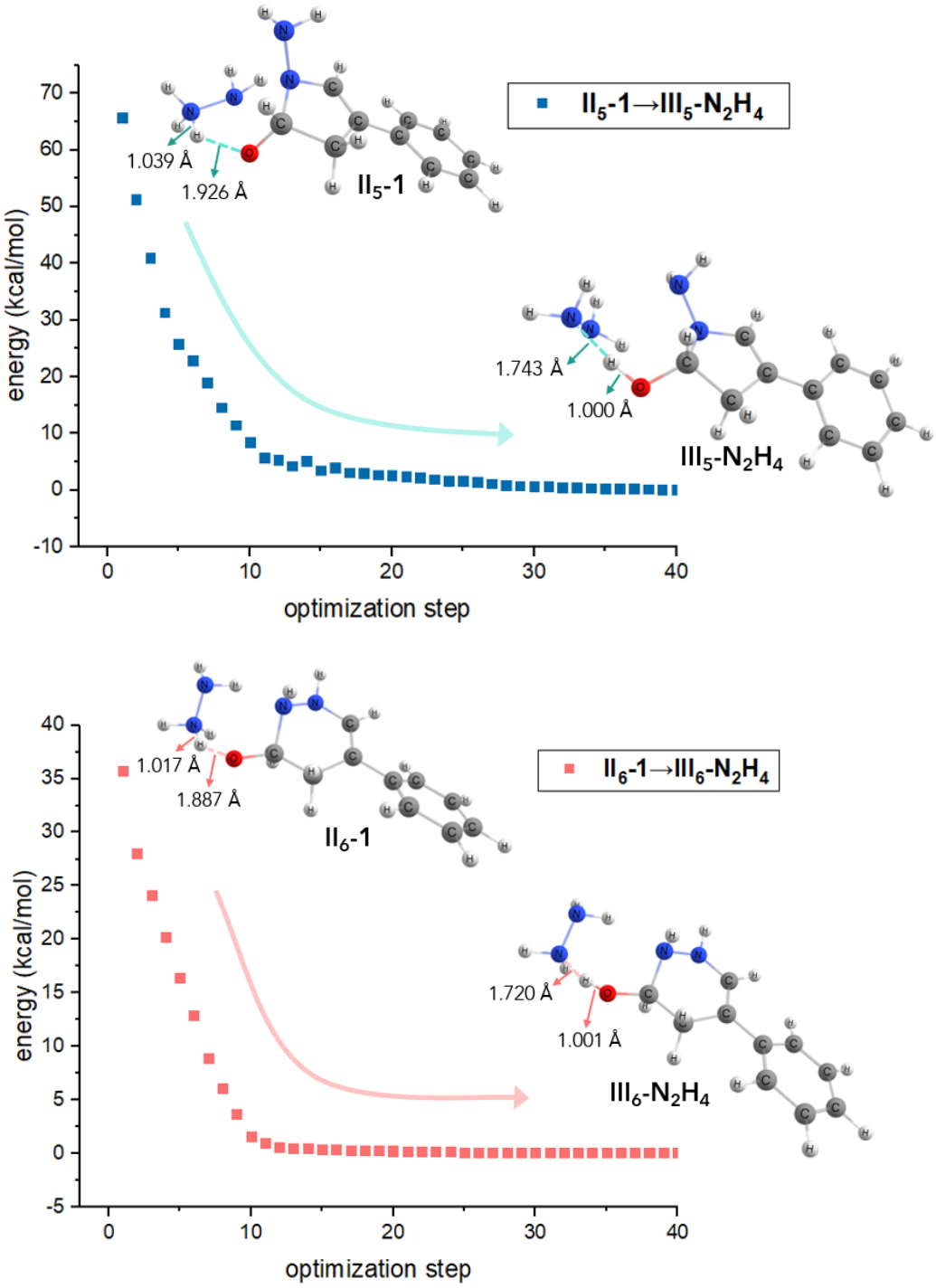

Figure S5. Results of structural conversion of **II_5-1** and **II_6-1** to **III_5-N_2H_4** and **III_6-N_2H_4** in geometry optimization.

Both **II_5-1** and **II_6-1** converged to **III_5-N_2H_4** and **III_6-N_2H_4**, respectively, during the geometry optimization.

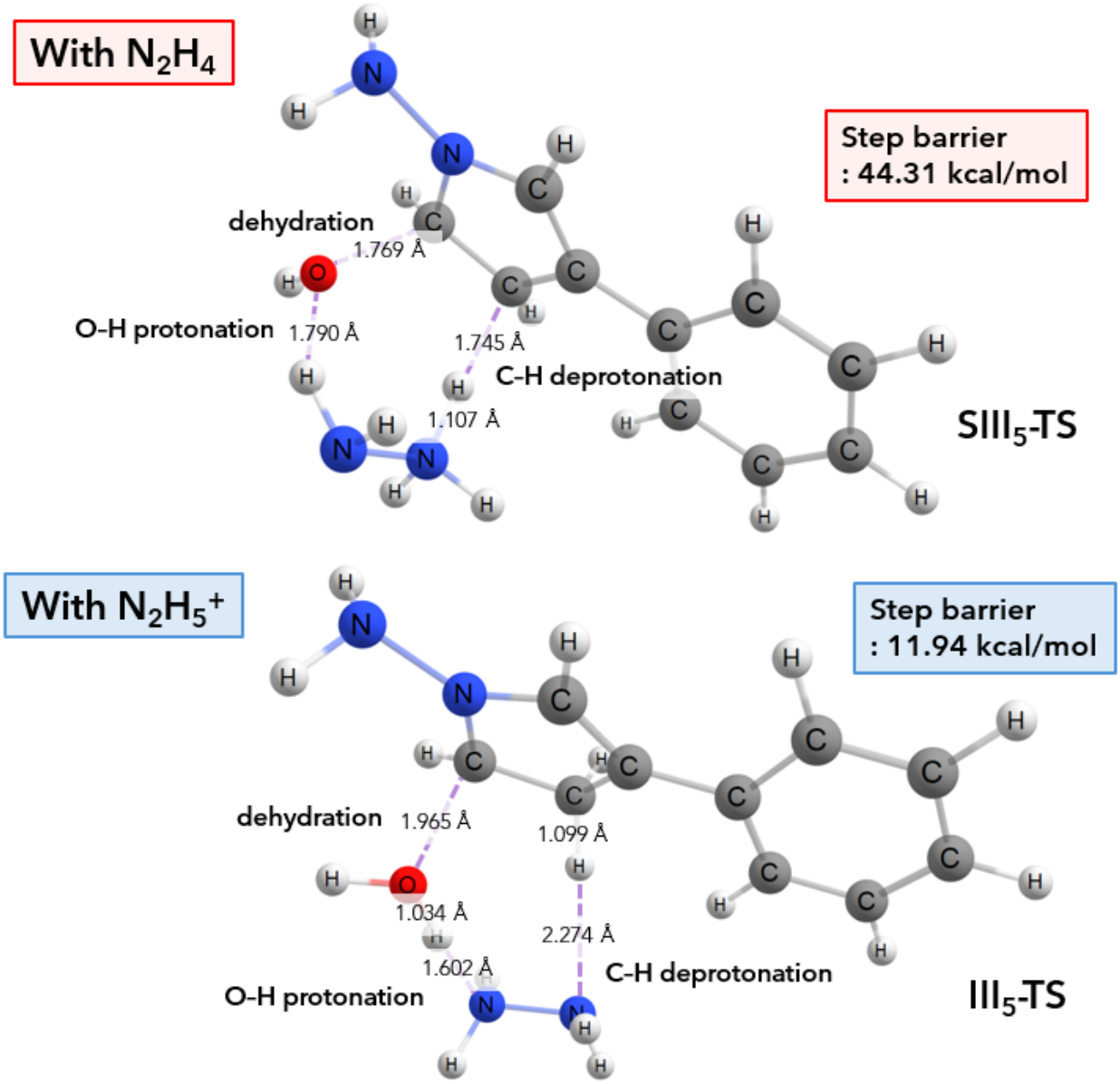

Figure S6. Comparison of dehydration step (**III_5** → **IV_5**) involving N_2H_4 (**$SIII_5$-TS**) and $N_2H_5^+$ (**III_5-TS**).

Acid assistance is required for the subsequent dehydration step (**III_5** → **IV_5**), as the calculated barrier decreases from 44.3 kcal/mol in the absence of acid assistance to 11.9 kcal/mol in the presence of hydrazinium salts.

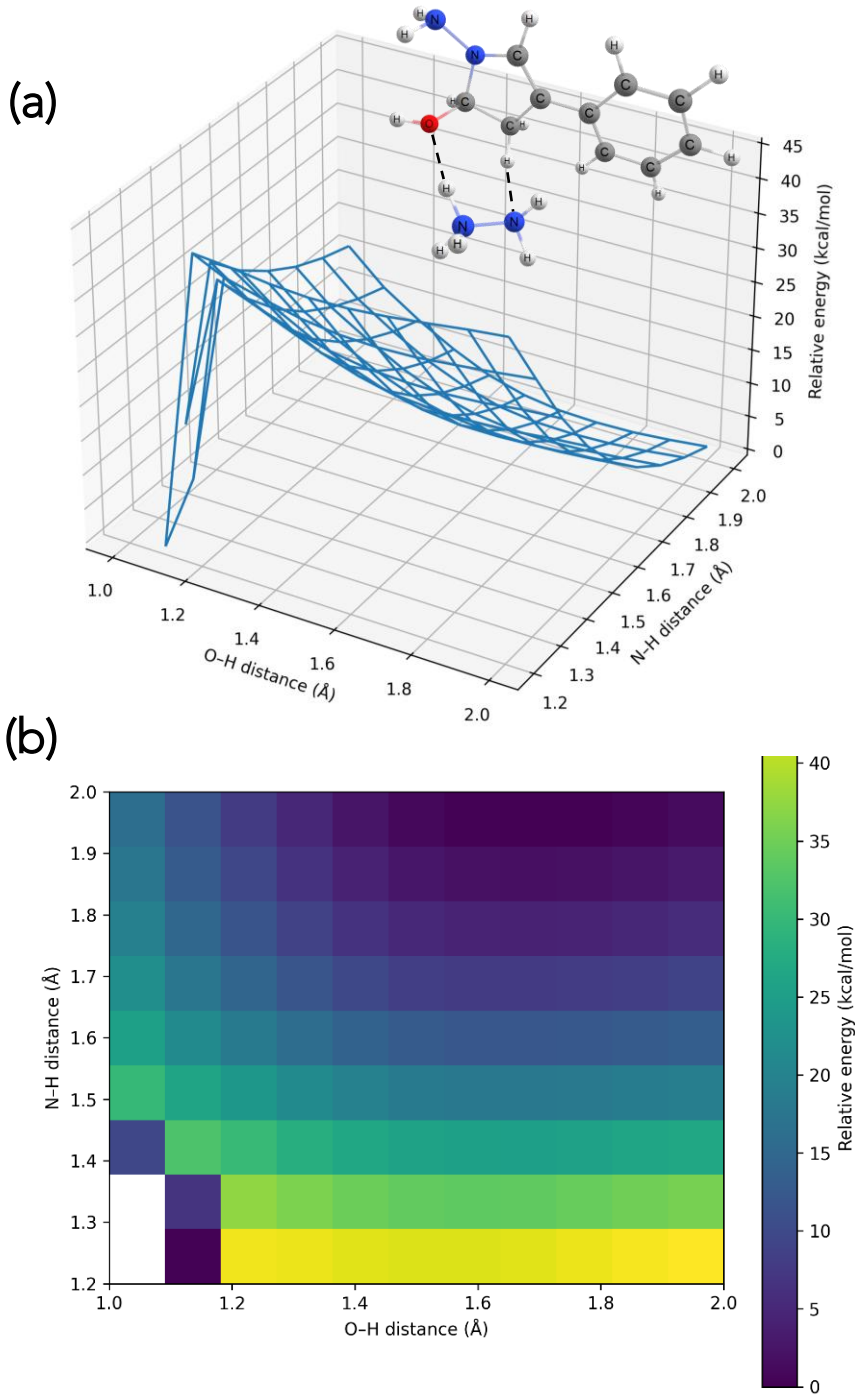

Figure S7. Validation of the dehydration transition-state assignment using two-dimensional relaxed scans. (a) 3D wireframe plot and (b) energy heatmap of the relaxed potential energy surface along the proton-transfer and water-elimination coordinates. The scans were performed using the LooseOpt keyword.

Two-dimensional relaxed scans were performed along the proton-transfer and water-elimination coordinates to examine the dehydration region (**Figure S7**). The resulting surfaces indicate that this region is highly sensitive to local electrostatic stabilization after water elimination, leading to abrupt stabilization in the product-like region rather than a smooth, well-separated concerted pathway. Concerted TS-like structures relaxed toward the corresponding stepwise intermediate upon further optimization. Therefore, the dehydration/proton-transfer sequence is best described as a stepwise dehydration process followed by rapid, essentially barrierless N–H deprotonation.

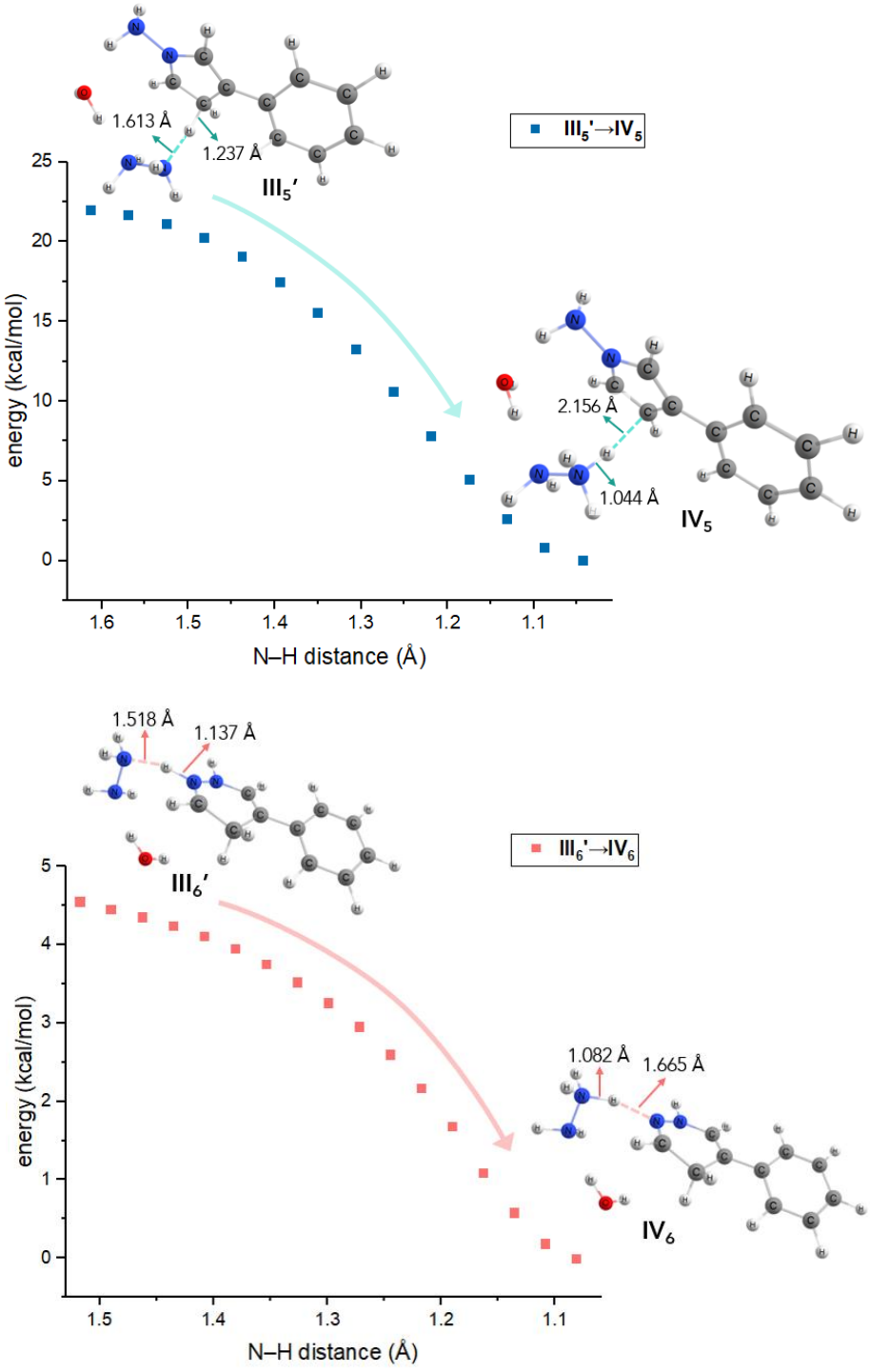

Figure S8. Potential energy surface (PES) scan of the conversion from **III$_5$′** and **III$_6$′** to **IV$_5$** and **IV$_6$**.

During the PES scan, **III$_5$′** and **III$_6$′** converged to **IV$_5$** and **IV$_6$**, respectively.

V. Mechanistic Studies

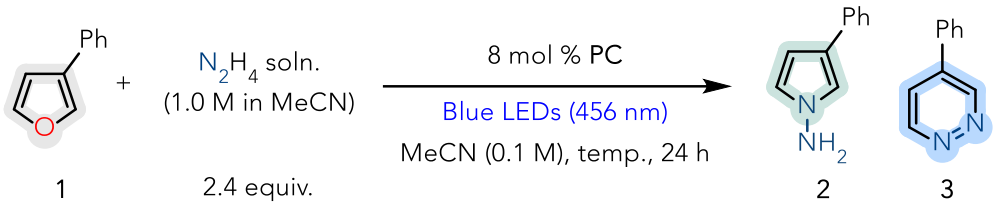

General procedure for the control experiments to determine ring topology. In an N_2-filled glovebox, 3-phenylfuran **1** (0.1 mmol, 1.0 equiv.), photocatalyst (0.008 mmol, 0.08 equiv.), and proper reagent were added to an oven-dried 4 mL vial. After the addition of the proper reagent, acetonitrile was added to the vial. A magnetic stir bar was charged, sealed with a screw cap and electrical tape, then removed from the glovebox. Under an N_2 atmosphere, hydrazine solution (1.0 M in MeCN) (0.24 mL, 2.4 equiv.) was added to the vial, and the mixture was stirred for 24 h under irradiation with Kessil™ PR160L 456 nm blue lamps (40 W, 100% intensity) using a household fan. After completion, about 10 mg of 1,3,5-trimethoxybenzene was added to the reaction mixture under an ambient atmosphere. Then, an aliquot of 0.05 mL of the resulting crude mixture was taken and directly transferred to an NMR tube. An additional 0.6 mL of $CDCl_3$ was added to the NMR cell, and the crude yield was analyzed by either 400 MHz or 500 MHz ^{1}H NMR spectroscopy using 1,3,5-trimethoxybenzene as an internal standard. The relaxation delay (d1), scan numbers (ns), and dummy scans (ds) were set to 20 seconds, 3 scans, and 1 scan, respectively, to accurately quantify the yield using ^{1}H NMR spectra.

Table S10. Control experiment for ring topology.

Entry	Photocatalyst	Temperature	^{1}H NMR Yield of **2** (%)	^{1}H NMR Yield of **3** (%)	Unreacted furan **1** (%)
1	**PC1**	23 °C	6	11	37
2	**PC2**	23 °C	7	44	0
3[a]	**PC1**	23 °C	0	13	75
4[a]	**PC2**	23 °C	0	48	0
5	**PC1**	80 °C	71	16	7
6	**PC2**	80 °C	69	21	0
7[a]	**PC1**	80 °C	31	32	6
8[a]	**PC2**	80 °C	4	28	36

[a] Use 1.0 equiv. of $Na_2S_2O_3 \cdot 5H_2O$ with MeCN:H_2O (4:1) as a solvent.

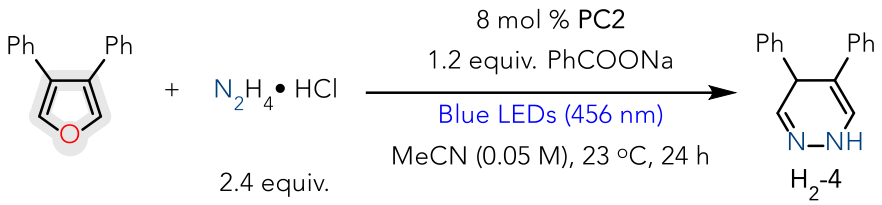

General procedure for the H_2-4 synthesis. In an N_2-filled glovebox, an oven-dried 4 mL vial was charged with 3,4-diphenyl furan (0.1 mmol, 1.0 equiv.), hydrazine monohydrochloride (0.24 mmol, 2.4 equiv.), and sodium benzoate (0.12 mmol, 1.2 equiv.), followed by 8 mol % of **PC2** (0.008 mmol, 0.08 equiv.). After the addition of the proper reagent, acetonitrile (2.0 mL) was added to the vial. A magnetic stir bar was charged, sealed with a screw cap and electrical tape, then removed from the glovebox. The reaction mixture was stirred for 24 h under irradiation at 23 °C with Kessil™ PR160L 456 nm blue lamps (40 W, 100% intensity) using a household fan. After completion, the crude mixture was concentrated under reduced pressure, then purified with silica gel flash column chromatography to afford the **H_2-4**.

4,5-diphenyl-1,4-dihydropyridazine (H_2-4)

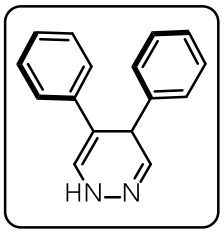

Light yellow solid (21.3 mg, 91%); Purified by silica chromatography with EtOAc/*n*-hexane (1:4) eluent; **^{1}H NMR (600 MHz, DMSO-*d*$_6$)** δ 9.57 (d, *J* = 3.9 Hz, 1H), 7.33 – 7.26 (m, 7H), 7.21 – 7.17 (m, 3H), 7.05 (t, *J* = 7.3 Hz, 1H), 6.71 (d, *J* = 4.3 Hz, 1H), 4.61 (d, *J* = 4.3 Hz, 1H); **^{13}C{^{1}H} NMR (151 MHz, DMSO-*d*$_6$)** δ 143.13, 137.68, 135.40, 128.78, 128.32, 127.21, 126.67, 125.62, 125.13, 123.38, 103.65; **HRMS** (ESI) m/z calcd. for $C_{16}H_{14}N_2$ $[M+H]^+$: 235.1230, found: 235.1238; Solid-state structure and its absolute configuration was characterized by X-ray diffraction analysis (CCDC 2554883).

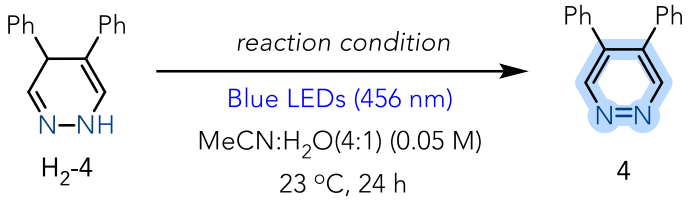

General procedure for the control experiments: synthesis of pyridazine 4 from H_2-4.

In an N_2-filled glovebox, **H_2-4** (0.03 mmol, 1.0 equiv.), and proper reagents were added to an oven-dried 4 mL vial. After the addition of the proper reagent, acetonitrile was added to the vial. A magnetic stir bar was charged, sealed with a screw cap and electrical tape, then removed from the glovebox. Under an N_2 atmosphere, degassed water (0.4 mL) was added to the vial, and the mixture was stirred for 24 h under irradiation at 23 °C with Kessil™ PR160L 456 nm blue lamps (40 W, 100% intensity) using a household fan. After completion, about 5 mg of 1,3,5-trimethoxybenzene was added to the reaction mixture under an ambient atmosphere. Then, an aliquot of 0.05 mL of the resulting crude mixture was taken and directly transferred to an NMR tube. An additional 0.6 mL of DMSO-d_6 was added to the NMR cell, and the crude yield was analyzed by either 400 MHz or 500 MHz ^{1}H NMR spectroscopy using 1,3,5-trimethoxybenzene as an internal standard. The relaxation delay (d1), scan numbers (ns), and dummy scans (ds)

were set to 20 seconds, 3 scans, and 1 scan, respectively, to accurately quantify the yield using ^{1}H NMR spectra.

Table S11. Control experiments for pyridazine synthesis

Entry	Deviation from optimal conditions	^{1}H NMR Yield of **4** (%)	Unreacted **H_2-4** (%)
1	none	99	0
2	MeCN	3	66
3	dark	0	99
4	8 mol % **PC2**	6	0
5	20 mol % $Na_2S_2O_3 \cdot 5H_2O$	80	27
6	8 mol % **PC2**, 20 mol % $Na_2S_2O_3 \cdot 5H_2O$	29	0

UV-Vis Absorption Analysis

General procedure for the UV-Vis measurement of H_2-4 and 4. Acetonitrile (CH_3CN) was used from SPS, followed by drying under 3 Å molecular sieves. All vials and quartz cells were dried in an oven prior to use. In an N_2-filled glovebox, 208, 104, 52, 26, and 13 μM of **H_2-4** and **4** solutions in acetonitrile are prepared and transferred to a custom-made fluorescence 10 mm cuvette cell with J-Young valves. The UV-Vis absorbance was measured with freshly made samples.

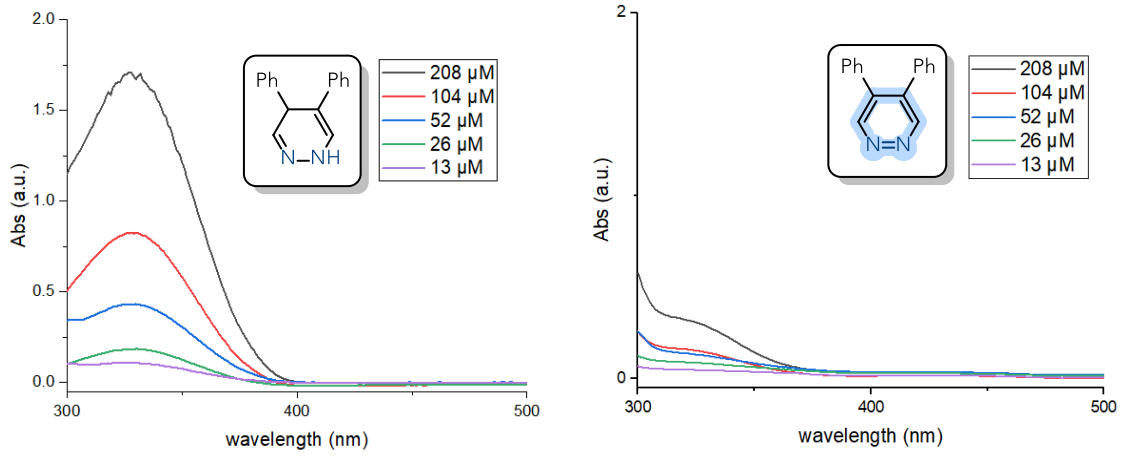

Figure S9. UV-vis absorption spectra of **H_2-4** (left) and **4** (right). *The sample was measured with a custom-made fluorescence 10 mm cuvette cell with J-Young valves in degassed acetonitrile.

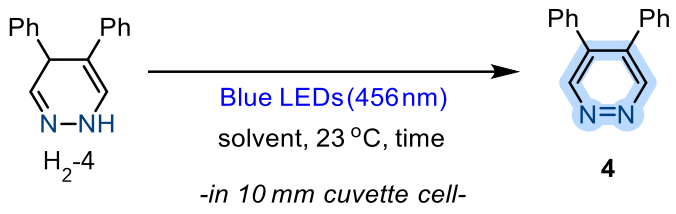

General procedure for the UV-Vis analysis of H_2-4 after irradiation. Acetonitrile (CH_3CN) was used from SPS, followed by drying under 3 Å molecular sieves. All vials and quartz cells were dried in an oven prior to use. In an N_2-filled glovebox, 104 μM of **H_2-4** solutions in acetonitrile are prepared and transferred to a custom-made fluorescence 10 mm cuvette cell with J-Young valves. Under an N_2 atmosphere, degassed water was added to a custom-made fluorescence 10 mm cuvette cell with J-Young valves, and the mixture was irradiated at 23 °C with Kessil™ PR160L 456 nm blue lamps (40 W, 100% intensity) using a household fan.

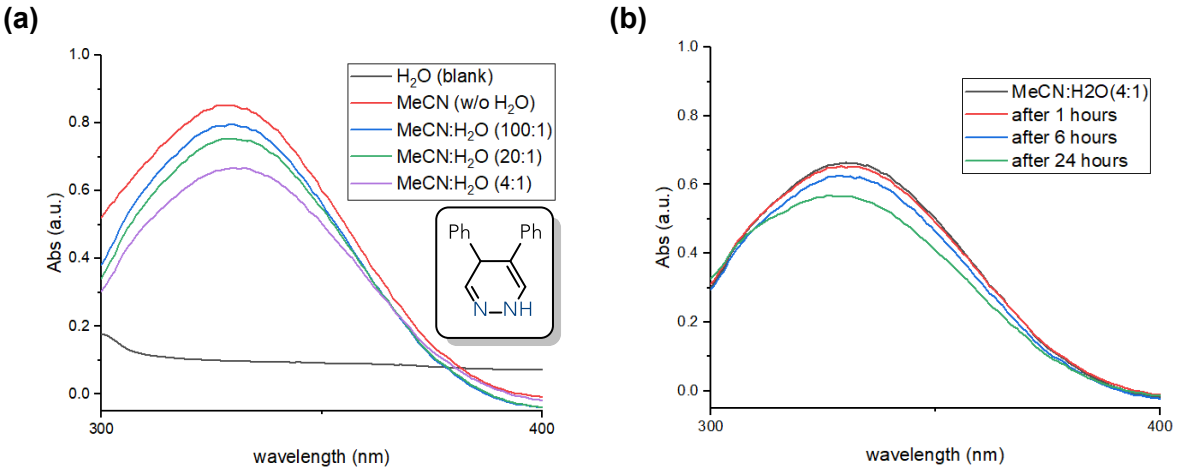

Figure S10. (a) UV-vis absorption spectra of **H_2-4** in MeCN, and MeCN:H_2O. (b) UV-vis absorption spectra of **H_2-4** in MeCN:H_2O (4:1) under 456 nm Blue LEDs irradiation in different time intervals. *The sample was measured with a custom-made fluorescence 10 mm cuvette cell with J-Young valves in degassed acetonitrile, and N_2-bubbled water.

VI. Crystallographic Data

1. Data for 2 (CCDC 2554884)

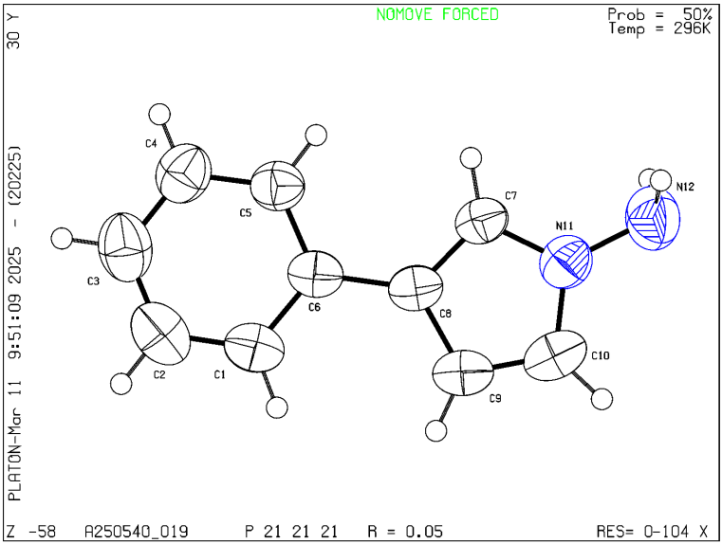

Figure S11. CheckCIF copy for **2**.

Table S12. Crystal data and structure refinement for **2**.

Empirical formula	C_{10} H_{10} N_2
Formula weight	158.20
Temperature	296(2) K
Wavelength	0.71073 Å
Crystal system	Orthorhombic
Space group	$P2_12_12_1$
Unit cell dimensions	a = 5.8167(4) Å b = 7.6196(6) Å c = 19.0009(16) Å α = 90 ° β = 90 ° γ = 90 °
Volume	842.14(11) $Å^3$
Z	4
Density (calculated)	1.248 Mg/m^3
Absorption coefficient	0.076 mm^{-1}
F(000)	336
Crystal size	0.089 x 0.056 x 0.022 mm^3
Theta range for data collection	2.880 to 28.063°.
Index ranges	–7<=h<=7, –10<=k<=10, –25<=l<=25
Reflections collected	12298
Independent reflections	2027 [R(int) = 0.0599]
Completeness to theta = 25.242°	99.1 %
Absorption correction	Semi-empirical from equivalents
Max. and min. transmission	0.7456 and 0.6787
Refinement method	Full-matrix least-squares on F^2
Data / restraints / parameters	2027 / 0 / 115
Goodness-of-fit on F^2	1.102
Final R indices [I>2sigma(I)]	R1 = 0.0531, wR2 = 0.0930
R indices (all data)	R1 = 0.1012, wR2 = 0.1113
Largest diff. peak and hole	0.106 and –0.135 $e·Å^{-3}$

2. Data for H_2-4 (CCDC 2554883)

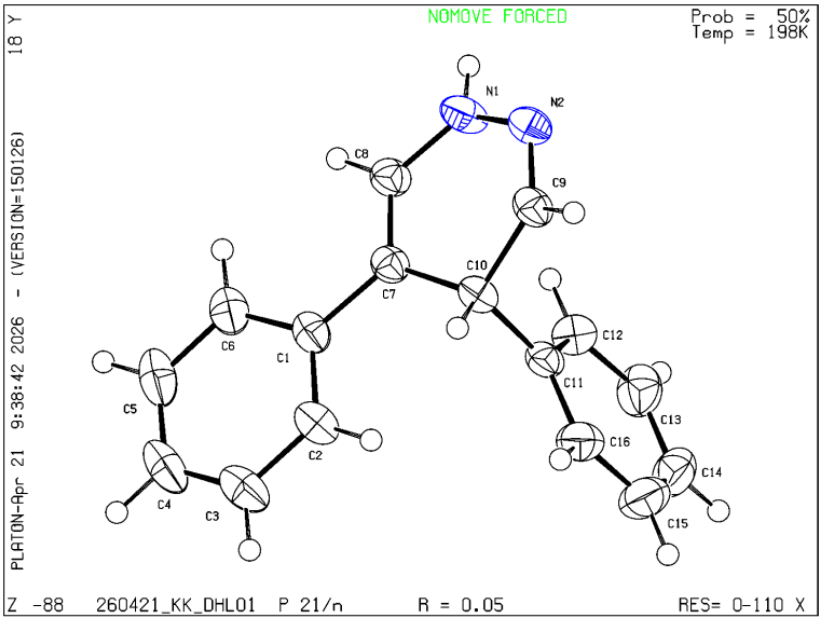

Figure S12. CheckCIF copy for **H_2-4** .

Table S13. Crystal data and structure refinement for **H_2-4** .

Empirical formula	C_{16} H_{14} N_2
Formula weight	234.29
Temperature	198(2) K
Wavelength	0.71073 Å
Crystal system	Monoclinic
Space group	$P2_1/n$
Unit cell dimensions	a = 13.9944(14) Å b = 5.6941(5) Å c = 16.6956(19) Å α = 90 ° β = 112.349(4) ° γ = 90 °
Volume	1230.5(2) Å^3
Z	4
Density (calculated)	1.265 Mg/m^3
Absorption coefficient	0.075 mm^{-1}
F(000)	496
Crystal size	0.170 x 0.080 x 0.060 mm^3
Theta range for data collection	2.407 to 26.430°.
Index ranges	–17<=h<=17, –7<=k<=7, –20<=l<=20
Reflections collected	38751
Independent reflections	2512 [R(int) = 0.1266]
Completeness to theta = 25.242°	100.0 %
Absorption correction	Semi-empirical from equivalents
Max. and min. transmission	0.7454 and 0.4800
Refinement method	Full-matrix least-squares on F^2
Data / restraints / parameters	2512 / 0 / 163
Goodness-of-fit on F^2	1.020
Final R indices [I>2sigma(I)]	R1 = 0.0462, wR2 = 0.1230
R indices (all data)	R1 = 0.0676, wR2 = 0.1456
Largest diff. peak and hole	0.240 and –0.280 e·Å^{-3}

3. Data for 4 (CCDC 2554882)

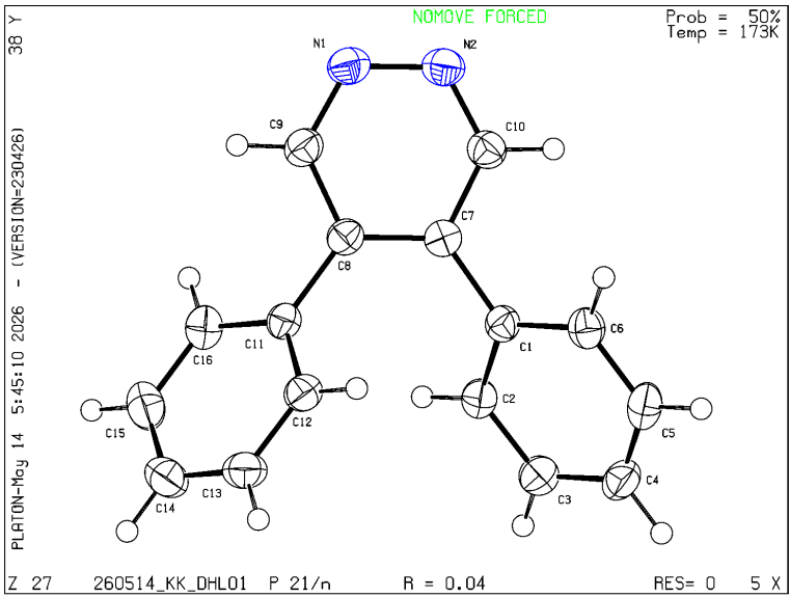

Figure S13. CheckCIF copy for **4**.

Table S14. Crystal data and structure refinement for **4**.

Empirical formula	$C_{16}H_{12}N_2$
Formula weight	232.28
Temperature	173(2) K
Wavelength	0.71073 Å
Crystal system	Monoclinic
Space group	$P2_1/n$
Unit cell dimensions	a = 6.5221(3) Å
	b = 12.6675(7) Å
	c = 14.7843(8) Å
	α = 90 °
	β = 100.902(2) °
	γ = 90 °
Volume	1199.41(11) $Å^3$
Z	4
Density (calculated)	1.286 Mg/m^3
Absorption coefficient	0.077 mm^{-1}
F(000)	488
Crystal size	0.150 x 0.070 x 0.070 mm^3
Theta range for data collection	2.806 to 26.401°.
Index ranges	–8<=h<=8, –15<=k<=15, –18<=l<=18
Reflections collected	28739
Independent reflections	2459 [R(int) = 0.0688]
Completeness to theta = 25.242°	99.9 %
Absorption correction	Semi-empirical from equivalents
Max. and min. transmission	0.7454 and 0.7094
Refinement method	Full-matrix least-squares on F^2
Data / restraints / parameters	2459 / 0 / 164
Goodness-of-fit on F^2	1.013
Final R indices [I>2sigma(I)]	R1 = 0.0357, wR2 = 0.1117
R indices (all data)	R1 = 0.0420, wR2 = 0.1210
Largest diff. peak and hole	0.184 and –0.159 $e·Å^{-3}$

4. Data for 45 (CCDC 2554885)

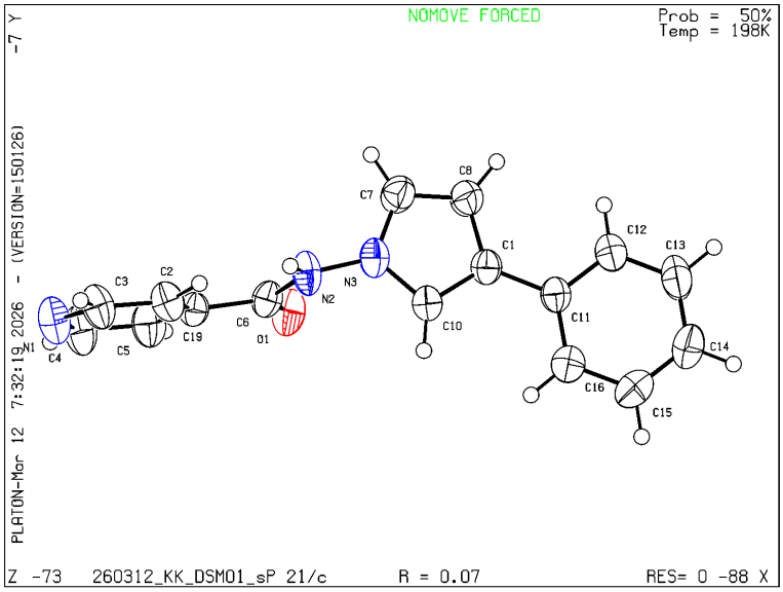

Figure S14. CheckCIF copy for **45**.

Table S15. Crystal data and structure refinement for **45**.

Empirical formula	$C_{16}H_{13}N_3O$
Formula weight	263.29
Temperature	198(2) K
Wavelength	0.71073 Å
Crystal system	Monoclinic
Space group	$P2_1/c$
Unit cell dimensions	a = 9.7927(6) Å b = 9.7276(7) Å c = 19.7920(14) Å α = 90 ° β = 103.471(2) ° γ = 90 °
Volume	1833.5(2) $Å^3$
Z	4
Density (calculated)	1.335 Mg/m^3
Absorption coefficient	0.506 mm^{-1}
F(000)	728
Crystal size	0.200 x 0.120 x 0.090 mm^3
Theta range for data collection	2.116 to 26.438°.
Index ranges	–12<=h<=11, –12<=k<=12, –24<=l<=24
Reflections collected	44124
Independent reflections	3779 [R(int) = 0.1043]
Completeness to theta = 25.242°	100.0 %
Absorption correction	Semi-empirical from equivalents
Max. and min. transmission	0.7454 and 0.5730
Refinement method	Full-matrix least-squares on F^2
Data / restraints / parameters	3779 / 0 / 184
Goodness-of-fit on F^2	1.042
Final R indices [I>2sigma(I)]	R1 = 0.0714, wR2 = 0.2372
R indices (all data)	R1 = 0.0926, wR2 = 0.2760
Largest diff. peak and hole	0.531 and –0.483 $e \cdot Å^{-3}$

VII. NMR Spectral Copies

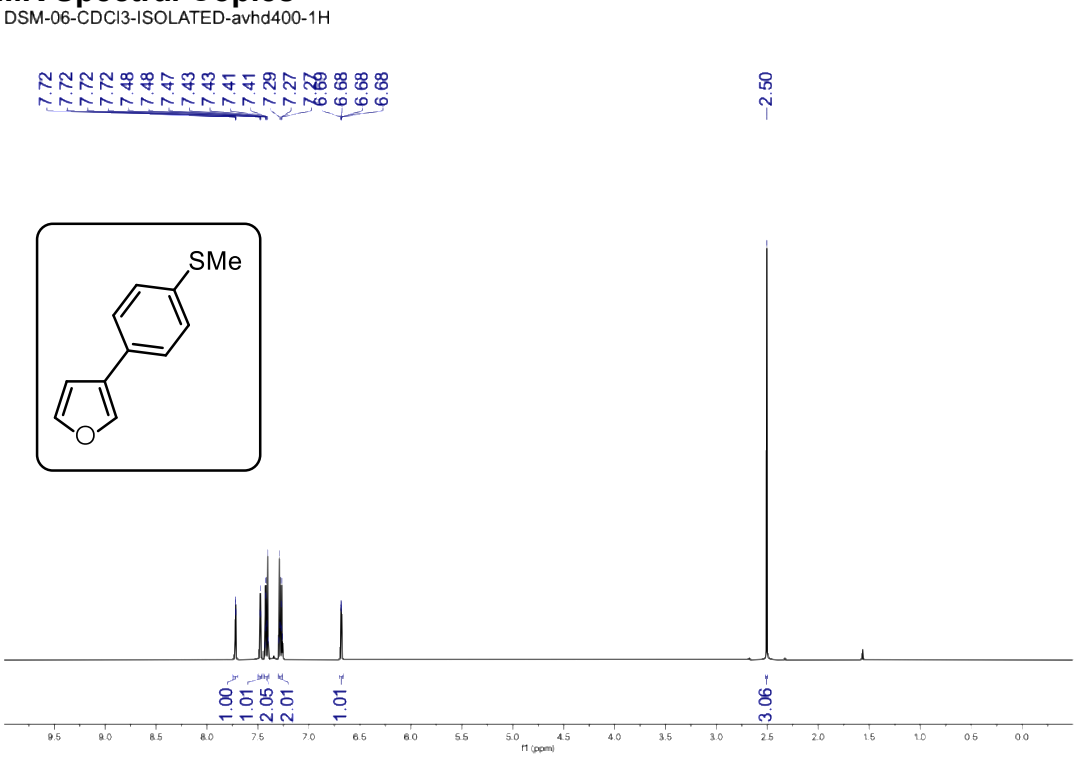

Figure S15. ^{1}H NMR spectrum of **3-(4-(methylthio)phenyl)furan** in $CDCl_3$ at 25 ^{o}C.

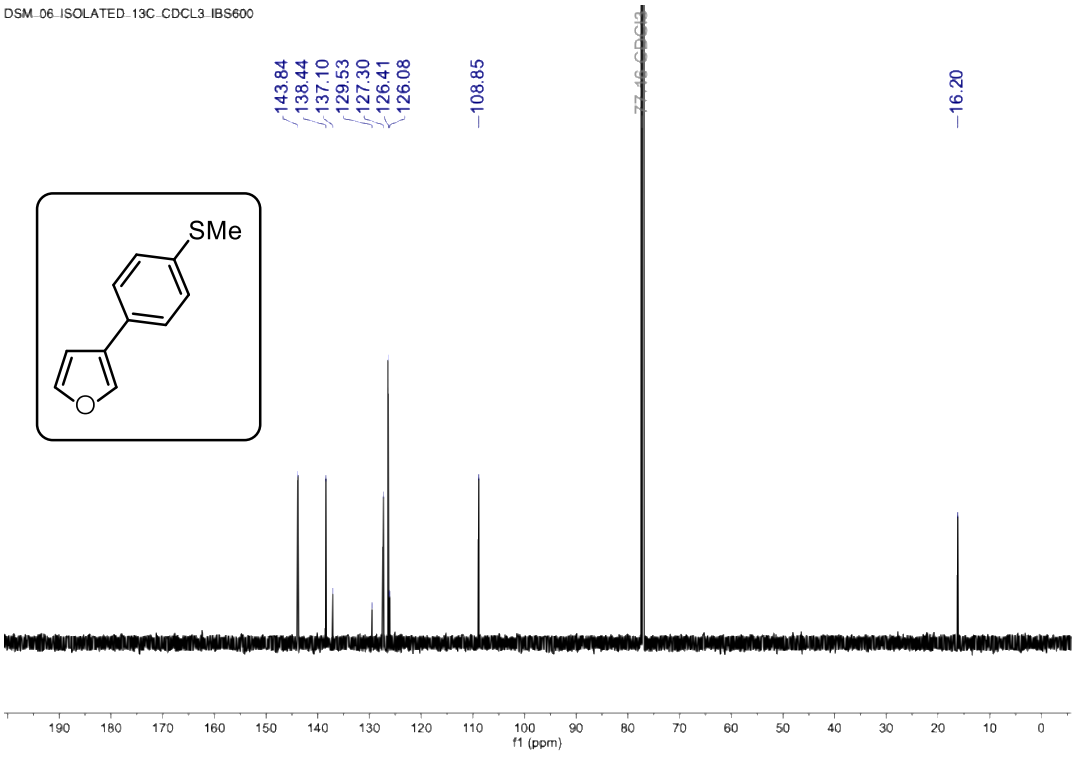

Figure S16. ^{13}C NMR spectrum of **3-(4-(methylthio)phenyl)furan** in $CDCl_3$ at 25 ^{o}C.

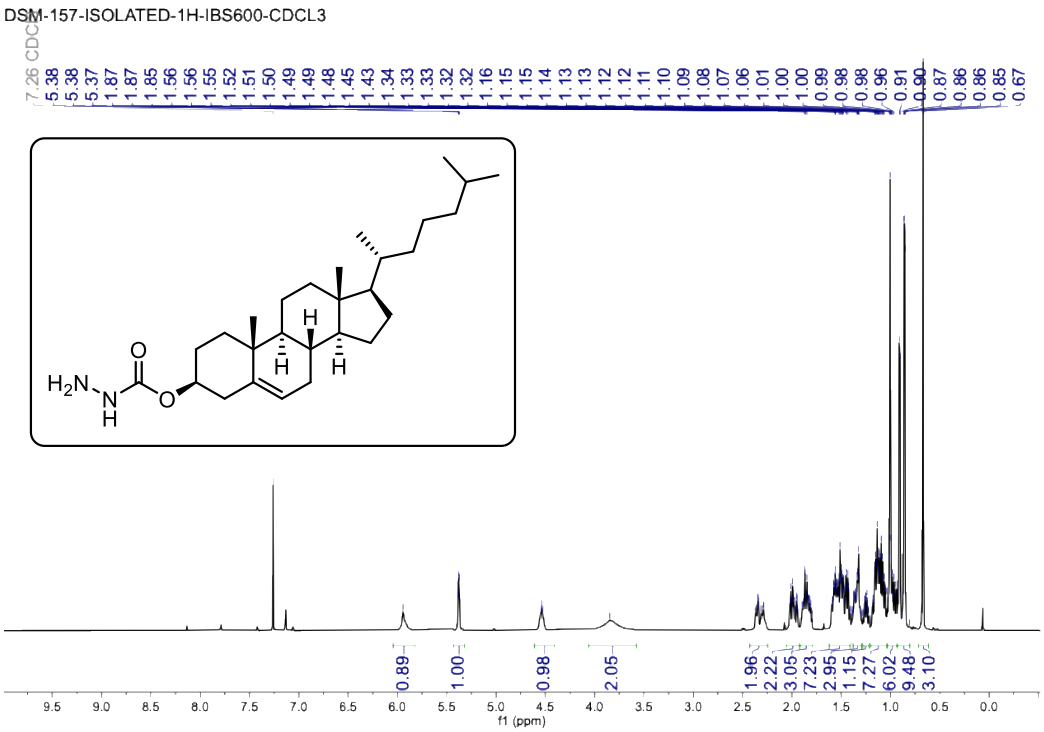

Figure S17. ^{1}H NMR spectrum of **(3*S*,8*S*,9*S*,10*R*,13*R*,14*S*,17*R*)-10,13-dimethyl-17-((*R*)-6-methylheptan-2-yl)-2,3,4,7,8,9,10,11,12,13,14,15,16,17-tetradecahydro-1*H*-cyclopenta[*a*] phenanthren-3-yl hydrazinecarboxylate** in $CDCl_3$ at 25 ºC.

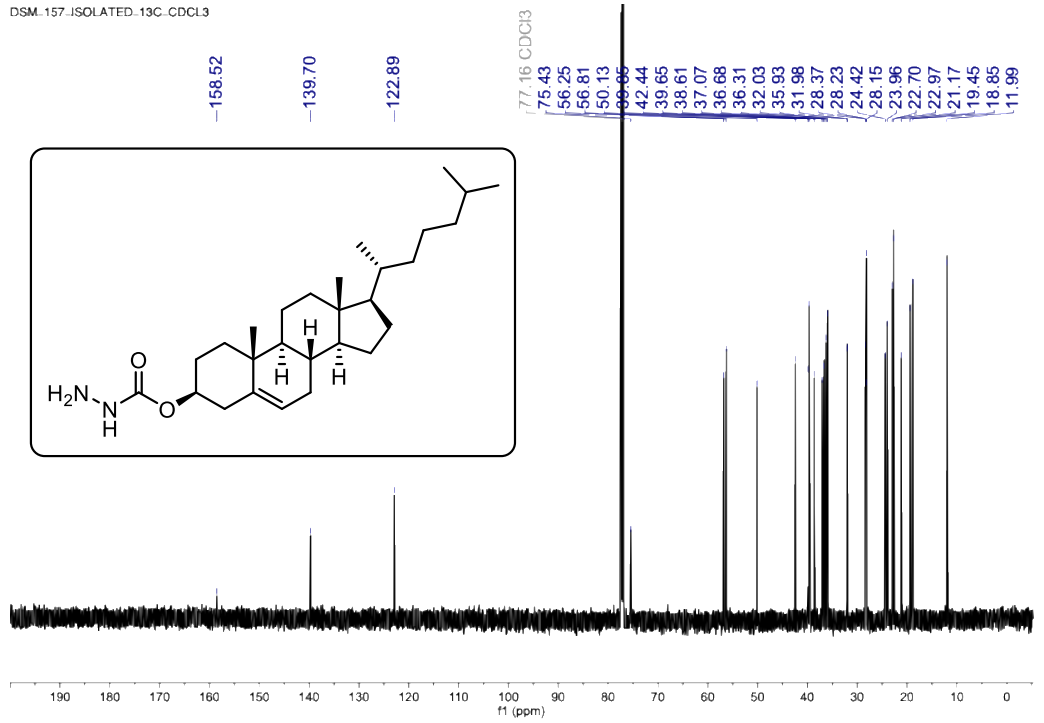

Figure S18. ^{13}C NMR spectrum of **(3*S*,8*S*,9*S*,10*R*,13*R*,14*S*,17*R*)-10,13-dimethyl-17-((*R*)-6-methylheptan-2-yl)-2,3,4,7,8,9,10,11,12,13,14,15,16,17-tetradecahydro-1*H*-cyclopenta[*a*] phenanthren-3-yl hydrazinecarboxylate** in $CDCl_3$ at 25 ºC.

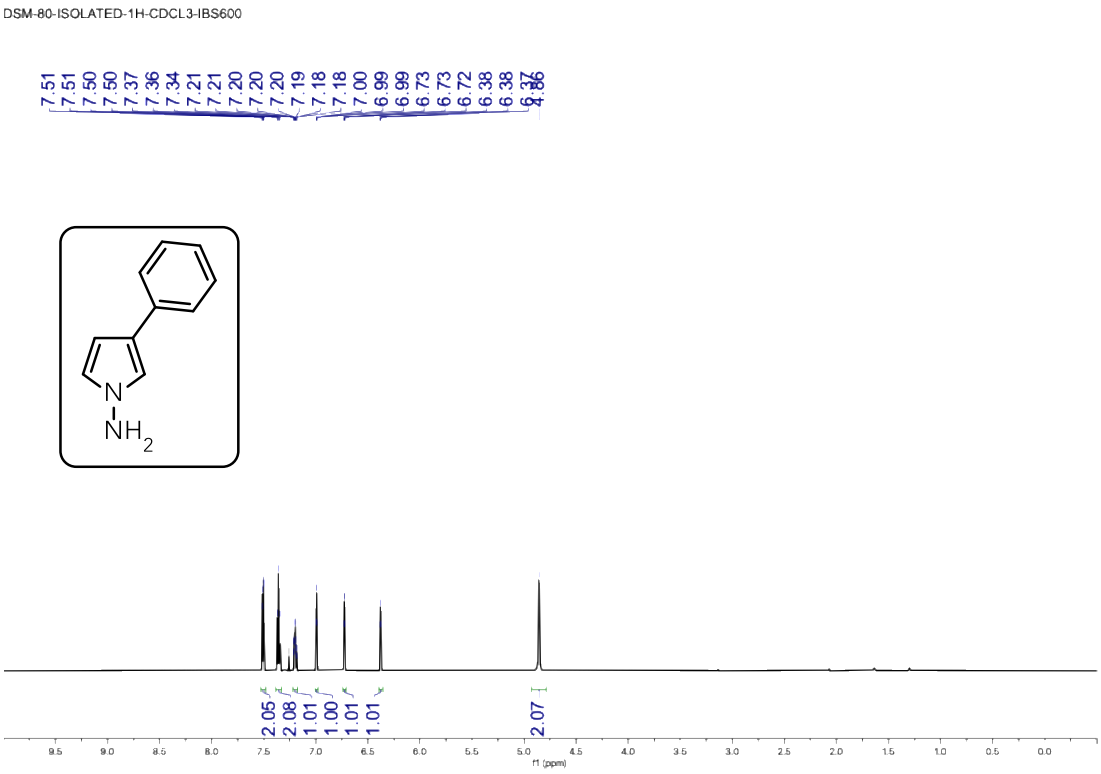

Figure S19. ^{1}H NMR spectrum of **2** in $CDCl_3$ at 25 ºC.

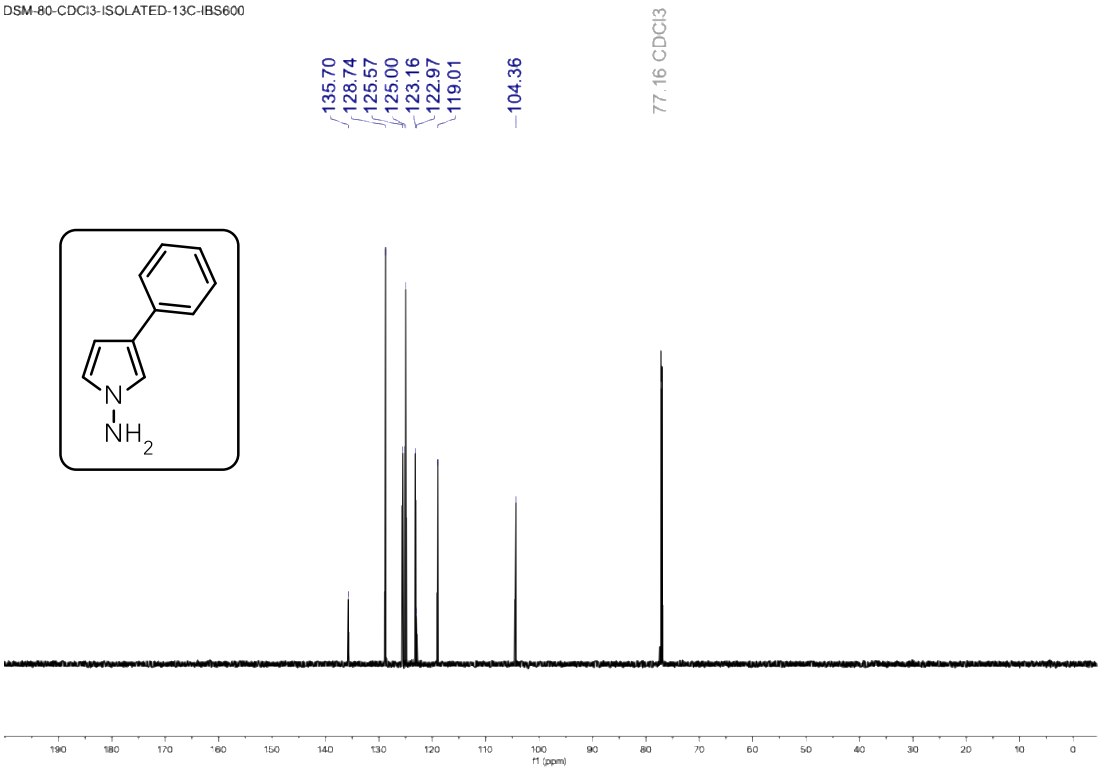

Figure S20. ^{13}C NMR spectrum of **2** in $CDCl_3$ at 25 ºC.

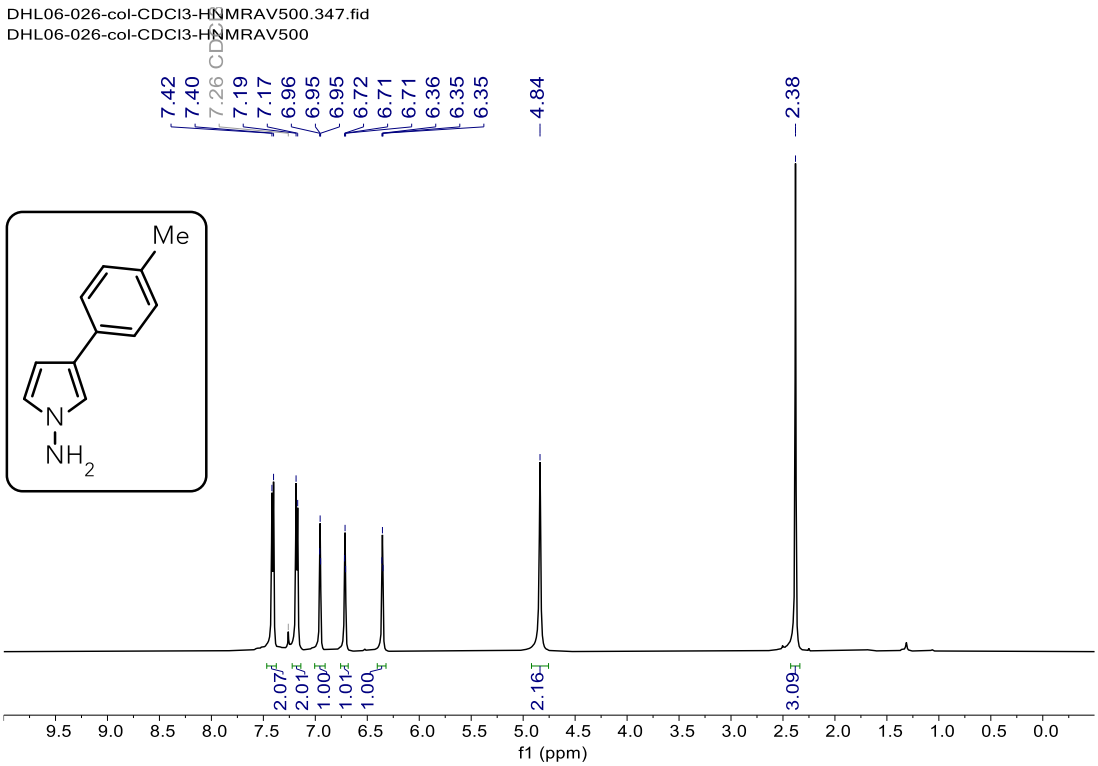

Figure S21. ^{1}H NMR spectrum of **5** in $CDCl_3$ at 25 ºC.

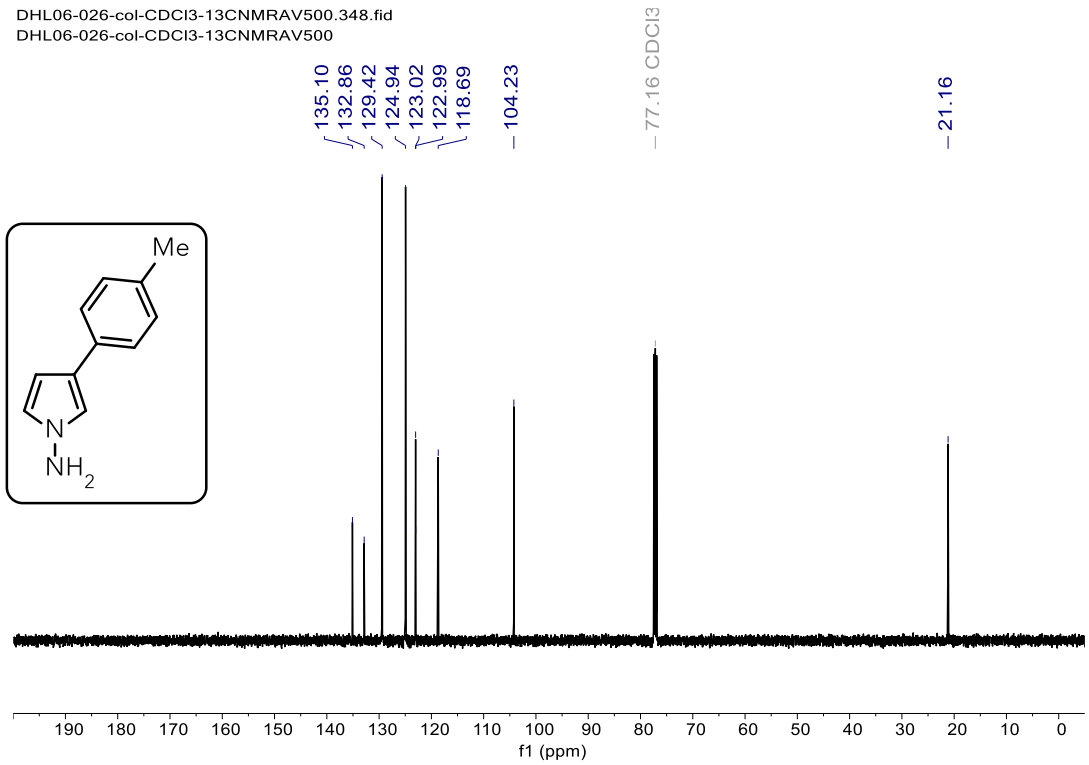

Figure S22. ^{13}C NMR spectrum of **5** in $CDCl_3$ at 25 ºC.

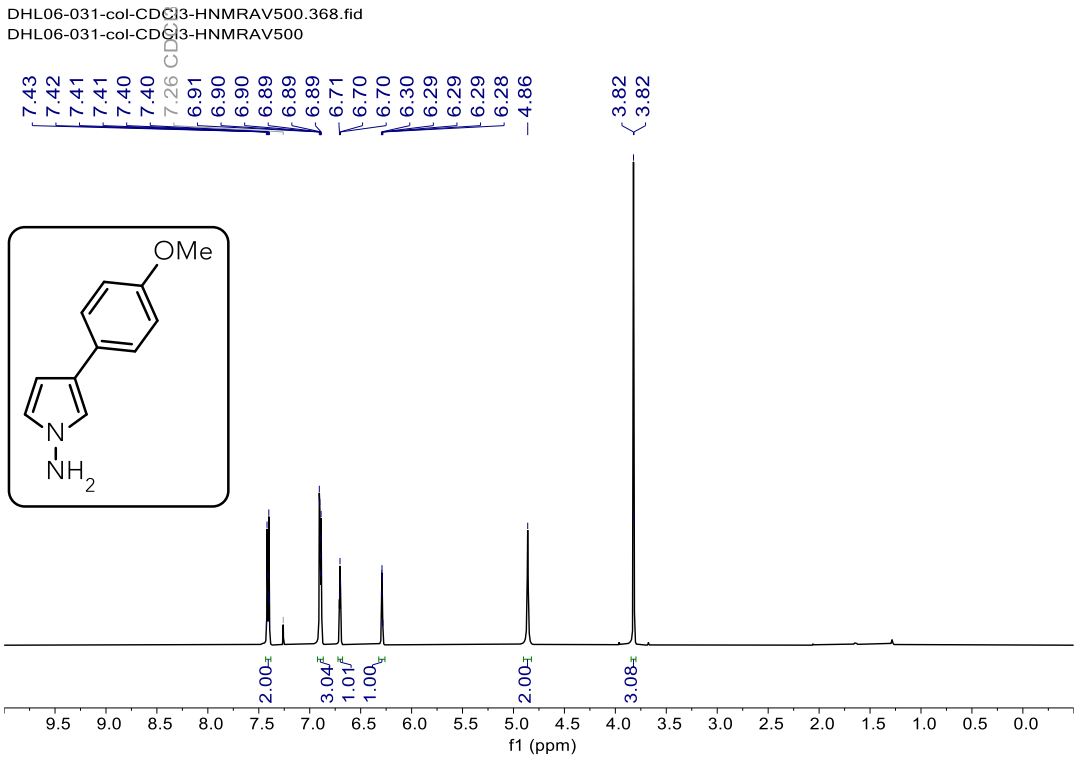

Figure S23. ^{1}H NMR spectrum of **6** in $CDCl_3$ at 25 ºC.

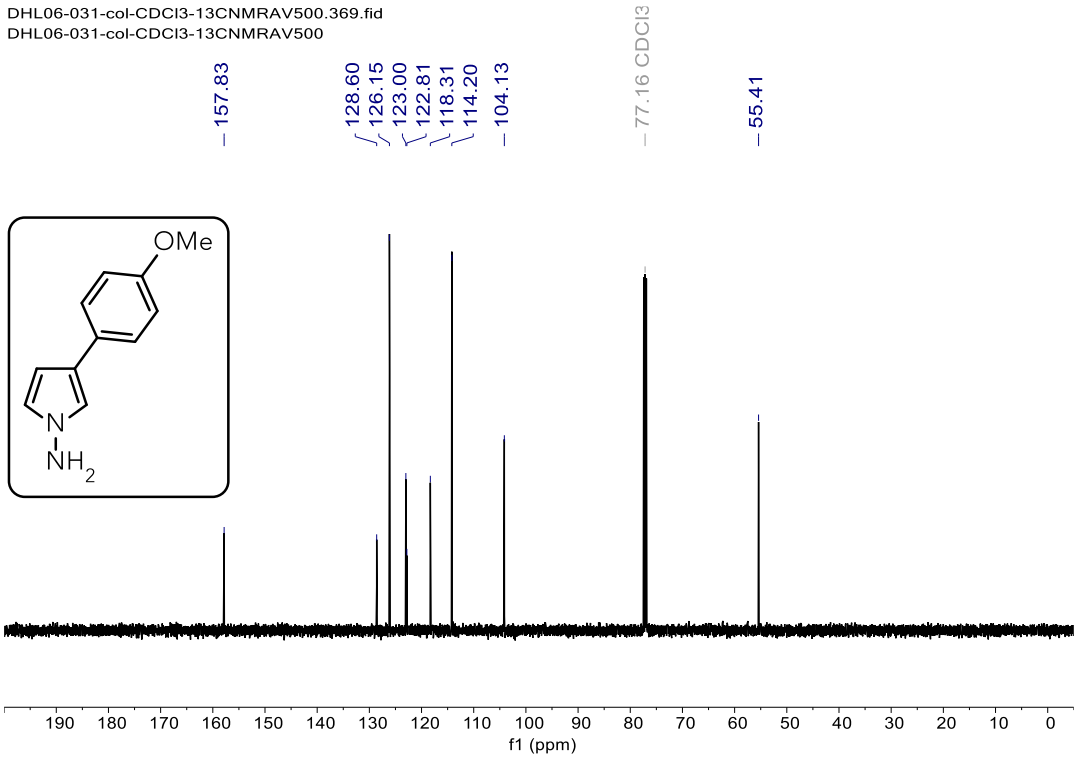

Figure S24. ^{13}C NMR spectrum of **6** in $CDCl_3$ at 25 ºC.

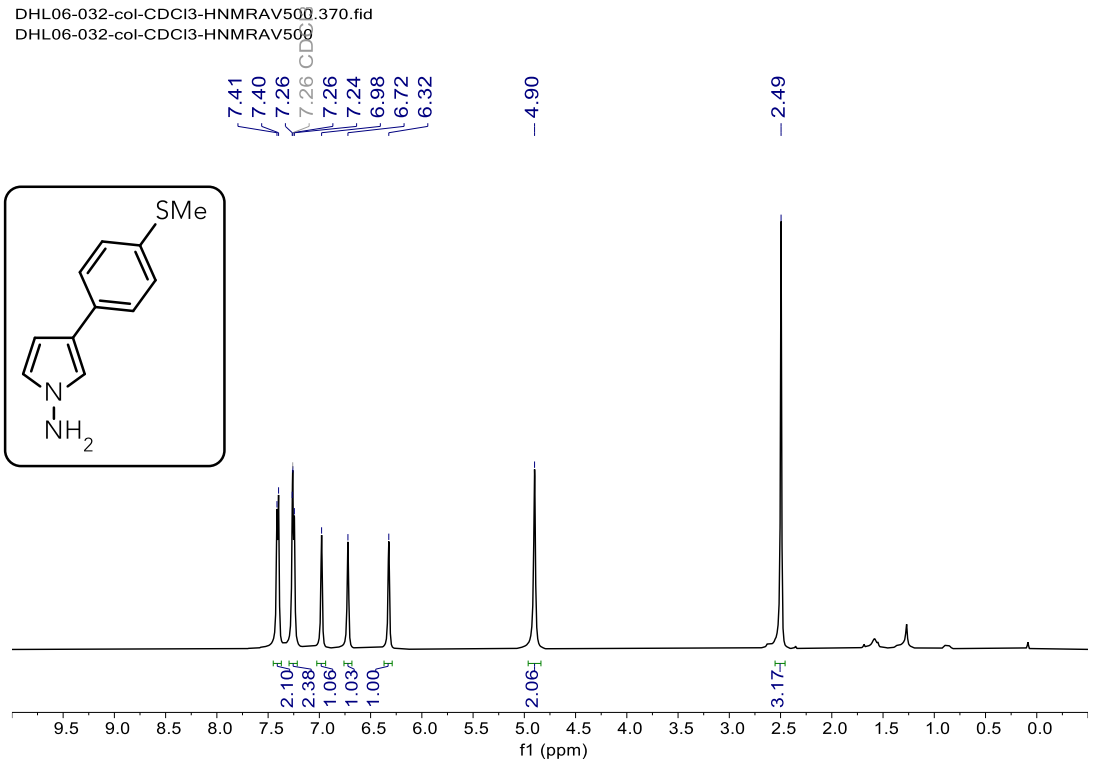

Figure S25. ^{1}H NMR spectrum of **7** in $CDCl_3$ at 25 ºC.

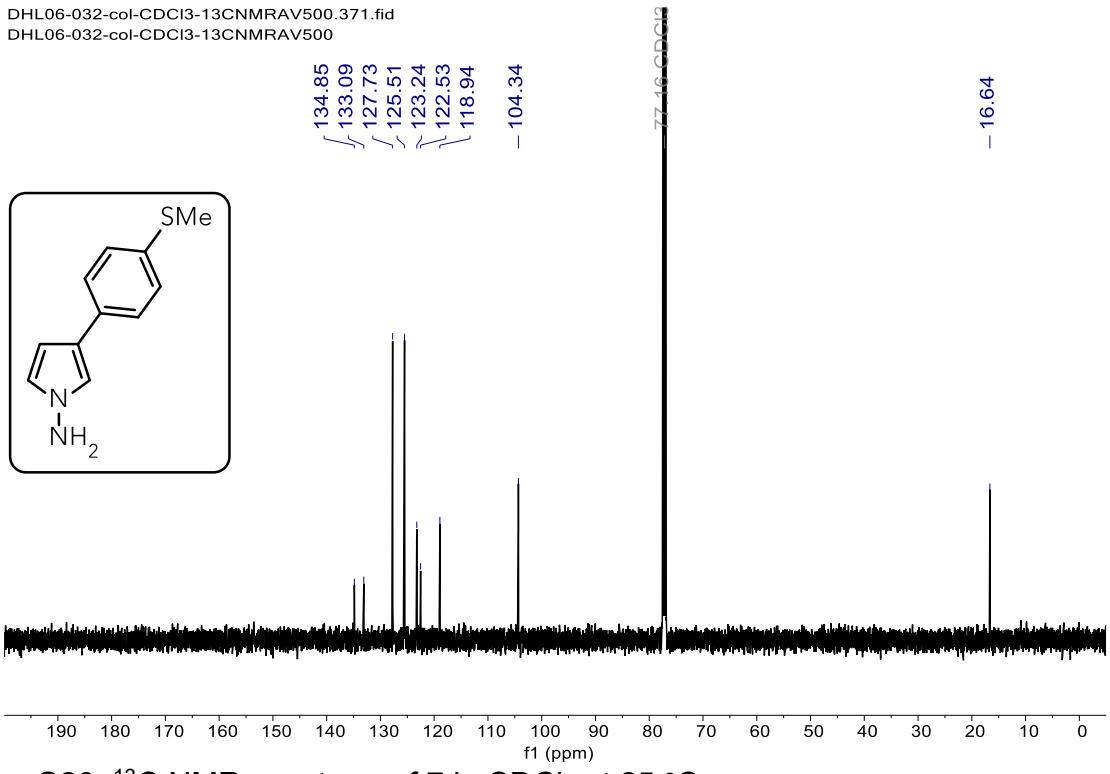

Figure S26. ^{13}C NMR spectrum of **7** in $CDCl_3$ at 25 ºC.

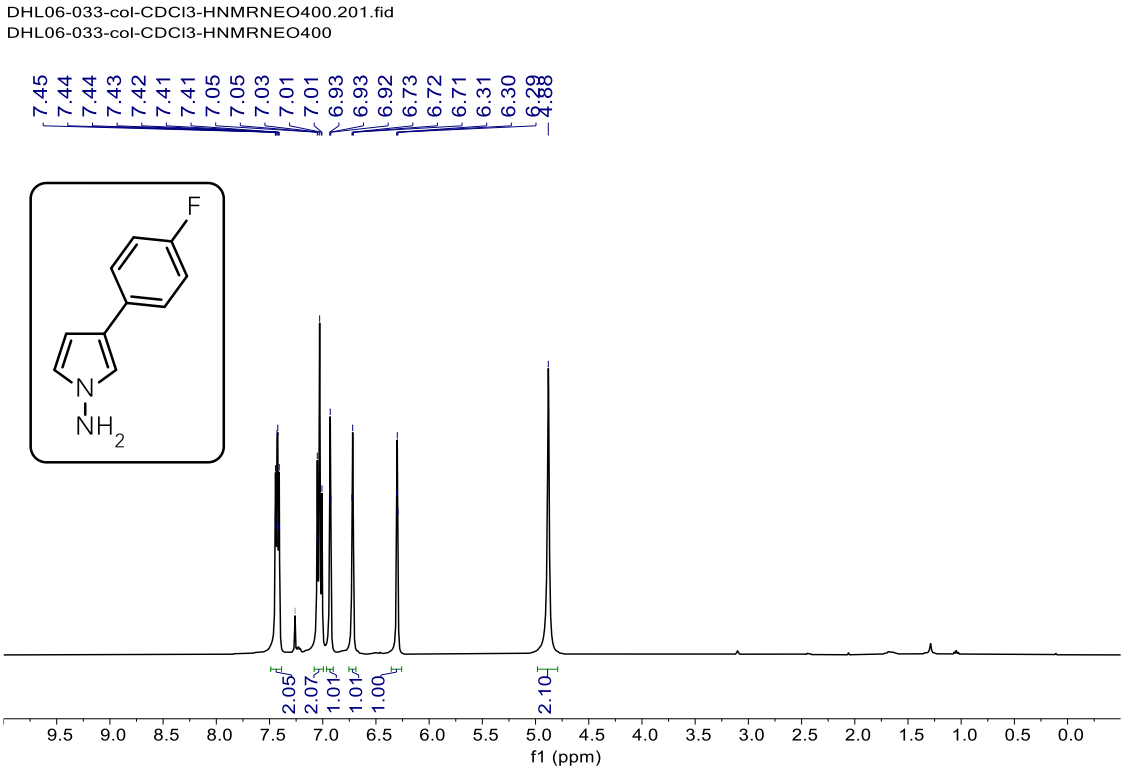

Figure S27. ^{1}H NMR spectrum of **8** in $CDCl_3$ at 25 ºC.

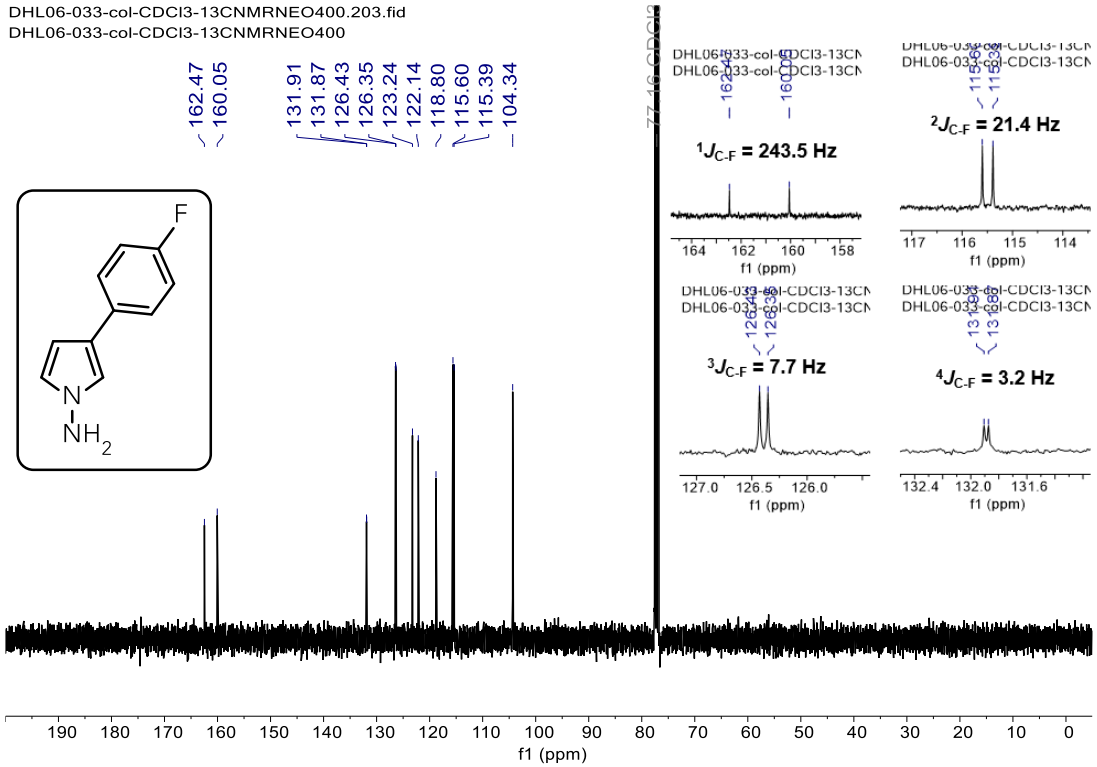

Figure S28. ^{13}C NMR spectrum of **8** in $CDCl_3$ at 25 ºC.

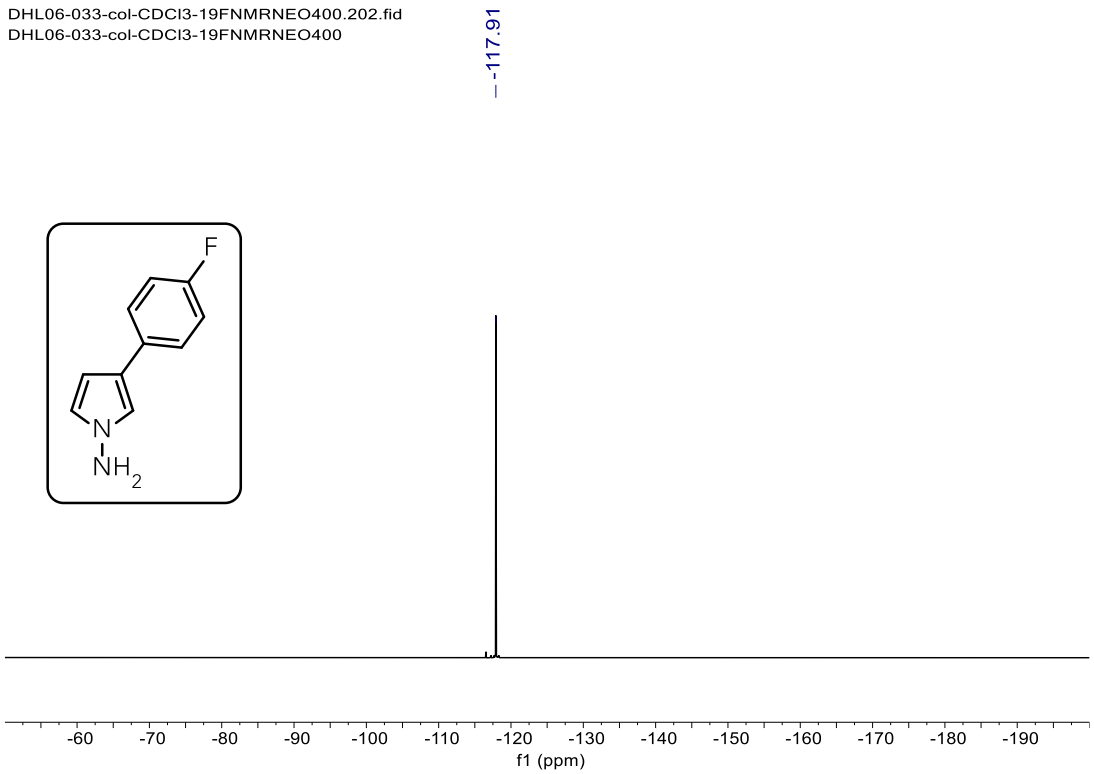

Figure S29. ^{19}F NMR spectrum of **8** in $CDCl_3$ at 25 °C.

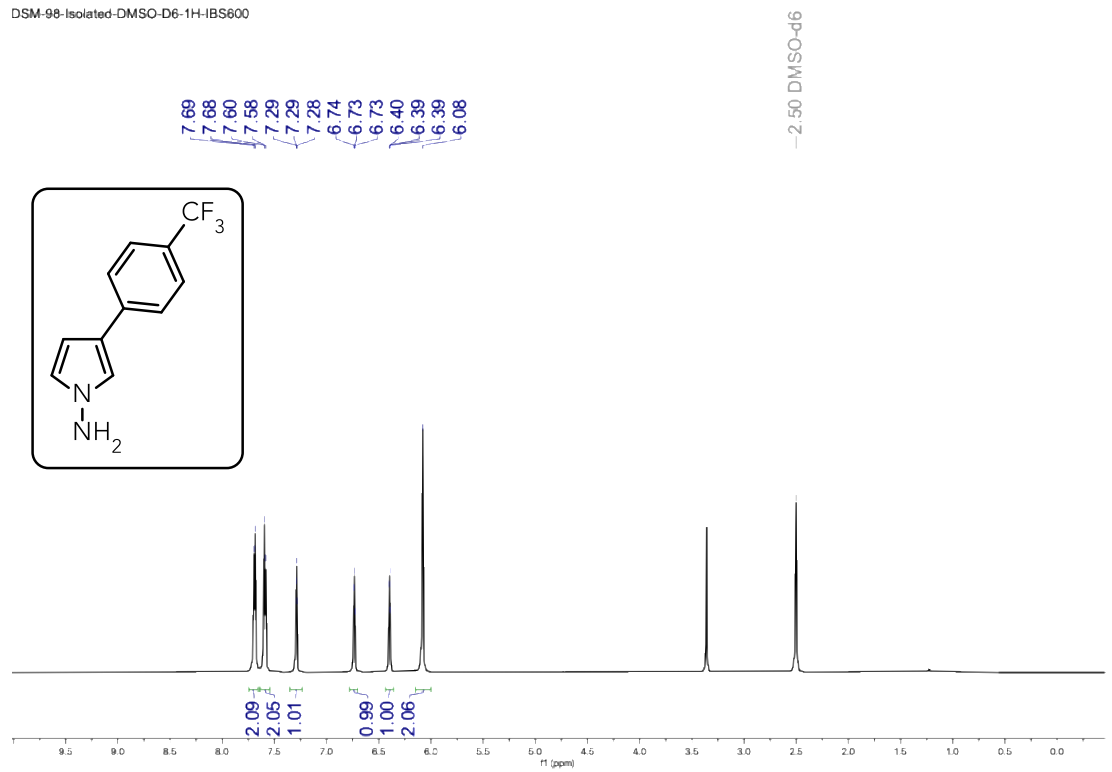

Figure S30. ^{1}H NMR spectrum of **9** in DMSO-d_6 at 25 ^{o}C.

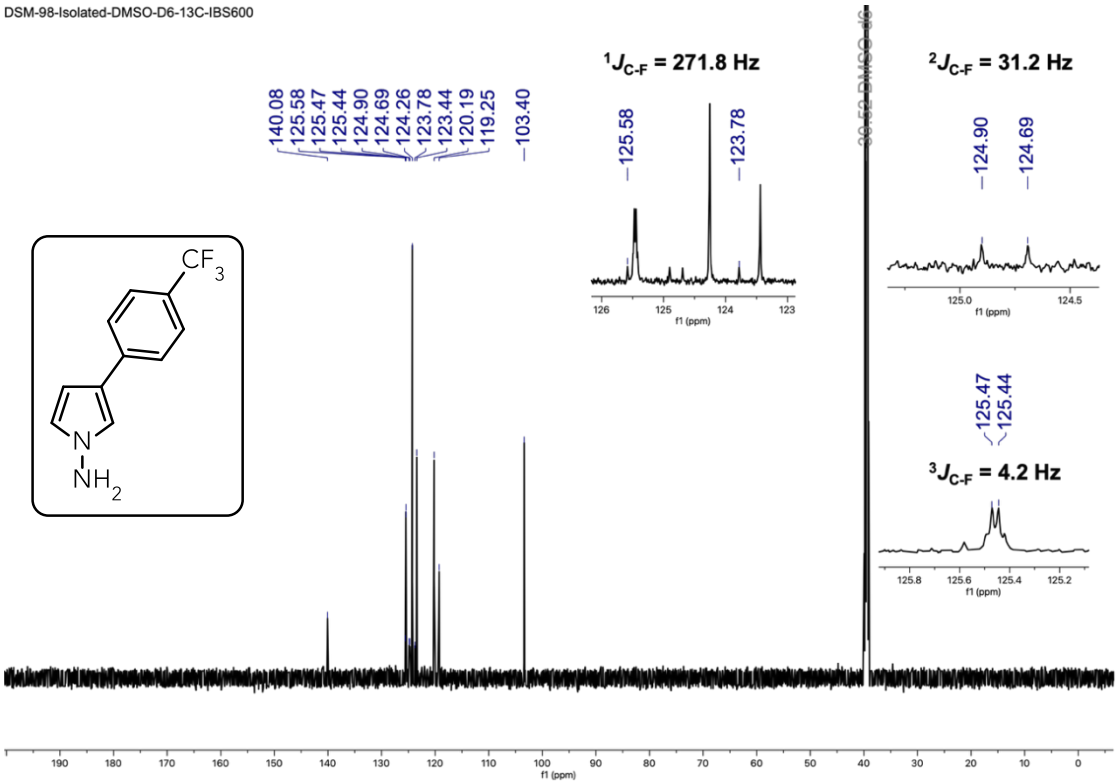

Figure S31. ^{13}C NMR spectrum of **9** in DMSO-d_6 at 25 ^{o}C.

Figure S32. ^{19}F NMR spectrum of **9** in DMSO-d_6 at 25 ºC.

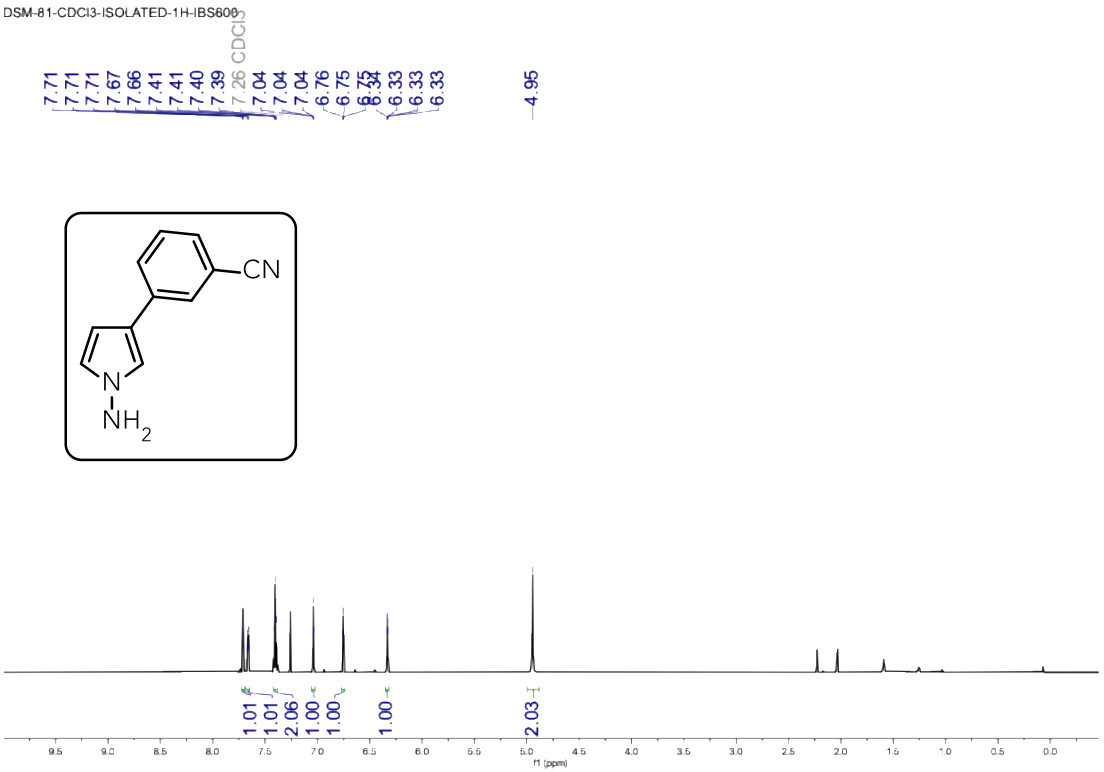

Figure S33. ^{1}H NMR spectrum of **10** in $CDCl_3$ at 25 ºC.

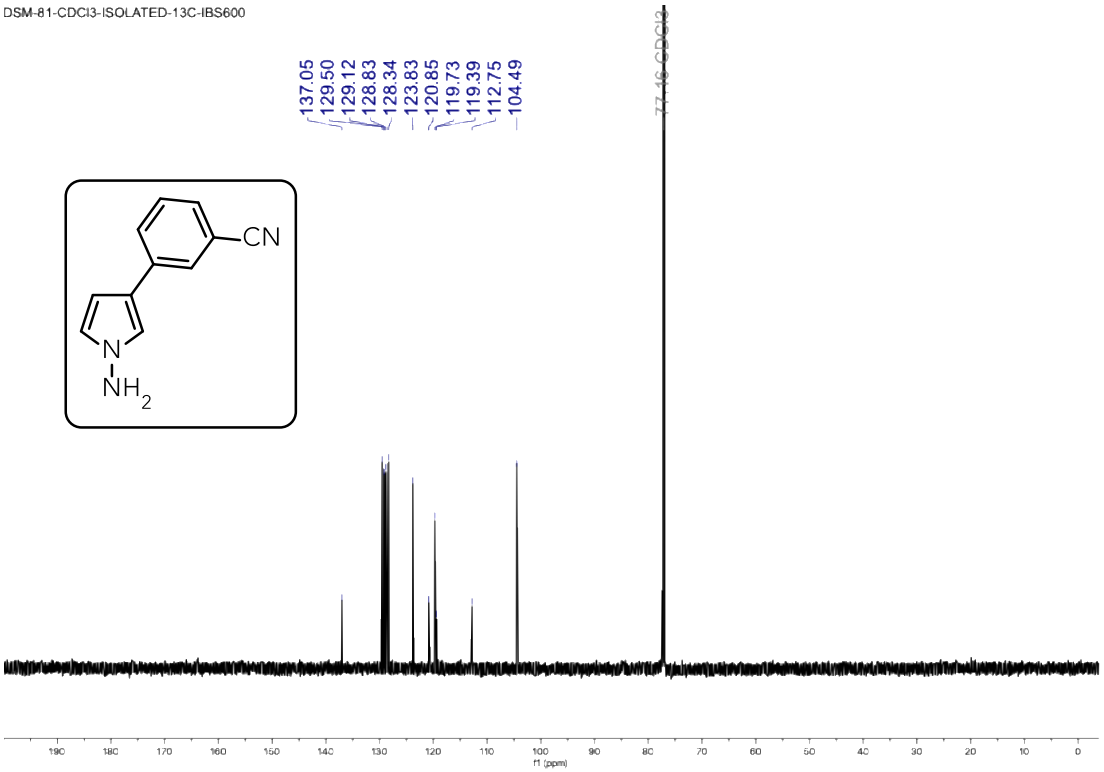

Figure S34. ^{13}C NMR spectrum of **10** in $CDCl_3$ at 25 ºC.

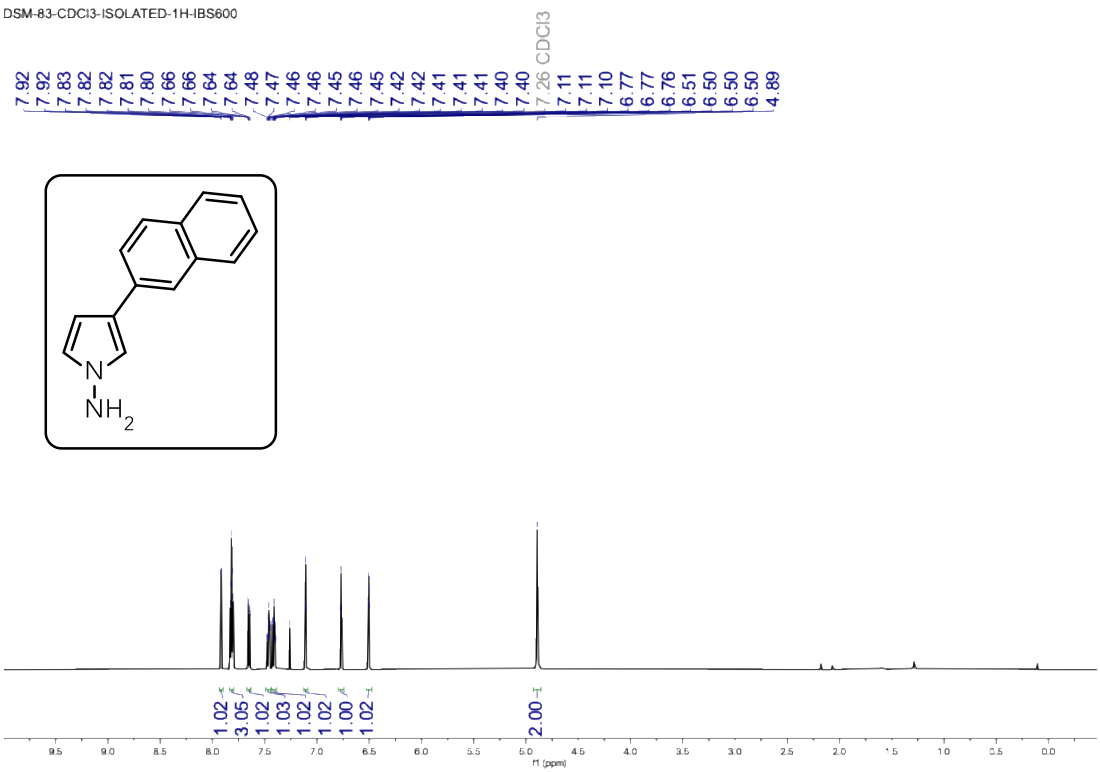

Figure S35. ^{1}H NMR spectrum of **11** in $CDCl_3$ at 25 ºC.

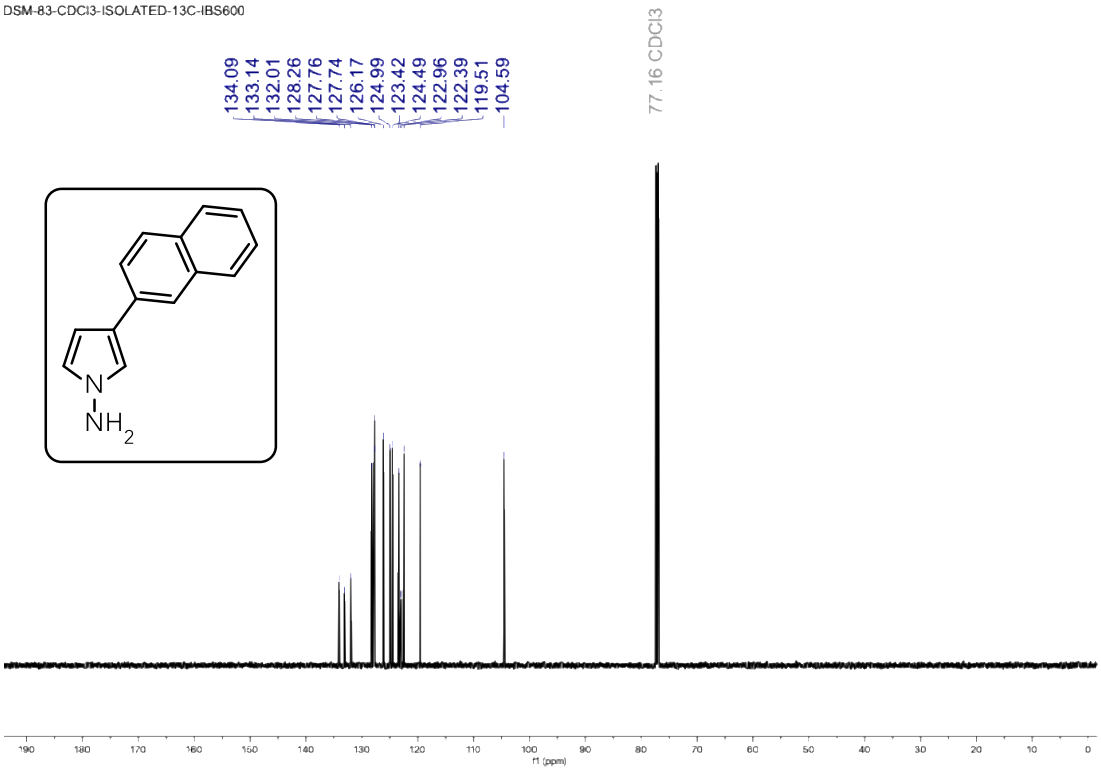

Figure S36. ^{13}C NMR spectrum of **11** in $CDCl_3$ at 25 ºC.

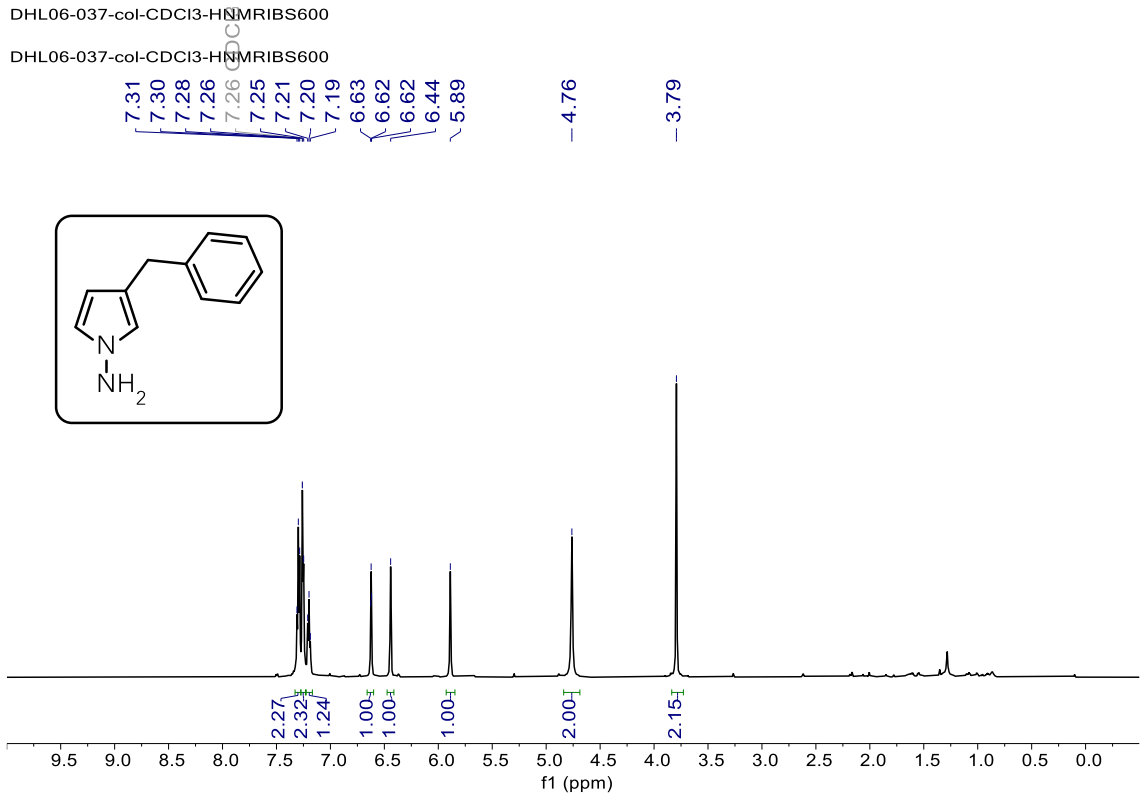

Figure S37. ^{1}H NMR spectrum of **12** in $CDCl_3$ at 25 ºC.

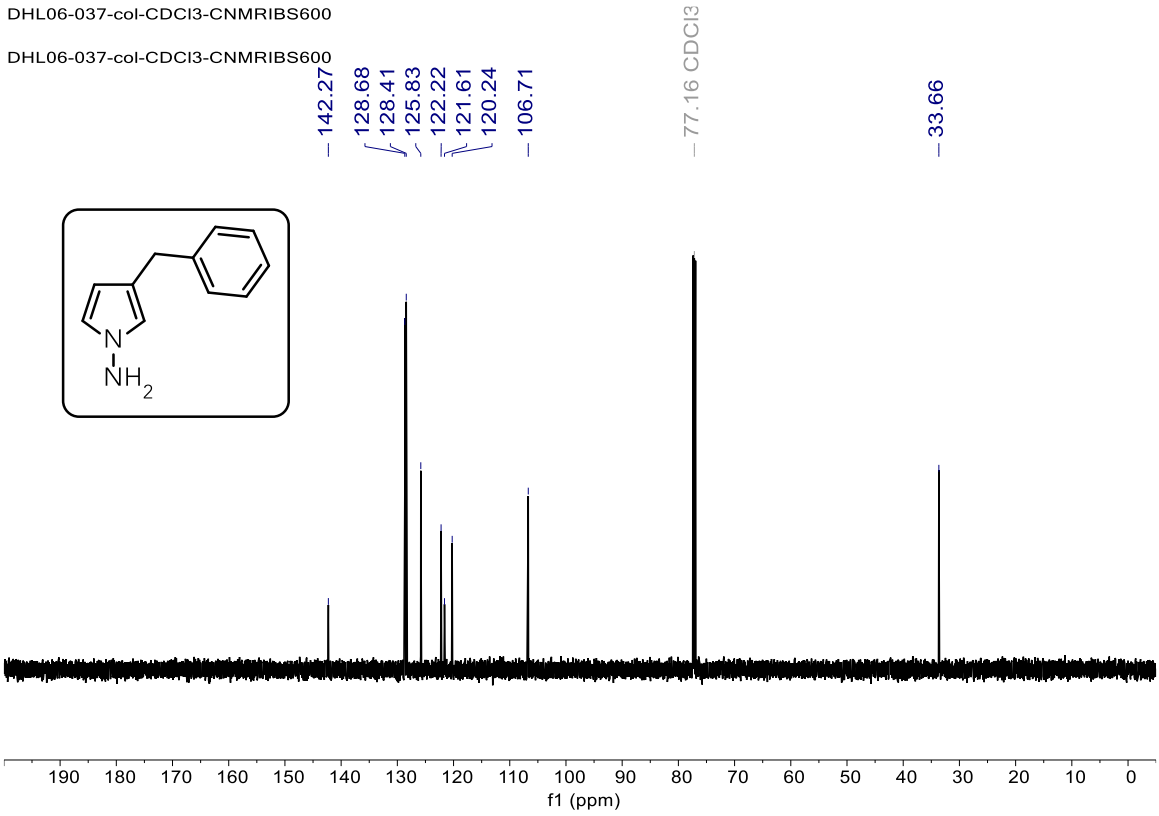

Figure S38. ^{13}C NMR spectrum of **12** in $CDCl_3$ at 25 ºC.

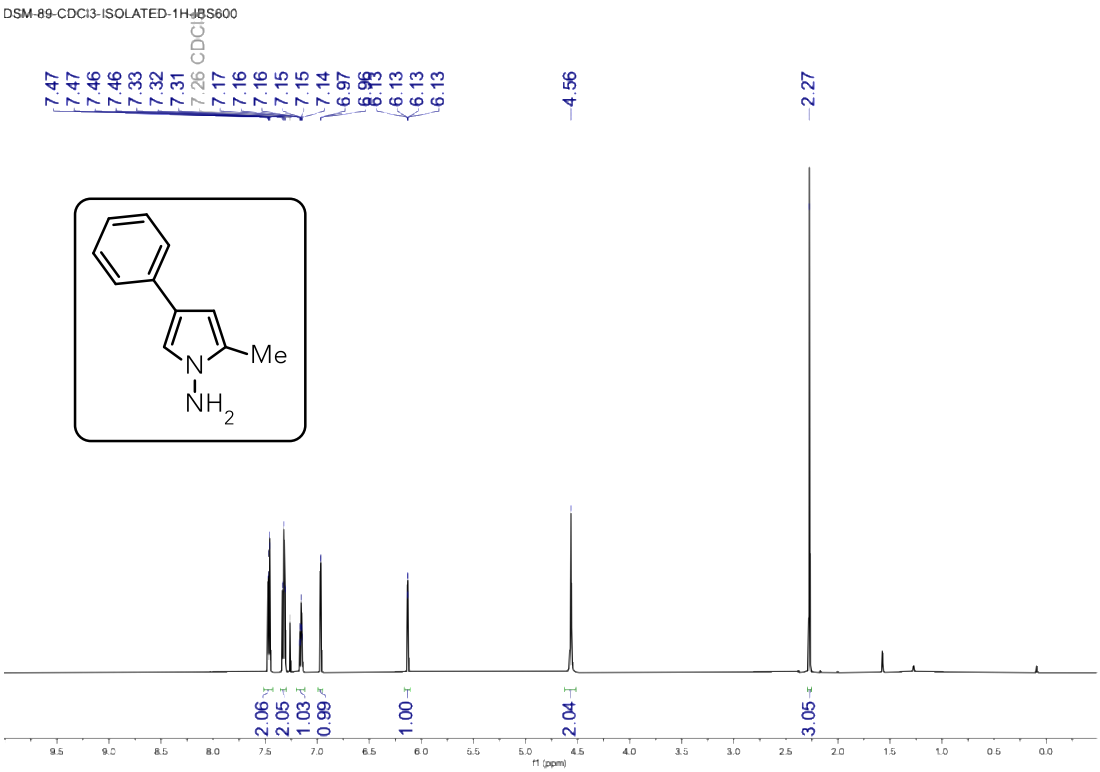

Figure S39. ^{1}H NMR spectrum of **13** in $CDCl_3$ at 25 ºC.

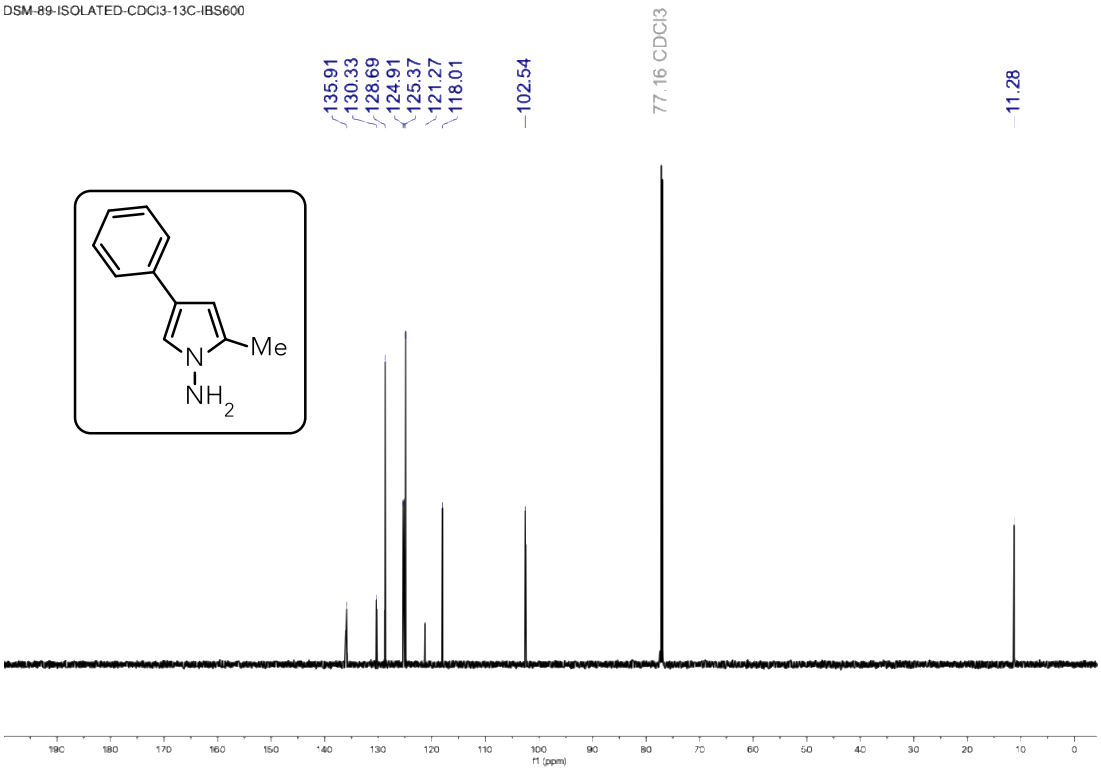

Figure S40. ^{13}C NMR spectrum of **13** in $CDCl_3$ at 25 ºC.

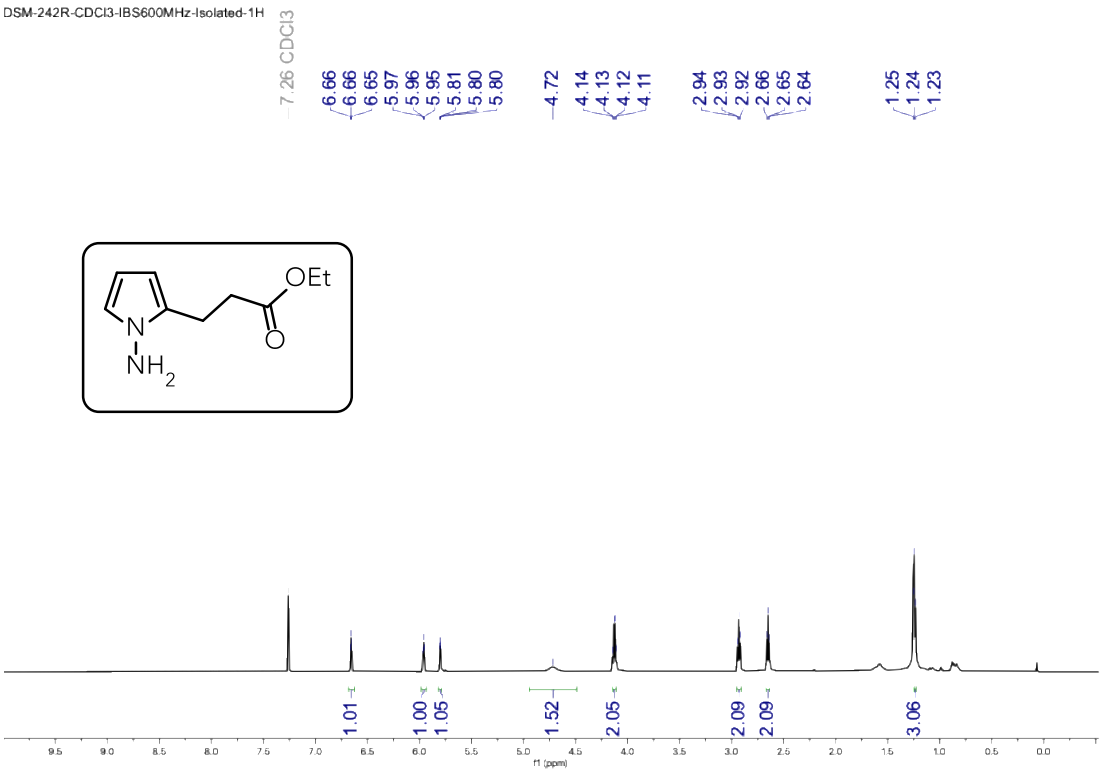

Figure S41. ^{1}H NMR spectrum of **14** in $CDCl_3$ at 25 ºC.

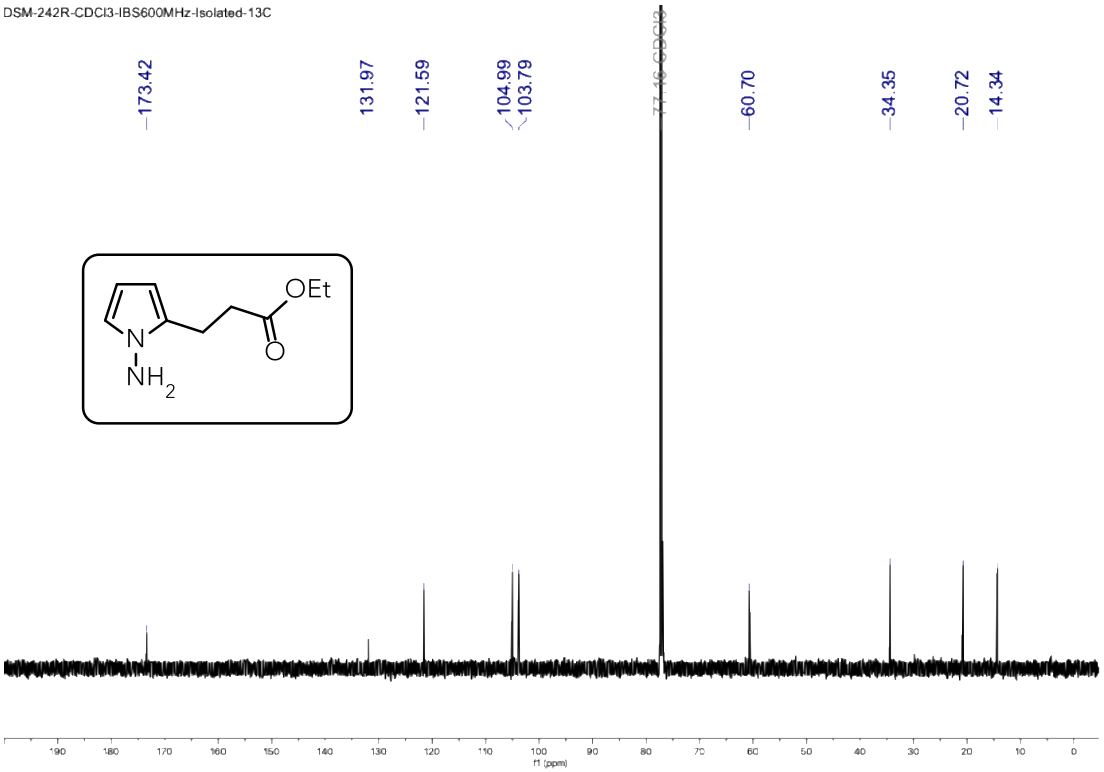

Figure S42. ^{13}C NMR spectrum of **14** in $CDCl_3$ at 25 ºC.

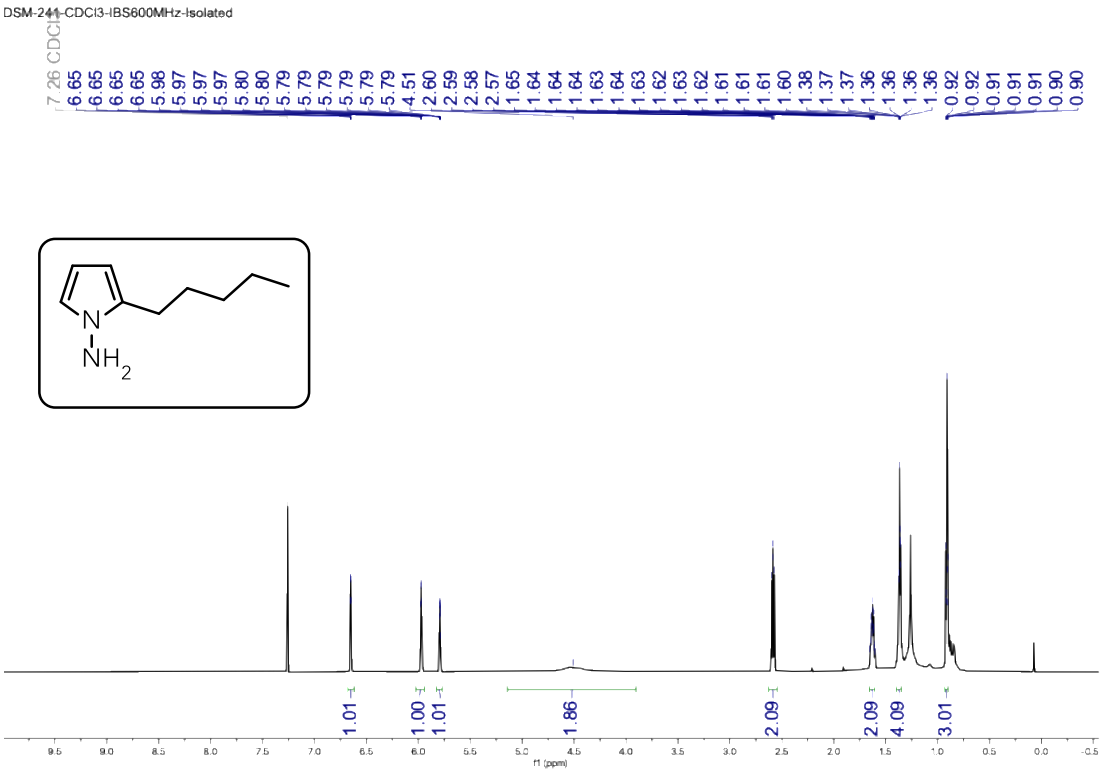

Figure S43. ^{1}H NMR spectrum of **15** in $CDCl_3$ at 25 ºC.

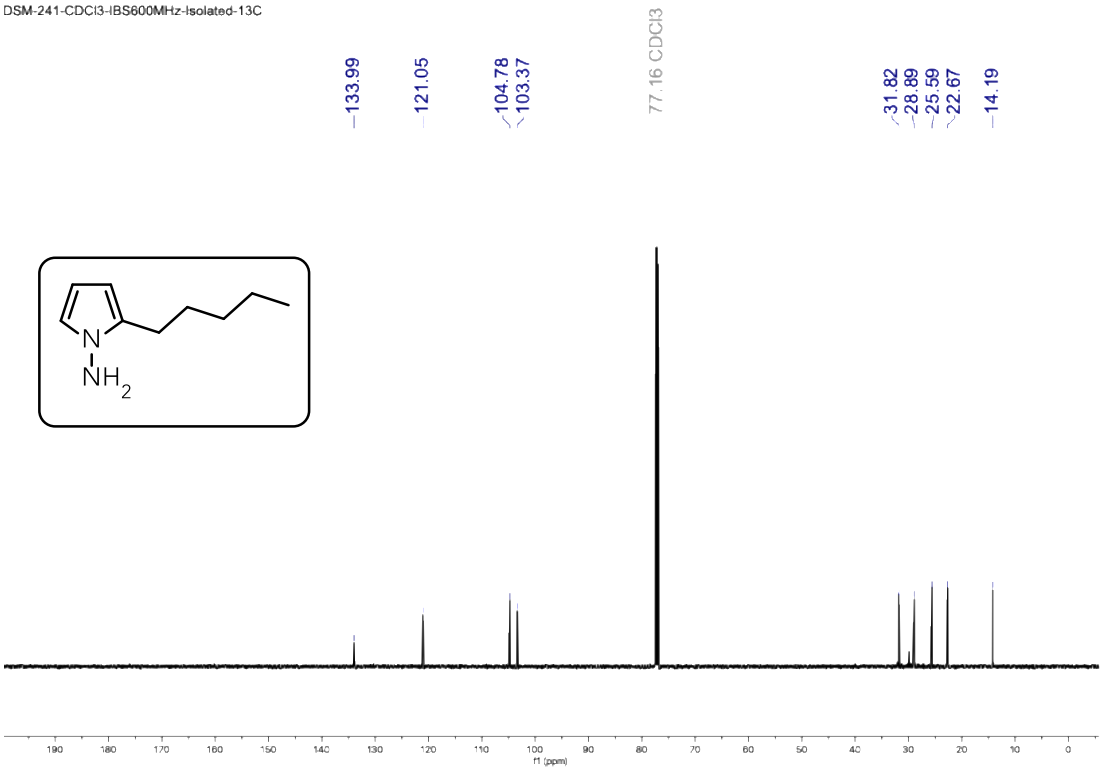

Figure S44. ^{13}C NMR spectrum of **15** in $CDCl_3$ at 25 ºC.

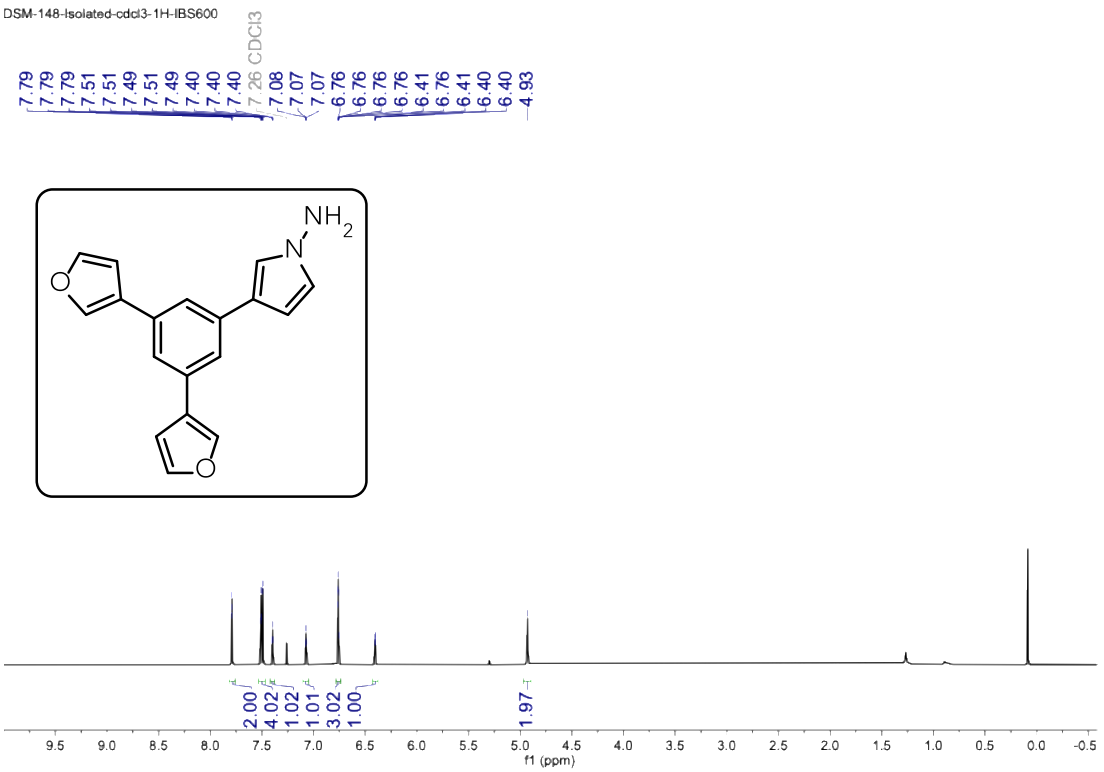

Figure S45. ^{1}H NMR spectrum of **16** in $CDCl_3$ at 25 ºC.

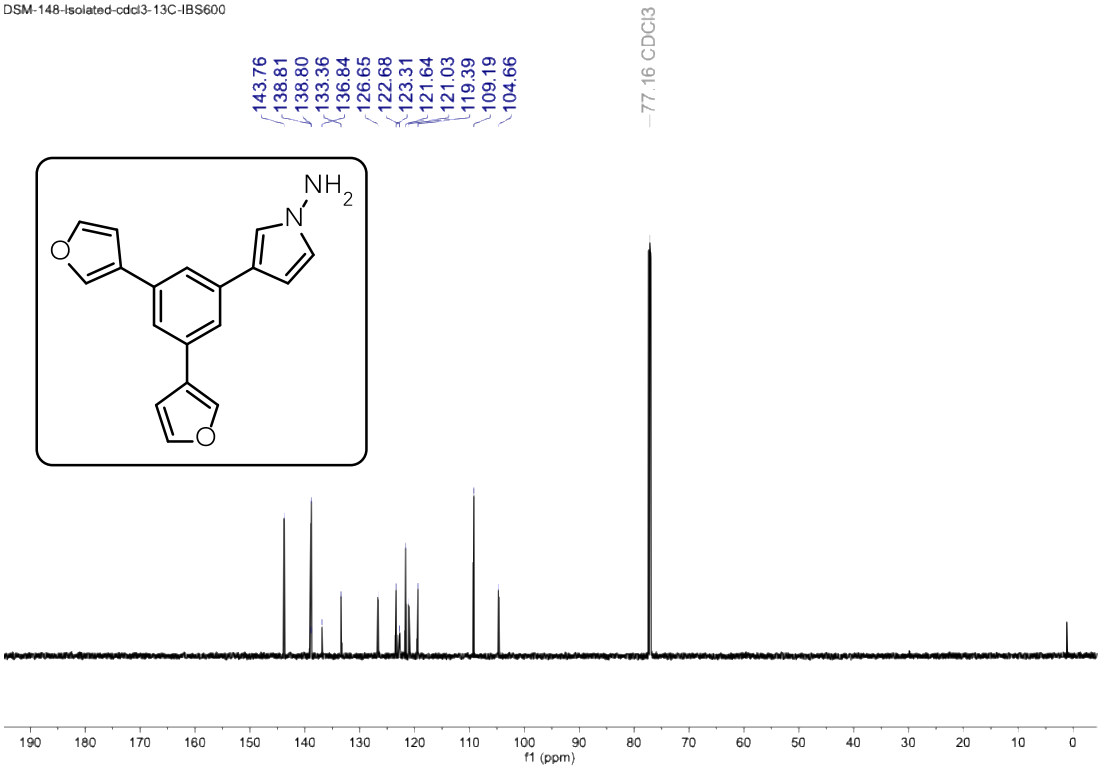

Figure S46. ^{13}C NMR spectrum of **16** in $CDCl_3$ at 25 ºC.

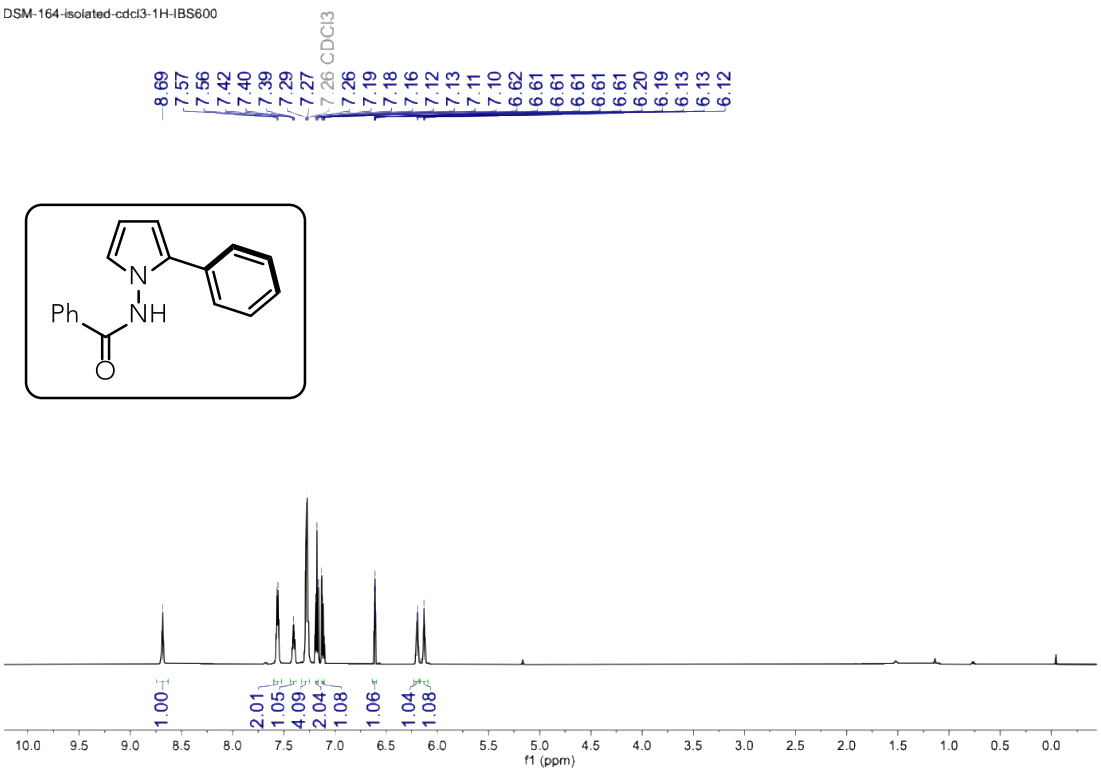

Figure S47. ^{1}H NMR spectrum of **17** in $CDCl_3$ at 25 ºC.

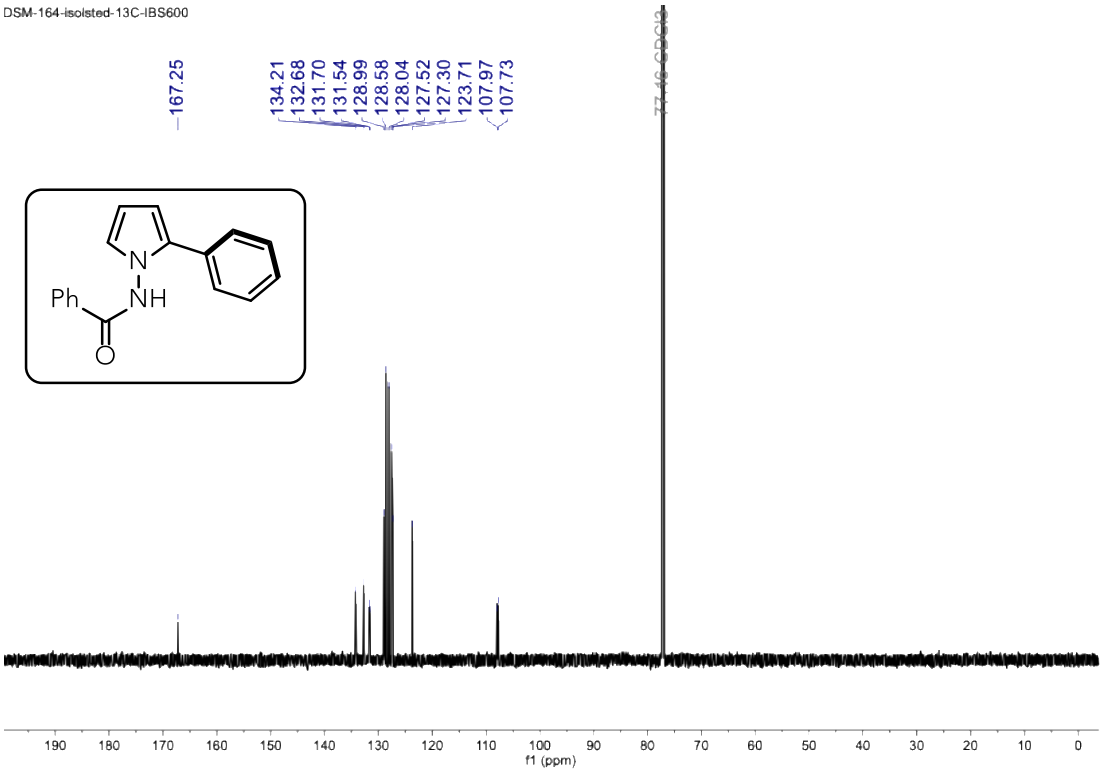

Figure S48. ^{13}C NMR spectrum of **17** in $CDCl_3$ at 25 ºC.

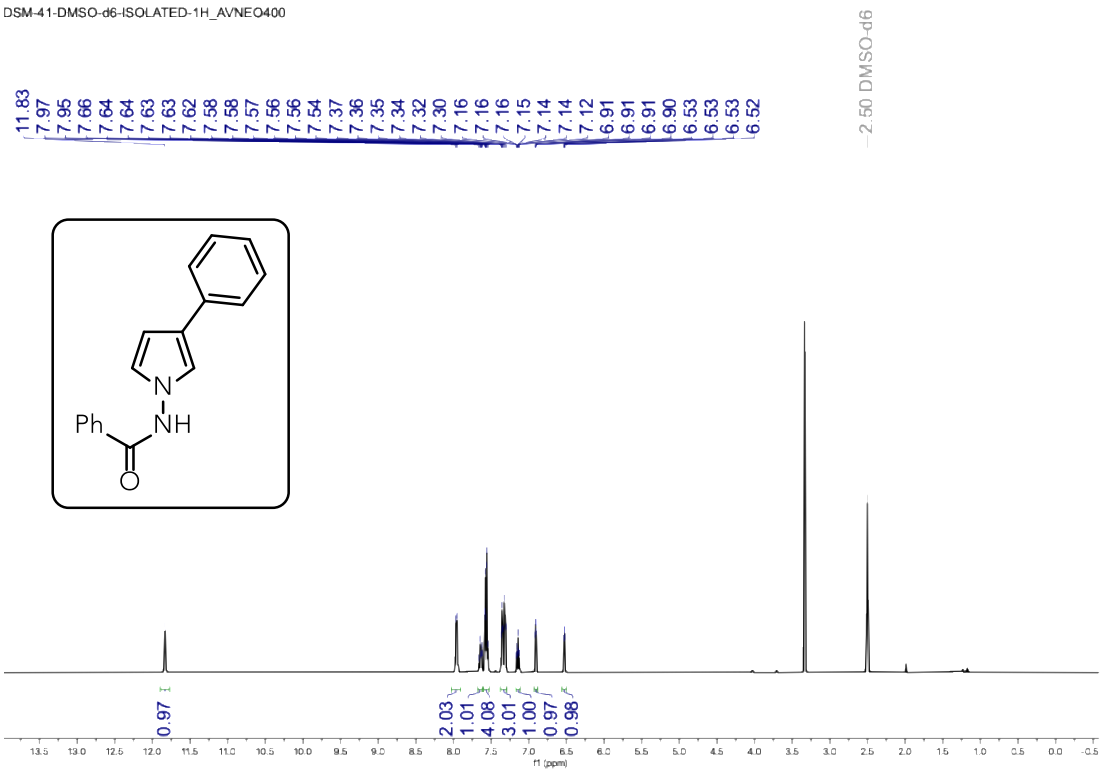

Figure S49. ^{1}H NMR spectrum of **18** in DMOS-d_6 at 25 ºC.

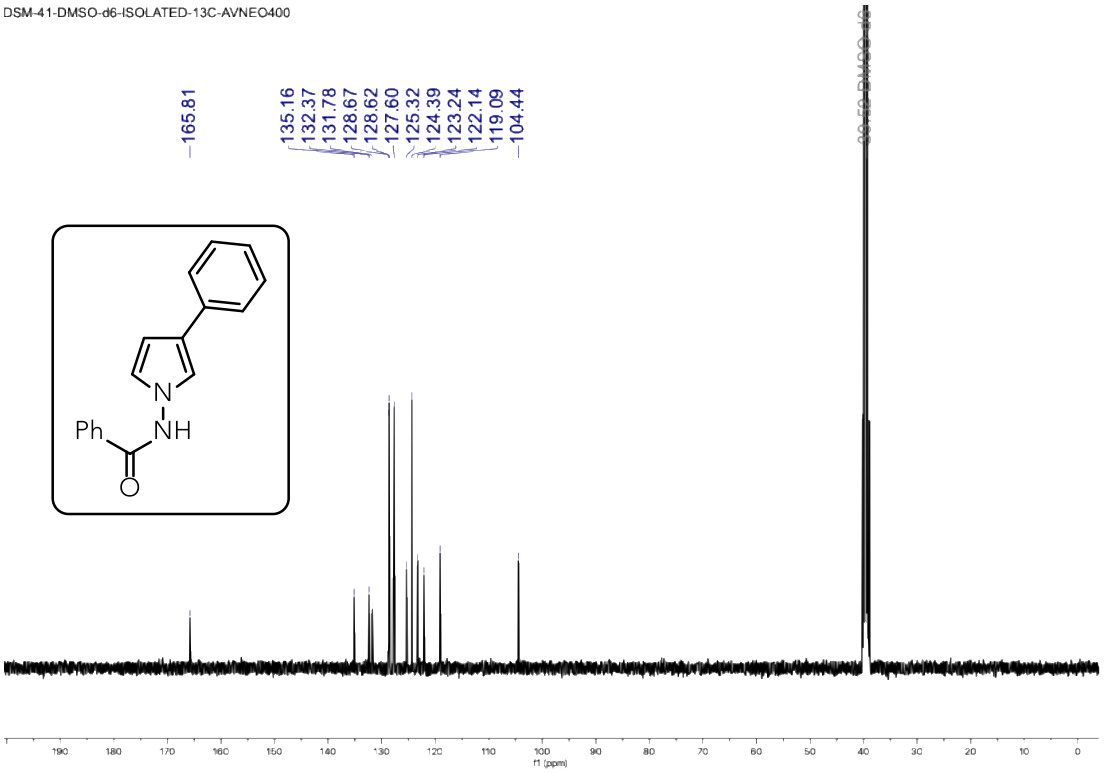

Figure S50. ^{13}C NMR spectrum of **18** in DMOS-d_6 at 25 ºC.

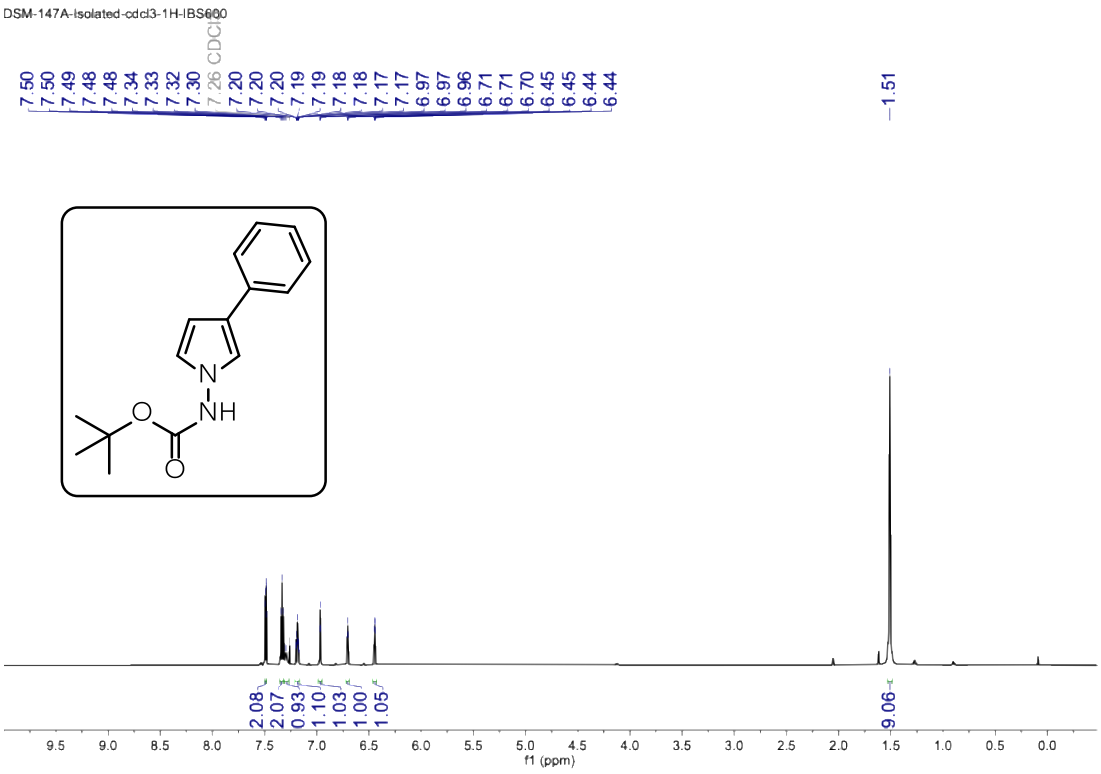

Figure S51. ^{1}H NMR spectrum of **19** in $CDCl_3$ at 25 ºC.

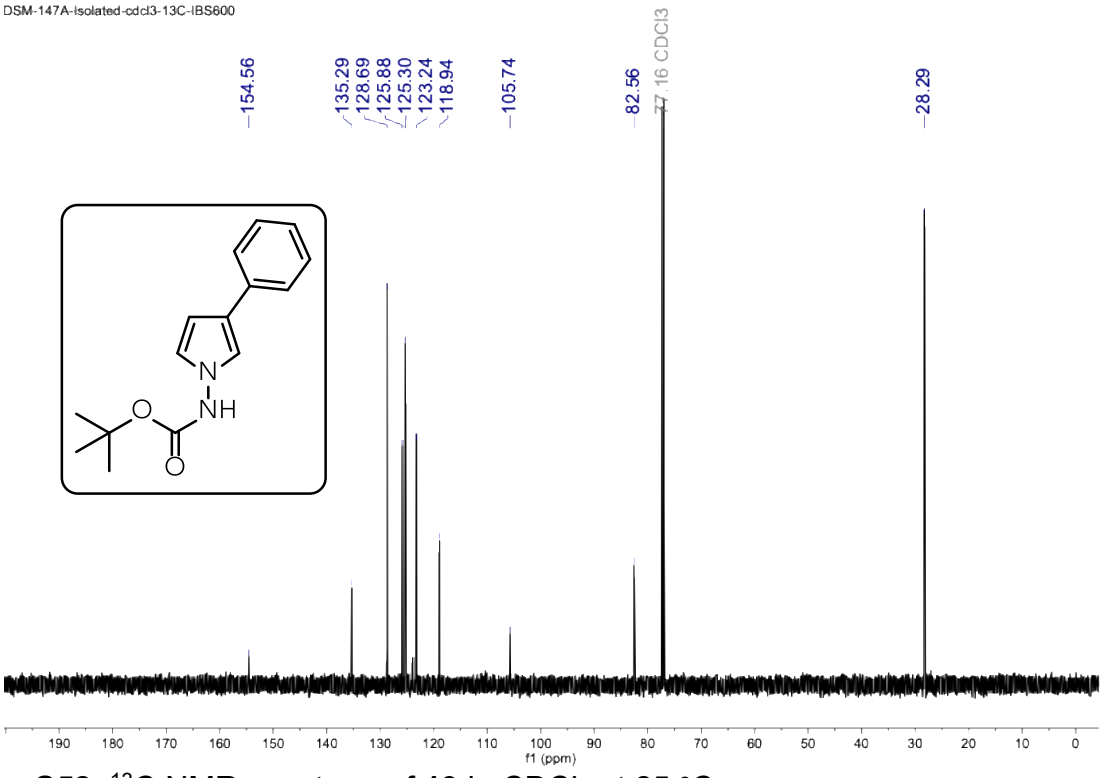

Figure S52. ^{13}C NMR spectrum of **19** in $CDCl_3$ at 25 ºC.

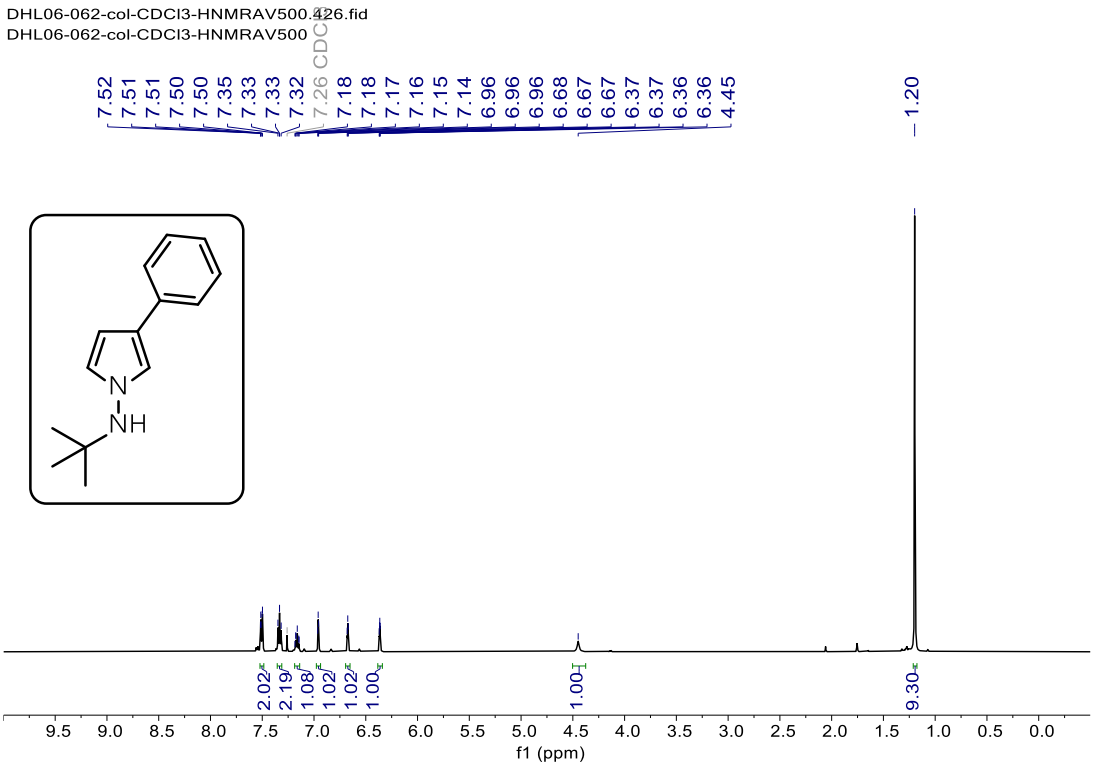

Figure S53. ^{1}H NMR spectrum of **20** in $CDCl_3$ at 25 ºC.

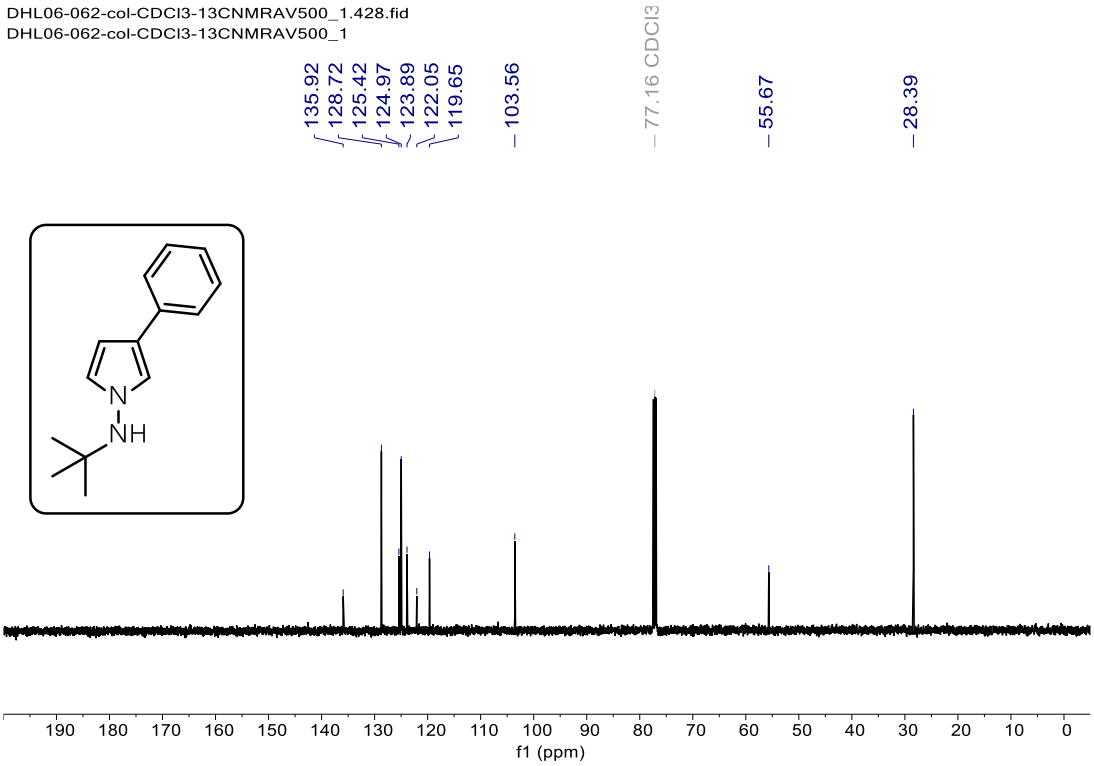

Figure S54. ^{13}C NMR spectrum of **20** in $CDCl_3$ at 25 ºC.

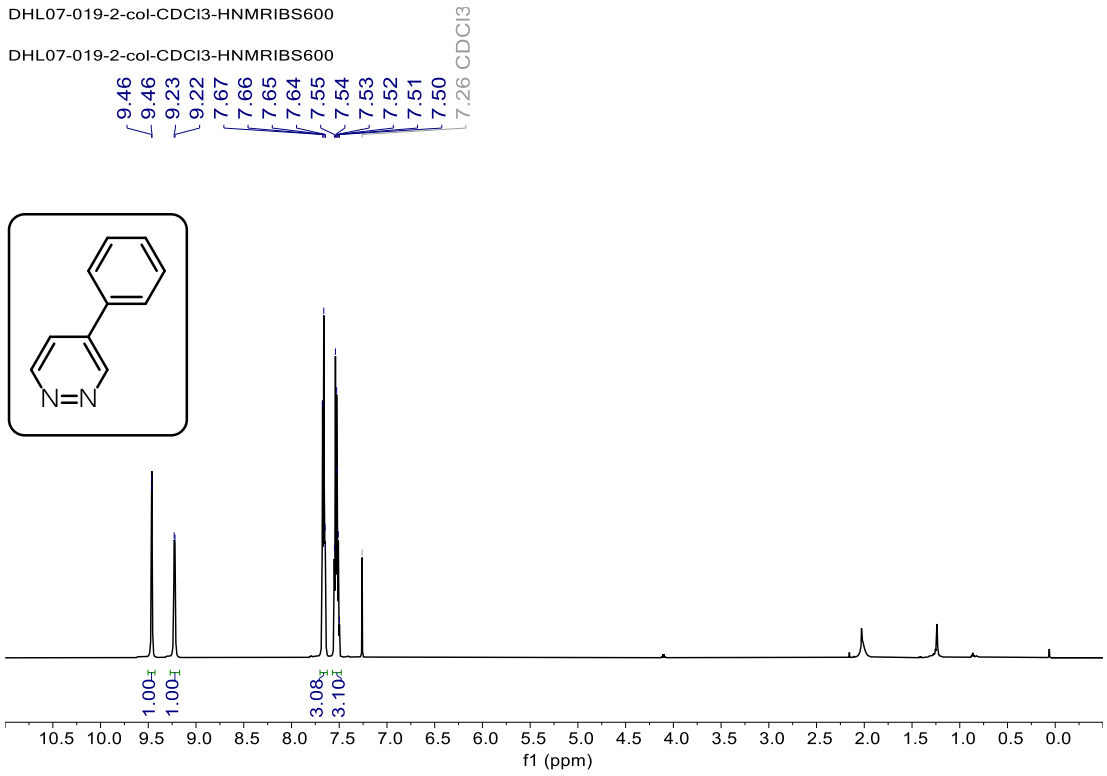

Figure S55. ^{1}H NMR spectrum of **3** in $CDCl_3$ at 25 ºC.

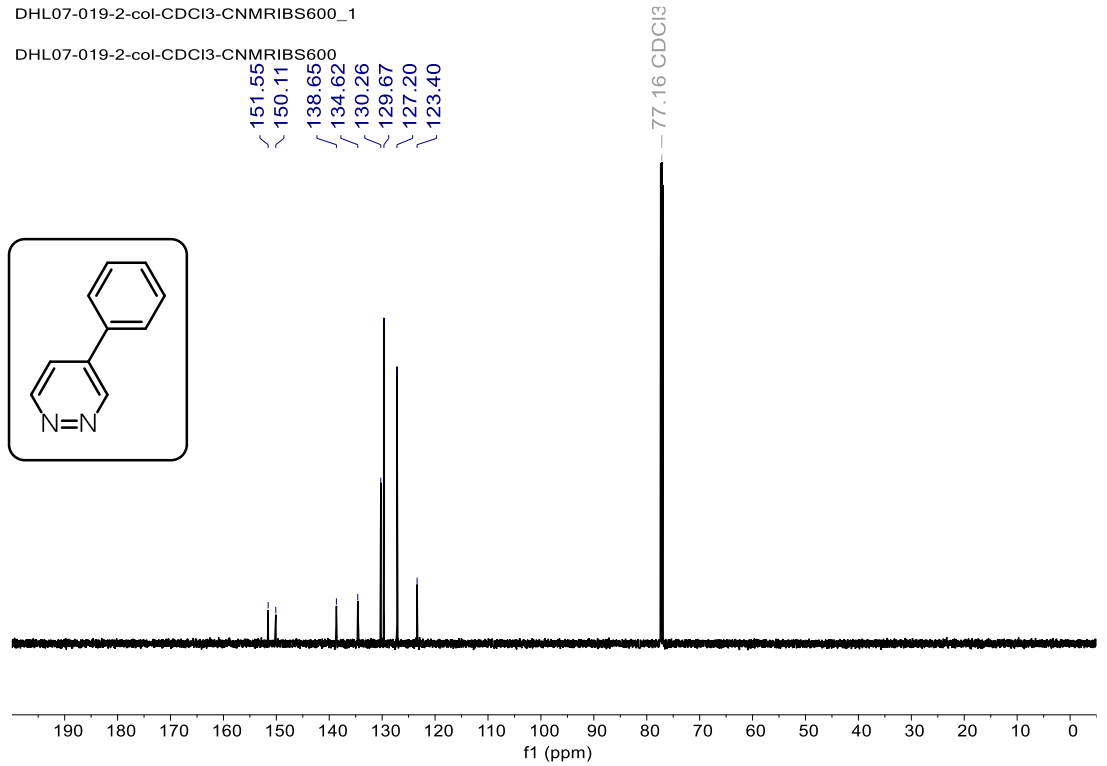

Figure S56. ^{13}C NMR spectrum of **3** in $CDCl_3$ at 25 ºC.

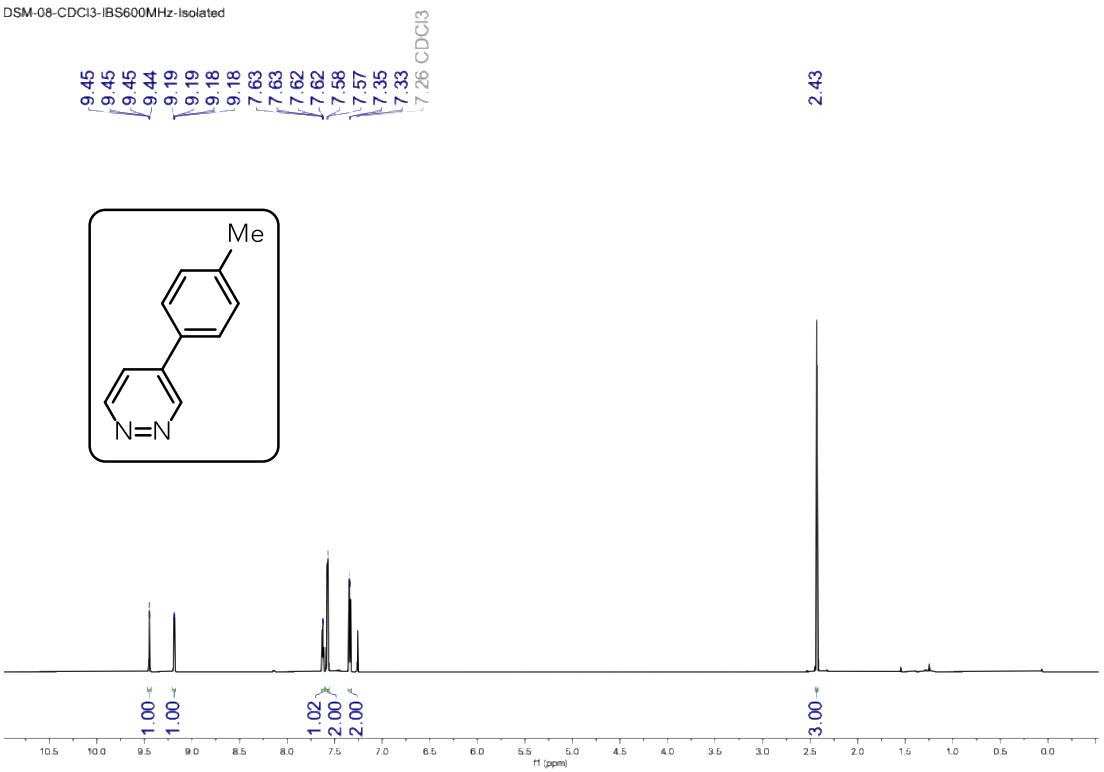

Figure S57. ^{1}H NMR spectrum of **21** in $CDCl_3$ at 25 ºC.

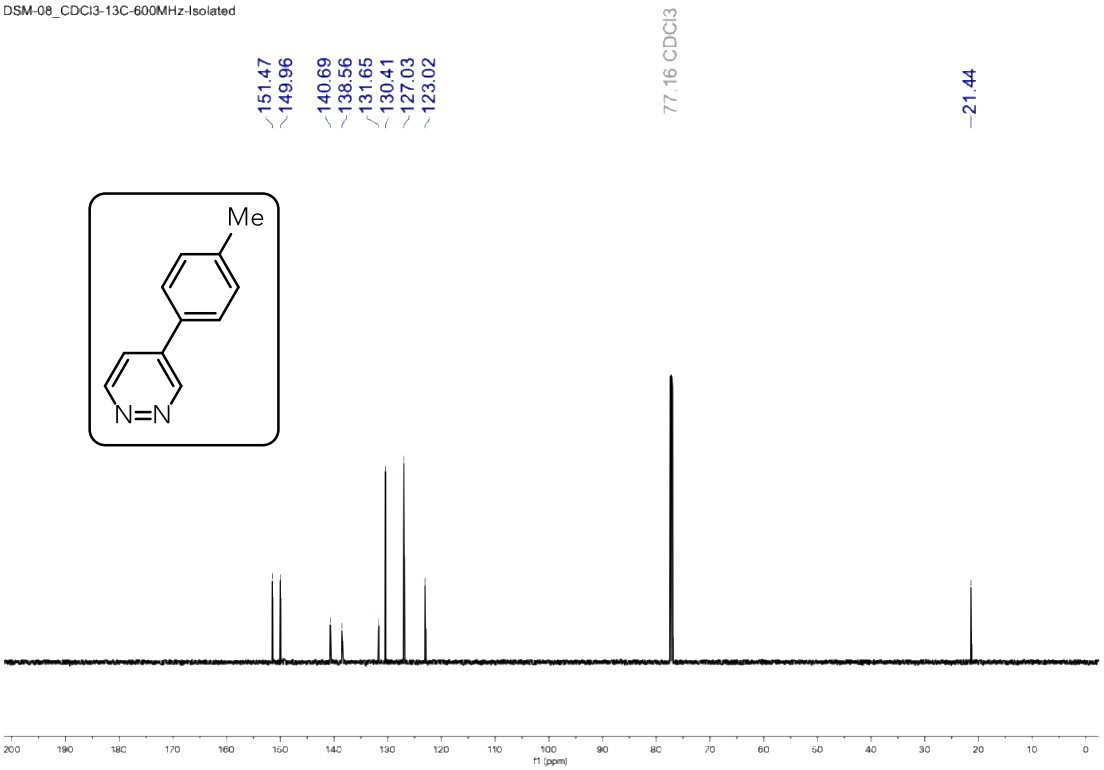

Figure S58. ^{13}C NMR spectrum of **21** in $CDCl_3$ at 25 ºC.

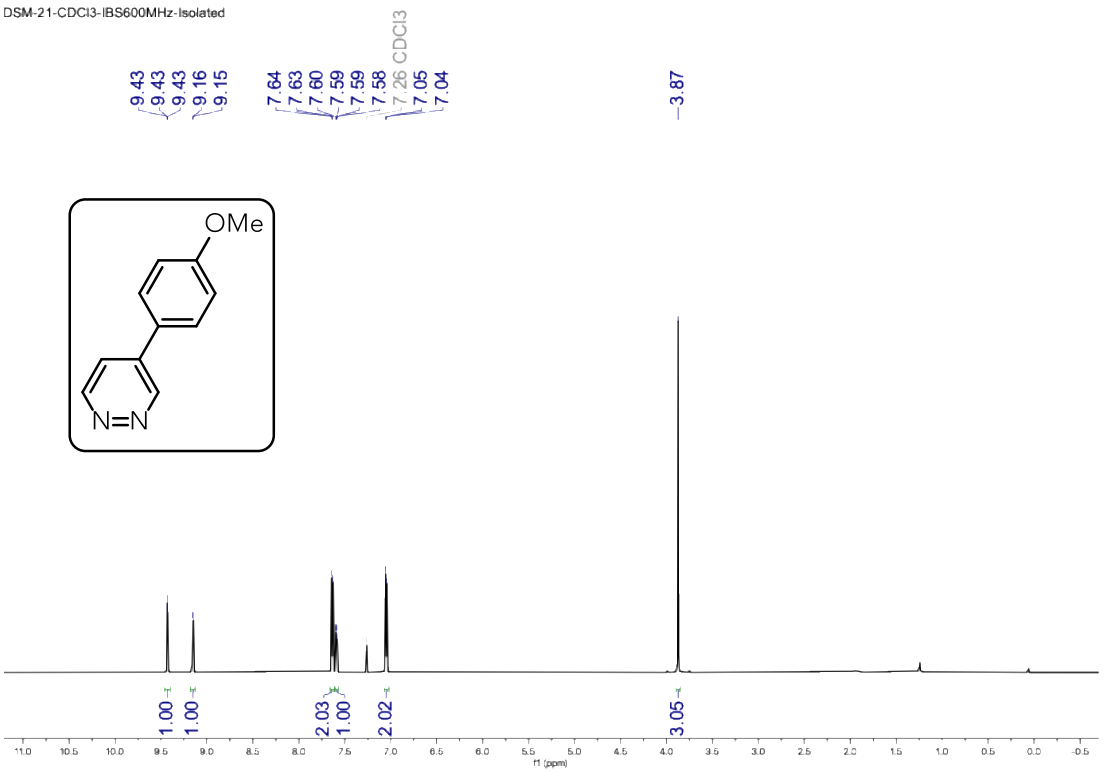

Figure S59. ^{1}H NMR spectrum of **22** in $CDCl_3$ at 25 ºC.

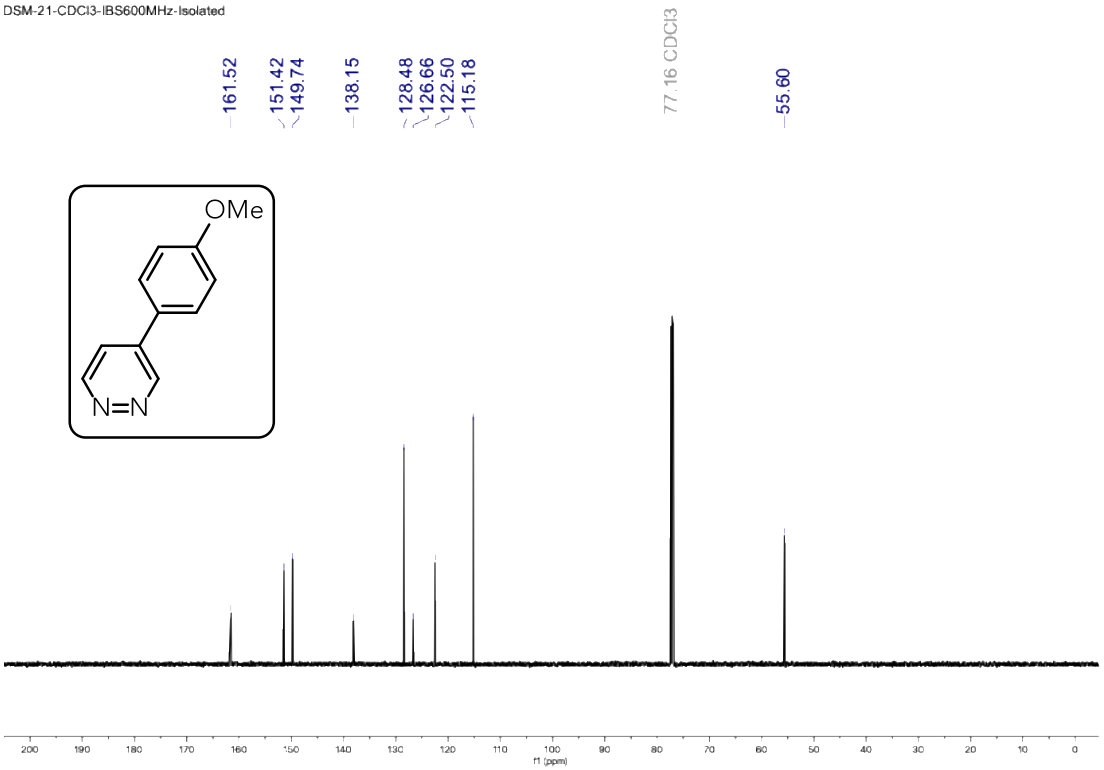

Figure S60. ^{13}C NMR spectrum of **22** in $CDCl_3$ at 25 ºC.

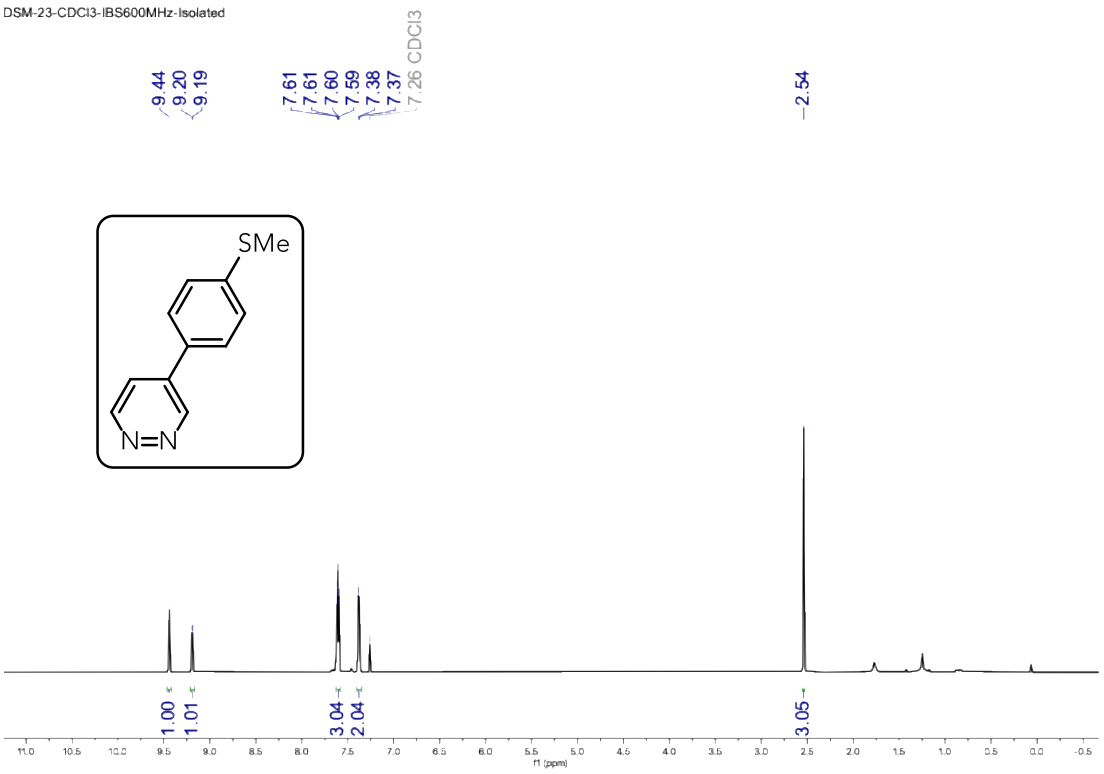

Figure S61. ^{1}H NMR spectrum of **23** in $CDCl_3$ at 25 ºC.

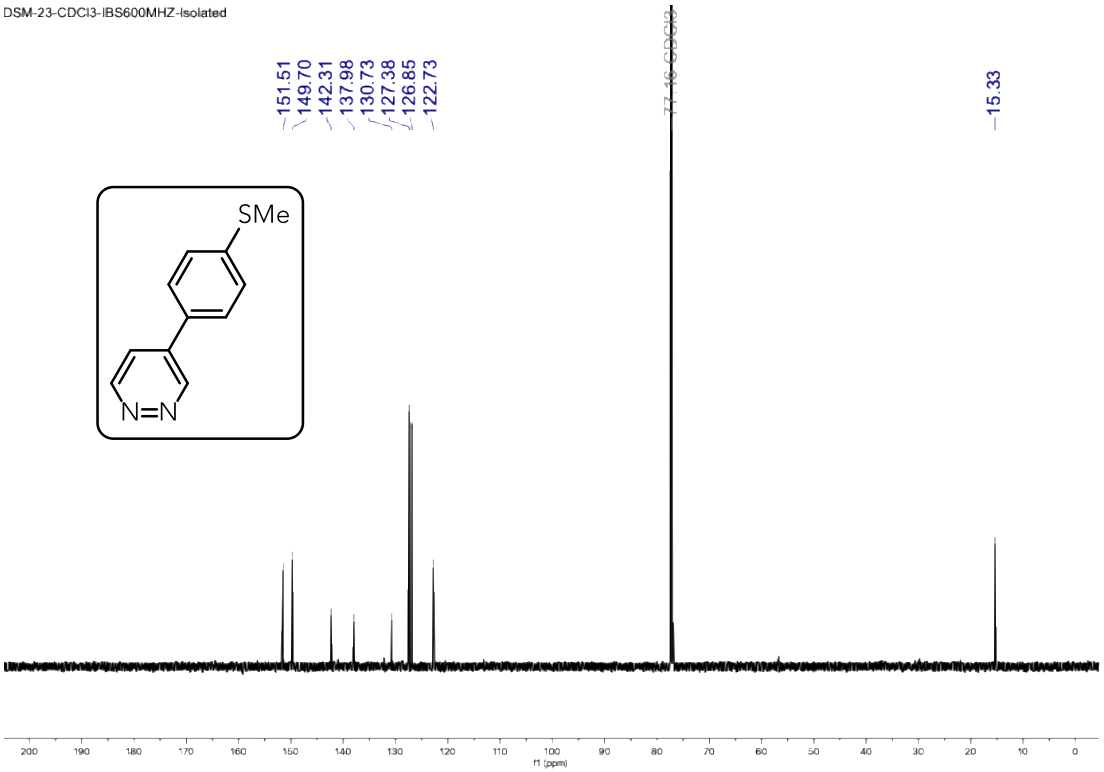

Figure S62. ^{13}C NMR spectrum of **23** in $CDCl_3$ at 25 ºC.

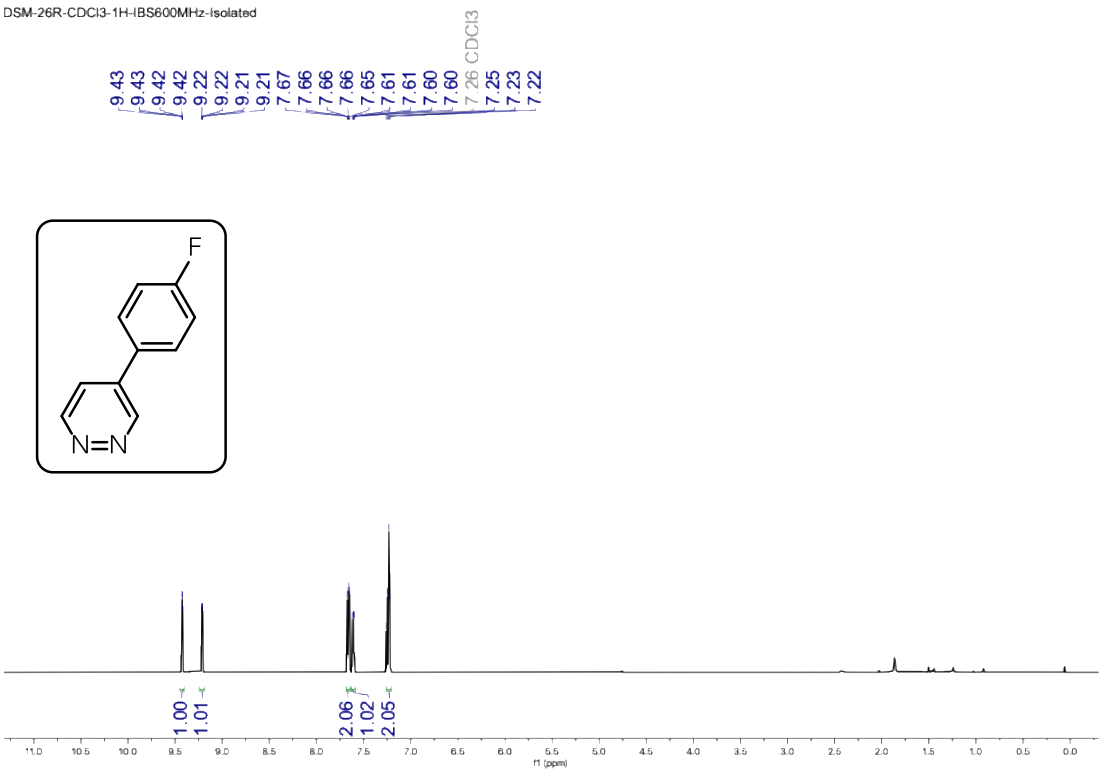

Figure S63. ^{1}H NMR spectrum of **24** in $CDCl_3$ at 25 °C.

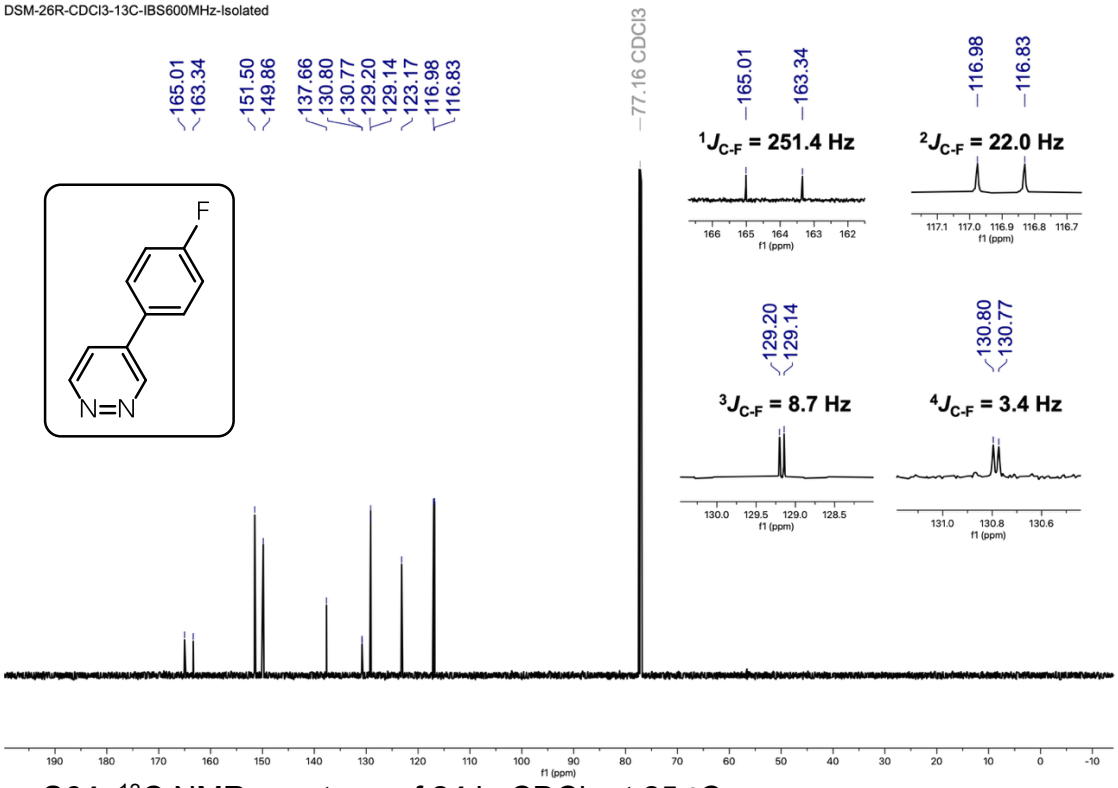

Figure S64. ^{13}C NMR spectrum of **24** in $CDCl_3$ at 25 °C.

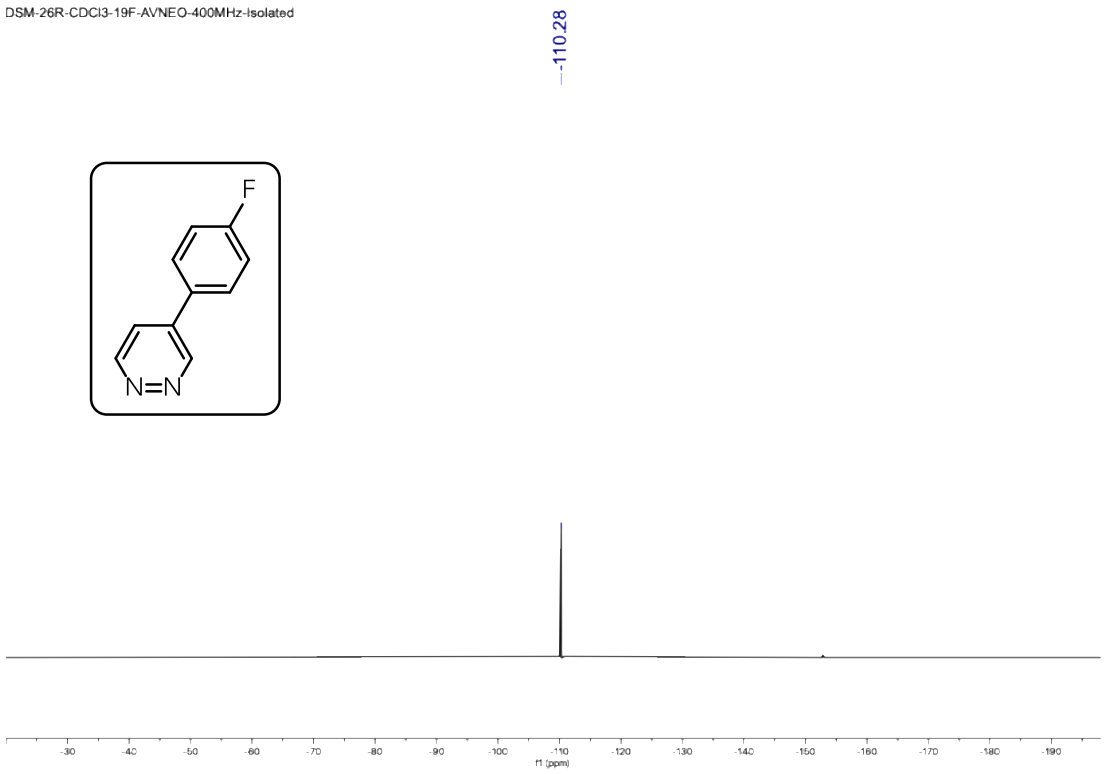

Figure S65. ^{19}F NMR spectrum of **24** in $CDCl_3$ at 25 ºC.

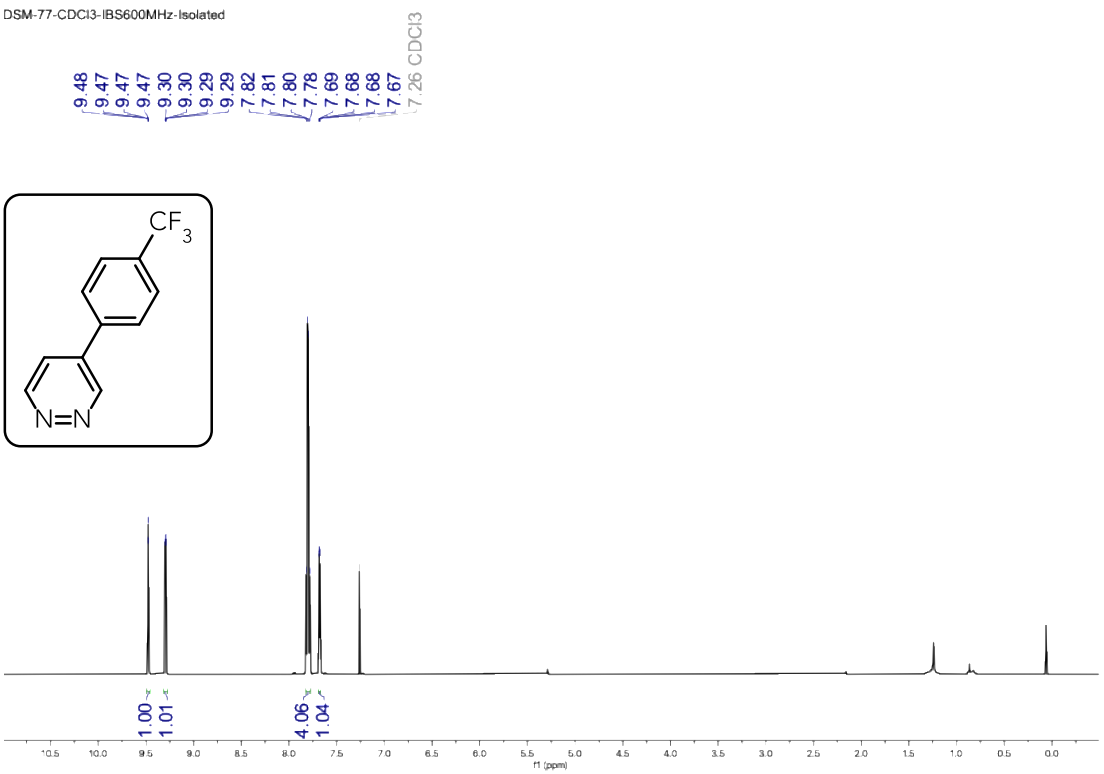

Figure S66. ^{1}H NMR spectrum of **25** in $CDCl_3$ at 25 ºC.

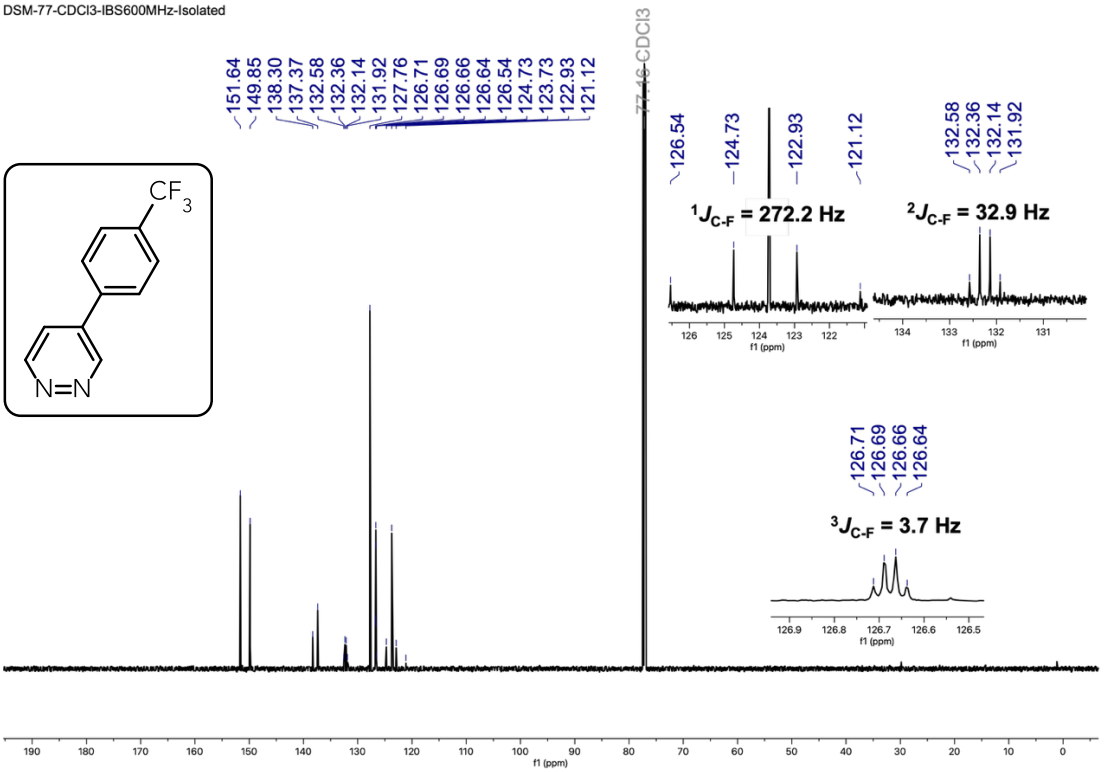

Figure S67. ^{13}C NMR spectrum of **25** in $CDCl_3$ at 25 ºC.

Figure S68. ^{19}F NMR spectrum of **25** in $CDCl_3$ at 25 ^{o}C.

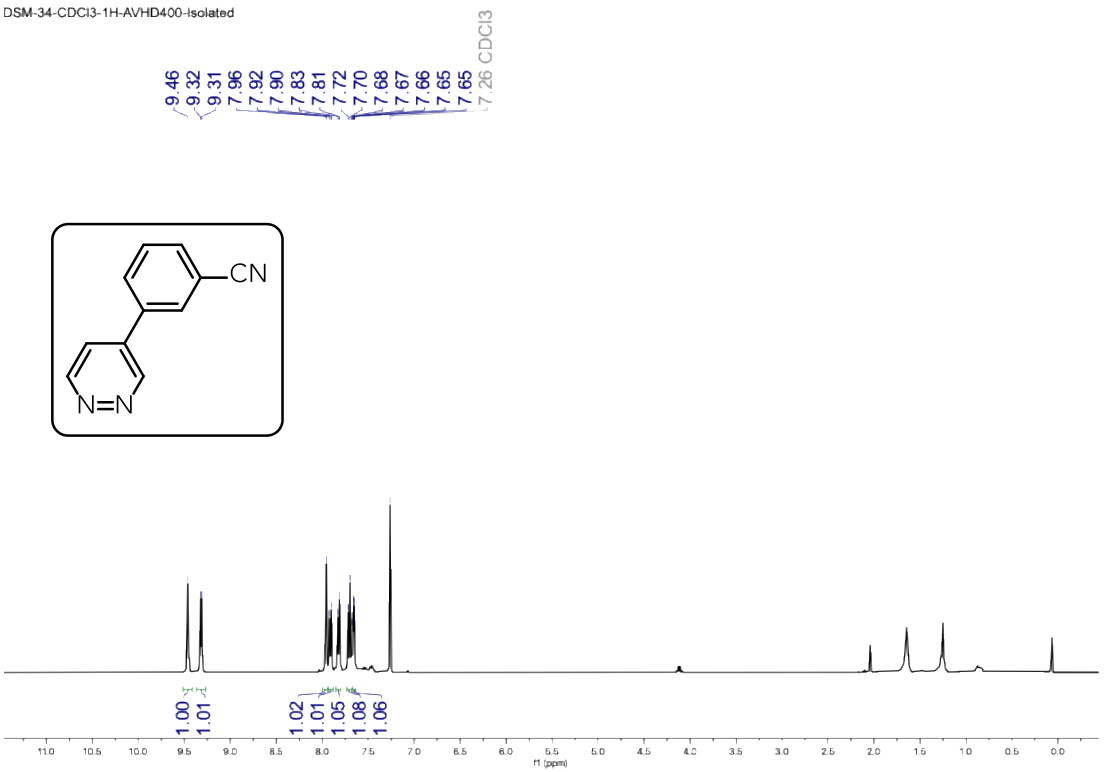

Figure S69. ^{1}H NMR spectrum of **26** in $CDCl_3$ at 25 ºC.

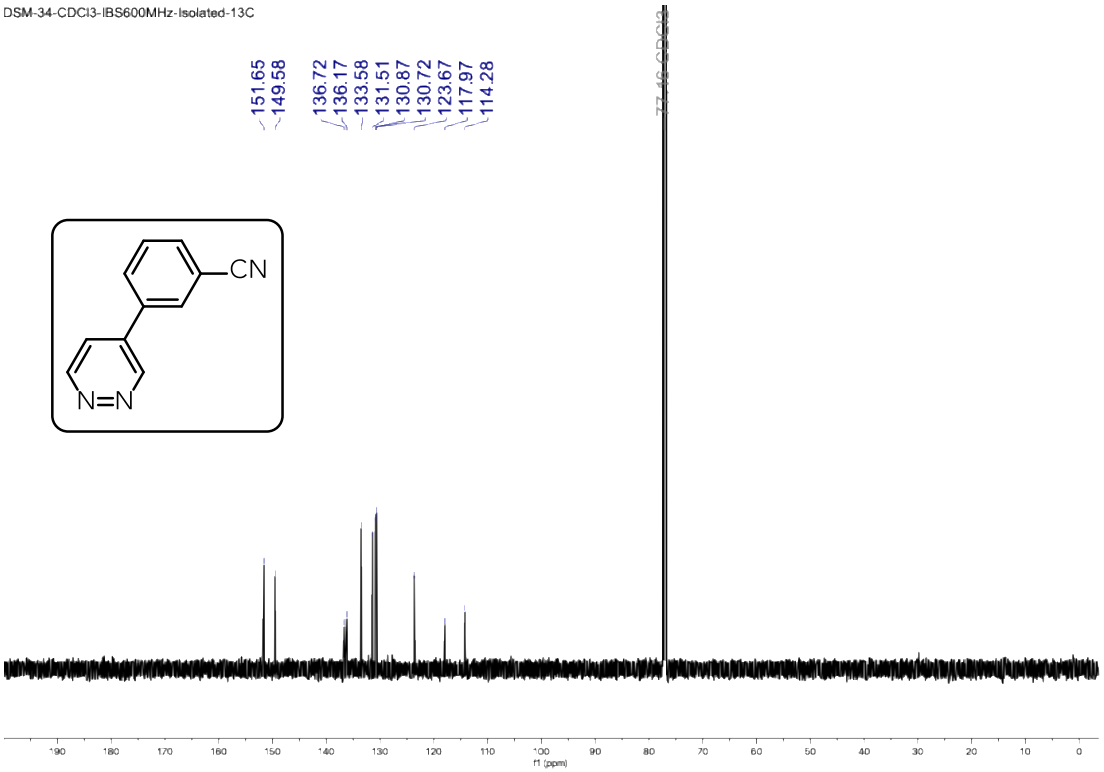

Figure S70. ^{13}C NMR spectrum of **26** in $CDCl_3$ at 25 ºC.

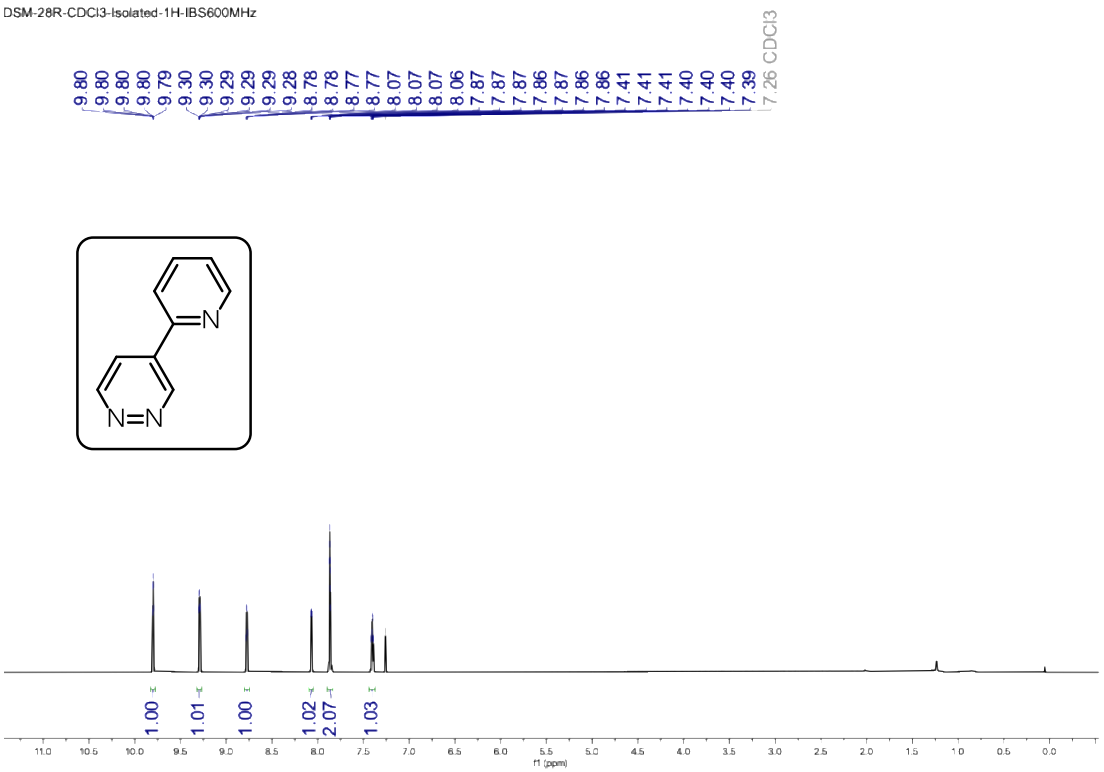

Figure S71. ^{1}H NMR spectrum of **27** in $CDCl_3$ at 25 ºC.

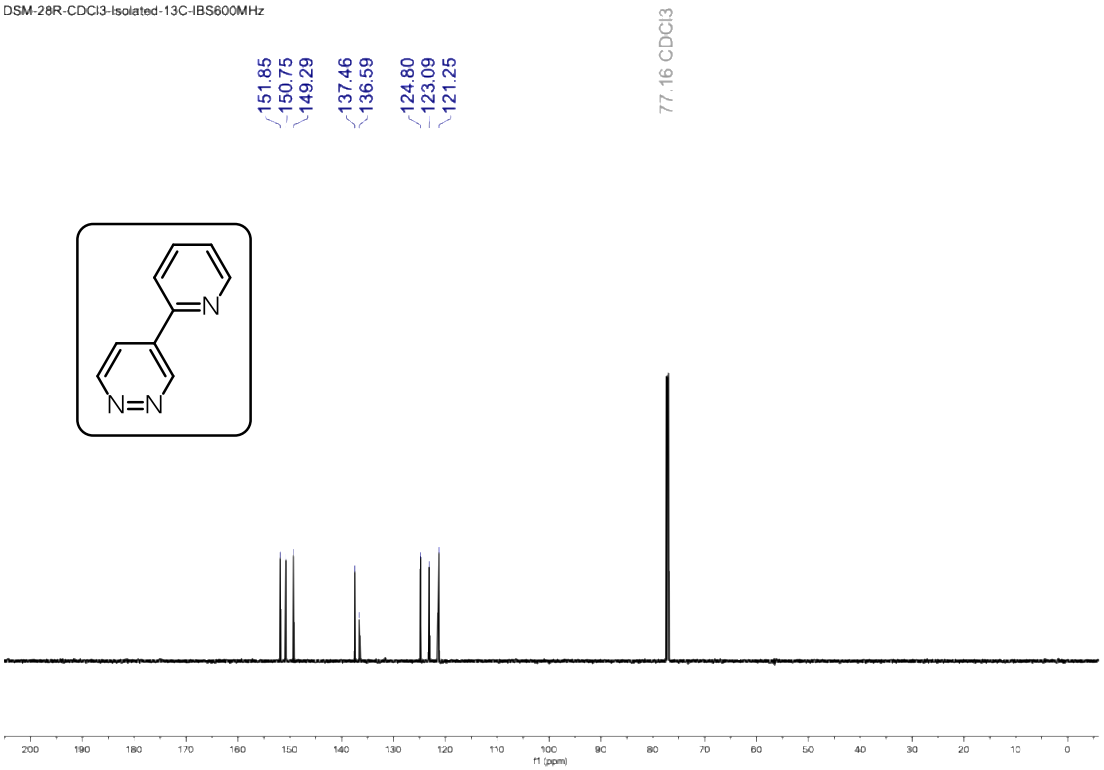

Figure S72. ^{13}C NMR spectrum of **27** in $CDCl_3$ at 25 ºC.

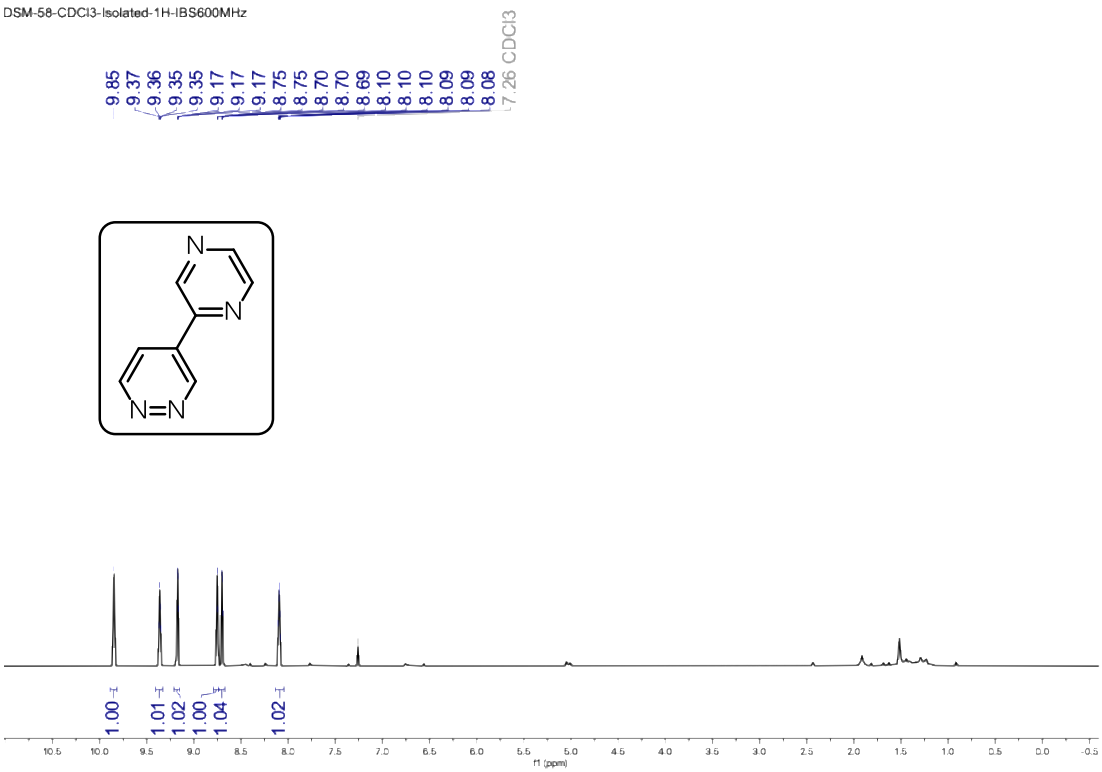

Figure S73. ^{1}H NMR spectrum of **28** in $CDCl_3$ at 25 ºC.

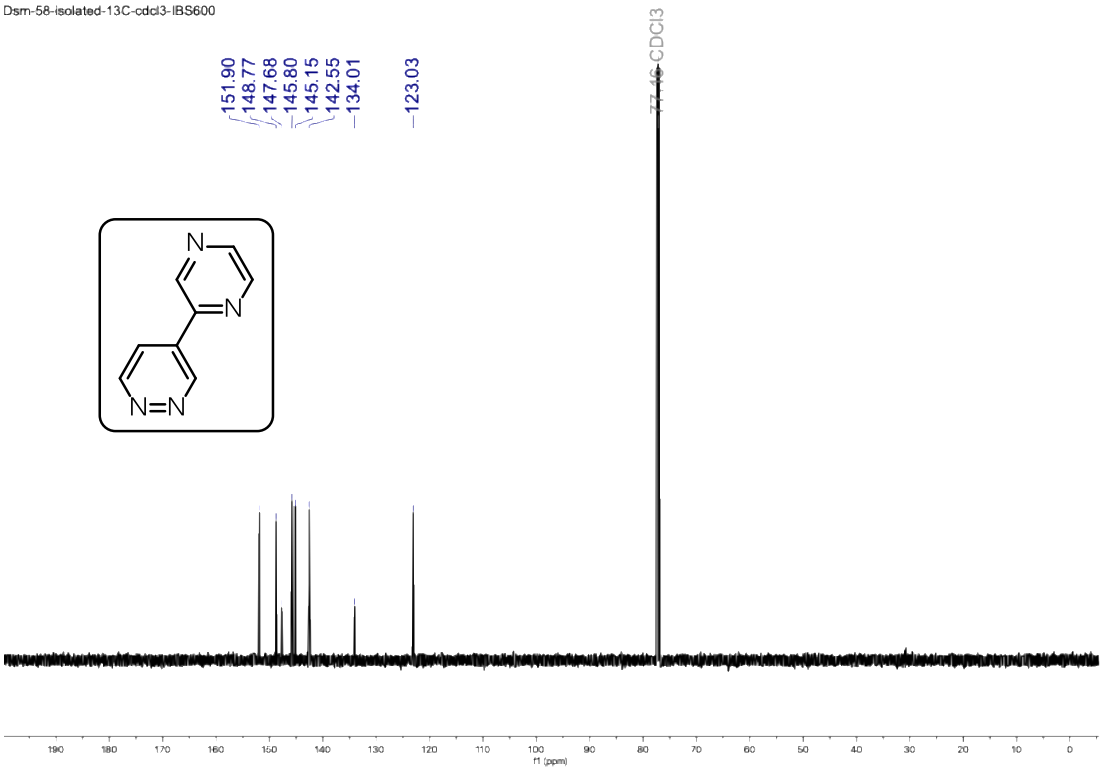

Figure S74. ^{13}C NMR spectrum of **28** in $CDCl_3$ at 25 ºC.

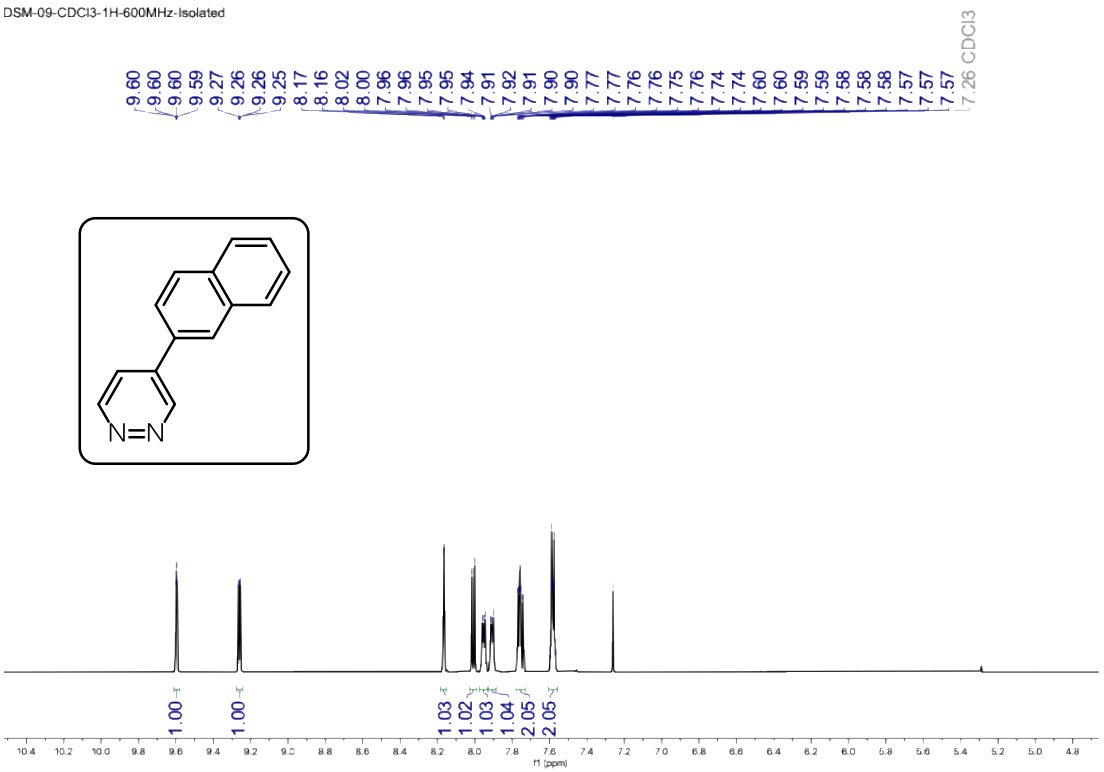

Figure S75. ^{1}H NMR spectrum of **29** in $CDCl_3$ at 25 ºC.

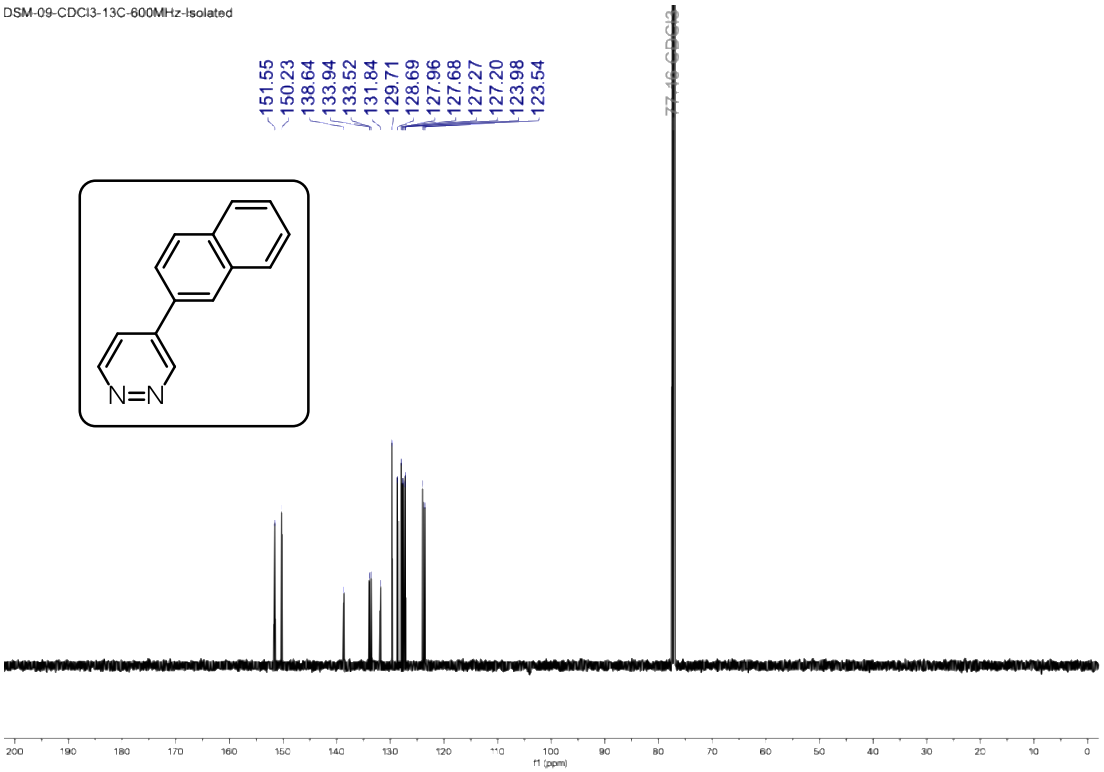

Figure S76. ^{13}C NMR spectrum of **29** in $CDCl_3$ at 25 ºC.

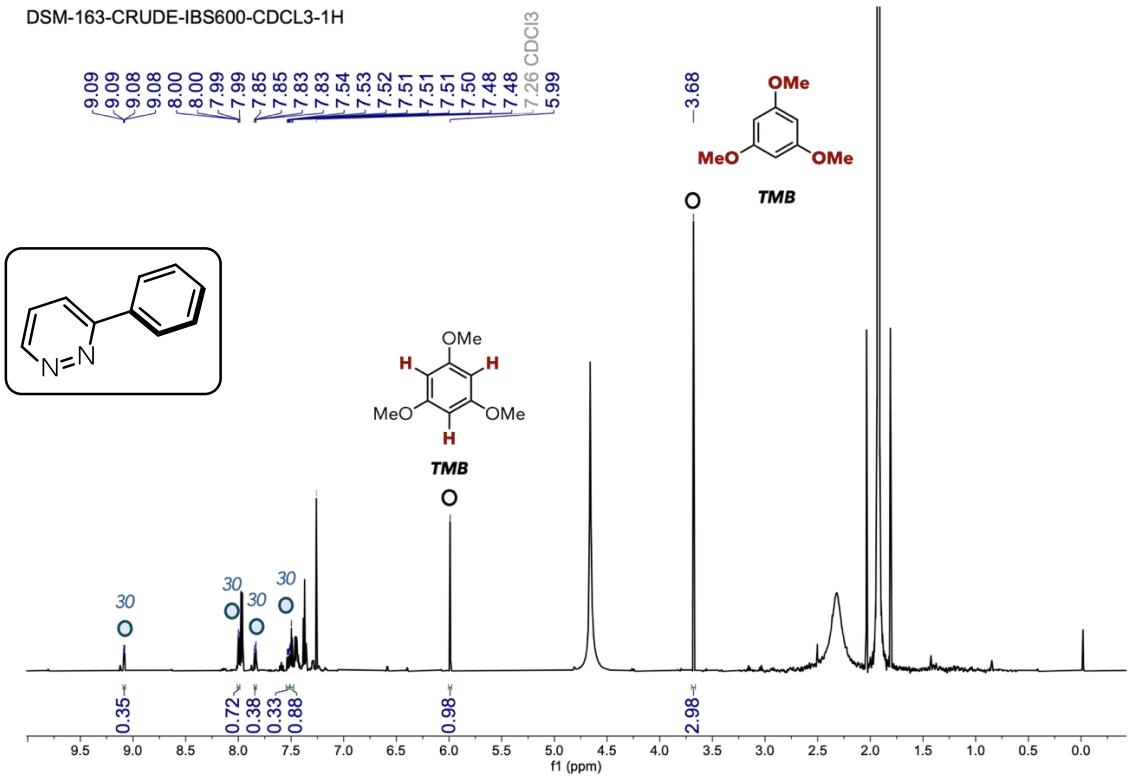

Figure S77. ^{1}H NMR spectrum of **30** in $CDCl_3$ at 25 °C.

* This NMR spectrum was obtained right after reaction completion with 1,3,5-trimethoxybenzene (TMB) as an internal standard.

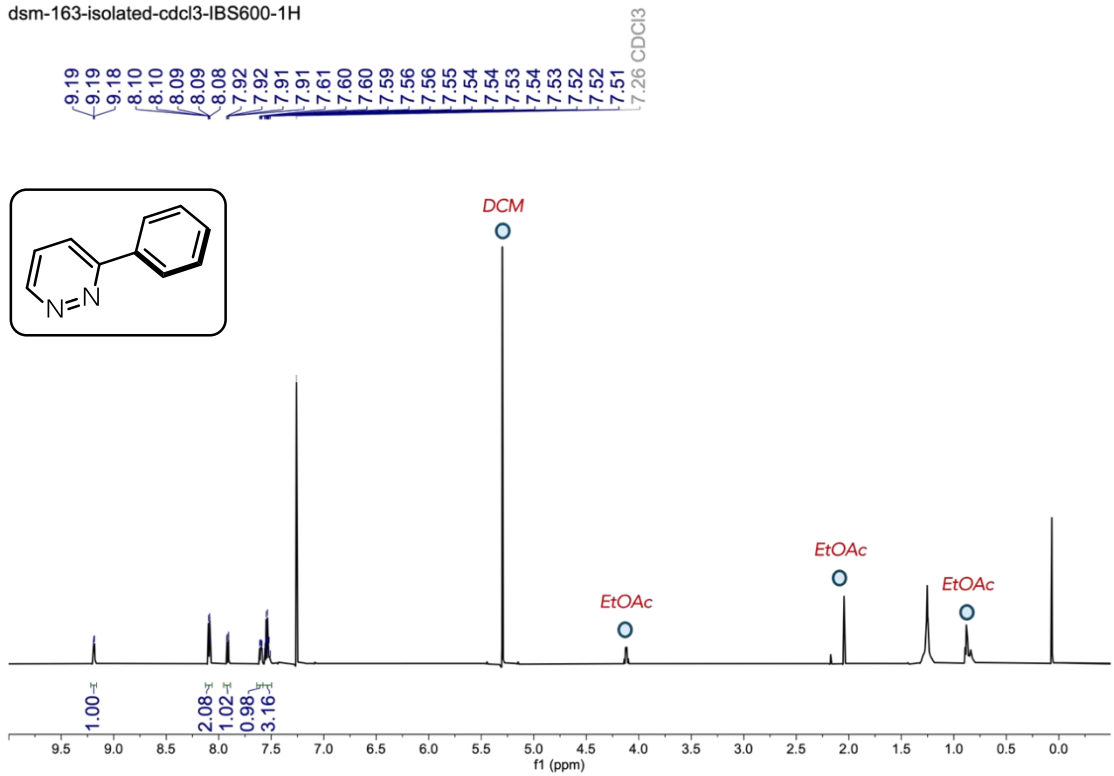

Figure S78. ^{1}H NMR spectrum of **30** in $CDCl_3$ at 25 °C.

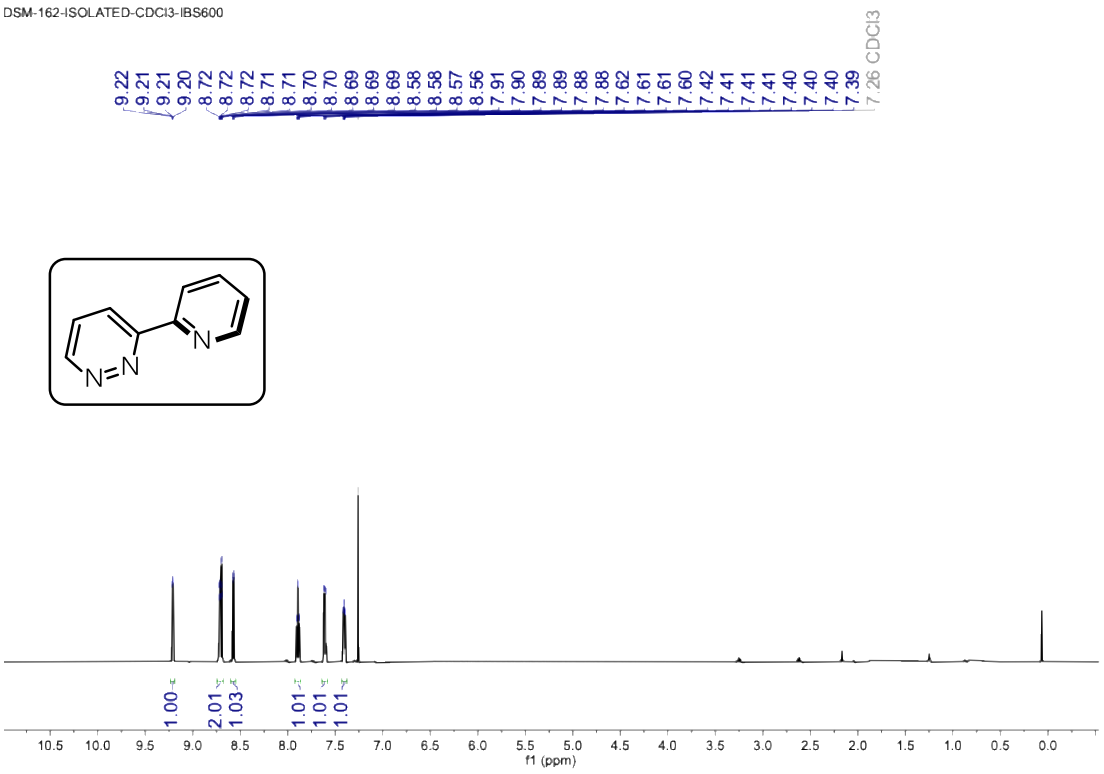

Figure S79. ^{1}H NMR spectrum of **31** in $CDCl_3$ at 25 ºC.

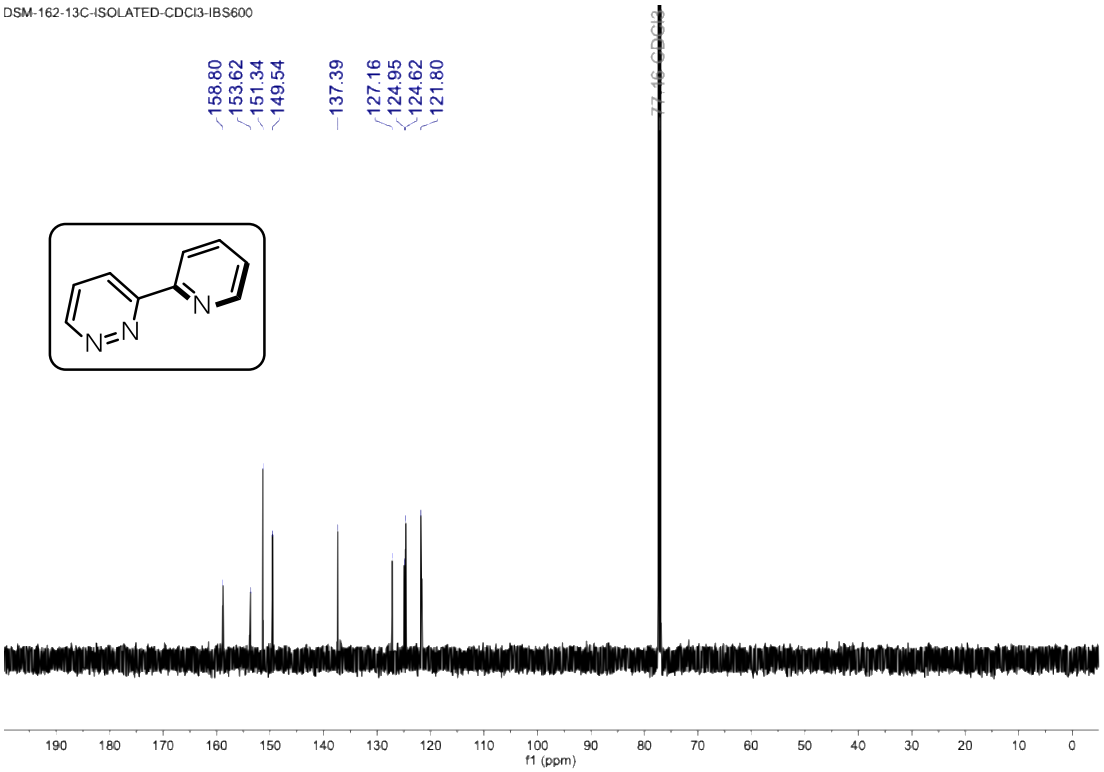

Figure S80. ^{13}C NMR spectrum of **31** in $CDCl_3$ at 25 ºC.

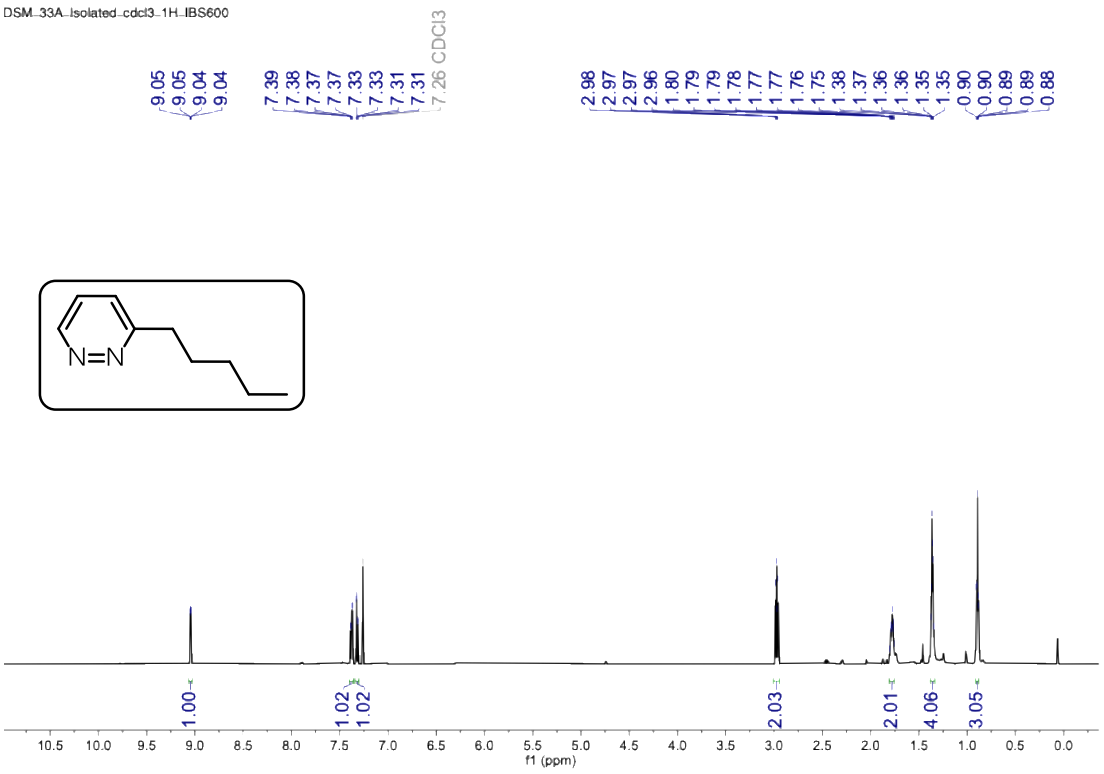

Figure S81. ^{1}H NMR spectrum of **32** in $CDCl_3$ at 25 ºC.

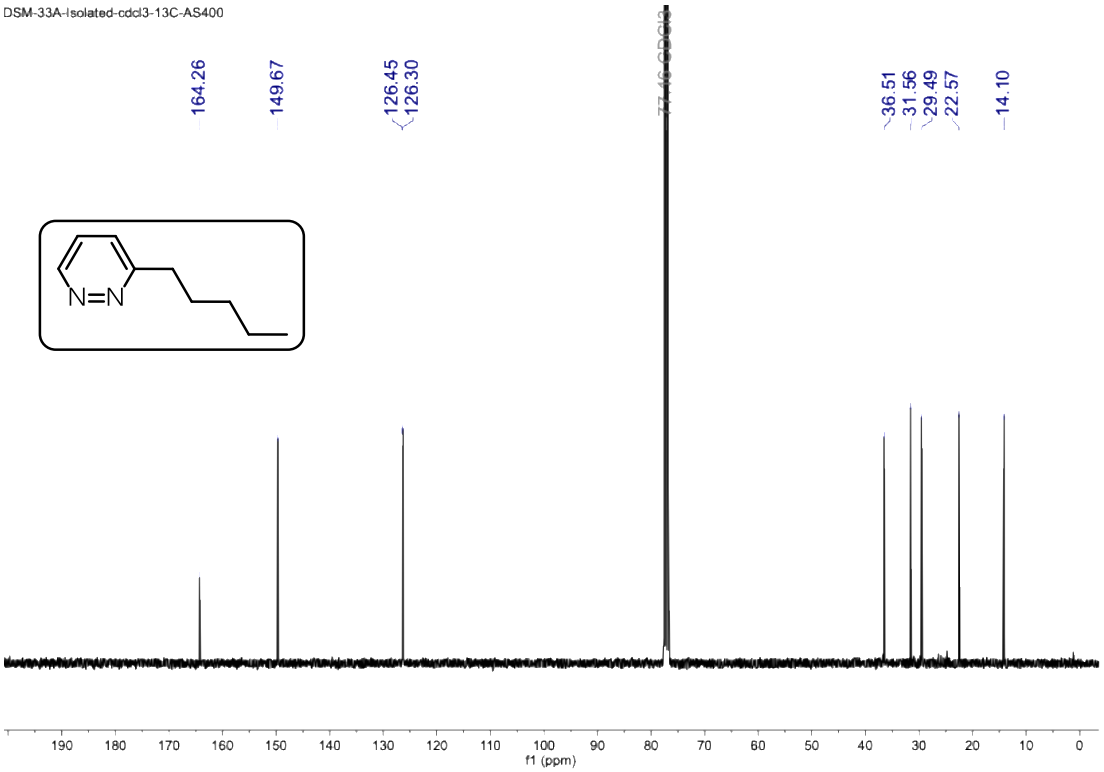

Figure S82. ^{13}C NMR spectrum of **32** in $CDCl_3$ at 25 ºC.

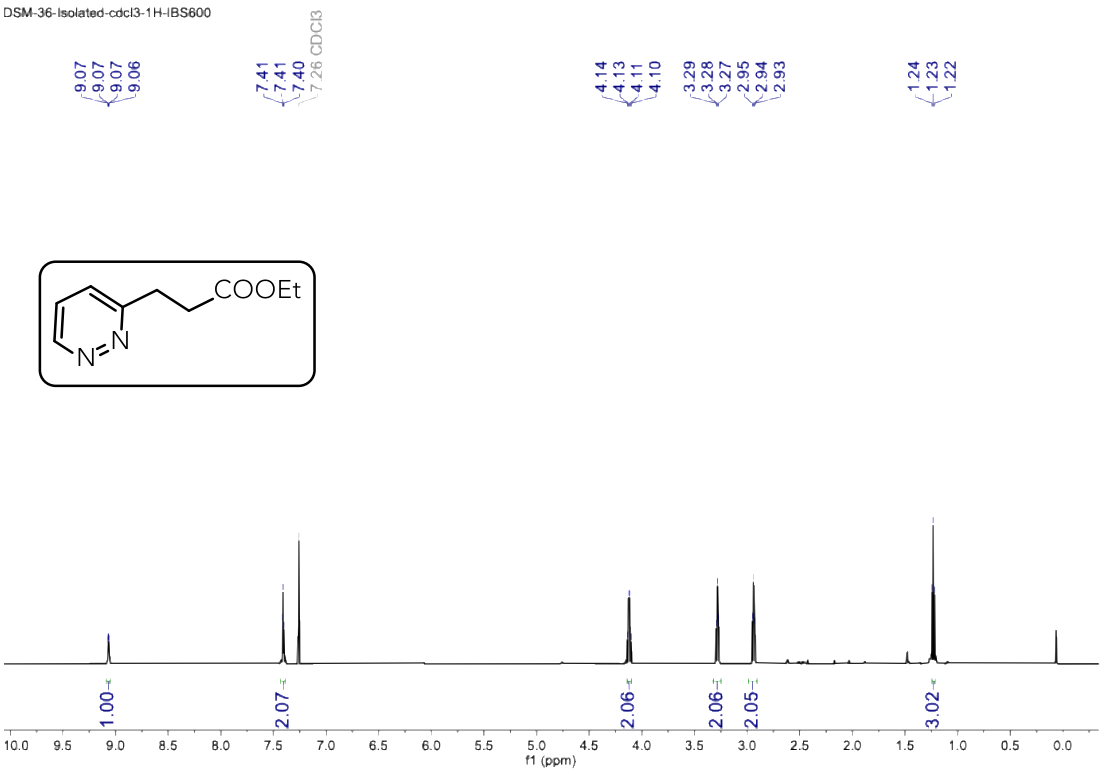

Figure S83. ^{1}H NMR spectrum of **33** in $CDCl_3$ at 25 ºC.

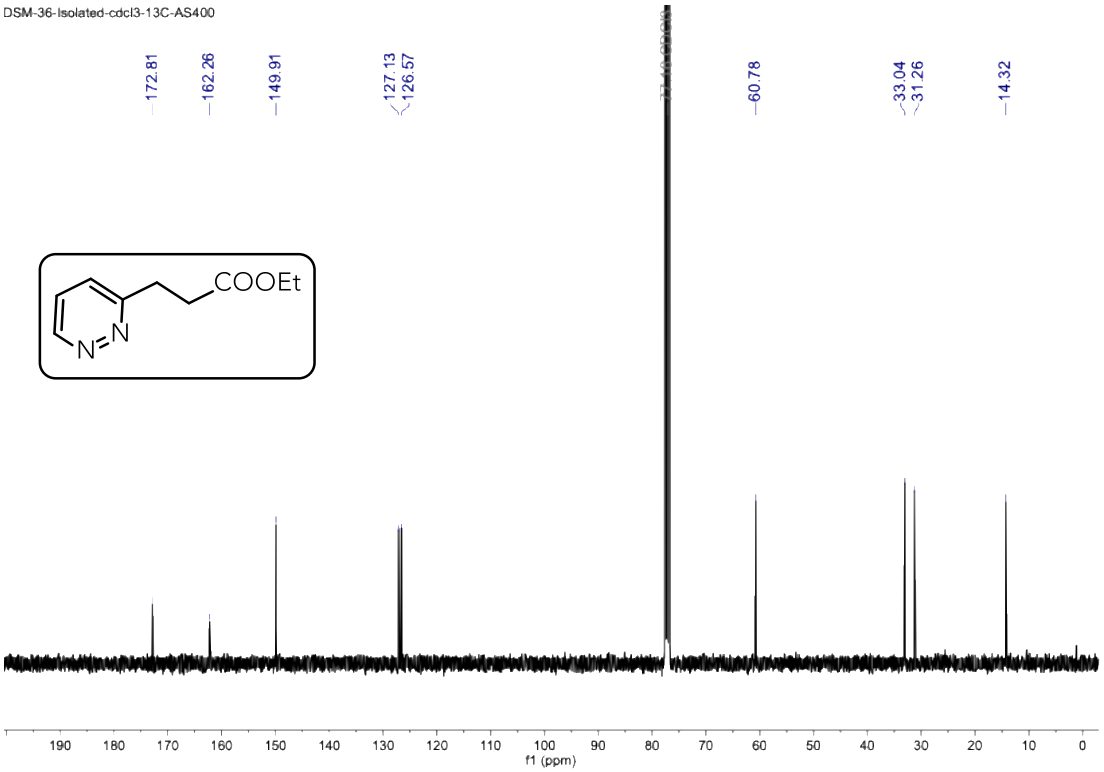

Figure S84. ^{13}C NMR spectrum of **33** in $CDCl_3$ at 25 ºC.

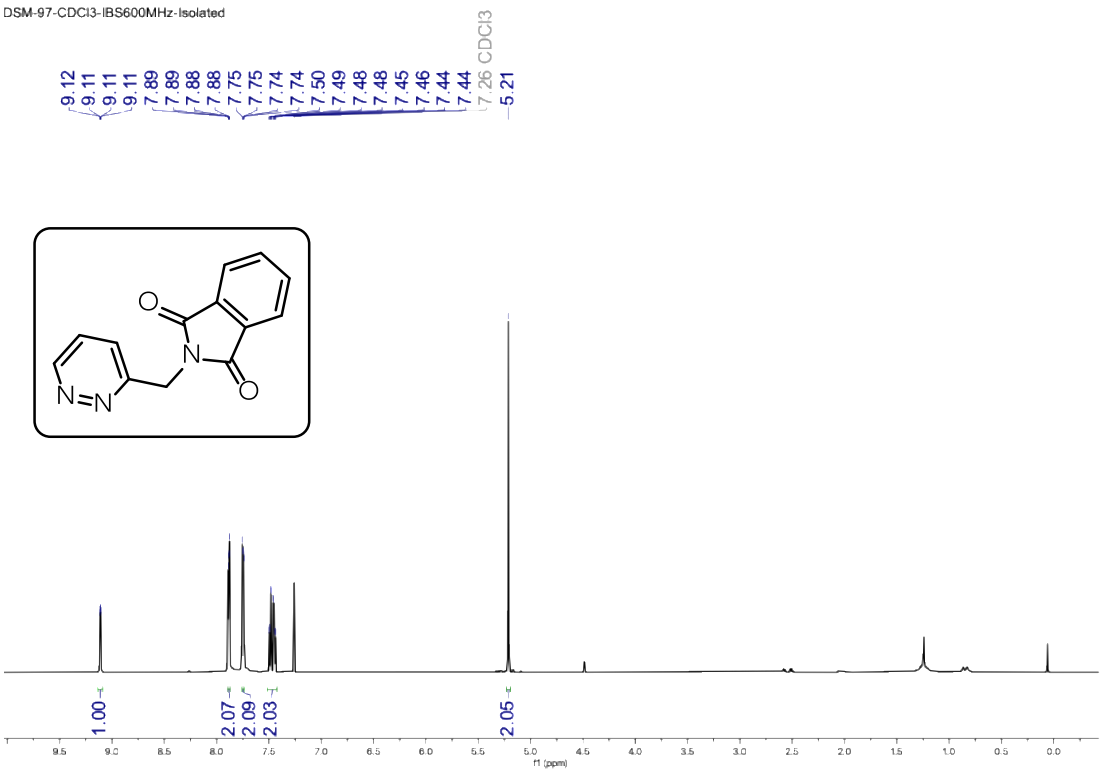

Figure S85. ^{1}H NMR spectrum of **34** in $CDCl_3$ at 25 ºC.

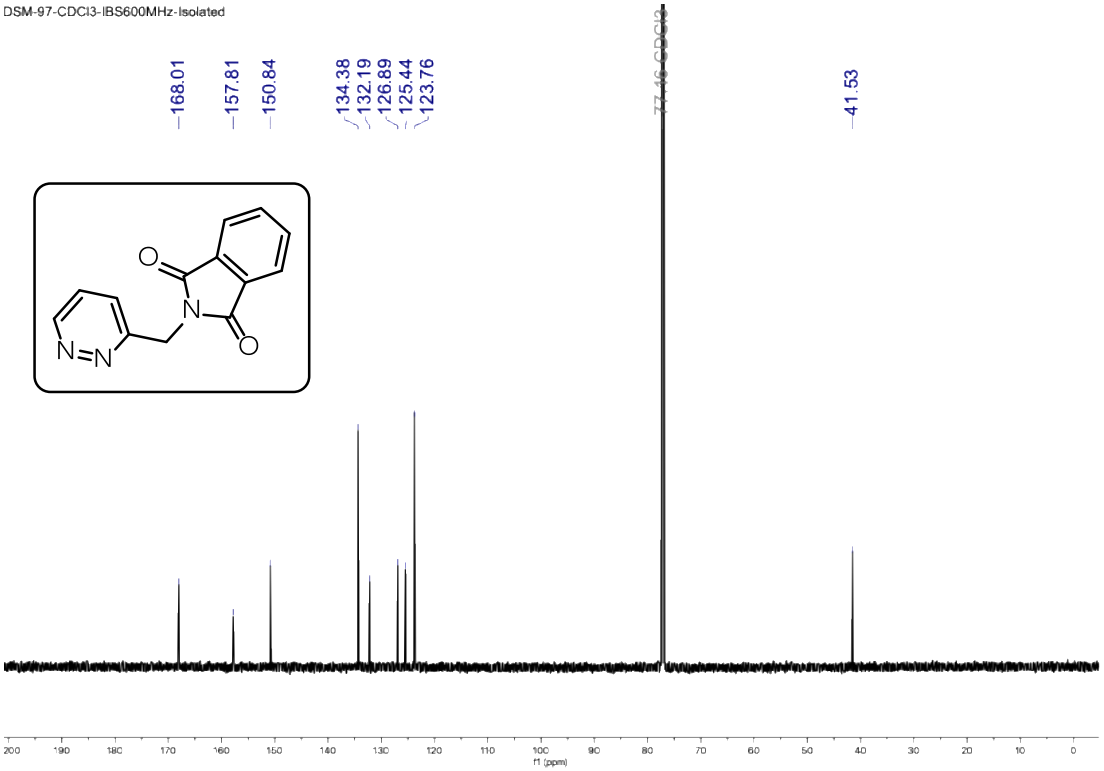

Figure S86. ^{13}C NMR spectrum of **34** in $CDCl_3$ at 25 ºC.

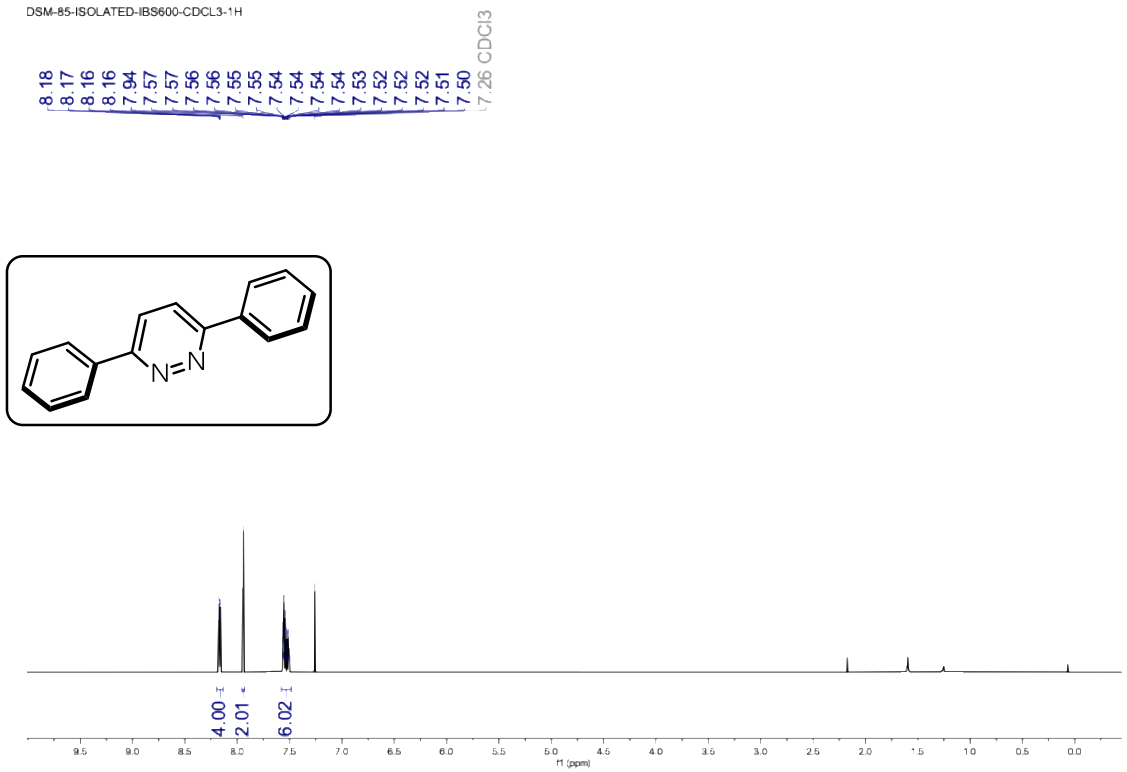

Figure S87. ^{1}H NMR spectrum of **35** in $CDCl_3$ at 25 ºC.

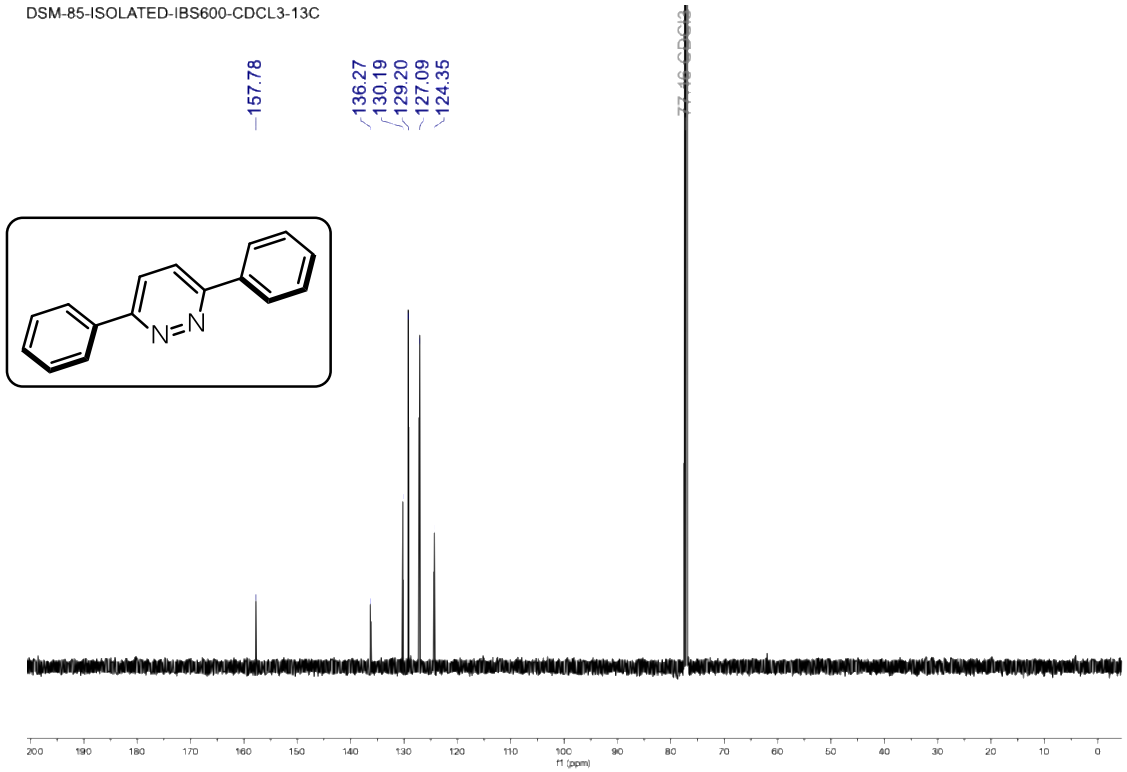

Figure S88. ^{13}C NMR spectrum of **35** in $CDCl_3$ at 25 ºC.

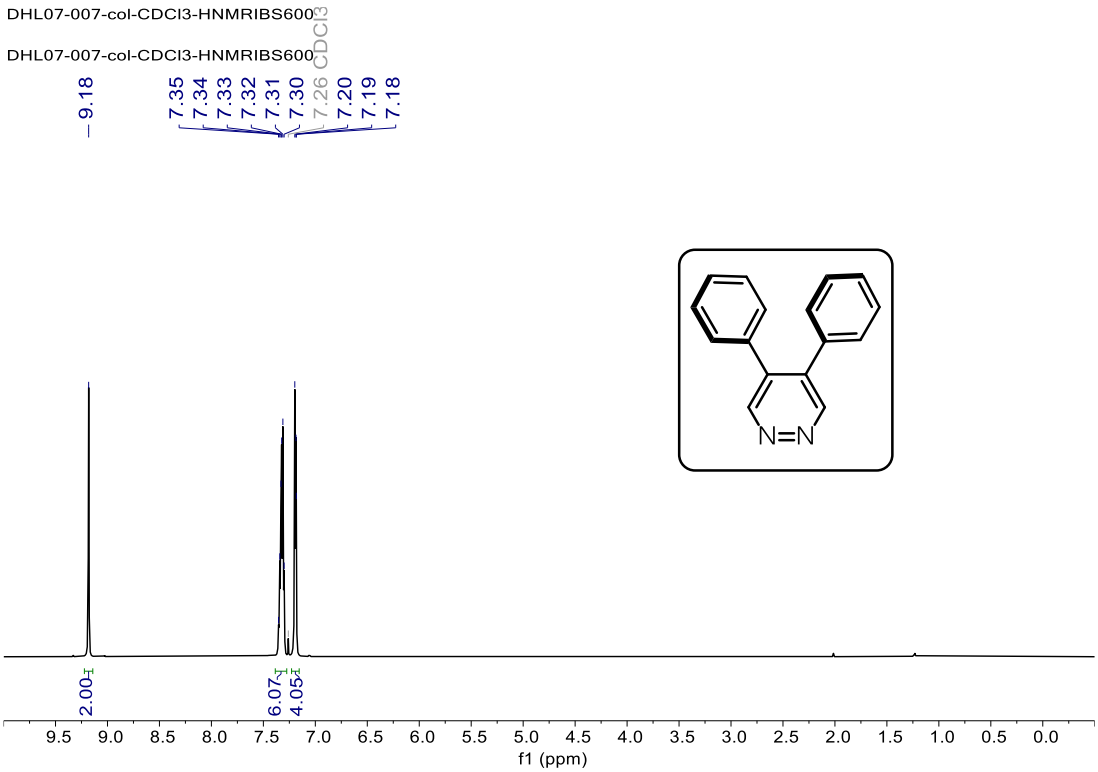

Figure S89. ^{1}H NMR spectrum of **4** in $CDCl_3$ at 25 ºC.

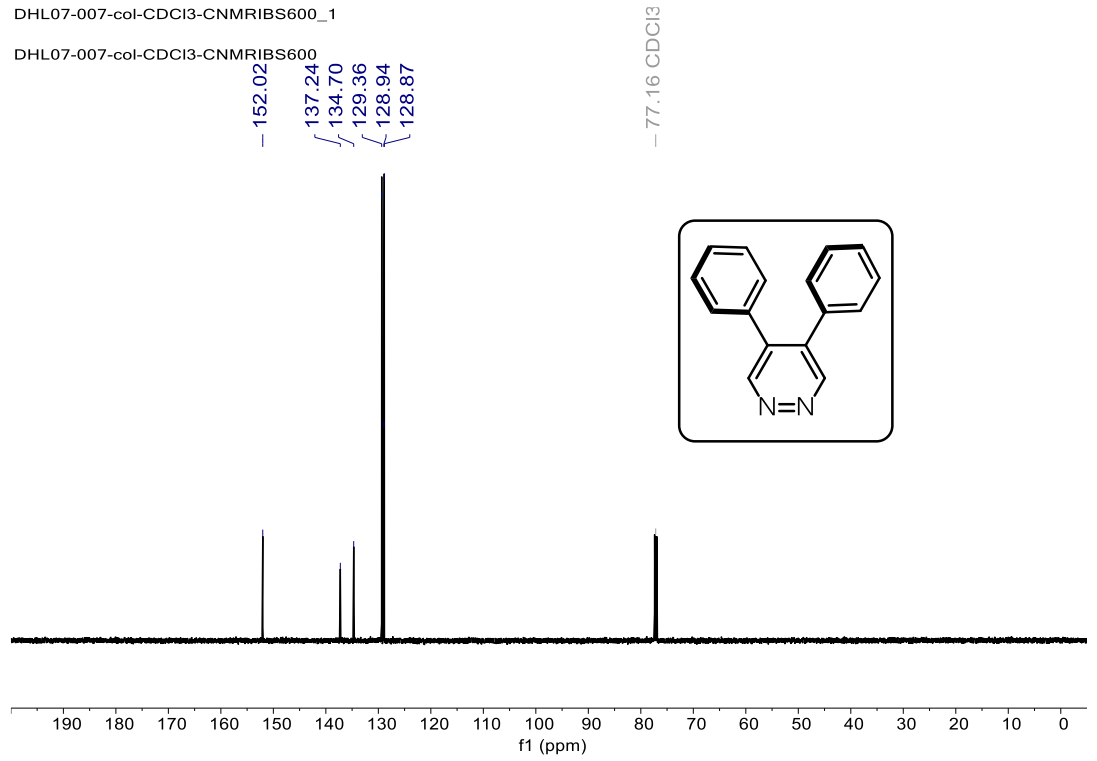

Figure S90. ^{13}C NMR spectrum of **4** in $CDCl_3$ at 25 ºC.

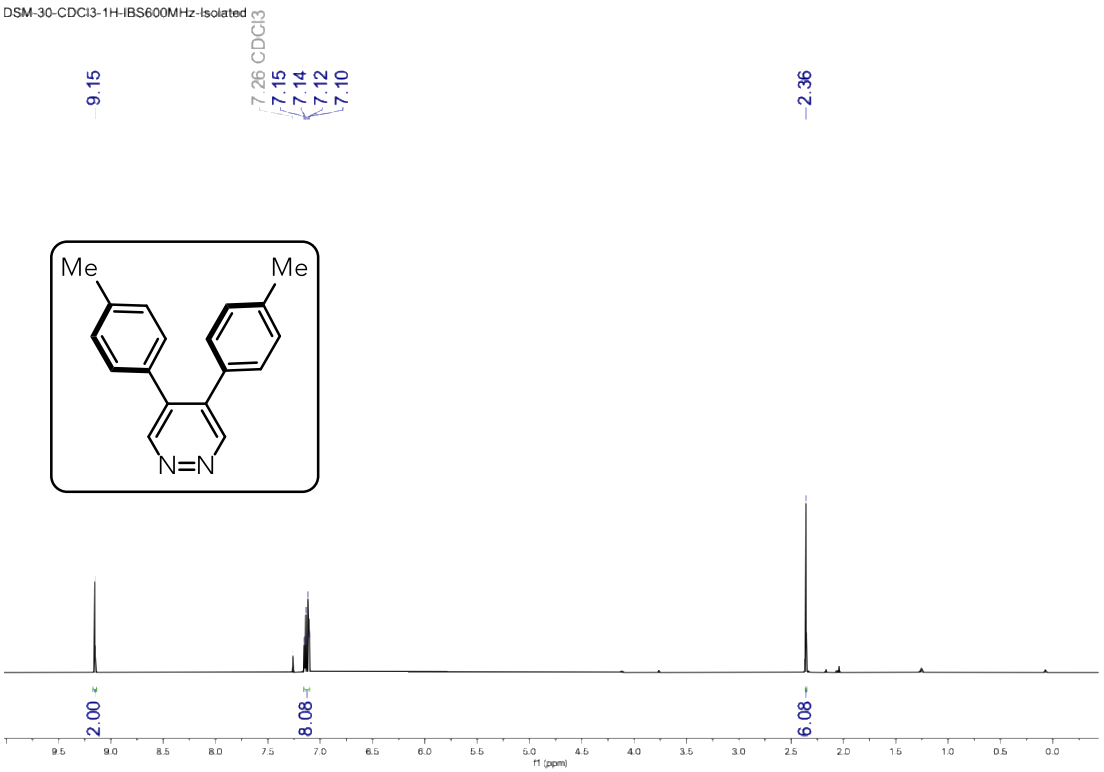

Figure S91. ^{1}H NMR spectrum of **36** in $CDCl_3$ at 25 ºC.

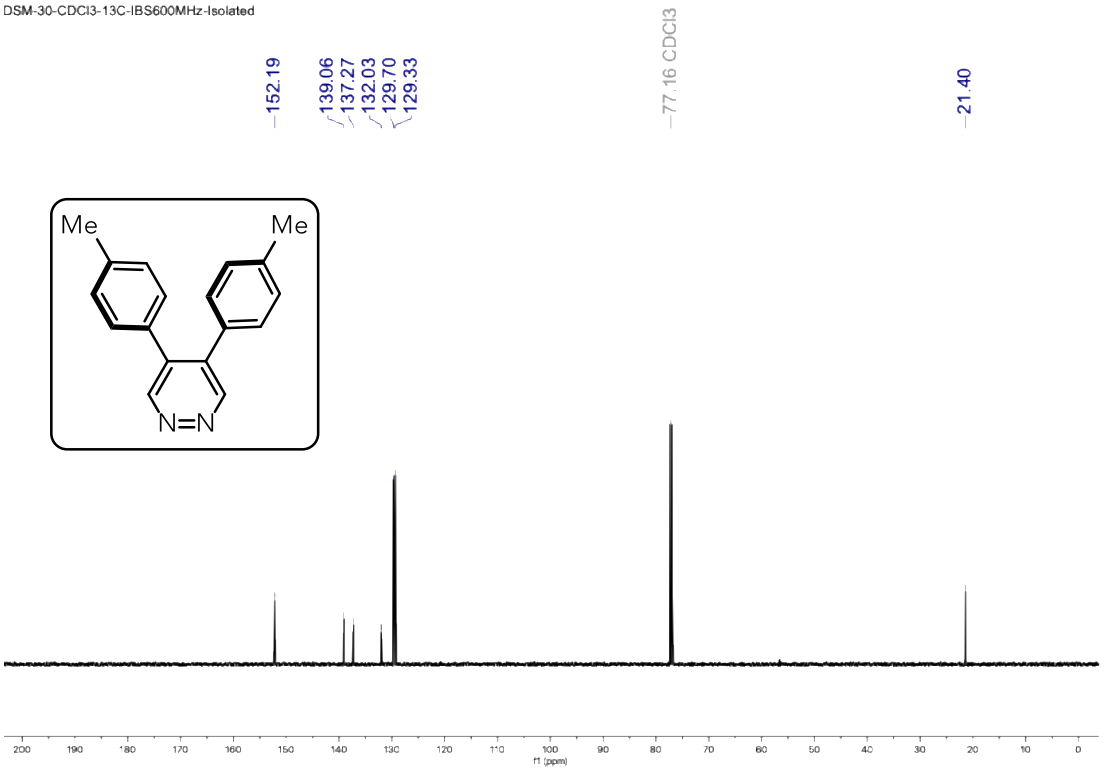

Figure S92. ^{13}C NMR spectrum of **36** in $CDCl_3$ at 25 ºC.

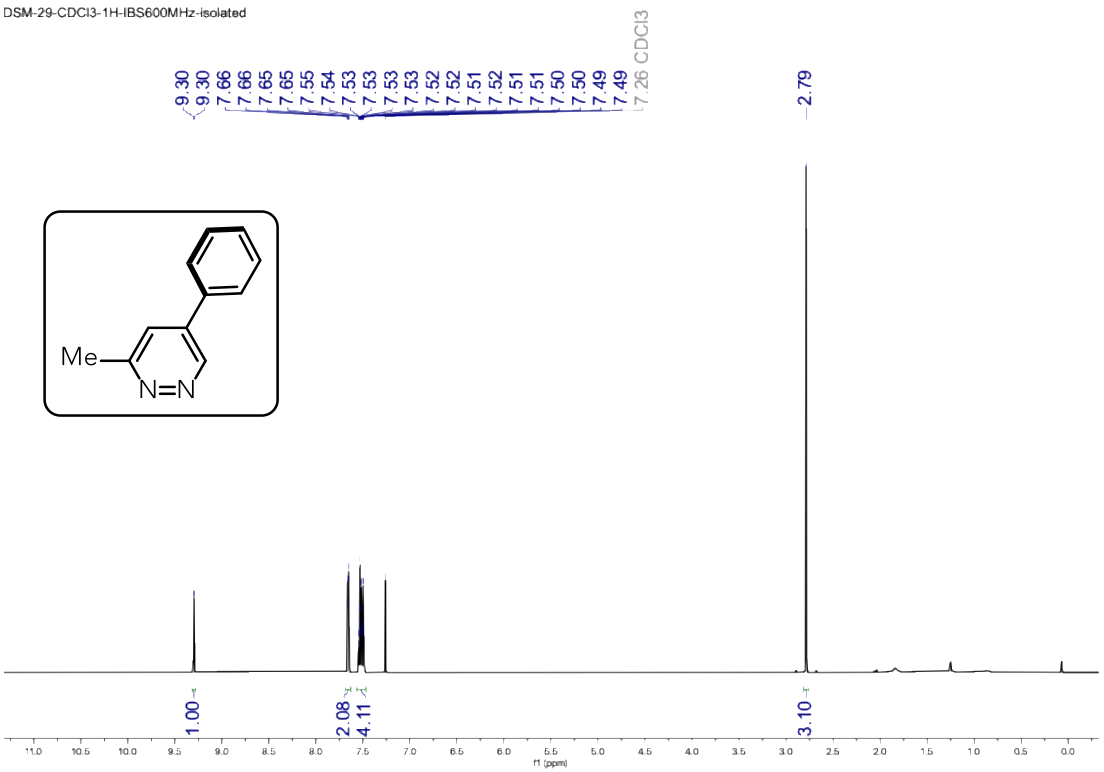

Figure S93. ^{1}H NMR spectrum of **37** in $CDCl_3$ at 25 °C.

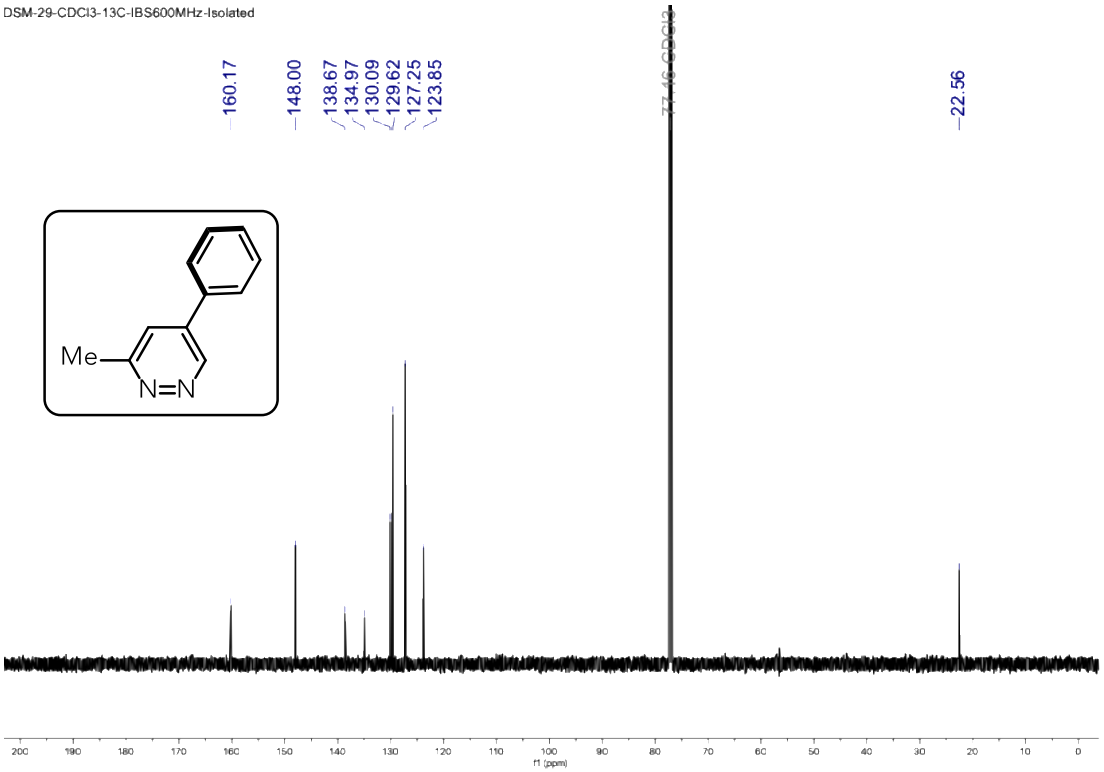

Figure S94. ^{13}C NMR spectrum of **37** in $CDCl_3$ at 25 °C.

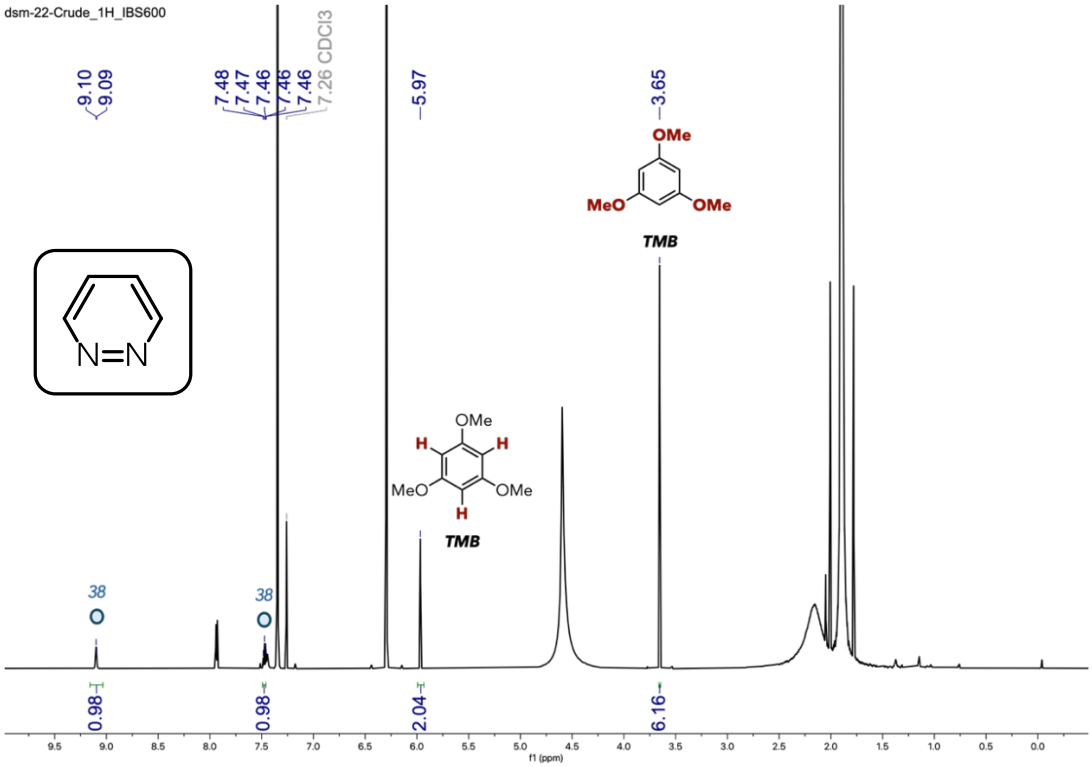

Figure S95. ^{1}H NMR spectrum of **38** in $CDCl_3$ at 25 °C.
* This NMR spectrum was obtained right after reaction completion with 1,3,5-trimethoxybenzene (TMB) as an internal standard.

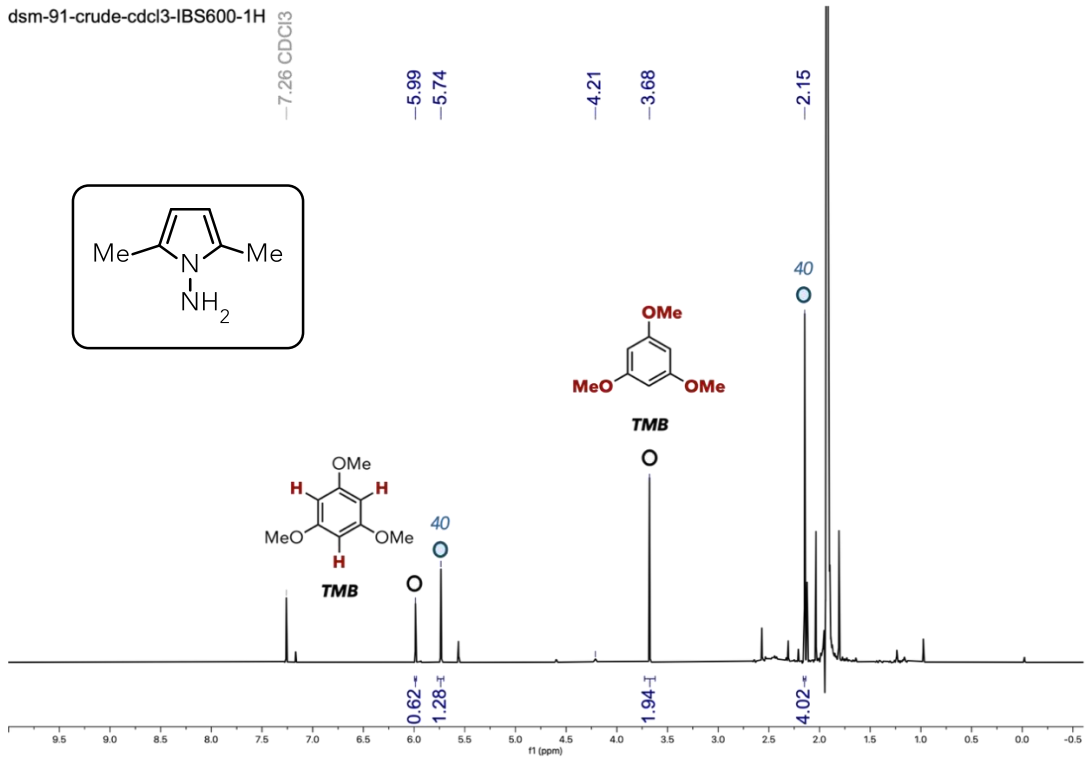

Figure S96. ^{1}H NMR spectrum of **39** in $CDCl_3$ at 25 °C.
* This NMR spectrum was obtained right after reaction completion with 1,3,5-trimethoxybenzene (TMB) as an internal standard.

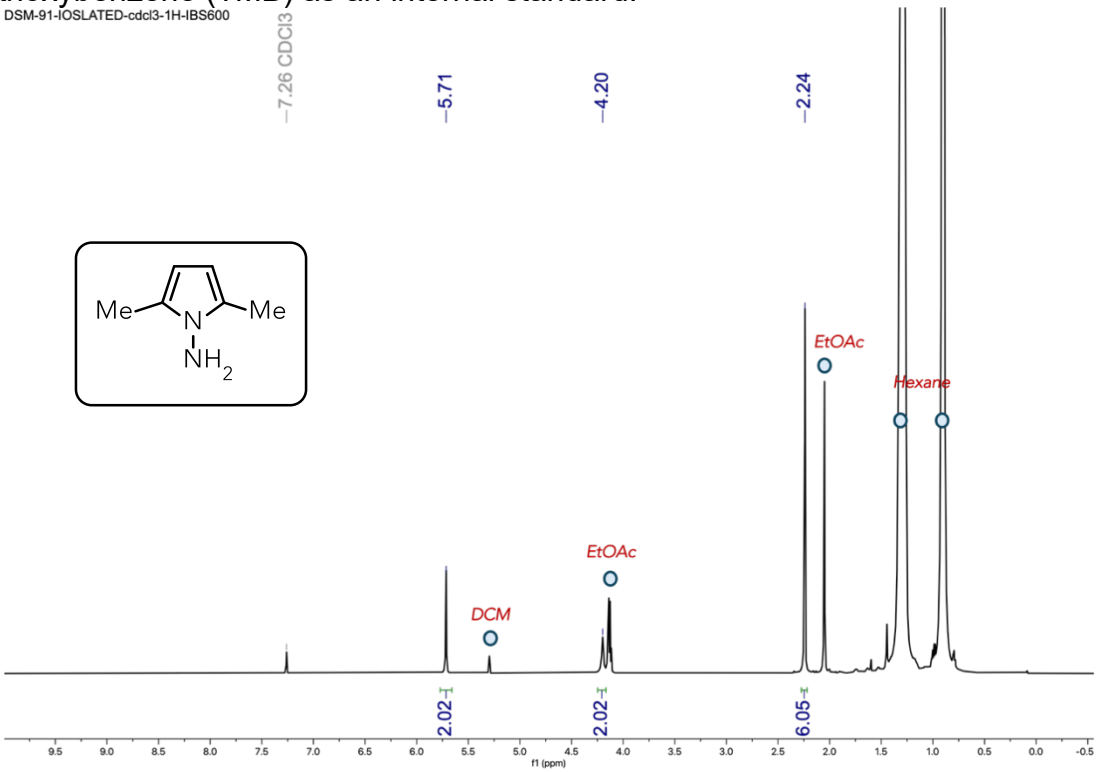

Figure S97. ^{1}H NMR spectrum of **39** in $CDCl_3$ at 25 °C.
* This NMR spectrum is obtained with a solvent because of volatility.

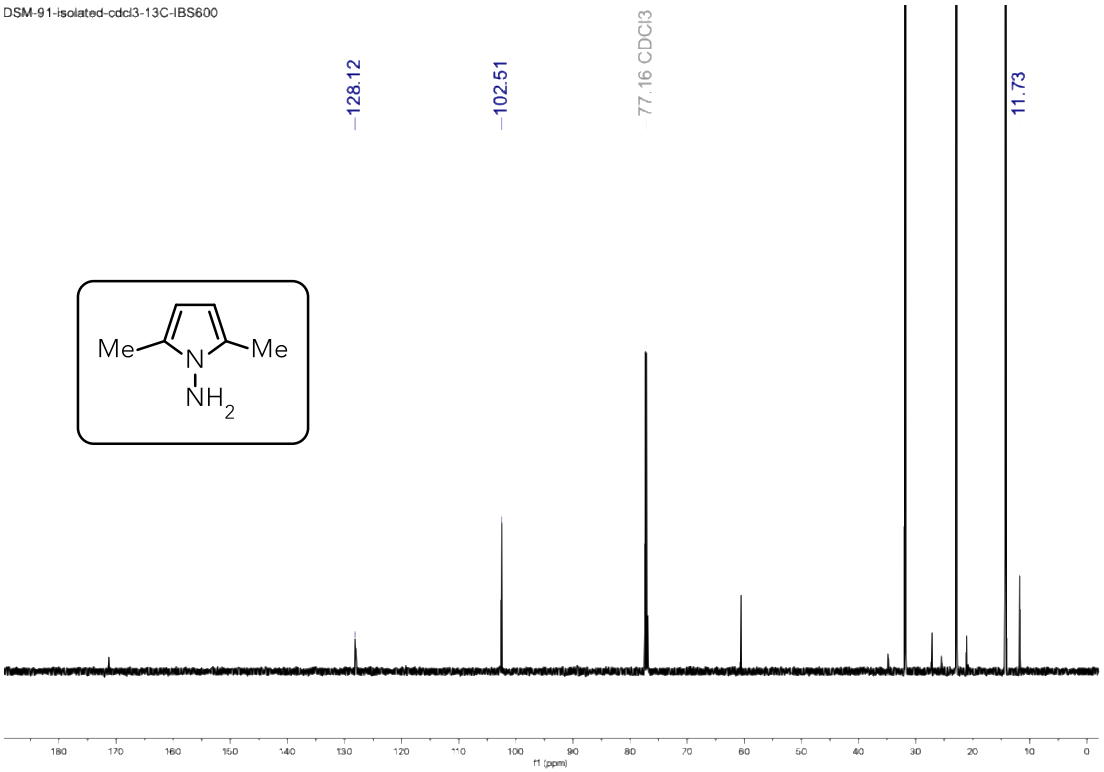

Figure S98. ^{13}C NMR spectrum of **39** in $CDCl_3$ at 25 ºC.
* This NMR spectrum is obtained with a solvent because of volatility.

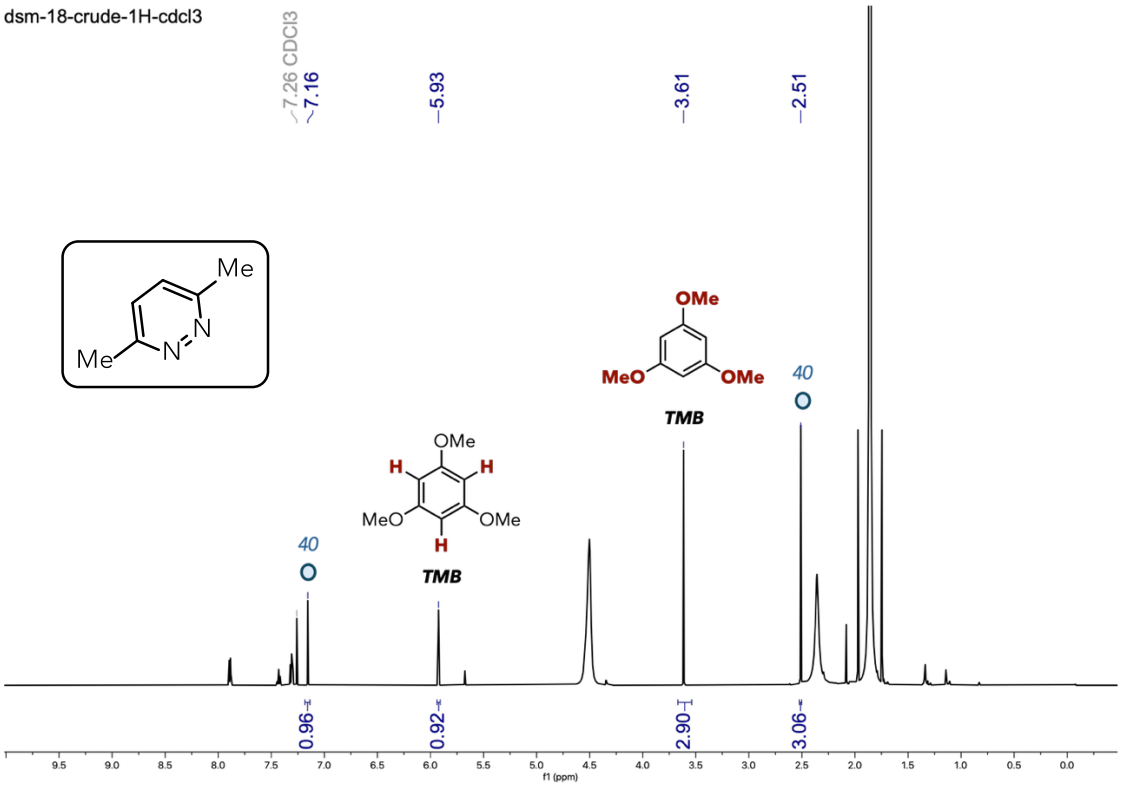

Figure S99. ^{1}H NMR spectrum of **40** in $CDCl_3$ at 25 ºC.
* This NMR spectrum was obtained right after reaction completion with 1,3,5-trimethoxybenzene (TMB) as an internal standard.

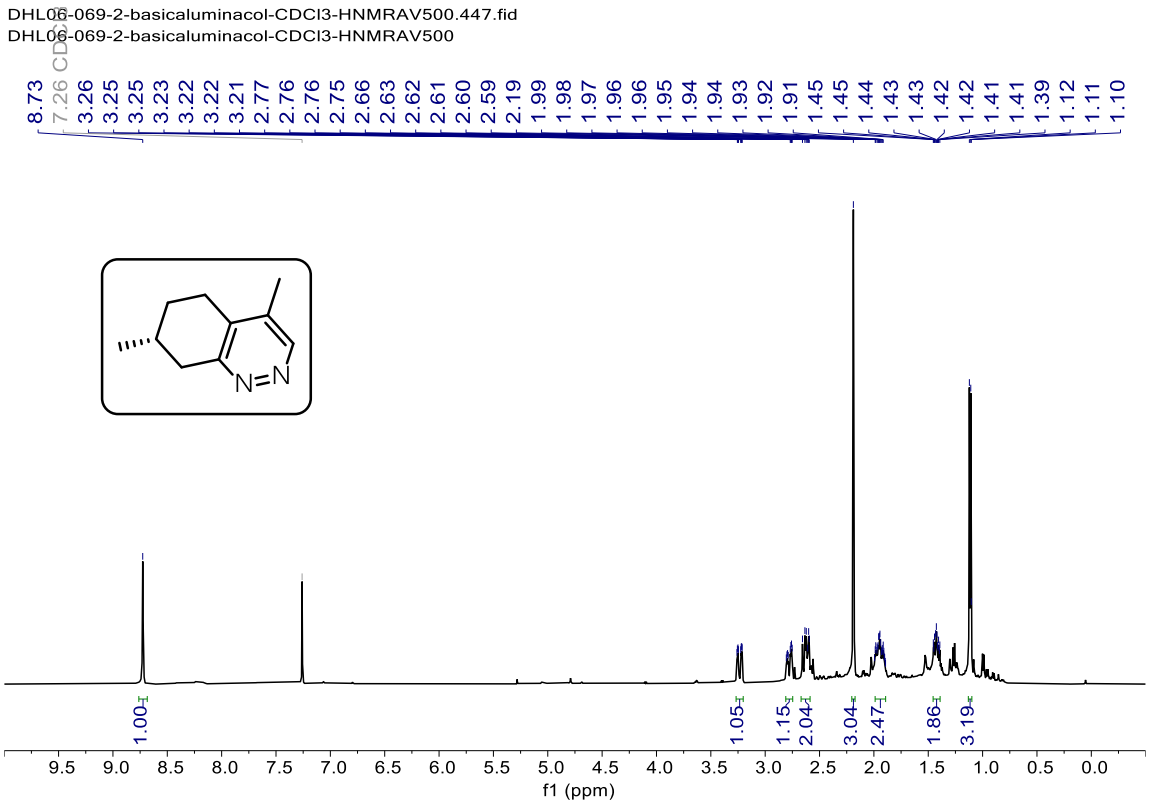

Figure S100. ^{1}H NMR spectrum of **41** in $CDCl_3$ at 25 °C.

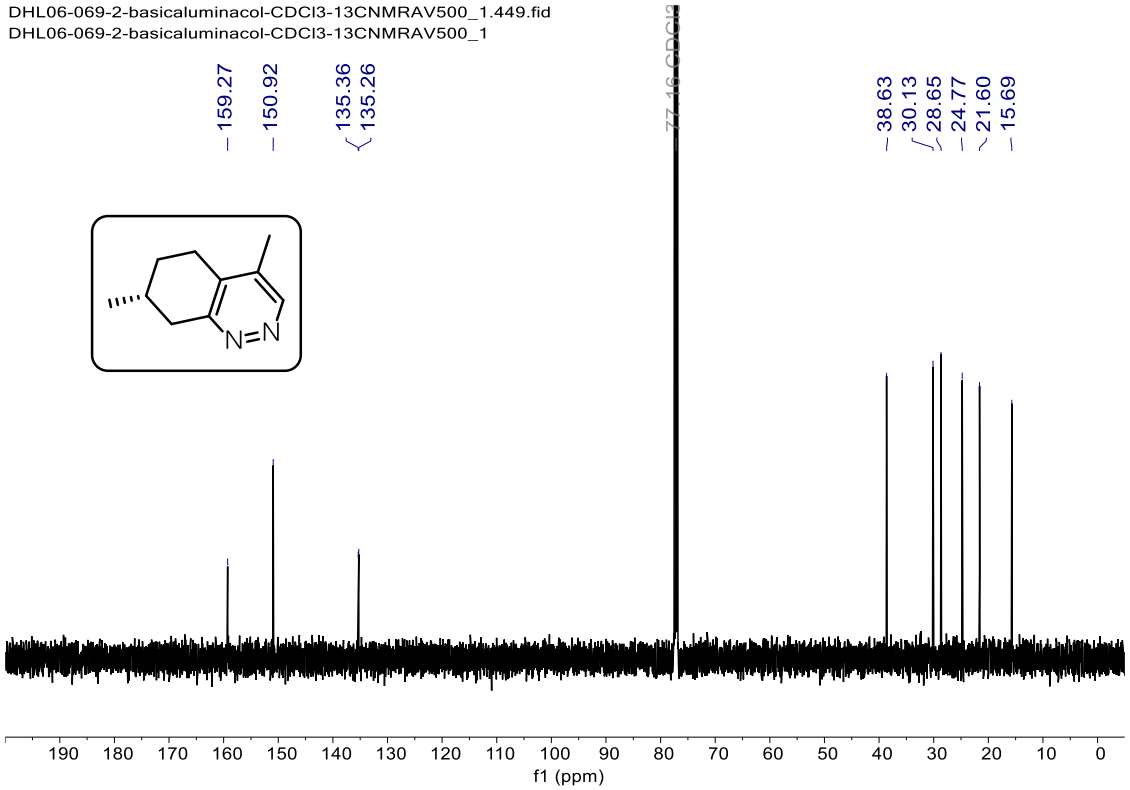

Figure S101. ^{13}C NMR spectrum of **41** in $CDCl_3$ at 25 °C.

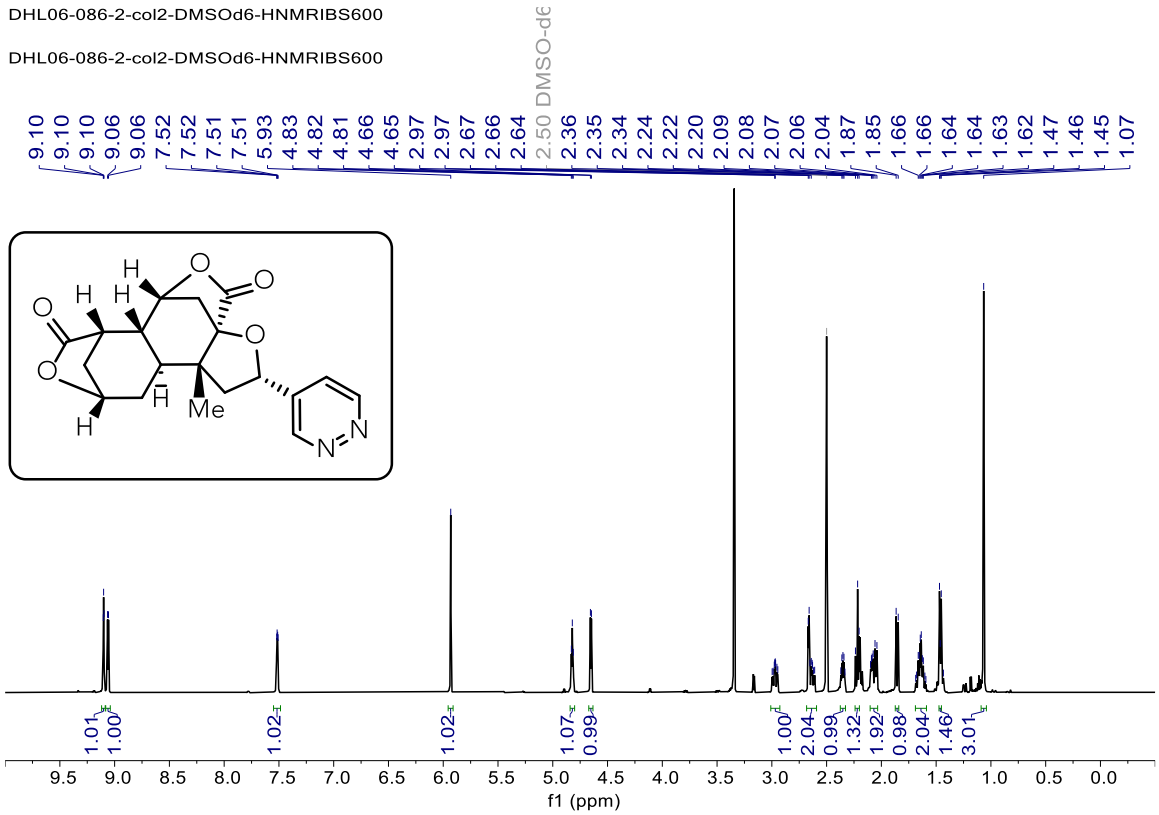

Figure S102. ^{1}H NMR spectrum of **42** in DMSO-d_6 at 25 °C.

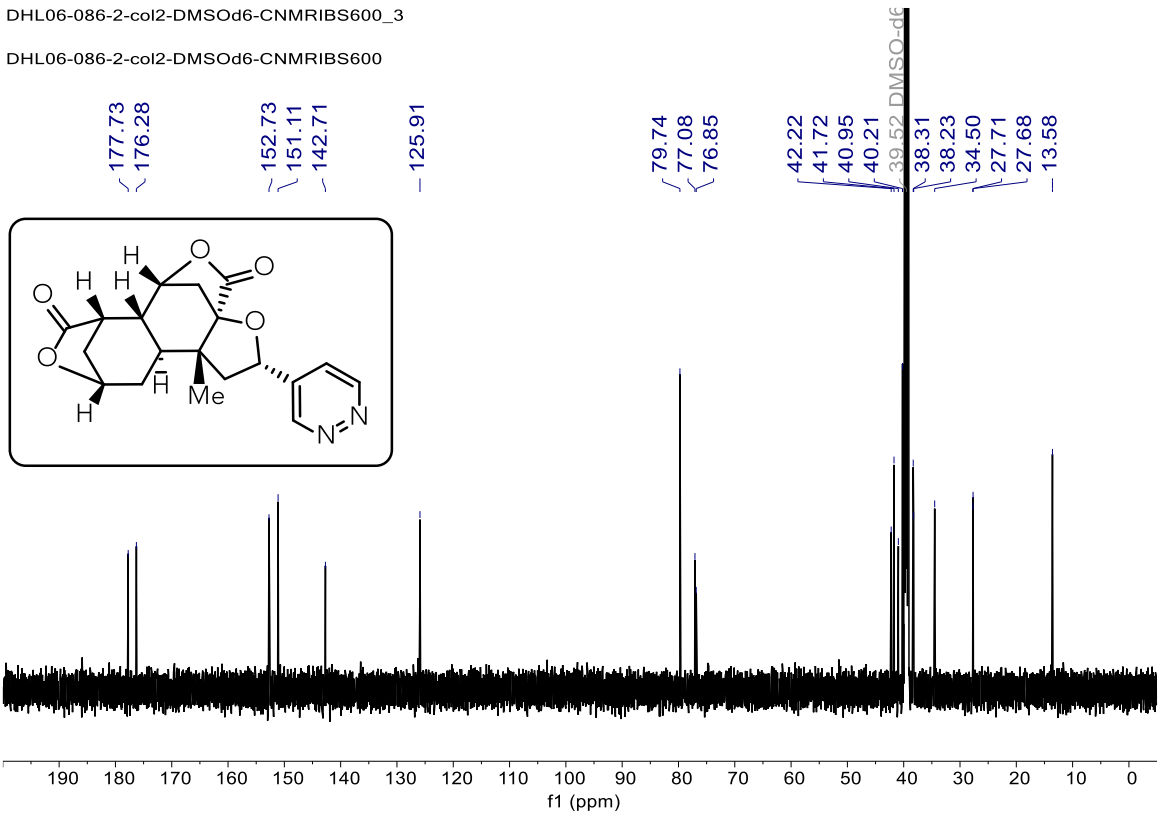

Figure S103. ^{13}C NMR spectrum of **42** in DMSO-d_6 at 25 °C.

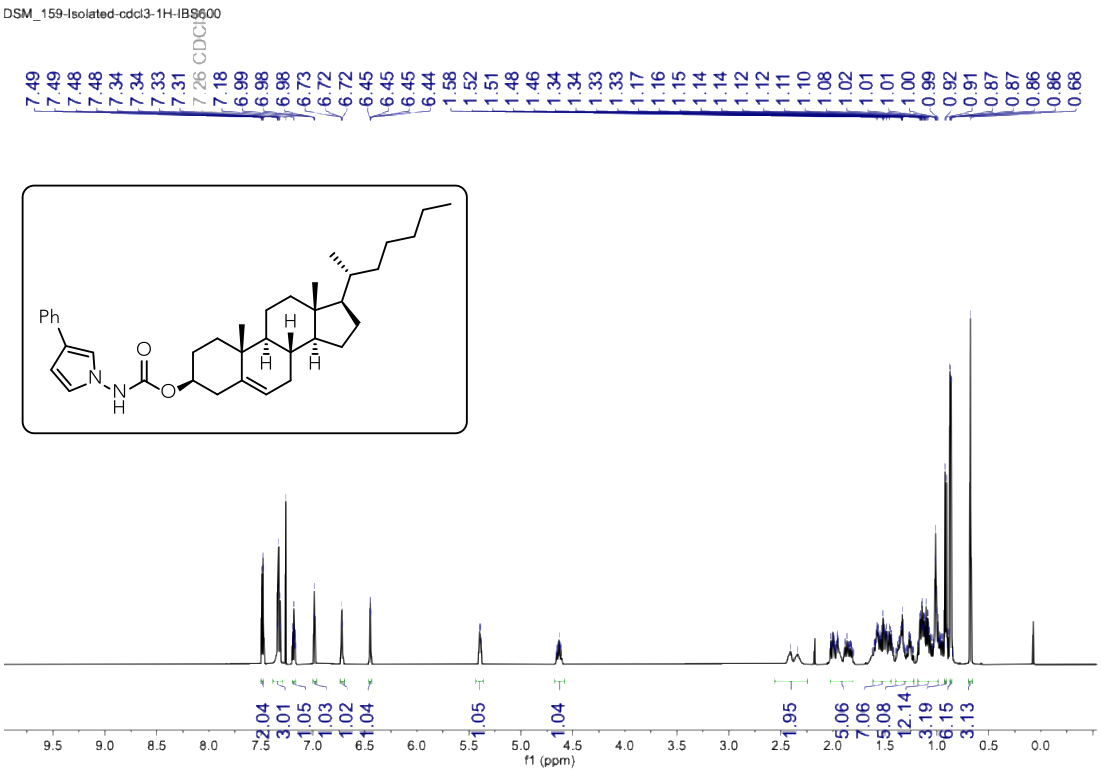

Figure S104. ^{1}H NMR spectrum of **43** in $CDCl_3$ at 25 °C.

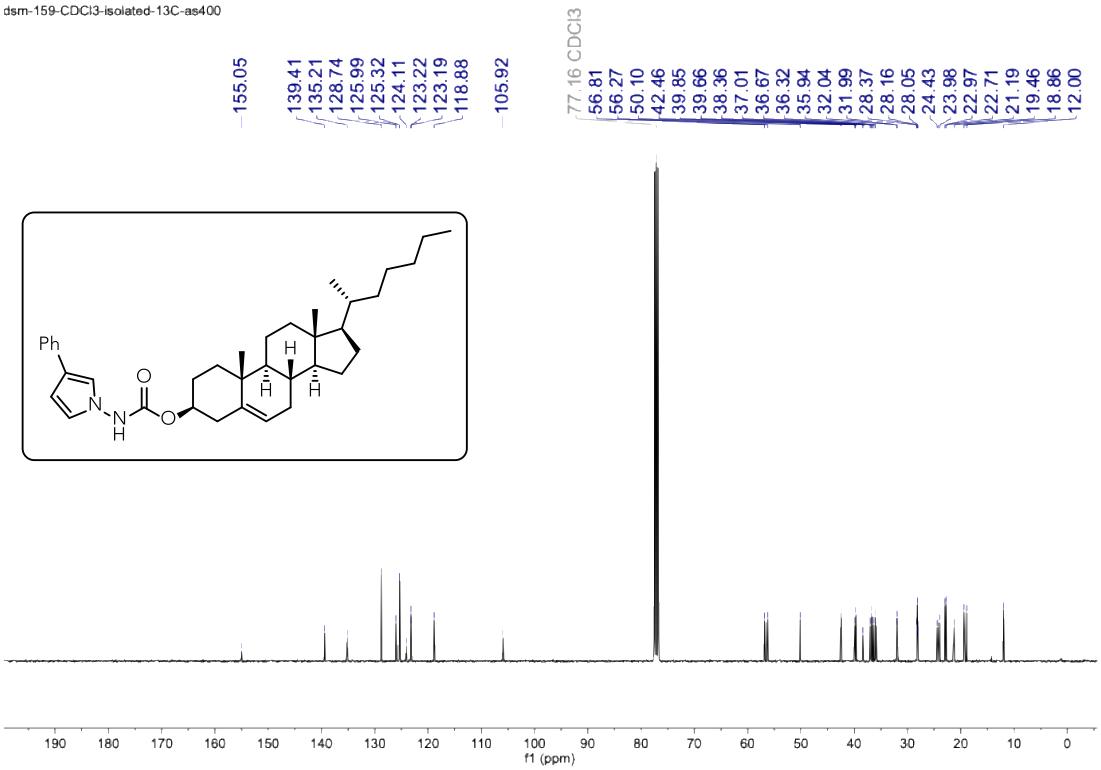

Figure S105. ^{13}C NMR spectrum of **43** in $CDCl_3$ at 25 °C.

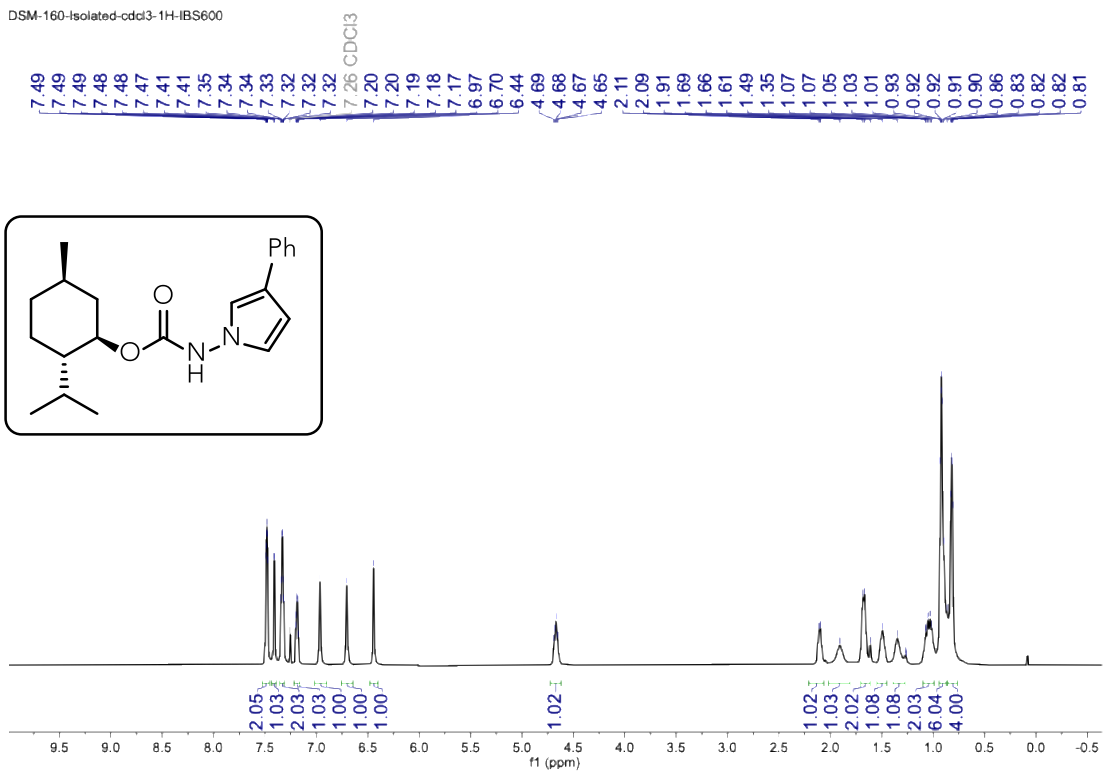

Figure S106. ^{1}H NMR spectrum of **44** in $CDCl_3$ at 25 °C.

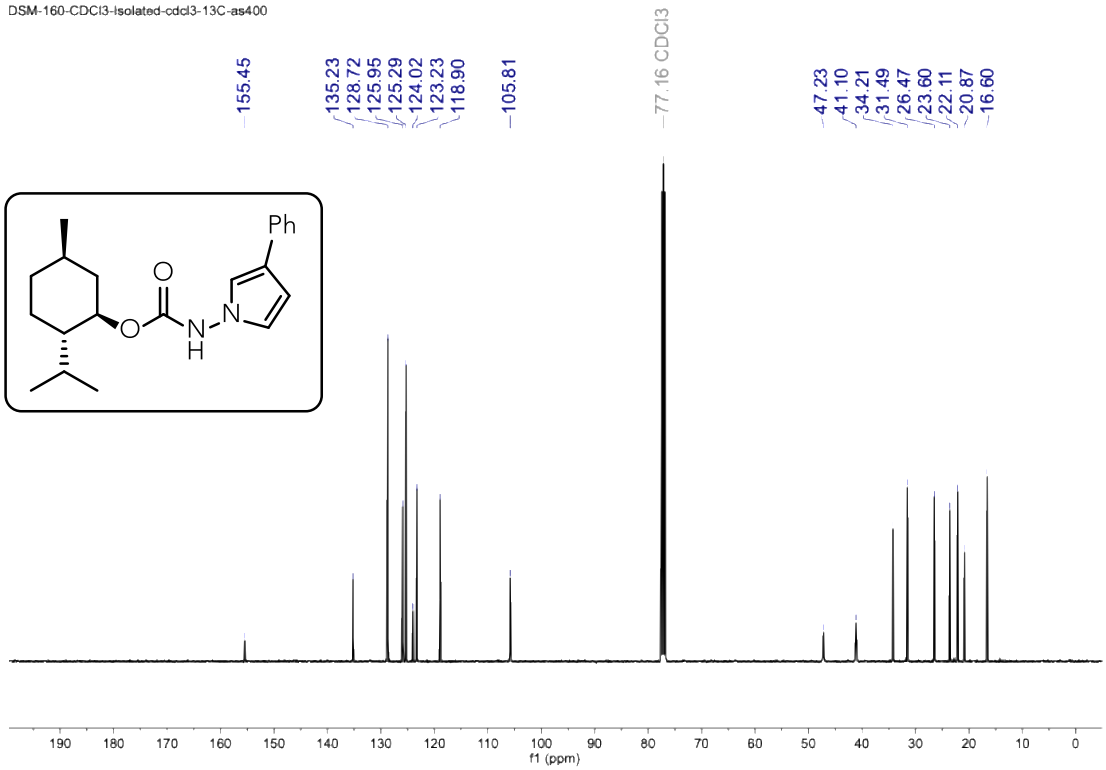

Figure S107. ^{13}C NMR spectrum of **44** in $CDCl_3$ at 25 °C.

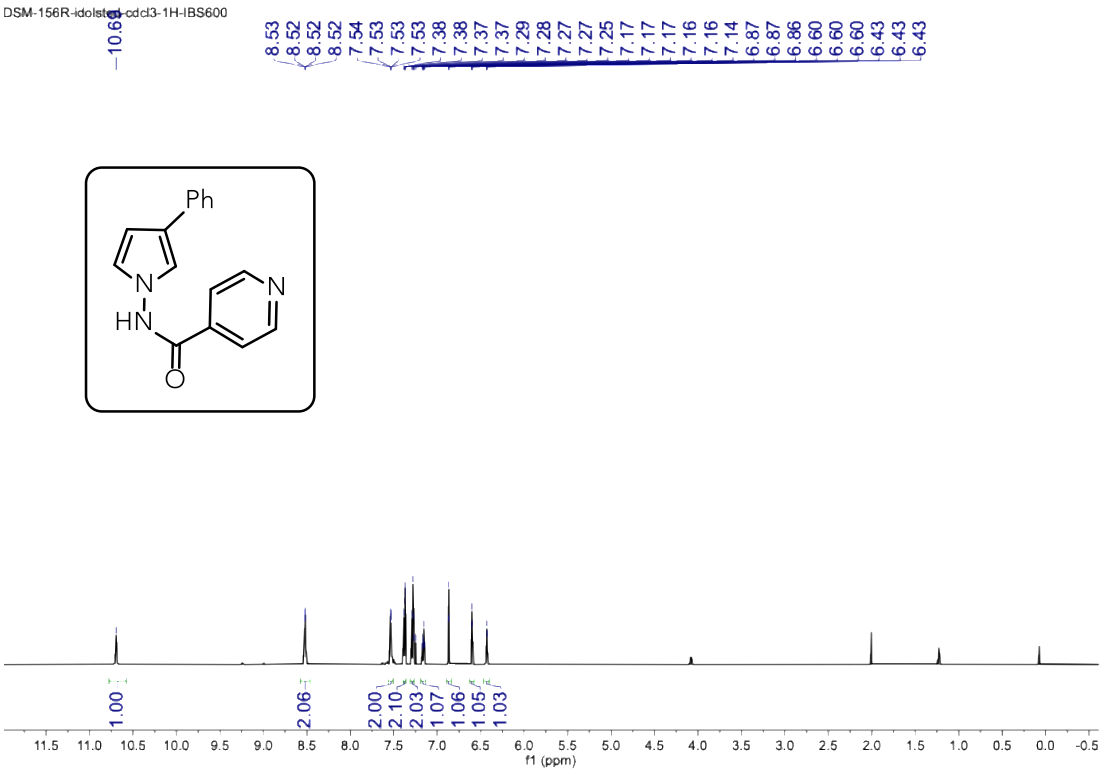

Figure S108. ^{1}H NMR spectrum of **45** in $CDCl_3$ at 25 °C.

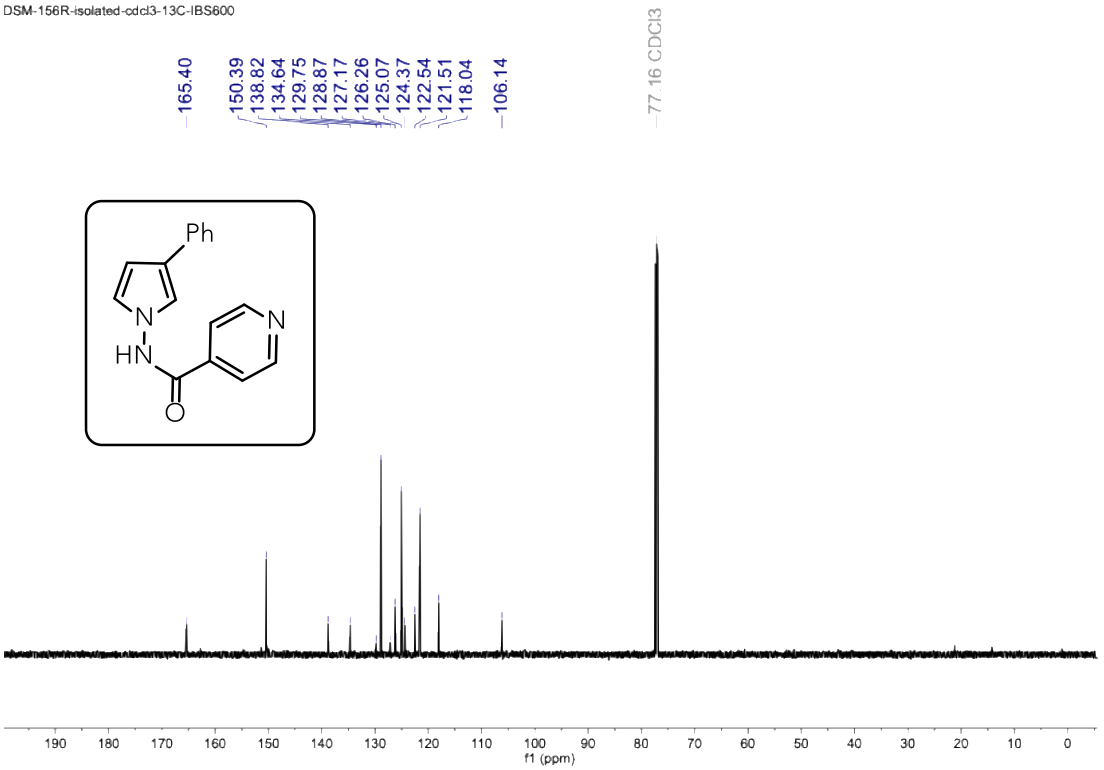

Figure S109. ^{13}C NMR spectrum of **45** in $CDCl_3$ at 25 °C.

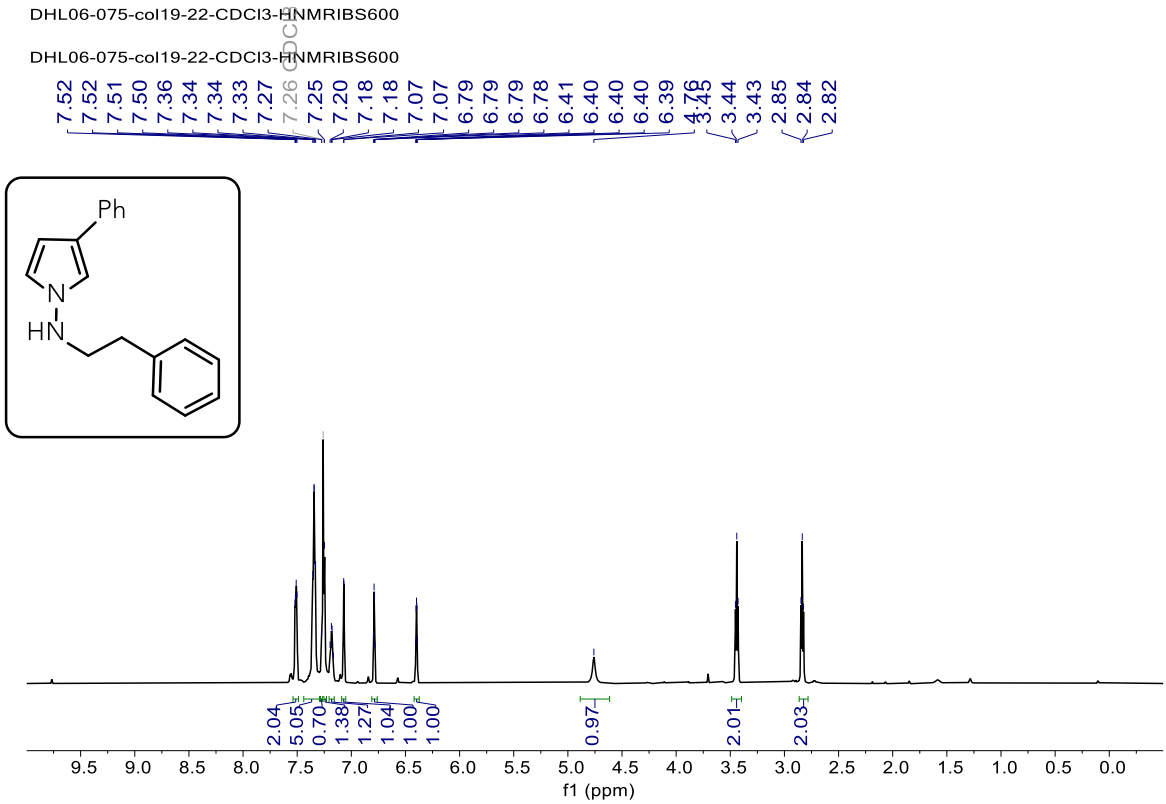

Figure S110. ^{1}H NMR spectrum of **46** in $CDCl_3$ at 25 °C.

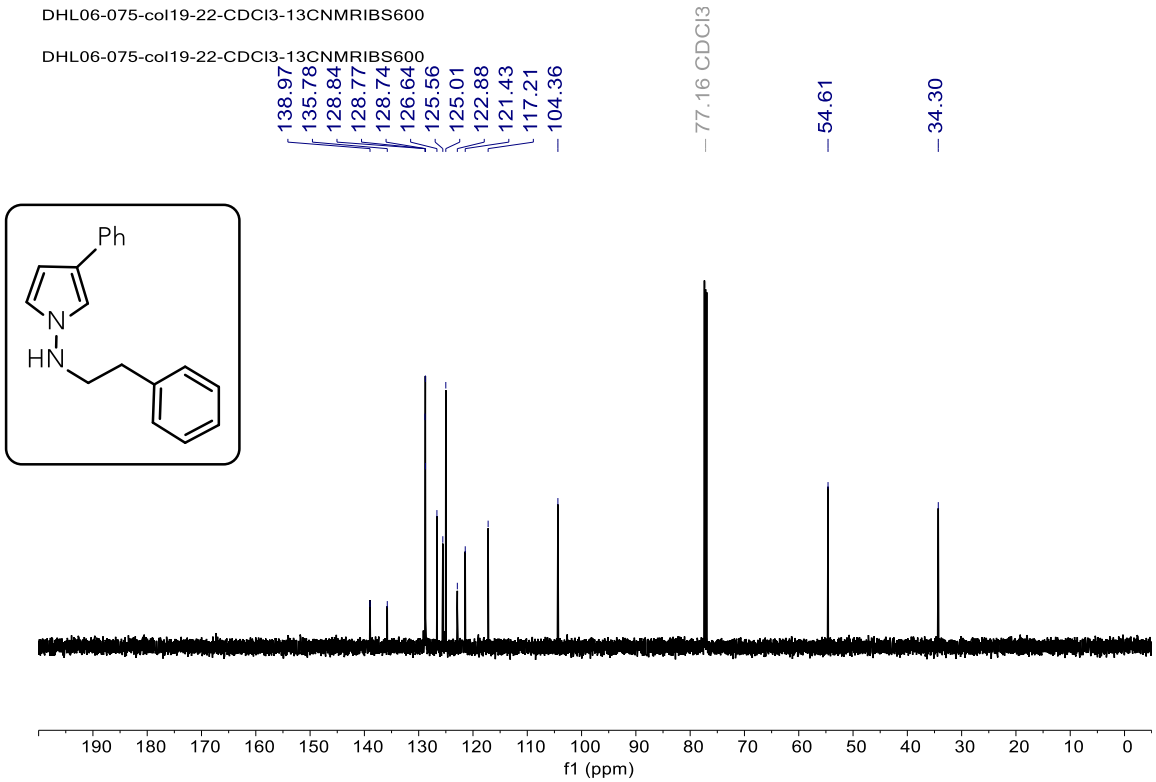

Figure S111. ^{13}C NMR spectrum of **46** in $CDCl_3$ at 25 °C.

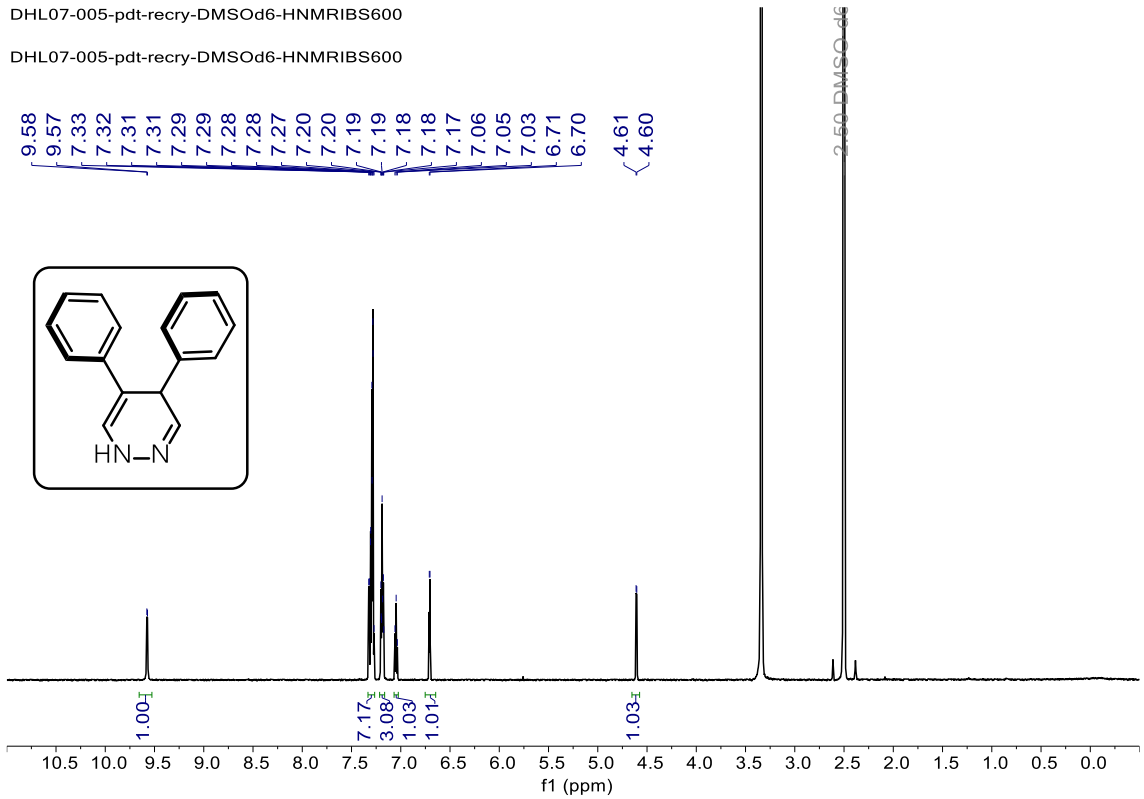

Figure S112. ^{1}H NMR spectrum of **H_2-4** in DMSO-d_6 at 25 ºC.

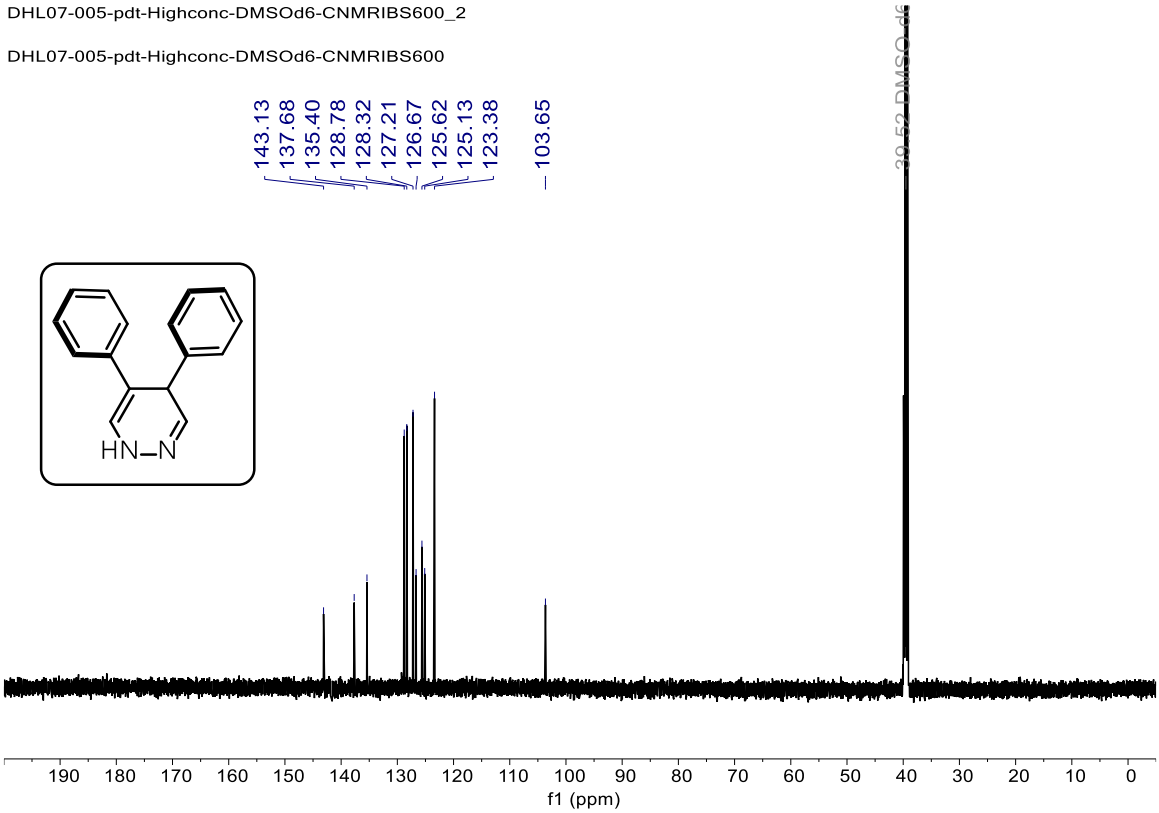

Figure S113. ^{13}C NMR spectrum of **H_2-4** in DMSO-d_6 at 25 ºC.

VIII. Cartesian Coordinates Obtained in Computational Studies

==========

I

# of Negative Frequency: 0
Charge: 0 Multiplicity: 1

==========

C	1.088603	1.501292	-0.376096
O	2.125637	1.972918	0.020281
H	1.082044	0.785204	-1.232332
C	-0.276042	1.849403	0.165256
C	-0.997909	3.979360	-1.086042
C	0.080040	4.694709	-0.529325
C	-1.973153	4.724027	-1.781712
C	0.187622	6.078257	-0.678006
C	-1.859905	6.102351	-1.935653
C	-0.776778	6.793728	-1.385690
H	0.863470	4.163376	0.013777
H	-2.849451	4.220755	-2.193938
H	1.038943	6.598393	-0.234160
H	-2.637673	6.644372	-2.477818
H	-0.692998	7.875535	-1.500642
C	-1.095626	2.513887	-0.922116
C	-1.838480	1.762236	-1.779683
H	-2.393502	2.232489	-2.594808
N	-1.970660	0.410310	-1.783787
H	-1.573136	-0.146017	-1.032171
H	-0.761280	0.913721	0.491089
H	-0.159325	2.492936	1.048344
N	-2.927121	-0.175195	-2.609049
H	-3.693323	-0.548634	-2.046332
H	-2.508264	-0.964148	-3.100137

==========

I_5-TS

# of Negative Frequency: 1
Charge: 0 Multiplicity: 1

==========

C	1.204534	-0.360007	-0.160661
C	2.069790	-1.403729	-0.523306
C	3.454098	-1.255796	-0.425867
C	4.001442	-0.057792	0.029852
C	3.151538	0.992966	0.387144
C	1.770875	0.844854	0.291758
C	-0.261353	-0.539406	-0.258207
C	-1.157479	0.176833	0.444174
N	-2.518030	-0.168808	0.279668
C	-2.222446	-1.164172	-1.656783
C	-0.851184	-1.598841	-1.157425
N	-2.969006	-1.289674	1.011366
H	1.657789	-2.351259	-0.875826
H	4.105118	-2.085352	-0.707665
H	5.083788	0.060740	0.103476
H	3.568231	1.939348	0.737080
H	1.124891	1.684081	0.556180
H	-0.888334	0.997975	1.115897
H	-2.228330	-0.164684	-2.146733
H	-0.211184	-1.757512	-2.040895
H	-0.968133	-2.568860	-0.648021
H	-3.573888	-0.973353	1.770955
H	-3.566788	-1.826823	0.373598
O	-3.158885	-1.938445	-1.792519
H	-3.200284	0.601742	0.297682
N	-5.545173	-0.248892	-0.496443
N	-5.156393	1.008089	0.041090
H	-6.342365	-0.147467	-1.126768
H	-4.775464	-0.610480	-1.063734
H	-5.737469	1.201684	0.855205
H	-5.321133	1.771754	-0.617834

==========

II_5

# of Negative Frequency: 0
Charge: 0 Multiplicity: 1

==========

C	1.207613	-0.340314	-0.154240
C	2.067075	-1.290495	-0.725295
C	3.451383	-1.132626	-0.653968
C	3.996992	-0.017393	-0.019165
C	3.150146	0.941482	0.543997
C	1.769023	0.783026	0.476156
C	-0.253982	-0.538487	-0.220198
C	-1.155777	0.080521	0.555463
N	-2.508031	-0.317377	0.282533
C	-2.387697	-1.154297	-1.248248
C	-0.895752	-1.521797	-1.163627
N	-3.065341	-1.216960	1.228782
H	1.649149	-2.168531	-1.221089
H	4.106474	-1.884405	-1.097479
H	5.079719	0.109005	0.033369
H	3.570872	1.822257	1.032185
H	1.117421	1.547096	0.904358
H	-0.969060	0.802699	1.351512
H	-2.517730	-0.249800	-1.891964
H	-0.437932	-1.490435	-2.163651
H	-0.806790	-2.553503	-0.784343
H	-3.910128	-0.775668	1.597442
H	-3.408209	-1.989239	0.629249
O	-3.271211	-2.068642	-1.300285
H	-3.187299	0.466995	0.113356
N	-5.545940	-0.218239	-0.435912
N	-4.862388	1.025520	-0.323517
H	-6.335056	-0.138388	-1.079052
H	-4.895109	-0.899281	-0.844377
H	-5.337399	1.599689	0.371904
H	-4.876261	1.556298	-1.197462

==========

II_5-TS

# of Negative Frequency: 1
Charge: 0 Multiplicity: 1

==========

C	1.184628	-0.288086	0.010006
C	1.904864	-0.774761	-1.091617
C	3.280664	-0.993965	-1.006230
C	3.959835	-0.737110	0.184229
C	3.252033	-0.259605	1.291636
C	1.880596	-0.039488	1.206531
C	-0.263742	-0.052043	-0.103893
C	-1.020384	0.694444	0.719054
N	-2.373848	0.781124	0.285998
C	-2.581437	-0.458525	-0.690064
C	-1.125664	-0.577583	-1.224157
N	-3.369646	0.828725	1.292693
H	1.382598	-0.973140	-2.029565
H	3.823812	-1.366312	-1.876830
H	5.035113	-0.910478	0.252955
H	3.773088	-0.064752	2.230751
H	1.335996	0.315320	2.084049
H	-0.716939	1.249182	1.609560
H	-2.713323	-1.279952	0.075423
H	-1.049538	0.051763	-2.129081
H	-0.882288	-1.611443	-1.510969
H	-3.148565	0.128824	2.006815
H	-3.313758	1.738195	1.753781
O	-3.546278	-0.316900	-1.544339
N	-4.367859	2.335747	-1.609964
N	-3.014696	2.687839	-1.337118
H	-4.614952	2.700933	-2.530235
H	-4.327046	1.299809	-1.676715
H	-2.616097	1.837424	-0.528908
H	-2.956441	3.629123	-0.942202
H	-2.402786	2.657331	-2.160272

==========

III_5

# of Negative Frequency: 0
Charge: 0 Multiplicity: 1

==========

C	0.996226	-0.248971	0.004165
C	1.367381	-1.584316	-0.231146
C	2.686478	-2.006449	-0.057970
C	3.667063	-1.105677	0.354897
C	3.312530	0.226477	0.593831
C	1.998847	0.649014	0.421322
C	-0.391602	0.173676	-0.185737
C	-0.944002	1.379220	0.065727
N	-2.324771	1.384705	-0.132385
C	-2.662987	0.202224	-0.926662
C	-1.507650	-0.755937	-0.627105
N	-2.997986	2.550640	-0.512976
H	0.612998	-2.303455	-0.555512
H	2.945367	-3.049720	-0.249494
H	4.698447	-1.435351	0.490288
H	4.069053	0.942635	0.920304

H	1.744983	1.693456	0.613820
H	-0.467330	2.289833	0.433558
H	-3.648352	-0.179623	-0.616316
H	-1.266932	-1.343714	-1.524756
H	-1.777087	-1.460718	0.176545
H	-3.210694	3.104813	0.314767
H	-2.415626	3.124568	-1.126704
O	-2.664469	0.500894	-2.297272
H	-3.357972	1.162631	-2.435364

==========

III_5-TS

of Negative Frequency: 1
Charge: 1 Multiplicity: 1

==========

N	-0.979313	-0.238682	-0.933209
H	-0.410962	-0.183018	-1.779679
N	-3.403319	-0.511142	3.489089
C	-3.502291	0.022991	2.280309
O	-3.261166	-1.507594	1.071334
H	-4.481243	0.270385	1.871526
C	-2.232845	0.756365	2.006589
C	0.114829	0.577970	3.186231
C	0.801066	1.053942	2.058112
C	0.822918	0.414533	4.389131
C	2.161361	1.355185	2.132120
C	2.180633	0.711925	4.458299
C	2.855784	1.185387	3.329675
H	0.274195	1.167567	1.108036
H	0.299792	0.065333	5.281685
H	2.681677	1.721057	1.245217
H	2.713621	0.582203	5.401766
H	3.919488	1.422851	3.385399
C	-1.315154	0.257273	3.100345
C	-2.065447	-0.465504	3.951933
H	-1.821581	-0.985290	4.876033
H	-1.859672	0.613243	0.982711
H	-2.428277	1.837150	2.132593
N	-4.386386	-1.221937	4.165045
H	-4.662028	-2.024591	3.596202
H	-5.203721	-0.623514	4.286077
N	-2.295145	-0.684615	-1.234133
H	-4.119525	-1.937476	0.937523
H	-0.542900	-0.944505	-0.338991
H	-2.948478	-1.198439	0.135200
H	-2.304715	-1.410682	-1.955566
H	-2.826030	0.103888	-1.606165

==========

IV_5

of Negative Frequency: 0
Charge: 0 Multiplicity: 1

==========

C	-0.771018	4.940702	13.741576
H	-0.463933	5.951391	13.467086
C	-1.915873	4.395168	13.161088
H	-2.486967	4.984252	12.440759
C	-2.333491	3.107028	13.498267
H	-3.230202	2.680836	13.045463
C	-1.589955	2.369821	14.422865
H	-1.901494	1.359706	14.695669
C	-0.445852	2.914788	15.001492
H	0.123979	2.320769	15.718731
C	-0.014149	4.211453	14.672991
C	2.000534	4.193400	16.246181
H	1.937224	3.228699	16.745061
C	1.195438	4.790714	15.285659
C	1.773932	6.072079	15.012576
H	1.410991	6.816883	14.308636
C	2.892110	6.199129	15.806998
H	3.620552	6.997967	15.919684
N	3.014204	5.056229	16.545508
N	4.046189	4.846719	17.455770
H	3.639057	4.664360	18.373778
H	4.554542	4.004439	17.183428

==========

I_6-TS

of Negative Frequency: 1
Charge: 0 Multiplicity: 1

==========

C	0.321620	0.969478	-1.332936
O	1.318182	0.323825	-0.971101
H	-0.110166	0.812348	-2.351178
C	0.088858	2.373591	-0.806971
C	-1.477698	4.389990	-1.062039
C	-0.520855	5.240383	-0.479052
C	-2.568984	4.992373	-1.717358
C	-0.659318	6.627794	-0.526772
C	-2.709419	6.377229	-1.761582
C	-1.756323	7.206106	-1.164800
H	0.341217	4.809931	0.033736
H	-3.309907	4.369912	-2.222738
H	0.097508	7.260388	-0.058583
H	-3.564361	6.815005	-2.280820
H	-1.863878	8.291227	-1.206885
C	-1.314271	2.918495	-0.977527
C	-2.403896	2.119926	-1.032700
H	-3.402286	2.548877	-1.140012
N	-2.424406	0.739385	-0.990311
H	-3.289963	0.326076	-0.651262
H	0.430825	2.397992	0.241748
H	0.791340	3.012171	-1.369534
N	-1.256776	0.117770	-0.553439
H	-1.172587	-0.835551	-0.964625
H	-1.167433	0.101533	0.468260
N	0.674562	-2.344797	-2.171216
N	-0.741200	-2.200647	-2.187096
H	1.030539	-2.492093	-3.116462
H	-1.167054	-3.123231	-2.108071
H	-1.076394	-1.807156	-3.069645
H	1.067449	-1.460098	-1.833089

==========

II_6

of Negative Frequency: 0
Charge: 0 Multiplicity: 1

==========

C	0.156526	0.925407	-1.472311
O	1.212556	0.287734	-1.094913
H	-0.141756	0.863298	-2.554269
C	0.044041	2.383994	-1.013835
C	-1.508993	4.441423	-1.075428
C	-0.510234	5.243969	-0.497720
C	-2.635959	5.088260	-1.616193
C	-0.642935	6.631686	-0.437880
C	-2.769089	6.472989	-1.555122
C	-1.774370	7.255200	-0.963008
H	0.381220	4.776256	-0.076223
H	-3.412875	4.504575	-2.113741
H	0.146462	7.227162	0.025048
H	-3.652546	6.946716	-1.987643
H	-1.877723	8.340682	-0.920421
C	-1.348628	2.968731	-1.106647
C	-2.421520	2.158040	-1.198265
H	-3.441724	2.540303	-1.255659
N	-2.358358	0.768692	-1.267701
H	-3.167799	0.276648	-0.896930
H	0.440416	2.427764	0.015803
H	0.738329	2.971083	-1.635948
N	-1.147156	0.205100	-0.836881
H	-1.075854	-0.805710	-1.194383
H	-1.033840	0.229804	0.186881
N	0.665484	-2.475669	-1.769110
N	-0.713750	-2.240096	-2.038095
H	1.121328	-2.862736	-2.596033
H	-1.252575	-3.072796	-1.801812
H	-0.891152	-2.052656	-3.028040
H	1.077399	-1.547620	-1.587580

==========

II_6-TS

of Negative Frequency: 1
Charge: 0 Multiplicity: 1

==========

C	0.088173	0.890806	-1.501002
O	1.185034	0.267332	-1.121891
H	-0.154807	0.860268	-2.601250
C	0.020714	2.362570	-1.056376
C	-1.515874	4.438048	-1.078145
C	-0.488479	5.228750	-0.532659
C	-2.660818	5.103855	-1.558659
C	-0.608238	6.616520	-0.447325
C	-2.781205	6.487815	-1.471647
C	-1.756190	7.256388	-0.912864
H	0.417225	4.749518	-0.156952
H	-3.464266	4.534550	-2.029849
H	0.205183	7.199446	-0.010417
H	-3.680428	6.972768	-1.857215

H	-1.850135	8.341724	-0.849795
C	-1.363959	2.968346	-1.139382
C	-2.435163	2.153192	-1.259500
H	-3.456745	2.531105	-1.331365
N	-2.343024	0.775849	-1.348443
H	-3.168835	0.244846	-1.092527
H	0.425506	2.395711	-0.028674
H	0.724407	2.938183	-1.680274
N	-1.144335	0.183897	-0.915842
H	-1.005413	-1.139306	-1.421289
H	-1.051094	0.248349	0.107411
N	0.682701	-2.379003	-1.621794
N	-0.687939	-2.158934	-1.951382
H	1.137436	-2.806071	-2.427802
H	-1.272789	-2.934859	-1.631103
H	-0.859887	-2.042706	-2.956100
H	1.068168	-1.410727	-1.479944

==========

III_6

of Negative Frequency: 0
Charge: 0 Multiplicity: 1

==========

C	0.028555	0.884533	-1.410265
O	1.149490	0.254217	-0.876373
H	0.026022	0.865304	-2.515643
C	0.009384	2.328902	-0.924422
C	-1.481037	4.426604	-1.092484
C	-0.491165	5.191323	-0.448125
C	-2.574625	5.121810	-1.647943
C	-0.595428	6.579518	-0.347259
C	-2.678917	6.505310	-1.545603
C	-1.690470	7.247678	-0.892428
H	0.371765	4.692348	-0.004025
H	-3.352174	4.576257	-2.185607
H	0.189797	7.139319	0.165109
H	-3.536223	7.012118	-1.993314
H	-1.772510	8.333153	-0.817237
C	-1.347037	2.958875	-1.171993
C	-2.395857	2.153767	-1.471276
H	-3.390124	2.543879	-1.696707
N	-2.290315	0.787703	-1.562841
H	-3.131371	0.225274	-1.580288
H	0.275584	2.326026	0.147650
H	0.798762	2.898256	-1.441397
N	-1.174135	0.161848	-0.995111
H	-1.229027	0.241398	0.028098
H	1.172205	-0.647860	-1.224635

==========

III_6-TS

of Negative Frequency: 1
Charge: 1 Multiplicity: 1

==========

C	-0.336230	0.690375	-1.137368
O	0.199395	0.897151	-2.901675
H	0.507037	0.036767	-0.907554
C	-0.265819	2.123687	-0.696591
C	-1.521240	4.331616	-1.112860
C	-0.527544	5.038078	-0.413653
C	-2.491375	5.076659	-1.809392
C	-0.516282	6.433539	-0.392918
C	-2.482296	6.468160	-1.782865
C	-1.494538	7.156804	-1.073238
H	0.245686	4.495645	0.133290
H	-3.254778	4.562650	-2.396371
H	0.266849	6.956320	0.159524
H	-3.247770	7.020260	-2.331559
H	-1.484366	8.247892	-1.059693
C	-1.527178	2.855865	-1.098979
C	-2.635083	2.136216	-1.377979
H	-3.601025	2.599472	-1.584979
N	-2.669423	0.756644	-1.462599
H	-3.493728	0.313082	-1.062700
H	-0.120092	2.130326	0.397808
H	0.632752	2.583147	-1.131693
N	-1.505983	0.067546	-1.115282
H	-1.499873	-0.916190	-1.461546
N	-0.936442	-1.257839	-3.862302
N	-0.978297	-2.156705	-2.757933
H	-0.191455	0.061729	-3.386878
H	-0.589323	-1.709578	-4.712854
H	-0.016208	-2.409871	-2.528478
H	-1.454529	-3.025065	-3.010183
H	-1.893600	-0.959317	-4.060371
H	-0.262209	1.665239	-3.280157

==========

IV_6

of Negative Frequency: 0
Charge: 0 Multiplicity: 1

==========

N	1.802637	5.749194	15.797669
C	2.716556	6.274220	16.521210
C	2.619416	6.526280	18.005596
C	1.595777	5.585393	18.604918
N	0.672308	5.331489	16.421524
H	3.625207	6.575148	15.990539
C	1.619791	5.304177	20.051437
C	0.947391	4.201007	20.612791
C	2.327630	6.152058	20.921066
C	0.963903	3.973415	21.985364
C	2.349058	5.918821	22.297285
C	1.665227	4.831499	22.838150
H	0.418740	3.499865	19.964048
H	2.860472	7.016336	20.520974
H	0.436176	3.109593	22.394333
H	2.906786	6.594622	22.948520
H	1.683382	4.646208	23.913428
C	0.651287	5.086872	17.778014
H	0.048576	4.803164	15.823662
H	-0.181875	4.468469	18.114833
H	3.611331	6.381920	18.462698
H	2.359340	7.587169	18.191113

==========

S1

of Negative Frequency: 0
Charge: 1 Multiplicity: 2

==========

O	-3.070026	-0.475960	3.325579
C	-3.181439	0.328149	2.215464
H	-4.163506	0.357206	1.750787
C	-1.998925	0.930864	1.938332
C	0.297744	0.808085	3.124146
C	0.947813	1.686889	2.216017
C	1.034144	0.264440	4.213438
C	2.279732	2.005959	2.393338
C	2.366393	0.593016	4.381516
C	2.991531	1.461129	3.475155
H	0.391463	2.108411	1.378334
H	0.554427	-0.411672	4.921581
H	2.777767	2.679937	1.696047
H	2.929170	0.176223	5.216785
H	4.043651	1.716138	3.612181
C	-1.078869	0.482546	2.939315
C	-1.841399	-0.397768	3.763609
H	-1.581670	-0.984399	4.643445
H	-1.809612	1.618242	1.118742

==========

S2

of Negative Frequency: 0
Charge: 1 Multiplicity: 2

==========

O	-3.028893	-0.642468	3.253779
C	-3.100881	0.195290	2.178950
H	-4.062910	0.243784	1.675500
C	-1.915673	0.849381	1.960151
C	0.367599	0.838209	3.167666
C	1.051011	1.619088	2.209328
C	1.059401	0.464015	4.340607
C	2.370655	1.999913	2.415910
C	2.381684	0.849864	4.540164
C	3.045000	1.616844	3.580486
H	0.539812	1.915085	1.291740
H	0.554911	-0.111382	5.120652
H	2.883163	2.596319	1.659163
H	2.896853	0.553284	5.455254
H	4.082435	1.915207	3.738571
C	-1.000325	0.432891	2.944534
C	-1.725606	-0.599984	3.756617
H	-1.746632	1.584136	1.176240
N	-1.147643	-2.003220	3.542001
H	-0.190381	-2.031829	3.925495
N	-1.115740	-2.489932	2.213666
H	-0.570573	-1.830694	1.653380
H	-2.075967	-2.486669	1.863900
H	-1.684881	-2.669504	4.117747

H	-1.727871	-0.466949	4.849413

==========

S3

of Negative Frequency: 0
Charge: 0 Multiplicity: 2

==========

O	-3.208150	-0.578222	3.213470
C	-3.232575	0.277018	2.178147
H	-4.185716	0.386201	1.663988
C	-2.021107	0.884308	1.951041
C	0.266114	0.747553	3.110054
C	0.942702	1.597024	2.201598
C	0.999554	0.250328	4.212510
C	2.279107	1.926303	2.387642
C	2.338353	0.586309	4.392676
C	2.989736	1.422909	3.483538
H	0.406767	1.994906	1.338019
H	0.512942	-0.395906	4.944645
H	2.775336	2.582211	1.669606
H	2.878355	0.191273	5.255329
H	4.039878	1.681626	3.627370
C	-1.118928	0.404255	2.916504
C	-1.870931	-0.607576	3.766791
H	-1.829808	1.610889	1.164231
N	-1.407861	-1.965099	3.759915
H	-0.769516	-2.161647	4.524370
N	-0.919315	-2.476939	2.547313
H	-0.337121	-1.784672	2.065175
H	-1.714312	-2.661465	1.936152
H	-1.935720	-0.301537	4.826028

==========

$SIII_5$-TS

of Negative Frequency: 1
Charge: 0 Multiplicity: 1

==========

N	-0.259085	0.038547	-2.386578
H	-0.574737	0.653334	-3.143792
N	-2.186557	-0.780655	1.039677
C	-2.415207	0.317777	0.211505
O	-2.899625	-0.483283	-1.289944
H	-3.372837	0.837323	0.338595
C	-1.157875	1.008326	0.136850
C	1.272465	0.425195	0.880259
C	1.847288	1.471956	0.136236
C	2.127871	-0.346063	1.692440
C	3.217767	1.730665	0.193260
C	3.494612	-0.090886	1.744386
C	4.051328	0.950979	0.994574
H	1.207222	2.087657	-0.499798
H	1.706220	-1.149291	2.300593
H	3.636657	2.549728	-0.395218
H	4.132971	-0.706546	2.381492
H	5.122765	1.153271	1.039918
C	-0.168609	0.163473	0.803540
C	-0.824338	-0.943423	1.273887
H	-0.463116	-1.858839	1.737525
H	-0.665769	0.429154	-1.433861
H	-1.078487	2.089158	0.018725
N	-3.106771	-1.812768	1.193878
H	-3.506516	-1.965168	0.263657
H	-3.873054	-1.478018	1.780997
N	-0.677167	-1.303805	-2.658707
H	-3.561693	0.088563	-1.702229
H	0.763887	0.104439	-2.362735
H	-1.645770	-1.293497	-2.278384
H	-0.143839	-1.887304	-2.010747

==========

II_5'

of Negative Frequency: 0
Charge: 0 Multiplicity: 1

==========

C	-1.637007	2.360117	-1.241776
C	-0.316053	2.548112	-1.674543
C	0.166691	3.826955	-1.953618
C	-0.666915	4.935909	-1.813571
C	-1.988383	4.759650	-1.393469
C	-2.469752	3.484515	-1.111682
C	-2.121113	1.000891	-0.928850
C	-3.208469	0.714153	-0.198448
N	-3.431699	-0.695366	-0.041290
C	-2.380585	-1.412440	-1.241034
C	-1.392494	-0.240178	-1.373381
N	-3.064248	-1.217255	1.226704
H	0.344844	1.686287	-1.783593
H	1.198976	3.957075	-2.282963
H	-0.291351	5.936239	-2.035681
H	-2.649169	5.622402	-1.292888
H	-3.508446	3.356864	-0.800969
H	-3.891684	1.413574	0.285433
H	-3.116710	-1.382607	-2.081639
H	-1.035066	-0.157849	-2.410702
H	-0.519194	-0.440659	-0.730430
H	-2.835133	-0.419279	1.822569
H	-3.965823	-1.572888	1.592860
O	-1.978276	-2.546379	-0.826765
H	-4.397302	-1.032778	-0.284508

==========

II_6'

of Negative Frequency: 0
Charge: 0 Multiplicity: 1

==========

C	0.156526	0.925407	-1.472311
O	1.212556	0.287734	-1.094913
H	-0.141756	0.863298	-2.554269
C	0.044041	2.383994	-1.013835
C	-1.508993	4.441423	-1.075428
C	-0.510234	5.243969	-0.497720
C	-2.635959	5.088260	-1.616193
C	-0.642935	6.631686	-0.437880
C	-2.769089	6.472989	-1.555122
C	-1.774370	7.255200	-0.963008
H	0.381220	4.776256	-0.076223
H	-3.412875	4.504575	-2.113741
H	0.146462	7.227162	0.025048
H	-3.652546	6.946716	-1.987643
H	-1.877723	8.340682	-0.920421
C	-1.348628	2.968731	-1.106647
C	-2.421520	2.158040	-1.198265
H	-3.441724	2.540303	-1.255659
N	-2.358358	0.768692	-1.267701
H	-3.167799	0.276648	-0.896930
H	0.440416	2.427764	0.015803
H	0.738329	2.971083	-1.635948
N	-1.147156	0.205100	-0.836881
H	-1.075854	-0.805710	-1.194383
H	-1.033840	0.229804	0.186881

==========

II_5''

of Negative Frequency: 0
Charge: 1 Multiplicity: 1

==========

C	-0.140872	-1.238280	-1.190989
C	0.460760	-2.342865	-1.810177
C	0.602104	-2.384818	-3.197067
C	0.136216	-1.328777	-3.979031
C	-0.472022	-0.226689	-3.370423
C	-0.610008	-0.180204	-1.987238
C	-0.256875	-1.197321	0.274973
C	-0.580751	-0.130073	1.015734
N	-0.504105	-0.443529	2.443413
C	-0.640890	-1.991285	2.469428
C	0.026673	-2.383946	1.162210
N	0.769221	-0.064198	2.978786
H	0.830957	-3.173231	-1.206328
H	1.078333	-3.246324	-3.667382
H	0.243631	-1.363029	-5.064452
H	-0.841571	0.599766	-3.979404
H	-1.095603	0.679663	-1.522225
H	-0.804148	0.898750	0.740731
H	-1.727765	-2.147999	2.421562
H	-0.393702	-3.321518	0.776643
H	1.109155	-2.519792	1.313494
H	0.788111	0.957771	2.987143
H	0.772564	-0.374971	3.953300
O	-0.060409	-2.518901	3.578646
H	-1.280821	-0.013782	2.967320
H	-0.703783	-2.577291	4.300800

==========

II_6''

of Negative Frequency: 0
Charge: 1 Multiplicity: 1

==========

C	-0.388655	-0.502598	-5.499736
O	0.337728	0.038082	-6.521781
H	-1.477594	-0.445394	-5.642481
C	0.047242	0.071686	-4.171001
C	-0.414574	-0.165191	-1.653454
C	0.410443	0.937368	-1.379942
C	-1.232086	-0.653974	-0.619504
C	0.435102	1.517148	-0.111133
C	-1.205539	-0.075683	0.646659
C	-0.369567	1.012226	0.909285
H	1.053067	1.346210	-2.161625
H	-1.918045	-1.481428	-0.809521
H	1.089563	2.369852	0.078645
H	-1.854958	-0.469633	1.430515
H	-0.352935	1.467901	1.900629
C	-0.416552	-0.772152	-3.005438
C	-0.812919	-2.039392	-3.212215
H	-1.150470	-2.699402	-2.412936
N	-0.890748	-2.643827	-4.475554
H	-0.720556	-3.648600	-4.483146
H	1.144706	0.179871	-4.187931
H	-0.371279	1.086196	-4.101013
N	-0.108323	-2.008778	-5.464501
H	-0.344269	-2.412629	-6.382217
H	0.908574	-2.149367	-5.326227
H	-0.142729	-0.041930	-7.359313

==========

N_2H_4

# of Negative Frequency: 0
Charge: 0 Multiplicity: 1
==========

N	-0.493919	-0.006566	-2.470281
N	-1.065163	0.007358	-1.167295
H	-1.037832	0.967873	-0.829107
H	-2.054850	-0.246031	-1.193715
H	-1.184448	0.243685	-3.180824
H	-0.222748	-0.966316	-2.677606

==========

$N_2H_5^+$

# of Negative Frequency: 0
Charge: 1 Multiplicity: 1
==========

H	2.380200	0.362037	-2.469067
H	2.593318	2.008454	-2.368996
N	0.921229	1.366474	-3.434802
N	2.263702	1.246407	-2.981237
H	2.899515	1.198827	-3.788294
H	0.853040	2.265132	-3.915761
H	0.335296	1.438407	-2.601468

==========

H_2O

# of Negative Frequency: 0
Charge: 0 Multiplicity: 1
==========

O	-0.702729	0.000000	-1.258583
H	-0.702729	0.752991	-0.654406
H	-0.702729	-0.752991	-0.654406

IX. Vibrational Frequencies Obtained in Computational Studies

==========

I

# of Negative Frequency: 0
Charge: 0 Multiplicity: 1
==========
45.44 60.10 79.69 90.40 117.64 124.82 202.43 255.60
267.88 333.18 355.07 381.33 423.50 457.40 475.86
522.50 554.60 604.25 630.13 639.67 725.99 769.87
792.62 875.69 882.03 948.12 950.15 979.02 991.37
1005.79 1023.97 1041.88 1051.24 1071.76 1092.07 1116.06
1152.65 1163.76 1192.83 1200.15 1269.63 1307.33 1315.68
1328.86 1355.28 1363.00 1373.52 1417.29 1445.25 1482.93
1515.97 1546.94 1647.45 1660.04 1686.52 1734.97 1864.68
2960.26 3071.18 3148.45 3209.07 3214.39 3223.43 3230.19
3232.55 3236.33 3497.02 3579.34 3587.99

==========

I_5-TS

# of Negative Frequency: 1
Charge: 0 Multiplicity: 1
==========
-121.38 39.84 49.69 60.14 80.04 102.56 131.61 138.05
158.73 188.48 211.35 211.96 235.19 283.43 306.51
333.71 388.13 420.38 427.14 447.07 470.66 536.52
567.81 595.91 628.85 681.13 727.04 794.43 828.95
854.50 883.63 890.16 897.41 903.25 967.36 1000.72
1010.46 1019.87 1028.31 1038.61 1049.24 1057.00 1062.17
1071.53 1076.20 1108.85 1148.08 1152.20 1187.76 1194.69
1251.20 1265.81 1308.61 1314.00 1334.41 1343.60 1353.54
1361.27 1378.03 1397.74 1416.71 1485.01 1517.96 1543.71
1639.45 1644.84 1663.46 1664.75 1693.63 1735.38 1787.64
2979.41 3066.08 3127.00 3190.35 3213.41 3218.43 3226.32
3230.09 3237.90 3383.23 3461.47 3480.94 3489.44 3547.54
3562.03 3586.34 -117.22 37.15 50.10 62.25 76.02 95.06
129.64 137.47 150.29 185.22 211.74 213.08 247.91
287.87 308.13 349.77 392.14 419.96 431.77 460.59
471.80 537.43 570.49 598.29 628.75 681.05 726.93
794.91 842.05 859.10 883.56 891.16 900.42 917.66
968.76 1002.51 1011.57 1025.51 1029.13 1041.00 1050.08
1061.34 1064.25 1076.33 1082.25 1108.32 1146.87 1152.28
1187.14 1192.94 1248.15 1262.33 1308.04 1310.57 1332.23
1347.26 1354.05 1360.52 1376.90 1394.86 1416.85 1485.13
1517.13 1543.53 1634.59 1640.93 1663.66 1669.79 1693.91
1736.45 1765.01 2976.08 3065.86 3125.76 3193.44 3213.54
3218.37 3226.03 3229.99 3238.02 3356.96 3449.72 3478.90
3490.11 3548.20 3559.69 3586.28

==========

II_5

# of Negative Frequency: 0
Charge: 0 Multiplicity: 1
==========
30.38 41.34 75.63 77.79 92.30 109.36 145.64 170.14
198.65 205.75 258.19 299.35 309.80 326.43 373.78
391.63 417.54 423.22 492.08 513.79 534.17 570.70
583.95 627.80 668.41 692.58 722.19 794.96 857.95
877.82 885.44 927.78 938.13 969.78 1003.54 1011.96
1027.46 1037.52 1046.58 1051.28 1061.94 1068.57 1077.81
1104.94 1143.49 1151.04 1164.16 1182.27 1210.27 1246.40
1263.56 1295.70 1300.17 1311.53 1323.72 1349.28 1361.26
1379.30 1381.43 1393.86 1425.83 1486.14 1519.31 1542.57
1568.05 1635.57 1643.05 1666.19 1688.59 1694.24 1741.72
2891.43 2982.99 3068.43 3134.36 3216.02 3221.51 3227.48
3232.84 3239.59 3247.30 3304.78 3417.82 3487.55 3535.43
3537.86 3580.46

==========

II_5-TS

# of Negative Frequency: 1
Charge: 0 Multiplicity: 1
==========
-804.33 40.48 46.98 76.35 96.37 114.31 139.27 155.26
210.46 230.93 249.70 284.73 319.81 340.74 371.98
390.71 420.34 458.48 500.00 541.68 546.93 567.50
589.94 627.39 636.48 645.62 719.83 742.47 794.61
847.81 874.70 895.22 960.99 962.75 976.45 997.71
1010.93 1021.55 1031.84 1044.49 1047.41 1063.23 1104.16
1116.42 1144.11 1149.56 1151.37 1171.50 1183.78 1198.18
1236.28 1274.97 1293.16 1311.84 1335.18 1346.90 1363.82
1368.41 1390.65 1420.78 1433.95 1468.67 1486.96 1543.03
1610.27 1621.92 1625.80 1665.98 1677.09 1695.00 1711.52
1737.83 2750.25 3052.90 3126.53 3213.45 3218.38 3225.19
3230.30 3237.34 3238.15 3277.45 3468.55 3475.59 3543.68
3563.86 3565.95 -717.14 31.23 44.49 62.19 89.98 112.95
140.68 156.04 210.43 229.37 255.52 294.13 321.57
345.62 374.87 406.33 420.93 460.92 510.13 542.94
549.37 574.30 603.79 622.02 628.22 653.68 721.63
766.99 794.34 845.82 875.41 901.95 960.74 963.11
985.16 1010.57 1015.35 1021.63 1031.03 1043.91 1046.76
1062.82 1103.30 1128.50 1143.17 1149.02 1150.49 1180.57
1183.51 1199.90 1235.53 1275.88 1291.11 1312.62 1336.64
1343.90 1363.32 1366.07 1386.13 1425.66 1435.79 1462.84
1486.89 1542.57 1603.32 1625.09 1644.84 1664.96 1676.96
1694.46 1715.09 1735.08 2735.53 3047.01 3122.77 3199.93
3212.38 3217.21 3224.27 3229.22 3233.75 3237.45 3459.39
3468.74 3545.98 3556.27 3564.37

==========

III_5

# of Negative Frequency: 0
Charge: 0 Multiplicity: 1
==========
33.33 71.59 124.27 148.21 182.61 234.45 268.84 303.85
356.81 398.78 414.04 419.76 442.73 503.12 546.94
600.46 627.94 662.30 705.57 718.84 790.95 869.81
870.31 896.33 909.56 927.96 952.38 964.92 1007.28
1007.73 1019.61 1027.53 1041.60 1062.74 1097.95 1106.30
1148.92 1183.98 1186.64 1213.43 1227.79 1266.04 1277.91
1311.42 1319.49 1332.17 1359.53 1379.02 1409.58 1427.97
1452.40 1488.77 1543.80 1633.69 1658.98 1692.25 1712.08
3071.35 3088.71 3136.24 3209.70 3214.60 3222.92 3227.37
3235.37 3242.43 3488.11 3587.25 3813.16

==========

III_5-TS

# of Negative Frequency: 1
Charge: 1 Multiplicity: 1
==========
-760.90 23.01 39.19 59.89 112.81 149.60 160.30 201.35
214.02 241.36 255.49 326.98 348.81 366.32 385.71
421.09 441.53 486.12 510.74 525.71 548.03 572.25
601.62 627.11 660.27 684.77 714.66 724.32 747.86
790.44 842.24 877.83 903.11 940.73 949.32 957.81
975.67 1007.75 1021.85 1023.17 1040.36 1043.35 1062.10
1088.30 1101.92 1136.16 1148.63 1182.53 1186.05 1198.58
1225.11 1247.12 1268.10 1288.75 1309.00 1320.55 1326.65
1348.36 1353.16 1357.34 1403.76 1456.96 1473.92 1494.84
1541.47 1563.48 1631.64 1639.91 1645.46 1654.81 1671.49
1687.74 1689.50 1761.30 1866.28 3050.41 3122.23 3137.47
3149.15 3204.27 3207.87 3218.24 3220.88 3232.67 3253.90
3406.38 3459.42 3525.62 3546.17 3723.74 -244.42 33.22
43.44 46.39 70.61 94.80 123.18 130.39 143.74 157.56
210.14 230.58 250.22 305.52 326.35 367.91 379.58
415.04 420.32 488.40 497.80 516.17 541.60 572.04
625.78 659.37 697.47 723.15 745.89 789.40 874.23
878.93 883.37 902.58 941.53 945.83 968.02 992.80
1009.94 1015.82 1026.25 1036.05 1049.98 1059.48 1065.96
1071.70 1106.15 1142.87 1149.00 1150.97 1162.13 1190.04
1222.57 1270.77 1302.67 1307.65 1321.73 1340.24 1362.48
1371.59 1376.66 1381.97 1412.99 1485.81 1541.99 1572.67
1633.92 1635.15 1644.61 1661.86 1666.17 1693.97 1722.13
2560.95 3067.32 3146.46 3212.57 3216.56 3224.03 3230.70
3238.48 3279.05 3290.73 3483.90 3499.26 3502.78 3572.12
3584.05 3594.66 3832.85

==========

IV_5

# of Negative Frequency: 0
Charge: 0 Multiplicity: 1
==========
12.75 98.39 139.19 205.85 231.39 319.93 323.06 369.75
415.61 490.90 523.62 626.44 628.24 666.15 672.66
718.24 727.60 741.51 788.43 847.01 868.92 902.58
935.48 954.86 973.54 1010.38 1017.20 1027.13 1039.74
1059.64 1069.07 1085.75 1105.26 1148.66 1183.43 1214.73
1264.21 1314.48 1345.57 1358.11 1420.40 1429.96 1457.94
1495.36 1539.33 1570.10 1619.22 1657.17 1669.31 1695.74
3209.83 3214.97 3222.73 3226.91 3234.48 3273.64 3280.92
3298.72 3504.25 3585.22

==========

I_6-TS

# of Negative Frequency: 1
Charge: 0 Multiplicity: 1
==========
-149.62 7.70 43.70 56.74 73.05 98.59 123.29 152.39
171.76 185.68 228.23 271.85 295.00 312.82 387.27
397.64 422.04 426.92 483.11 495.99 508.52 542.72
559.46 616.71 628.79 724.11 727.78 773.11 791.28
874.80 891.43 923.80 931.17 938.06 960.55 1003.64
1018.08 1022.07 1042.26 1063.77 1067.47 1076.21 1088.81
1108.20 1148.23 1150.16 1161.29 1184.38 1188.24 1228.28
1261.64 1292.98 1312.12 1320.33 1333.15 1356.55 1363.21
1382.51 1389.55 1401.43 1419.82 1483.12 1519.78 1539.87
1636.28 1651.60 1654.72 1662.79 1685.23 1688.08 1748.50
2913.49 3051.58 3085.96 3102.61 3209.62 3215.06 3223.42
3227.33 3234.99 3236.32 3424.51 3477.60 3481.15 3537.06
3571.98 3574.39 -140.78 28.38 47.31 67.95 83.33 100.67
122.08 152.91 175.55 185.01 230.77 277.05 294.05
312.26 385.78 395.05 421.17 425.69 481.51 496.25
505.32 541.33 559.23 615.66 628.73 724.29 724.93
764.18 791.71 875.53 888.71 924.21 929.64 941.91
961.72 1003.39 1017.30 1022.63 1043.20 1063.67 1068.36
1077.14 1090.25 1108.09 1148.20 1148.55 1151.29 1179.93
1187.77 1226.09 1262.14 1293.43 1312.93 1320.40 1333.29
1355.89 1363.12 1382.87 1387.56 1402.16 1419.71 1483.15
1518.94 1539.48 1637.29 1650.75 1659.53 1662.49 1684.51
1687.52 1748.20 2916.17 3051.93 3102.86 3122.27 3210.04
3215.37 3223.57 3227.54 3234.46 3236.23 3426.52 3479.44
3484.04 3542.31 3572.07 3575.22

==========

II_6

of Negative Frequency: 0
Charge: 0 Multiplicity: 1
==========
31.38 49.39 74.46 84.78 104.89 140.08 172.88 186.14
196.61 267.56 283.71 324.80 342.80 380.56 404.71
419.89 452.09 466.05 505.71 515.02 542.92 560.87
585.12 628.65 662.51 722.75 772.00 794.55 874.67
907.40 921.93 941.16 949.57 961.86 973.89 1007.84
1022.13 1039.13 1043.34 1059.02 1067.80 1091.93 1100.04
1107.96 1149.39 1153.55 1186.23 1199.52 1244.76 1274.11
1303.33 1310.78 1316.08 1326.21 1335.25 1352.05 1360.36
1388.77 1411.45 1428.57 1452.20 1483.75 1499.75 1538.25
1542.20 1628.84 1654.82 1664.01 1687.07 1690.61 1752.51
2596.84 2819.21 3051.13 3111.06 3210.30 3215.85 3223.73
3228.57 3236.15 3244.36 3315.59 3426.15 3483.24 3538.04
3573.53 3586.25

==========

II_6-TS

of Negative Frequency: 1
Charge: 0 Multiplicity: 1
==========
-578.43 22.12 44.87 76.42 93.90 108.30 161.68 177.32
211.86 214.95 294.46 334.35 368.69 417.20 419.59
437.34 453.75 465.55 508.25 539.89 547.32 554.75
575.06 628.70 653.22 704.72 722.96 789.46 827.67
875.24 924.48 933.01 957.49 973.32 998.11 1010.81
1018.42 1022.04 1042.40 1061.27 1067.32 1071.57 1106.15
1115.76 1137.45 1149.23 1186.02 1188.66 1212.82 1245.74
1274.45 1283.40 1293.93 1314.70 1337.54 1340.64 1360.82
1383.78 1392.95 1426.86 1437.79 1464.13 1484.07 1512.50
1541.08 1611.18 1660.31 1675.13 1688.11 1693.10 1723.95
1744.43 2777.39 3038.89 3040.97 3098.52 3209.39 3214.83
3223.09 3228.57 3235.49 3237.61 3413.82 3470.94 3552.08
3562.45 3609.66 -415.58 29.62 44.01 79.40 96.48 109.36
164.01 177.84 213.83 216.00 301.53 335.10 372.91
418.12 424.09 437.93 453.15 458.95 511.50 537.64
547.28 565.80 579.03 628.66 705.71 722.51 745.63
790.86 850.00 874.22 925.94 933.19 957.87 977.64
1000.79 1012.26 1021.28 1029.49 1041.47 1061.65 1068.26
1075.02 1106.23 1113.31 1140.36 1149.18 1186.70 1197.88
1215.61 1246.23 1274.56 1278.99 1294.51 1314.55 1336.95
1342.32 1361.16 1383.43 1396.79 1424.56 1436.39 1479.76
1484.63 1512.75 1541.09 1606.92 1659.90 1676.13 1687.36
1694.14 1720.59 1737.89 2772.15 2941.09 3038.33 3095.71
3209.17 3214.63 3222.97 3228.55 3235.02 3236.66 3413.58
3468.19 3547.30 3564.33 3617.35

==========

III_6

of Negative Frequency: 0
Charge: 0 Multiplicity: 1
==========
40.98 77.15 132.74 164.61 213.87 234.00 293.43 333.70
359.00 389.19 418.25 460.93 484.75 515.94 553.73
568.30 587.69 628.78 715.91 721.45 792.15 869.12
875.21 931.69 939.53 958.63 964.45 1003.69 1018.49
1020.05 1041.71 1046.29 1064.88 1099.58 1109.51 1124.97
1151.00 1184.88 1192.26 1223.75 1264.65 1272.93 1305.74
1316.46 1346.53 1362.37 1366.70 1387.85 1434.87 1456.95
1468.27 1486.03 1518.64 1543.02 1657.86 1685.82 1721.83
3042.27 3049.50 3104.62 3208.87 3213.93 3223.48 3227.98
3235.30 3239.57 3420.80 3653.66 3837.58

==========

III_6-TS

of Negative Frequency: 1
Charge: 1 Multiplicity: 1
==========
-315.33 23.90 39.21 49.50 79.46 126.69 133.67 163.37
179.02 204.61 282.29 295.42 313.48 339.32 390.78
407.98 421.15 450.84 469.80 483.70 537.73 558.89
569.64 603.62 626.54 656.34 722.71 741.23 792.64
816.09 875.08 886.86 922.15 951.39 958.79 972.57
991.63 1006.98 1012.71 1023.55 1033.12 1046.04 1060.53
1074.32 1086.29 1111.22 1139.07 1151.25 1154.48 1192.07
1209.82 1221.99 1246.63 1293.25 1305.92 1324.28 1340.87
1351.59 1364.97 1397.41 1411.42 1439.37 1483.54 1512.51
1543.80 1560.75 1627.56 1634.38 1655.90 1660.41 1668.10
1691.51 1740.90 2428.15 3064.13 3125.08 3135.41 3212.47
3217.35 3225.62 3230.13 3237.51 3244.31 3244.71 3481.88
3497.29 3564.50 3581.36 3584.51 3779.83 -313.25 29.12
41.76 49.74 74.90 127.27 137.05 163.76 180.91 203.57
289.05 295.33 313.65 338.99 388.22 408.12 420.97
460.15 471.15 488.17 540.32 559.43 571.87 604.26
626.66 656.98 721.95 741.43 792.04 814.08 873.05
884.53 920.54 950.90 958.29 972.90 989.80 1006.98
1012.41 1022.07 1033.29 1045.12 1061.16 1074.75 1086.21
1111.24 1139.06 1150.89 1153.38 1191.88 1209.56 1220.64
1242.96 1292.69 1305.91 1324.21 1341.58 1353.11 1365.05
1395.81 1411.91 1439.80 1483.63 1511.95 1544.04 1566.77
1630.41 1634.13 1659.83 1662.02 1672.46 1691.89 1742.71
2452.56 3064.08 3116.94 3133.60 3212.58 3217.50 3225.71
3230.21 3237.57 3245.74 3246.22 3482.29 3497.21 3565.65
3582.12 3582.72 3782.32

==========

IV_6

of Negative Frequency: 0
Charge: 0 Multiplicity: 1
==========
59.20 84.52 140.82 168.96 292.90 329.39 402.30 422.26
459.06 484.35 551.41 589.52 605.72 627.17 649.17
721.78 758.72 790.72 863.57 872.53 922.70 943.75
957.02 991.29 1006.57 1016.14 1019.42 1028.06 1042.25
1056.90 1074.26 1108.73 1149.38 1188.42 1194.18 1235.56
1303.75 1322.38 1344.27 1362.68 1380.38 1399.86 1447.55
1484.40 1506.23 1543.72 1661.17 1689.27 1726.37 1768.02
3005.98 3090.50 3202.91 3212.02 3218.01 3226.08 3231.19
3236.69 3246.22 3652.92

==========

S1

of Negative Frequency: 0
Charge: 1 Multiplicity: 2
==========
77.80 95.23 170.31 256.75 354.02 393.81 432.95 469.07
565.59 607.60 644.07 673.83 683.54 795.91 816.99
841.83 850.59 906.99 921.23 940.31 986.93 1002.36
1024.08 1031.15 1045.41 1059.32 1078.97 1106.88 1129.96
1158.61 1192.87 1232.31 1280.50 1325.53 1375.40 1392.02
1418.08 1483.65 1501.04 1580.11 1605.87 1612.31 1660.91
3237.22 3245.85 3247.73 3255.94 3258.22 3297.49 3302.62
3324.40

==========

S2

of Negative Frequency: 0
Charge: 1 Multiplicity: 2
==========
57.50 82.96 128.87 137.81 147.44 207.19 280.47 305.39
344.20 374.95 419.86 448.51 496.73 580.26 624.76
631.12 691.85 715.86 741.81 790.48 834.11 851.37
869.59 877.04 909.26 928.36 956.89 973.02 1002.42
1022.84 1023.82 1046.25 1054.65 1072.56 1088.44 1112.53
1150.24 1151.69 1186.37 1192.12 1238.49 1250.19 1319.17

1332.67 1341.42 1357.85 1362.32 1443.25 1452.39 1482.92
1495.15 1520.94 1558.25 1578.15 1640.14 1650.24 1673.17
3120.73 3207.09 3221.51 3229.31 3235.61 3242.13 3285.52
3307.70 3427.21 3472.29 3502.39 3596.94

==========

S3

# of Negative Frequency: 0
Charge: 0 Multiplicity: 2

==========

47.22 51.49 109.17 134.03 167.06 221.53 304.80 339.04
363.64 396.56 417.39 494.44 513.33 562.50 610.13
625.26 663.77 709.38 722.68 758.77 790.29 847.47
856.36 880.09 897.23 927.41 938.88 975.33 999.58
1013.66 1019.17 1036.84 1054.31 1071.47 1103.87 1112.93
1148.70 1183.14 1192.23 1232.89 1253.12 1301.22 1321.75
1341.10 1352.34 1360.88 1377.68 1443.14 1484.02 1486.71
1527.24 1560.90 1644.01 1652.70 1669.34 3061.63 3213.85
3219.34 3228.19 3234.22 3239.27 3268.87 3285.94 3451.23
3566.13 3608.89

==========

$SIII_5$-TS

# of Negative Frequency: 1
Charge: 0 Multiplicity: 1

==========

-481.89 31.42 45.26 51.89 58.71 112.86 129.97 166.38
174.08 197.21 247.83 259.82 281.74 331.73 342.33
361.54 377.25 393.47 421.43 432.61 507.42 518.25
547.05 609.89 627.95 653.09 662.96 709.67 722.11
744.50 805.24 834.93 877.06 923.13 950.38 999.94
1006.38 1014.48 1021.59 1034.26 1040.56 1047.12 1048.50
1062.72 1098.38 1100.79 1133.57 1146.55 1179.98 1206.61
1228.21 1249.78 1293.26 1307.11 1323.70 1334.64 1344.61
1356.96 1414.85 1478.92 1489.58 1498.13 1539.89 1556.42
1588.36 1614.16 1631.52 1649.20 1656.99 1663.47 1687.52
2096.01 3131.07 3185.87 3205.05 3208.90 3217.69 3221.82
3229.17 3232.60 3276.08 3467.59 3484.87 3537.64 3542.42
3554.09 3835.94

==========

II_5''

# of Negative Frequency: 0
Charge: 1 Multiplicity: 1

==========

40.43 75.96 130.15 148.45 198.18 256.30 290.48 330.75
365.27 414.22 424.52 448.25 461.26 519.92 569.78
590.72 626.23 663.35 708.99 720.24 773.69 790.00
855.85 864.94 874.79 959.85 977.22 995.29 1011.62
1024.66 1028.62 1046.18 1052.54 1061.13 1065.58 1108.74
1147.51 1153.11 1160.43 1186.95 1235.07 1251.83 1263.63
1301.49 1311.39 1330.50 1363.98 1371.46 1388.90 1425.31
1426.52 1443.34 1487.38 1494.76 1545.71 1624.22 1668.77
1694.77 1748.17 3098.88 3140.72 3174.87 3219.92 3224.45
3230.90 3236.84 3242.92 3285.56 3418.93 3499.84 3588.33
3819.13

==========

II_6''

# of Negative Frequency: 0
Charge: 1 Multiplicity: 1

==========

51.06 90.06 129.24 178.03 196.95 279.20 326.58 356.94
420.11 424.57 455.69 467.17 491.27 529.92 536.15
558.85 623.17 628.04 711.32 720.38 788.36 842.49
873.39 907.38 918.25 957.05 965.25 990.44 1011.98
1022.51 1044.88 1048.69 1060.23 1069.38 1090.22 1109.43
1150.34 1187.84 1193.38 1218.61 1244.69 1273.71 1291.59
1308.07 1329.21 1347.20 1361.84 1385.68 1397.67 1412.47
1438.88 1487.15 1505.53 1543.81 1544.65 1599.10 1665.72
1695.42 1762.50 3077.22 3136.45 3147.27 3214.66 3220.24
3227.20 3232.14 3238.73 3257.72 3365.51 3467.49 3581.41
3817.20

==========

N_2H_4

# of Negative Frequency: 0
Charge: 0 Multiplicity: 1

==========

416.40 896.79 1035.36 1151.25 1312.08 1357.39 1646.73
1655.92 3483.82 3489.22 3573.79 3582.18

==========

$N_2H_5^+$

# of Negative Frequency: 0
Charge: 1 Multiplicity: 1

==========

321.92 972.60 1073.72 1112.87 1234.34 1448.12 1554.03
1608.33 1613.37 1654.02 3413.47 3495.72 3514.76 3517.60
3599.20

==========

H_2O

# of Negative Frequency: 0
Charge: 0 Multiplicity: 1

==========

1611.62 3844.15 3920.66

X. References

1 Pangborn, A. B., Giardello, M. A., Grubbs, R. H., Rosen, R. K. & Timmers, F. J. Safe and Convenient Procedure for Solvent Purification. *Organometallics* **15**, 1518–1520 (1996). https://doi.org/10.1021/om9503712

2 Hubschle, C. B., Sheldrick, G. M. & Dittrich, B. ShelXle: a Qt graphical user interface for SHELXL. *J. Appl. Crystallogr.* **44**, 1281–1284 (2011). https://doi.org/doi:10.1107/S0021889811043202

3 Sheldrick, G. Crystal structure refinement with SHELXL. *Acta Crystallogr., C Struct. Chem.* **71**, 3–8 (2015). https://doi.org/doi:10.1107/S2053229614024218

4 Kim, D. *et al.* Photocatalytic furan-to-pyrrole conversion. *Science* **386**, 99–105 (2024). https://doi.org/10.1126/science.adq6245

5 Rieke, R. D., Suh, Y. & Kim, S.-H. Heteroaryl manganese reagents: direct preparation and reactivity studies. *Tetrahedron Lett.* **46**, 5961–5964 (2005). https://doi.org/https://doi.org/10.1016/j.tetlet.2005.06.092

6 Tofi, M., Georgiou, T., Montagnon, T. & Vassilikogiannakis, G. Regioselective Ortho Lithiation of 3-Aryl and 3-Styryl Furans. *Org. Lett.* **7**, 3347–3350 (2005). https://doi.org/10.1021/ol051205l

7 Li, J. J. *et al.* Synthesis and structure–Activity relationship of 2-amino-3-heteroaryl-quinoxalines as non-peptide, small-Molecule antagonists for interleukin-8 receptor. *Bioorg. Med. Chem.* **11**, 3777–3790 (2003). https://doi.org/https://doi.org/10.1016/S0968-0896(03)00399-7

8 Wu, X. *et al.* Alkoxide-Catalyzed Hydrosilylation of Cyclic Imides to Isoquinolines via Tandem Reduction and Rearrangement. *Org. Lett.* **20**, 5610–5613 (2018). https://doi.org/10.1021/acs.orglett.8b02287

9 Yang, Y. & N.C. Wong, H. Regiospecific synthesis of 3,4-disubstituted furans and 3-substituted furans using 3,4-Bis(tri-n-butylstannyl)furan and 3-(tri-n-butylstannyl)f. *Tetrahedron* **50**, 9583–9608 (1994). https://doi.org/https://doi.org/10.1016/S0040-4020(01)85528-9

10 Cao, Z., Wang, M., Gao, H., Li, L. & Ren, S. Porous Organic Polymers via Diels–Alder Reaction for the Removal of Cr(VI) from Aqueous Solutions. *ACS Macro Lett.* **11**, 447–451 (2022). https://doi.org/10.1021/acsmacrolett.2c00052

11 Wang, H. *et al.* Dearomative ring expansion of thiophenes by bicyclobutane insertion. *Science* **381**, 75–81 (2023). https://doi.org/10.1126/science.adh9737

12 Fukumoto, Y., Tamura, Y., Iyori, Y. & Chatani, N. Conversion of 3,3,3-Trisubstituted Prop-1-ynes with tert-Butylhydrazine into 3,3,3-Trisubstituted Propionitriles Catalyzed by TpRh(C2H4)2/P(2-furyl)3. *J. Org. Chem.* **81**, 3161–3167 (2016). https://doi.org/10.1021/acs.joc.6b00116

13 Thondur, J. R., Gowda, P. S., Sharada, D. S. & Satyanarayana, G. Electrochemical Regioselective C-3 Alkoxycarbonylation of 2H-Indazoles. *J. Org. Chem.* **90**, 7435–7448 (2025). https://doi.org/10.1021/acs.joc.5c00785

14 Zhang, J. *et al.* A Variation of the Fischer Indolization Involving Condensation of Quinone Monoketals and Aliphatic Hydrazines. *Angew. Chem. Int. Ed.* **52**, 1753–1757 (2013). https://doi.org/https://doi.org/10.1002/anie.201207533

15 Mutungi, M. M., Ho, C. C., Bissember, A. C. & Smith, J. A. Facilitating the Isolation of Polar Natural Products: Mild 1,1′-Carbonyldiimidazole-Enabled Method for Derivatization of Acids and Alcohols. *Eur. J. Org. Chem.* **28**, e202500231 (2025). https://doi.org/https://doi.org/10.1002/ejoc.202500231

16 Xu, J. *et al.* Electrochemical deoxygenative amination of stabilized alkyl radicals from activated alcohols. *Nature Communications* **15**, 6116 (2024). https://doi.org/10.1038/s41467-024-50596-3

17 Do, H.-Q., Khan, R. M. K. & Daugulis, O. A General Method for Copper-Catalyzed Arylation of Arene C−H Bonds. *J. Am. Chem. Soc.* **130**, 15185–15192 (2008). https://doi.org/10.1021/ja805688p
18 Choi, W., Jang, A. & Hong, S. Pyridine-to-Pyridazine Skeletal Editing. *J. Am. Chem. Soc.* **147**, 42042–42050 (2025). https://doi.org/10.1021/jacs.5c15601
19 Al Dulayymi, A. R. & Baird, M. S. Pyridazines by addition of diazoalkanes to 1-bromo- and 1,2-dibromocyclopropenes. *Tetrahedron* **54**, 12897–12906 (1998). https://doi.org/https://doi.org/10.1016/S0040-4020(98)00781-9
20 Wang, W., Meng, W. & Du, H. B(C6F5)3-catalyzed metal-free hydrogenation of 3,6-diarylpyridazines. *Dalton Trans.* **45**, 5945–5948 (2016). https://doi.org/10.1039/C5DT03872C
21 Ledovskaya, M. S., Polynski, M. V. & Ananikov, V. P. One-Pot and Two-Chamber Methodologies for Using Acetylene Surrogates in the Synthesis of Pyridazines and Their D-Labeled Derivatives. *Chem. Asian J.* **16**, 2286–2297 (2021). https://doi.org/https://doi.org/10.1002/asia.202100562
22 Kinjo, R., Donnadieu, B. & Bertrand, G. Gold-Catalyzed Hydroamination of Alkynes and Allenes with Parent Hydrazine. *Angew. Chem. Int. Ed.* **50**, 5560–5563 (2011). https://doi.org/https://doi.org/10.1002/anie.201100740
23 Pridmore, S. J., Slatford, P. A., Taylor, J. E., Whittlesey, M. K. & Williams, J. M. J. Synthesis of furans, pyrroles and pyridazines by a ruthenium-catalysed isomerisation of alkynediols and in situ cyclisation. *Tetrahedron* **65**, 8981–8986 (2009). https://doi.org/https://doi.org/10.1016/j.tet.2009.06.108
24 Parr, R. G. in *Horizons of Quantum Chemistry.* (eds Kenichi Fukui & Bernard Pullman) 5–15 (Springer Netherlands).
25 Neese, F., Wennmohs, F., Becker, U. & Riplinger, C. The ORCA quantum chemistry program package. *J. Chem. Phys.* **152**, 224108 (2020). https://doi.org/10.1063/5.0004608
26 Neese, F. Software Update: The ORCA Program System—Version 6.0. *WIREs Comput. Mol. Sci* **15**, e70019 (2025). https://doi.org/https://doi.org/10.1002/wcms.70019
27 Zhao, Y. & Truhlar, D. G. The M06 suite of density functionals for main group thermochemistry, thermochemical kinetics, noncovalent interactions, excited states, and transition elements: two new functionals and systematic testing of four M06-class functionals and 12 other functionals. *Theor. Chem. Acc.* **120**, 215–241 (2008). https://doi.org/10.1007/s00214-007-0310-x
28 Weigend, F. & Ahlrichs, R. Balanced basis sets of split valence, triple zeta valence and quadruple zeta valence quality for H to Rn: Design and assessment of accuracy. *Phys. Chem. Chem. Phys.* **7**, 3297–3305 (2005). https://doi.org/10.1039/B508541A
29 Weigend, F. Accurate Coulomb-fitting basis sets for H to Rn. *Phys. Chem. Chem. Phys.* **8**, 1057–1065 (2006). https://doi.org/10.1039/B515623H
30 Cossi, M., Rega, N., Scalmani, G. & Barone, V. Energies, structures, and electronic properties of molecules in solution with the C-PCM solvation model. *J. Comput. Chem.* **24**, 669–681 (2003). https://doi.org/https://doi.org/10.1002/jcc.10189